Technische Universität München
Department of Mathematics
Chair of Mathematical Finance (M13)

First-exit times and their applications in default risk management

Peter A. Hieber

Vollständiger Abdruck der von der Fakultät für Mathematik der Technischen Universität München zur Erlangung des akademischen Grades eines

Doktors der Naturwissenschaften (Dr. rer. nat.)

genehmigten Dissertation.

Vorsitzende:		Univ.-Prof. Dr. Claudia Klüppelberg
Prüfer der Dissertation:	1.	Univ.-Prof. Dr. Matthias Scherer
	2.	Prof. Dr. Hansjörg Albrecher *Universität Lausanne/Schweiz*
	3.	Prof. Marcos Escobar, Ph.D. *Ryerson University, Toronto/Kanada*

Die Dissertation wurde am **02.07.2013** bei der Technischen Universität München eingereicht und durch die Fakultät für Mathematik am **14.10.2013** angenommen.

Abstract

Im Verlauf der letzten zwei Jahrzehnte sind sowohl Markt- als auch Ausfallrisiken angestiegen. Als Folge der zunehmenden globalen Vernetzung nimmt außerdem die Abhängigkeit von Aktienrenditen und Ausfallereignissen zu. Risikomanagement (und speziell die Risikostreuung) wird deswegen zu einer immer größeren Herausforderung. Quantitative Modelle, die Firmen helfen, ihre Risiken besser zu analysieren und zu verstehen, werden zunehmend wichtiger. Diese Arbeit leistet einen Beitrag auf dem Gebiet der sogenannten strukturellen Ausfallmodelle, bei denen ein Ausfall durch die Unterschreitung einer Ausfallschranke definiert wird. Für zustandsabhängige Sprungdiffusionsmodelle und zeitveränderte Brown'sche Bewegung wird gezeigt, wie Ausfallwahrscheinlichkeiten effizient berechnet werden können. Diese Aktienkursmodelle berücksichtigen viele empirisch beobachtete statistische Eigenschaften von Aktien-, Rohstoff- und Kreditmärkten. Verschiedene Ansätze der Modellierung von Abhängigkeiten zwischen den Ausfallzeiten werden außerdem diskutiert. Die Ergebnisse der Arbeit haben Relevanz für viele Anwendungen im Finanz- und Versicherungsbereich. Beispielhaft wird die Bewertung von Derivaten und das Risikomanagement von Private Equity Transaktionen behandelt.

Abstract

Over the last two decades, default rates as well as market risks have increased substantially. Furthermore, a consequence of the growing global interlacing is a strong dependence between both individual stock returns and credit events. Risk management – especially risk diversification – is much more challenging, since. Quantitative models that assist firms to better analyse, measure, and comprehend the risks they face are required. This thesis contributes to the growing literature on structural credit risk models, where the time of default is modeled as a first-exit time, i.e. the first time point a stochastic process crosses some default boundary. It is shown how first-exit time probabilities can efficiently be computed for time-changed Brownian motion and regime switching jump-diffusion models. These models take into account most of the stylized statistical facts of today's stock, commodity, and credit markets. Different approaches for the modeling of dependence between default times are discussed. The results of this thesis are interesting for many applications in financial engineering. We exemplarily treat the pricing of financial derivatives and the risk management process of Private Equity transactions.

Contents

1 Introduction **1**

2 First-exit time probabilities **7**

2.1 Motivation and literature review 7

2.2 Definition and notation 11

2.3 Brownian motion 12

2.3.1 First-exit time probabilities 12

2.3.2 Brownian bridge probabilities 14

2.4 Time-changed Brownian motion 18

2.4.1 Theoretical results 19

2.4.2 Examples 21

2.4.3 Error bounds 25

2.5 Regime switching jump-diffusion model 29

2.5.1 Skeleton 33

2.5.2 Brownian bridge algorithm 34

2.5.3 Functionals of the first-exit time 42

2.6 Numerical examples 43

3 Default–linked contracts in Finance and Insurance **49**

3.1 Pricing barrier derivatives 50

3.1.1 Stochastic volatility model 52

3.1.2 Regime switching jump-diffusion model 65

3.1.3 Model calibration . . . 66
3.1.4 Numerical examples . . . 71
3.2 The risk appetite of Private Equity (PE) sponsors . . . 85
3.2.1 Structural default model . . . 86
3.2.2 Data description: PE database . . . 92
3.2.3 Risk factors of PE investments . . . 94
3.2.4 Summary and Conclusion . . . 101
3.3 Insurance risk . . . 103

4 Multivariate extensions 106
4.1 Structural approach . . . 107
4.2 Copula approach . . . 108
4.2.1 Dependence measurement . . . 113
4.2.2 Numerical example . . . 116
4.3 Credit risk management: Prepayment risk . . . 119
4.3.1 Distribution of the portfolio loss and notional . . . 121
4.3.2 Pricing loan-credit-default-swaps (LCDS) . . . 124
4.3.3 Numerical example . . . 126
4.3.4 Summary and Conclusion . . . 128

5 Conclusion 129

A Proofs and formulas 132
A.1 Parameters of the Stein–Stein model . . . 132
A.2 Proof of Theorem 11 . . . 133
A.3 $V_E(0)$ and $\partial V_E(0)/\partial S_0$ in Theorem 6 . . . 137

Bibliography 139

Chapter 1

Introduction

The current financial crisis has revealed massive deficits in the risk management practices used in the banking and insurance industry. There is an urgent need for improvements to avoid or attenuate financial bubbles that result from an inadequate measurement of risks. Investors in public equity have to cope with at least two major challenges:

- Increasing default risk: *Figure 1.1* presents the number of insolvencies (bar graph) together with the default rate, i.e. the number of insolvencies divided by the total number of firms (black line) in Germany from 1950 until today. It can be observed that the number of insolvencies rose from 6 000 in 1980 to 30 000 in 2012. Relative to the total number of companies the default rate has tripled in the same period. This observation of an increased default risk is not restricted to the German economy, similar observations hold for most industrialized countries. It is even more pro-

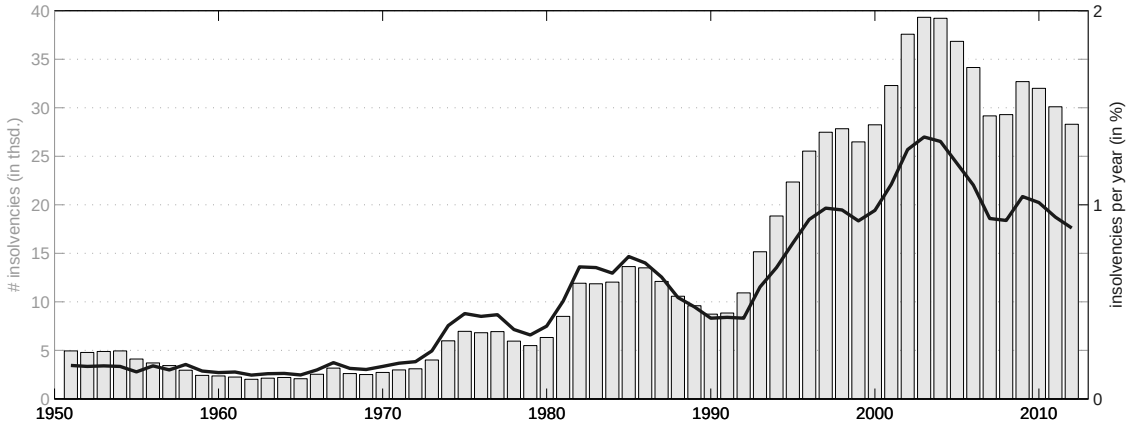

Figure 1.1: Number of insolvencies (bar graph) and insolvencies divided by the total number of firms (black line) in Germany from 1950–2012. (Data source: `http://www.destatis.de`.)

nounced for companies that are not quoted on stock markets (the interested reader is referred to *Section 3.2*, see also Cochrane [2005]).

- Increasing stock market risk: The increasing riskiness is not only reflected in default rates, but also in the volatility of public stock markets. Stapf and Werner [2003], for example, provide evidence for a significant increase of stock and index volatility in Germany after 1997.

- Increasing dependence: In a globalized world, macroeconomic factors turn out to be more and more important. Regional crises like the Hongkong banking crisis 1997/98

Figure 1.2: Average linear pairwise correlation (estimated on one year rolling windows) of the 5 stock market indices Nikkei (Japan), Hang Seng (China), EuroSTOXX (Europe), Bovespa (Brasil)*, and* S&P (US) *from 1988 to today (top) and of a representative sample of 20 German stocks from 1996 to today (below).* (Data source: *Reuters*.)

or the crisis in the US housing market crisis in 2007/08 might quickly spill over to the worldwide economy, simultaneously affecting companies from completely different industries and regions. This is also strongly reflected in the dependence of stock market returns. *Figure 1.2 (top)* presents the average pairwise linear correlation[1] (estimated based on one year rolling windows) of the 5 stock market indices *Nikkei (Japan), Hang Seng (China), EuroSTOXX (Europe), Bovespa (Brasil)*, and *S&P (US)* from 1988 to today. One observes a persistent and visible increase in the average correlation from about 0.2 (1988) to 0.4 (2013). This increase in dependence can also be observed within countries. Taking 20 major German stocks – a representative sample of the most important German industries – we observe a very similar evolution of the average pairwise correlation of single stocks (see *Figure 1.2 (below)*).

Those developments complicate risk diversification and increase the need for a careful risk management adequately reflecting empirical observations but also taking into account possibly changing economic environments. Therefore, it is necessary to develop tools and quantitative models that assist firms to better comprehend the risks they face. In the past risks and their dependence have often been modeled too simplistic, sometimes leading to a significant underestimation of risk. This thesis aims to present numerical tools and quantitative models to estimate default risks and their dependence.

From a theoretical point of view, this thesis further develops so-called *structural default models* (see the seminal papers of Merton [1974] and Black and Cox [1976]). Here, the time of default is modeled as a first-exit time, i.e. the first time point a stochastic process crosses some threshold level or default boundary. *Figure 1.3* gives two examples: While the company on the left defaults, the company on the right stays solvent during the considered time horizon. First-exit times have many applications in finance, engineering, and physics. In this thesis, the focus of such applications is on the pricing of derivatives, credit, and insurance risk. The structure of the thesis is as follows:

Chapter 2 introduces to the theory of first-exit times. The aim of this chapter is to derive the two-sided first-exit times for a large variety of stochastic processes. After a literature review and some basic notation, we first recapitulate the barrier hitting probabilities if the underlying process is a Brownian motion (*Section 2.3*). In *Section 2.4*, we extend those results to the case of (continuously) time-changed Brownian motion. This result is very convenient since we are still able to derive the barrier hitting probabilities analytically. We give several exemplary parameterizations for the time change and discuss the implementa-

[1] Heuristically speaking, a correlation of 0 indicates that the indices behave as "almost independent", if the correlation is 1 their evolution tends to be very similar.

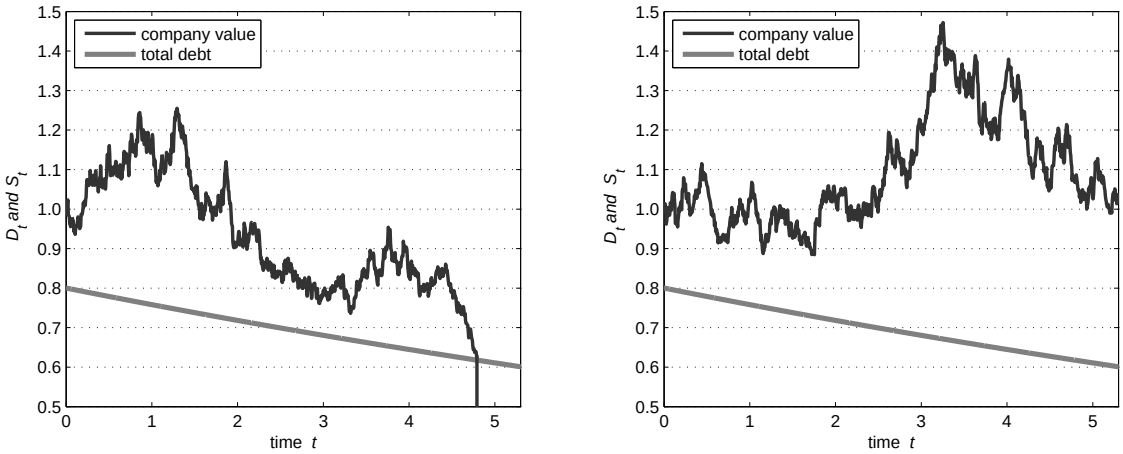

Figure 1.3: Concept of a structural default model*. A company defaults whenever its firm value (*black line*) hits the current face vale of debt (*grey line*).*

tion of the first-exit time probabilities. In *Section 2.5*, we finally deal with the most general model class captured in this thesis, namely regime switching jump-diffusion models. In this generality, the first-exit time probabilities cannot be solved analytically, instead one has to rely on numerical schemes. In this section, we extend an efficient and unbiased Monte–Carlo algorithm of Metwally and Atiya [2002] to regime switching parameters and to the case of two barriers. Finally, our results are compared to its numerical alternatives, for example finite elements schemes or brute–force Monte–Carlo simulations.

In *Chapter 3*, the theoretical results in *Chapter 2* are applied to the pricing of default-linked contracts in Finance and Insurance. First, *Section 3.1* discusses the pricing of barrier derivatives. The focus of this section is on derivatives that depend on whether or not certain thresholds are crossed during the lifetime of the contract (for example *(double) barrier options, digital options, (corridor) bonus certificates*). The results on time-changed Brownian motion have a nice interpretation in Mathematical Finance: The stochastic clock can be seen as a "measure of activity" or "business clock" and thus takes into account that calm markets with a low volatility alternate with periods of distress with a high volatility. Nevertheless, in order to not underestimate especially short term barrier hitting probabilities, it makes sense to further include jumps to the stock price processes (see, e.g., Giesecke [2006]). That is why, we adapt the Monte–Carlo algorithms described in *Chapter 2* to the pricing of financial contracts.

Our first-exit time setting can also be used to explain credit spreads. We apply the concept of structural credit risk models to the usually very risky asset class Private Equity (PE). The term "Private" stands for investments that are not listed on stock exchanges, that is why the main issue of this asset class is the scarcity of available data. Calculating risk indicators for PE-sponsored companies is considerably more difficult since – in contrast to public stocks – we rarely observe the company value. We provide a valuation model that explicitly accounts for the characteristics of PE (i.e. high leverage, high default risk, scarcity of data,...) and allows us to obtain implied risk measures. Within a cooperation with the *Center for Entrepreneurial and Financial Studies, Technische Universität München* (Prof. Dr. Dr. A.-K. Achleitner), we were able to test our results empirically on a unique PE database. This allowed us to examine the risk of PE transactions over time and to identify factors that determine the riskiness of a PE transaction.
Finally, *Section 3.3* gives a short note on applications of first-exit times in the insurance industry. Every insurance company has to ensure that its risk reserves are sufficient to cover the claims of all its policyholder. In the worst case, negative risk reserves lead to a default of the insurance company.

As discussed earlier in this introduction, it is important for the pricing and risk management of financial contracts to adequately model the dependence structure. *Chapter 4* introduces two possibilities on how to link the univariate processes from *Chapter 2*. The first one links them dynamically and thereby defines joint first-exit times. Unfortunately this approach is not very convenient from a numerical point of view: For high dimensions one usually has to rely on expensive numerical schemes.
The second one is a copula approach. Here, we abandon the economic interpretation of linked "trigger processes" and work with a fixed time horizon, i.e. the copula model is static with respect to time. However, this class is very tractable and works pretty well when calibrated to empirical data. We apply the copula approach to portfolio credit risk management and price loan-credit-default-swaps (LCDS) – an extension of credit-default-swaps (CDS) where the borrower is allowed to redeem the debt at any point in time.

The thesis concludes with a summary of the main results and an acknowledgment.

To summarize, the main contributions of this thesis are threefold:

- We present analytic expressions for the two-sided first-exit times of continuously time-changed Brownian motion extending single barrier results by, for example, Kammer [2007], Hurd [2009], and Hurd and Kuznetsov [2009]. From a numerical point of view the resulting expressions turn out to be more convenient than the Fourier integrals by Hurd [2009]. We show how these results can be used to price barrier derivatives (see **Hieber and Scherer [2012], Escobar et al. [2013]**).

- We extend the Brownian bridge algorithms of Metwally and Atiya [2002] to regime switching parameters and two barriers (see **Hieber and Scherer [2010], Fernández et al. [2013]**) and show how those algorithms can be adapted to price many exotic barrier derivatives.

- Finally, we show that – apart from barrier derivatives – our results have many interesting practical applications. Using a large and unique database on private equity transactions, we determine drivers of private equity sponsors' risk appetite (see **Braun et al. [2011]**). Furthermore, we propose a portfolio model to price loan-credit-default-swaps (LCDS) (see **Hieber and Scherer [2013]**).

Chapter 2

First-exit time probabilities

One- and two-sided exit problems for stochastic processes are classical mathematical problems with various applications in finance, engineering, biology, and physics. This chapter presents first-exit time probabilities for a large variety of stochastic processes. First, *Section 2.1* gives a historic overview on first-exit time results focusing on applications in Mathematical Finance.

2.1 Motivation and literature review

First-exit time problems first occurred in physics, sequential analysis, and statistics, for example to study irregularly moving particles (see, e.g., Schrödinger [1915], Darling and Siegert [1953], Feller [1966], Folks and Chhikara [1978]).

Presumably the first time that first-exit time problems were introduced to Mathematical Finance is the structural default model of Black and Cox [1976]. This seminal paper monitors a geometric Brownian motion as an "ability-to-pay" process continuously in time and controls whether it remains above a time-dependent default boundary. If the threshold is hit, i.e. if the company is unable to pay its obligations, the company defaults, an approach often referred to as *structural credit risk model*. For (geometric) Brownian motion, this approach yields an analytical first-exit time distribution, see also *Section 2.3*. Here, the probability of first hitting a lower (or an upper) threshold has extensively been treated in the literature. Analytical solutions exist for Brownian motion on constant (see, e.g., Darling and Siegert [1953], Geman and Yor [1996], Pelsser [2000]), on linear (see, e.g., Kunitomo and Ikeda [1992], Dominé [1996], Hall [1997]), or (at least in sufficient approximation) on any continuous (see, e.g., Novikov et al. [1999]) barriers. First-exit

time problems frequently appear in the area of option pricing – for instance – when barrier options are to be priced (see, e.g., Kunitomo and Ikeda [1992], Geman and Yor [1996], Bertoin [1998], Lin [1999], Pelsser [2000], Kyprianou [2000], Rogers [2000], Sepp [2004], and Hurd [2009]). For most stochastic processes a closed-form expression for the first-exit time probabilities is unknown. The aforementioned case of (geometric) Brownian motion is a convenient exception. However, financial modeling using (geometric) Brownian motion (the corresponding model is referred to as Black–Scholes model) is often criticized for its unrealistic simplicity. Thus, various extensions have been proposed:

- *Exponential Lévy models*: Lévy processes beyond Brownian motion are jump processes with stationary and independent increments. Many examples have been proposed in the literature, for example, CGMY, Variance Gamma, Normal inverse Gaussian, or the Kou model (see, among many others, Merton [1976], Kyprianou [2000], Cont and Tankov [2003]).

- *Stochastic volatility models*: In stochastic volatility models, volatility is a time-dependent stochastic process. Examples are regime switching models, the CEV, Heston, or Stein–Stein model (see, e.g., Jeanblanc et al. [2009]). A stochastic volatility can also be introduced by a stochastic time change (see, e.g., Geman et al. [2000], Carr and Wu [2004], Hurd [2009]).

- *Sato models*: A possibility to extend Lévy models to inhomogeneous increments are Sato models (see, e.g., Sato [1991], Carr et al. [2007]).

In this thesis, we mainly work with exponential Lévy models and with stochastic volatility models relying on a stochastic time change. To this end, as a first step, we replace calendar time by some suitably increasing stochastic process and show how several first-exit time results can be generalized to the situation of a continuous time shift (see, e.g., Kammer [2007], Hurd [2009], Hieber and Scherer [2012]). In financial applications, the interpretation of such a time change is a "business clock" or a "measure of economic activity". Clark [1973] gave the following motivation: *"The different evolutions of price series on different days is due to the fact that information is available to traders at a varying rate. On days when no new information is available, trading is slow, and the price process evolves slowly. On days when new information violates old expectations, trading is brisk, and the price process evolves much faster"*. Geman et al. [2000] examine time series empirically and show that a time change represents a measure of trading activity. There exist a large variety of different parameterizations for the "business clock", for example, integrated basic affine or shot-noise type processes. For such a specification, the first-exit

time probabilities turn out to be infinite series of functionals of the Laplace transform of the time change. Those series are easy to implement and allow for a straightforward error control. In contrast to Fourier integrals (see, e.g., Hurd [2009]), we avoid possibly oscillating integrals on the complex plane. Furthermore, a numerical implementation of the series turns out to be significantly faster than Fourier techniques.

However, a continuous time shift leads to continuous asset processes and thus cannot explain several empirical observations concerning market returns and its underlying derivative's prices (see the discussions in, e.g., Chahal and Wang [1997], Das [2002], Cont and Tankov [2003], Jarrow and Protter [2004]). For example, when used as firm-value process in structural credit risk models, continuous diffusion implies vanishing credit spreads for short-dated bonds/CDS (see, e.g., Jones et al. [1984], Giesecke [2006]).

That motivates why, in a second step, we consider jump-diffusion processes. The first-exit time of jump-diffusions, however, is mathematically challenging. In rare cases, at least the Laplace transforms of the first-exit times are available. This is the case if the jump size distribution is phase-type, if it, for example, follows a single- or double-exponential distribution (see, e.g., Boyarchenko and Levendorskiĭ [2002], Kou and Wang [2003]), or if the jump size distribution is a spectrally one-sided Lévy process (see, e.g., Rogers [2000]). Those results can often be extended to two barriers, for example, in the double-exponential jump-diffusion model, see Sepp [2004]. For arbitrary jump-size distributions or extensions like, for example, state-dependent drift, volatility, and jump size, state of art is to rely on numerical schemes. The most frequent approaches are recalled in the following:

- *Wiener–Hopf factorization*: The Laplace transform of the first-exit time probabilities can numerically be computed using the so-called Wiener-Hopf factorization (see, e.g., Kyprianou [2000], Boyarchenko and Levendorskiĭ [2002], Boyarchenko and Levendorskiĭ [2012], Mijatović and Pistorius [2013], and the references therein).

- *PIDE techniques*: First-exit time problems result in partial integro-differential equations (PIDEs) that can be solved numerically (see, e.g., Cont and Voltchkova [2005], Hilber et al. [2013] and the references therein).

- *Monte–Carlo simulation*: Another strand of literature focuses on Monte–Carlo techniques. The straightforward approach of a (brute-force) simulation on a discrete grid has been extended or improved (see, e.g., Metwally and Atiya [2002], Giesecke and Smelov [2011], Figueroa-López and Tankov [2012], and many others).

(Brute-force) Monte–Carlo simulations exhibit two disadvantages (see, e.g., Zhou [2001a], Platen and Bruti-Liberati [2010]): First, even for a daily grid, we obtain a significant

discretization bias. Second, computation time increases rapidly if one has to simulate on a fine grid. However, there are ways to remove or reduce this bias, especially for jump-diffusion models. Figueroa-López and Tankov [2012] develop an adaptive discretization scheme for the simulation of functionals of killed Lévy processes with controlled bias. Giesecke and Smelov [2011] present an unbiased sampling algorithm applying a technique called "acceptance/rejection" (see, e.g., von Neumann [1951]). Metwally and Atiya [2002] provide an unbiased, fast, and accurate alternative based on the so-called "Brownian bridge technique". Since the latter approach is one of the main topics of this thesis it is explained in more detail. In Brownian bridge algorithms, one proceeds as follows: First, the jump-instants of the process as well as the process immediately before and after the jump times are simulated. In between these generated points, one has a pure diffusion with fixed endpoints. Here, the so-called Brownian bridge probabilities provide an analytical expression for the first-exit time on a given threshold. This simulation technique turns out to be (1) unbiased and (2) significantly faster than the brute-force Monte–Carlo simulation. It has various applications in finance and can, for example, be used to derive efficient algorithms for pricing single barrier options in jump-diffusion models (see, e.g., Metwally and Atiya [2002], Ruf and Scherer [2011]) or regime-switching models (see, e.g., Hieber and Scherer [2010], Henriksen [2011]).

An extension of the Brownian bridge algorithms to two barriers is possible and has been considered in, e.g., Shevchenko [2003], Gobet [2009]. We further exploit their ideas mainly concentrating on three aspects: (1) We extend the model by a regime switching component, i.e. the diffusion can now switch between a finite number of states with distinct mean and volatility. This allows us to depart from the assumption of independent increments in Lévy models. (2) We are able to compute not only the first-exit time probabilities, but also expectations of arbitrary functionals of the first-exit time. (3) Apart from the barrier hitting probabilities, we also estimate the probability which one of the two barriers was hit first. The latter two features are important in many financial applications: In credit risk, the first-exit time (and not only the first-exit time probability) is vital to adequately model relevant payment streams. A second barrier allows to model – apart from default – a second exit event, i.e. an Initial Public Offering (IPO) or an early repayment of debt (see, e.g., Dobránszky and Schoutens [2008, 2009], Hieber and Scherer [2013]). For some exotic derivatives, for example corridor bonus certificates, the two thresholds trigger distinct events and have to be treated separately.

The remaining chapter is organized as follows: After introducing basic notation, various first-exit time results on Brownian motion are reviewed in *Section 2.3*. In *Section 2.4*, it is shown how those results can be extended to (continuously) time-changed Brownian motion providing error bounds and details on implementation. For more flexible processes, one

has to rely on numerical schemes: *Section 2.5* presents the Brownian bridge algorithms to estimate the first-exit time probabilities of regime switching jump-diffusions, extending results by Metwally and Atiya [2002], Shevchenko [2003], and Gobet [2009]. The chapter concludes by a numerical example, comparing different models and numerical techniques.

2.2 Definition and notation

Throughout, we work on the probability space $(\Omega, \mathcal{F}, \mathbb{P})$, supporting all required stochastic processes. We consider a stochastic process $B = \{B_t\}_{t\geq 0}$ with initial value $B_0 = 0$[1]. Assume that there are two constant barriers $b < B_0 = 0 < a$ and define the first-exit time

$$T_{ab} := \inf\{t \geq 0 \,:\, B_t \notin (b, a)\}\,, \tag{2.1}$$

where $\inf\{\emptyset\}=\infty$, $T_{ab}^{+} := \{T_{ab} \,|\, T_{ab} = T_{a,-\infty}\}$, $T_{ab}^{-} := \infty$ if $B_{T_{ab}} \geq a$ and $T_{ab}^{+} := \infty$, $T_{ab}^{-} := \{T_{ab} \,|\, T_{ab} = T_{\infty,b}\}$ if $B_{T_{ab}} \leq b$, i.e. if the lower barrier b is hit first, the first-exit time is $T_{ab} = T_{ab}^{-}$; if the upper barrier a is hit first, the first-exit time is $T_{ab} = T_{ab}^{+}$. Theorems, lemmas, and algorithms in this chapter focus on the upper barrier first-exit

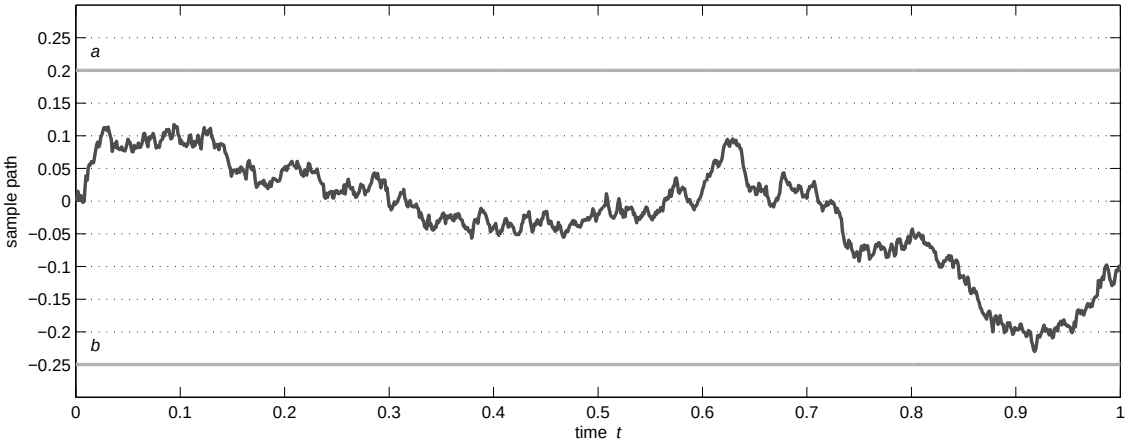

Figure 2.1: Continuous sample path $B = \{B_t\}_{0\leq t\leq 1}$ together with the two constant barriers $b < B_0 = 0 < a$. In this example, the path stays within the corridor $(b, a) = (-0.25, 0.20)$.

time T_{ab}^{+}. By symmetry (in the case of Brownian motion, one for example has to reverse the signs of a, b, μ, and B_0), the results can (in most cases) similarly be derived for T_{ab}^{-}. To demonstrate the first-exit time setting, a sample path together with the two barriers a

[1] If one is interested in the first-exit time of a process $\tilde{B}$ with $\tilde{B}_0 := x \neq 0$ on two constant barriers $\tilde{b} < x < \tilde{a}$, the results in this chapter are still valid if $B_t = \tilde{B}_t - x$ for all $t \geq 0$, $a = \tilde{a} - x$, and $b = \tilde{b} - x$.

and b is given in *Figure 2.1.* In the following, we want to derive first-exit time probabilities for different stochastic processes B on the finite interval $[0, T]$, where $T < \infty$.

2.3 Brownian motion

The simplest model is a Brownian motion with drift, i.e. the process B satisfies the stochastic differential equation (sde) $dB_t = \mu\, dt + \sigma dW_t$, where $W = \{W_t\}_{t\geq 0}$ is a standard Brownian motion, i.e. B has constant drift $\mu \in \mathbb{R}$ and volatility $\sigma > 0$.

2.3.1 First-exit time probabilities

The single barrier first-exit time probability is originally due to Schrödinger [1915], a review is given in Folks and Chhikara [1978]. Lemma 1 recalls this well–known result.

Lemma 1 (Exit time probability for a Brownian motion with drift)
Consider a time to maturity $T < \infty$ and a Brownian motion B with $B_0 = 0$, drift $\mu \in \mathbb{R}$, and volatility $\sigma > 0$. The first-exit time probability on a constant upper barrier $a > B_0 = 0$ is given by

$$\mathbb{P}(T_{a,-\infty} \leq T) = \Phi\left(\frac{-a+\mu T}{\sigma\sqrt{T}}\right) + \exp\left(\frac{2\mu a}{\sigma^2}\right)\Phi\left(\frac{-a-\mu T}{\sigma\sqrt{T}}\right), \tag{2.2}$$

where $\Phi(\,\cdot\,)$ denotes the standard normal cumulative distribution function.

Lemma 2 extends this result to two barriers, see also Darling and Siegert [1953]. In the literature, two parameterizations of those first-exit time probabilities are used, displayed as representation (a) and (b) in Lemma 2. The connection between the two is possible by the *Jacobi transformation formula* (see, e.g., Fernández et al. [2013]).

Lemma 2 (Double exit time probabilities for a Brownian motion with drift)
Consider a time to maturity $T < \infty$ and a Brownian motion B with $B_0 = 0$, drift $\mu \in \mathbb{R}$, and volatility $\sigma > 0$. Then, there are two representations known for the first-exit time probabilities on two constant barriers $b < B_0 = 0 < a$.

Representation (a):

$$\begin{aligned}\mathbb{P}(T_{ab}^{+} \leq T) = \sum_{n=1}^{\infty}\Bigg[&\exp\Big(-\frac{\mu}{\sigma^2}k_{n-1}\Big)\Phi\left(\frac{\mu T - k_{n-1} - a}{\sigma\sqrt{T}}\right)\\ &- \exp\Big(-\frac{\mu}{\sigma^2}(k_n - a)\Big)\Phi\left(\frac{\mu T - k_n + a}{\sigma\sqrt{T}}\right)\Bigg]\\ + \sum_{n=1}^{\infty}\Bigg[&\exp\Big(\frac{\mu}{\sigma^2}(k_n + b)\Big)\Phi\left(\frac{-\mu T - k_{n-1} - a}{\sigma\sqrt{T}}\right) - \exp\Big(\frac{\mu}{\sigma^2}k_n\Big)\Phi\left(\frac{-\mu T - k_n + a}{\sigma\sqrt{T}}\right)\Bigg],\end{aligned}$$

$$\mathbb{P}(T_{ab} \le T) = \sum_{n=-\infty}^{\infty} \exp\Big(\frac{\mu}{\sigma^2}k_n\Big)\left[\Phi\left(\frac{\mu T + k_n - a}{\sigma\sqrt{T}}\right) - \Phi\left(\frac{\mu T + k_n - b}{\sigma\sqrt{T}}\right)\right]$$
$$+ \exp\Big(\frac{\mu}{\sigma^2}(k_n - a)\Big)\left[\Phi\left(\frac{\mu T - k_n + a}{\sigma\sqrt{T}}\right) - \Phi\left(\frac{\mu T - k_{n-1} + b}{\sigma\sqrt{T}}\right)\right],$$

where $k_n := 2n(a-b)$ *and the standard normal cumulative distribution function is denoted* $\Phi(\,\cdot\,)$.

Representation (b):[2]

$$\mathbb{P}(T_{ab}^{+} \le T) = \frac{\exp\big(-\frac{2\mu b}{\sigma^2}\big) - 1}{\exp\big(-\frac{2\mu b}{\sigma^2}\big) - \exp\big(-\frac{2\mu a}{\sigma^2}\big)} + \exp\Big(\frac{\mu a}{\sigma^2}\Big)K_T^{\infty}(b), \tag{2.3}$$

$$\mathbb{P}(T_{ab} \le T) = 1 - \Big(\exp\Big(\frac{\mu b}{\sigma^2}\Big)K_T^{\infty}(a) - \exp\Big(\frac{\mu a}{\sigma^2}\Big)K_T^{\infty}(b)\Big), \tag{2.4}$$

where

$$K_T^N(k) := \frac{\sigma^2\pi}{(a-b)^2}\sum_{n=1}^{N}\frac{n(-1)^{n+1}}{\frac{\mu^2}{2\sigma^2} + \frac{\sigma^2 n^2\pi^2}{2(a-b)^2}}\ \exp\left(-\left(\frac{\mu^2}{2\sigma^2} + \frac{\sigma^2 n^2\pi^2}{2(a-b)^2}\right)T\right)\sin\left(\frac{n\pi k}{a-b}\right).$$

Proof. A proof of representation (a) is provided in Lin [1999], see also *Appendix A.2*.

To obtain representation (b), denote by $f_{ab}^{+}(t)$, $f_{ab}^{-}(t)$, and $f_{ab}(t)$ the first-exit time intensities[3] corresponding to T_{ab}^{+}, T_{ab}^{-}, and T_{ab}. Their Laplace transforms $\hat{f}_{ab}(\lambda) := \int_0^{\infty}\exp(-\lambda t)f_{ab}(t)dt$ are derived in Darling and Siegert [1953] as

$$\hat{f}_{ab}^{+}(\lambda) = \exp\Big(\frac{\mu a}{\sigma^2}\Big)\frac{\sinh\Big(\frac{\sqrt{\mu^2+2\sigma^2\lambda}}{\sigma^2}b\Big)}{\sinh\Big(\frac{\sqrt{\mu^2+2\sigma^2\lambda}}{\sigma^2}(b-a)\Big)},\ \hat{f}_{ab}^{-}(\lambda) = -\hat{f}_{ba}^{+}(\lambda).$$

From Laplace inversion tables, e.g. Oberhettinger and Badii [1973], p. 295, one obtains

$$\mathcal{L}^{-1}\big[f_{ab}^{+}\big](t) = \frac{\sigma^2\pi}{(a-b)^2}\sum_{n=1}^{\infty}n(-1)^n\exp\left(\frac{\mu a}{\sigma^2} - \Big(\frac{\mu^2}{2\sigma^2} + \frac{\sigma^2 n^2\pi^2}{2(a-b)^2}\Big)t\right)\sin\Big(\frac{n\pi b}{a-b}\Big).$$

Then, the first-exit time probability is $\mathbb{P}(T_{ab}^{+} \le T) = \int_0^T f_{ab}^{+}(t)dt$. To simplify this expression, one can use the identity $\sinh(kx) = \frac{2}{\pi}\sinh(k\pi)\sum_{n=1}^{\infty}\frac{(-1)^{n+1}n}{n^2+k^2}\sin(nx)$ (see, e.g.,

[2] For $\mu = 0$, the first term in Equation (2.3) has to be replaced by $\lim_{\mu\to 0}\frac{\exp\left(-\frac{2\mu b}{\sigma^2}\right)-1}{\exp\left(-\frac{2\mu b}{\sigma^2}\right)-\exp\left(-\frac{2\mu a}{\sigma^2}\right)} = -\frac{b}{a-b}$.

[3] Note that we use the term "intensities" instead of "densities", since there is a non-zero probability that the upper, respectively lower, barrier is not hit.

Rottmann [2008], p. 126). If we set $x = \pi b/(a-b)$, $k = \pm(a-b)\mu/(\pi\sigma^2)$, and use that $\sinh(-y) = -\sinh(y)$ for all $y \in \mathbb{R}$, we find that

$$\exp\Big(\frac{\mu a}{\sigma^2}\Big)\frac{\pi\sigma^2}{(a-b)^2}\sum_{n=1}^{\infty}\frac{(-1)^{n+1}n}{\frac{\mu^2}{2\sigma^2}+\frac{\sigma^2 n^2\pi^2}{2(a-b)^2}}\sin\Big(\frac{n\pi b}{a-b}\Big)$$
$$= \exp\Big(\frac{\mu a}{\sigma^2}\Big)\frac{\sinh\Big(-\frac{b\mu}{\sigma^2}\Big)}{\sinh\Big(\frac{(b-a)\mu}{\sigma^2}\Big)} = \frac{1-\exp\big(-\frac{2\mu b}{\sigma^2}\big)}{\exp\big(-\frac{2\mu b}{\sigma^2}\big)-\exp\big(-\frac{2\mu a}{\sigma^2}\big)}.$$

Similarly, $\mathbb{P}(T_{ab}^- \le T)$ can be derived. The expression for $\mathbb{P}(T_{ab}^+ \le T) + \mathbb{P}(T_{ab}^- \le T) = \mathbb{P}(T_{ab} \le T)$ is also displayed in Darling and Siegert [1953][4] and in Dominé [1996].

□

2.3.2 Brownian bridge probabilities

Due to its convenient mathematical structure, Brownian motion is analytically very tractable. Consequently, we aim at exploiting this tractability for more complicated processes. For this purpose, we need so-called Brownian bridges that later constitute a major part of the Brownian bridge algorithms in *Section 2.5*. Therefore, consider a fixed time interval (t_{i-1}, t_i), where $0 \le t_{i-1} < t_i < \infty$, $i \in \mathbb{N}$. Define, conditional on the path values at the edges of this time interval, i.e. $B_{t_{i-1}} =: x_{i-1} \in (b,a)$ and $B_{t_i} =: x_i$, Brownian bridge probabilities

$$BB_{ab}^+(t_{i-1}, t_i, x_{i-1}, x_i) := \mathbb{P}\big(t_{i-1} < T_{ab}^+ < t_i \,|\, B_{t_{i-1}} = x_{i-1},\, B_{t_i} = x_i\big), \tag{2.5}$$

$$BB_{ab}^-(t_{i-1}, t_i, x_{i-1}, x_i) := \mathbb{P}\big(t_{i-1} < T_{ab}^- < t_i \,|\, B_{t_{i-1}} = x_{i-1},\, B_{t_i} = x_i\big), \tag{2.6}$$

$$BB_{ab}(t_{i-1}, t_i, x_{i-1}, x_i) := BB_{ab}^+(t_{i-1}, t_i, x_{i-1}, x_i) + BB_{ab}^-(t_{i-1}, t_i, x_{i-1}, x_i). \tag{2.7}$$

For $x_{i-1} \notin (b,a)$, we set $BB_{ab}^+(t_{i-1}, t_i, x_{i-1}, x_i) = BB_{ab}^-(t_{i-1}, t_i, x_{i-1}, x_i) = 0$. In the single barrier case, the Brownian bridge probabilities are surprisingly simple. We find that (see, e.g., Jeanblanc et al. [2009], p. 240)

$$\lim_{b\to-\infty} BB_{ab}(t_{i-1}, t_i, x_{i-1}, x_i) = \begin{cases} \exp\Big(-\frac{2(x_{i-1}-a)(x_i-a)}{\sigma^2(t_i-t_{i-1})}\Big), & \max(x_i, x_{i-1}) < a, \\ 1, & \text{else.} \end{cases} \tag{2.8}$$

As in the case of the unconditional first-exit time probabilities, the extension to two barriers yields rapidly sloping infinite series. Again, we provide two different representations for

[4] Note that the expression in Darling and Siegert [1953], p. 633, contains two typos: π^2 has to be replaced by π and $(-1)^n$ by $(-1)^{n+1}$.

the probabilities. Representation (a) refers to Anderson [1960]; representation (b) to, e.g., Cox and Miller [1965]. The Brownian bridge probabilities for two barriers are presented in Theorem 1.

Theorem 1 (Brownian bridge probabilities)
Consider a time interval (t_{i-1}, t_i), where $0 \leq t_{i-1} < t_i < \infty$, and a Brownian motion B_t with volatility $\sigma > 0$. Assume that $x_{i-1} := B_{t_{i-1}} \in (b, a)$. Then, there are two representations for the Brownian bridge probabilities on two constant barriers $b < B_0 < a$.

Representation (a):

For $x_i := B_{t_i} \in (b, a)$ we get

$$BB_{ab}(t_{i-1}, t_i, x_{i-1}, x_i) = \sum_{n=-\infty}^{\infty} \left[\exp\left(-\frac{2n(a-b)}{\sigma^2(t_i - t_{i-1})} \big(x_{i-1} - x_i + n(a-b)\big) \right) + \exp\left(-\frac{2\big(x_i - na + (n-1)b\big)\big(x_{i-1} - na + (n-1)b\big)}{\sigma^2(t_i - t_{i-1})} \right) \right] - 1. \tag{2.9}$$

If $x_i := B_{t_i} \in (-\infty, a)$,

$$BB^{+}_{ab}(t_{i-1}, t_i, x_{i-1}, x_i) = \sum_{n=1}^{\infty} \left[\exp\left(-\frac{2\big(x_{i-1} - na + (n-1)b\big)\big(x_i - na + (n-1)b\big)}{\sigma^2(t_i - t_{i-1})} \right) - \exp\left(-\frac{2n(a-b)}{\sigma^2(t_i - t_{i-1})} \big(x_{i-1} - x_i + n(a-b)\big) \right) \right]. \tag{2.10}$$

Representation (b):

For $x_i := B_{t_i} \in (b, a)$ we find that

$$BB_{ab}(t_{i-1}, t_i, x_{i-1}, x_i) := 1 - \frac{2\sqrt{2\pi}\sigma\sqrt{t_i - t_{i-1}}}{a-b} \exp\left(\frac{(x_i - x_{i-1})^2}{2\sigma^2(t_i - t_{i-1})} \right) \cdot \sum_{n=1}^{\infty} \exp\left(-\frac{n^2\pi^2\sigma^2}{2(a-b)^2}(t_i - t_{i-1}) \right) \sin\Big(\frac{n\pi(x_{i-1} - b)}{a-b}\Big) \sin\Big(\frac{n\pi(x_i - b)}{a-b}\Big). \tag{2.11}$$

If $x_i := B_{t_i} \notin (b, a)$, one of the barriers was hit for sure, i.e. $BB_{ab}(t_{i-1}, t_i, x_{i-1}, x_i) = 1$.

If $x_i > a$, the probability of hitting the level a first is

$$BB^{+}_{ab}(t_{i-1}, t_i, x_{i-1}, x_i) := 1 - BB^{+}_{-b\,-a}(t_{i-1}, t_i, -x_{i-1}, -x_i). \tag{2.12}$$

Proof. For a proof of representation (a), we refer to Anderson [1960]. In a sometimes more convenient notation the formulas are displayed in Novikov et al. [1999], Remark 2. For a proof of the expression $BB_{ab}(t_{i-1}, t_i, x_{i-1}, x_i)$, see, e.g., Geman and Yor [1996]. The connection to the first-exit time probabilities is given in, e.g., Fernández et al. [2013].

Representation (b) is to be found in, e.g., Cox and Miller [1965], Pelsser [2000]. □

In some applications, we are not only interested in the (conditional) first-exit time probabilities, but also in the time $t_{i-1} < t < t_i$ this first exit event takes place. Therefore, we denote Brownian bridge first-exit time intensities[5] by

$$g^+_{ab}(t, x_{i-1}, x_i) := \mathbb{P}\big(T^+_{ab} \in dt \,|\, B_{t_{i-1}} = x_{i-1},\, B_{t_i} = x_i\big), \tag{2.13}$$

$$g^-_{ab}(t, x_{i-1}, x_i) := \mathbb{P}\big(T^-_{ab} \in dt \,|\, B_{t_{i-1}} = x_{i-1},\, B_{t_i} = x_i\big). \tag{2.14}$$

Figure 2.2 gives one numerical example. The intensities indicate the likelihood of a barrier crossing within the interval $(t_{i-1}, t_i) = (0, 5)$. In this example, we observe that this event is most likely during the first year $(0, 1)$.

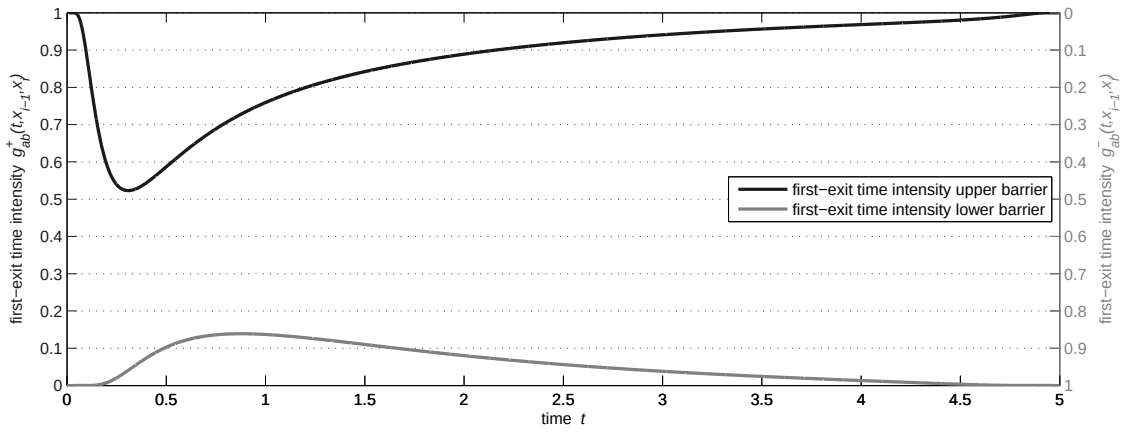

Figure 2.2: The first-exit time intensities $g^+_{ab}(t, x_{i-1}, x_i)$ and $g^-_{ab}(t, x_{i-1}, x_i)$ in the interval $(t_{i-1}, t_i) = (0, 5)$ using the parameters $x_{i-1} = x_i = 0$, $\sigma = 10\%$, upper barrier $a = \ln(1.10)$, and lower barrier $b = \ln(0.85)$.

Theorem 2 first presents the intensities on one barrier.

[5]Note that we use the term "intensities" instead of "densities", since there is a non-zero probability that the upper, respectively lower, barrier is not hit and thus $\int_{t_{i-1}}^{t_i} g^+_{ab}(t, x_{i-1}, x_i)\, dt \leq 1$.

Theorem 2 (First-exit time intensity I)
Consider a constant barrier $a > B_0 = 0$ and a Brownian bridge B_t with volatility $\sigma > 0$. Assume that $x_{i-1} := B_{t_{i-1}} < a$. For $x_i := B_{t_i}$ and $0 \leq t_{i-1} < t < t_i < \infty$ we get the Brownian bridge first-exit time intensity

$$g^+_{a,-\infty}(t, x_{i-1}, x_i) = \frac{a - x_{i-1}}{\sqrt{2\pi\sigma^2} y (t - t_{i-1})^{\frac{3}{2}} (t_i - t)^{\frac{1}{2}}} \exp\left(-\frac{(a - x_i)^2}{2(t_i - t)\sigma^2} - \frac{(a - x_{i-1})^2}{2(t - t_{i-1})\sigma^2} \right),$$

where $y = \exp\left(-\frac{(x_i - x_{i-1})^2}{2\sigma^2(t_i - t_{i-1})}\right) / \sqrt{t_i - t_{i-1}}$.

Proof. See, e.g., Feller [1966], Metwally and Atiya [2002], Ruf and Scherer [2011]. □

Adapting the main ideas by Feller [1966] and Metwally and Atiya [2002], it is possible to generalize Theorem 2 to two constant barriers $b < B_{t_{i-1}} < a$. Theorem 3 presents the resulting analytical expressions for $g^+_{ab}(t, x_{i-1}, x_i)$,

Theorem 3 (First-exit time intensity II)
Consider two constant barriers $b < B_0 < a$ and a Brownian motion B_t with volatility $\sigma > 0$. Assume that $x_{i-1} := B_{t_{i-1}} \in (b, a)$. For $x_i := B_{t_i}$ and $0 \leq t_{i-1} < t < t_i < \infty$ the Brownian bridge first-exit time intensity is given by

$$\begin{aligned} g^+_{ab}(t, x_{i-1}, x_i) = &\frac{\sigma^2 \pi}{(a-b)^2} \frac{\sqrt{t_i - t_{i-1}}}{\sqrt{t_i - t}} \exp\left(\frac{(x_i - x_{i-1})^2}{2\sigma^2(t_i - t_{i-1})} - \frac{(x_i - a)^2}{2\sigma^2(t_i - t)} \right) \\ &\cdot \sum_{n=1}^{\infty} (-1)^n n \exp\left(-\frac{\pi^2 n^2 \sigma^2}{2(a-b)^2} (t - t_{i-1}) \right) \sin\left(\frac{\pi n (b - x_{i-1})}{a - b} \right). \end{aligned} \tag{2.15}$$

Proof. See, e.g., Fernández et al. [2013]. □

2.4 Time-changed Brownian motion[6]

Brownian motion is a relatively simple model that enjoys a high level of analytical tractability. However, the underlying model assumptions of, for example, constant volatility are often not justified. One simple way to include a stochastic volatility is to introduce a stochastic time-scale, i.e. instead of $\{B_t\}_{t\geq 0}$, we consider $\{B_{\Lambda_t}\}_{t\geq 0}$ for a suitable time-change $\Lambda = \{\Lambda_t\}_{t\geq 0}$, independent of B. Λ is assumed to be a (pathwise) continuous and increasing stochastic process with $\Lambda_0 = 0$ and $\lim_{t\to\infty} \Lambda_t = \infty$ $\mathbb{P}$-a.s.. The model parameters are usually set such that on average we are back in the situation of Brownian motion, i.e. $\mathbb{E}[\Lambda_t] = t$.

Especially in the context of financial applications, this extension is frequently used for two reasons: (1) It is still analytically tractable, and (2) the time change allows for an economically reasonable interpretation as a measure of activity in an economy: On days when no new information is available, markets are calm and only slightly volatile. If, however, new and unexpected information arrives, markets move much faster (see, e.g., Clark [1973]). Several authors worked on first-exit time probabilities for time–changed Brownian motion on a single barrier. Overbeck and Schmidt [2005] treat the case of a deterministic and continuous time change. Kammer [2007] extends those results to stochastic and continuous time changes with known density. Time change densities, however, are rarely available as usually only the Laplace transform of the time change is known (see, e.g., the examples presented in *Section 2.4.2*). That motivates why Hurd [2009] presents the first-exit time probability on one barrier in terms of a Fourier integral.

We extend and improve those existing results in two aspects: First, in contrast to Overbeck and Schmidt [2005], Kammer [2007], and Hurd [2009], we present first-exit time probabilities on both an upper and a lower threshold. Second, instead of Fourier integrals, rapidly converging infinite series for the first-exit time probabilities are derived. Those series are straightforward to implement and allow for an easy error control. We show that those infinite series are numerically superior to Fourier integrals (see *Section 3.1.4*).

Time change models are frequently applied in Finance (see *Section 3.1.4*, *Chapter 3*). For specific parameterizations, it is possible to represent (special cases of) several well-known asset price models as a continuously time-changed Brownian motion. Some authors price barrier derivatives analytically for special cases of the stochastic volatility models of Heston (see, e.g., [Lipton, 2001, p. 235], Carr et al. [2003], Sepp [2006], Götz [2011], Kiesel and Lutz [2011], Escobar et al. [2011]) and Stein–Stein (see, e.g., Götz [2011]).

[6] This section is based on: Hieber, P. and Scherer, M. (2012): *A note on first-passage times of continuously time-changed Brownian motion*, Statistics and Probability Letters, Vol. 82, No. 1, pp. 165-172.

The remainder of this section is organized as follows: *Section 2.4.1* introduces the theoretical results on the first-exit times of time-changed Brownian motion. Several sample parameterizations for the time change are given in *Section 2.4.2*. Finally, error bounds to truncate the infinite series are presented in *Section 2.4.3*.

2.4.1 Theoretical results

The idea to approach exit problems for (continuously) time-changed Brownian motion is conceptually surprisingly simple. Conditioned on the time change Λ_T, we are back in the case of Brownian motion (with Λ_T as new maturity), a situation that was already solved. When we integrate out the distribution of Λ_T to obtain unconditional probabilities, we observe that the required quantities can be interpreted as functions of the Laplace transform of the time change Λ_T, for which we exploit the specific structure of representation (b) in Theorem 1. Fortunately, this Laplace transform is known for most popular specifications of Λ, see the examples in *Section 2.4.2*.

As a slight extension of Lemma 1, Theorem 4 presents first-exit time probabilities on a constant upper barrier a for a continuously time-changed Brownian motion; a result by Hurd [2009].

Theorem 4 (Exit time probability for a time-changed Brownian motion)
Consider a time-changed Brownian motion B_{Λ_t} with drift $\mu \in \mathbb{R}$, volatility $\sigma > 0$, initial value $B_0 = 0$, and a (pathwise) continuous time change Λ, independent of B. Denote the Laplace transform of Λ_T by $\vartheta_T(u) := \mathbb{E}[\exp(-u\Lambda_T)]$, $u \geq 0$. The first-exit time on a constant upper barrier $a > B_0 = 0$ is given by

$$\mathbb{P}(T_{a,-\infty} \leq T) = \frac{1 + \exp\left(\frac{2\mu a}{\sigma^2}\right)}{2} + \frac{2\exp\left(\frac{\mu a}{\sigma^2}\right)}{\pi} \operatorname{Re}\left[\int_0^\infty \frac{\sinh\left(\frac{\mu a}{\sigma^2} + iua\right)}{iu}\, \vartheta_T\Big(\frac{\sigma^2 u^2}{2} - iu\mu\Big)\, du\right]. \tag{2.16}$$

where $\operatorname{Re}(x + iy) = x$ denotes the real part of the complex number $x + iy$, $x, y \in \mathbb{R}$.

Proof. See, e.g., Hurd [2009]. □

This result can be extended to the case of two barriers, following an idea by Hieber and Scherer [2012]. The advantage of this result is the fact that one avoids the Fourier integral in Equation (2.16) and can instead rely on a rapidly converging infinite series. Error bounds to truncate this series are derived in *Section 2.4.3*.

Theorem 5 (Double exit time probabilities for a time-changed Brownian motion)
Consider a time-changed Brownian motion B_{Λ_t} with drift $\mu \in \mathbb{R}$, volatility $\sigma > 0$, initial value $B_0 = 0$, and a (pathwise) continuous time change Λ, independent of B. Denote the Laplace transform of Λ_T by $\vartheta_T(u) := \mathbb{E}[\exp(-u\Lambda_T)]$, $u \geq 0$. Then, we obtain the first-exit times on two constant barriers $b < B_0 = 0 < a$ as [7]

$$\mathbb{P}(T_{ab}^{+} \leq T) = \frac{\exp\left(-\frac{2\mu b}{\sigma^2}\right) - 1}{\exp\left(-\frac{2\mu b}{\sigma^2}\right) - \exp\left(-\frac{2\mu a}{\sigma^2}\right)} + \exp\left(\frac{\mu a}{\sigma^2}\right) K_{\Lambda_T}^{\infty}(b), \tag{2.17}$$

$$\mathbb{P}(T_{ab} \leq T) = 1 - \left(\exp\left(\frac{\mu b}{\sigma^2}\right) K_{\Lambda_T}^{\infty}(a) - \exp\left(\frac{\mu a}{\sigma^2}\right) K_{\Lambda_T}^{\infty}(b)\right), \tag{2.18}$$

where

$$K_{\Lambda_T}^{N}(k) := \frac{\sigma^2\pi}{(a-b)^2} \sum_{n=1}^{N} \frac{n(-1)^{n+1}}{\frac{\mu^2}{2\sigma^2} + \frac{\sigma^2 n^2 \pi^2}{2(a-b)^2}} \vartheta_T\left(\frac{\mu^2}{2\sigma^2} + \frac{\sigma^2 n^2 \pi^2}{2(a-b)^2}\right) \sin\left(\frac{n\pi k}{a-b}\right).$$

Proof. Recall from Lemma 2 the first-exit time probabilities of Brownian motion ($\Lambda_t \equiv t$). Then,

$$\begin{aligned} K_{\Lambda_T}^{\infty}(k) &= \mathbb{E}\Big[\mathbb{E}\big[K_{\tilde{T}}^{\infty}(k) \,\big|\, \tilde{T} = \Lambda_T\big]\Big] \\ &= \frac{\sigma^2\pi}{(a-b)^2} \sum_{n=1}^{\infty} \frac{n(-1)^{n+1}}{\frac{\mu^2}{2\sigma^2} + \frac{\sigma^2 n^2 \pi^2}{2(a-b)^2}} \mathbb{E}\left[\exp\left(-\left(\frac{\mu^2}{2\sigma^2} + \frac{\sigma^2 n^2 \pi^2}{2(a-b)^2}\right)\Lambda_T\right)\right] \sin\left(\frac{n\pi b}{a-b}\right) \\ &= \frac{\sigma^2\pi}{(a-b)^2} \sum_{n=1}^{\infty} \frac{n(-1)^{n+1}}{\frac{\mu^2}{2\sigma^2} + \frac{\pi^2 n^2 \sigma^2}{2(a-b)^2}} \vartheta_T\left(\frac{\mu^2}{2\sigma^2} + \frac{\pi^2 n^2 \sigma^2}{2(a-b)^2}\right) \sin\left(\frac{\pi n b}{a-b}\right). \end{aligned}$$

Note that the first equality holds for continuous time changes only; if there is a jump in time, one might not observe a barrier crossing (see Remark 1 and *Figure 2.3*). Hence, this theory does not generalize to Lévy subordinators. □

Remark 1 (Restriction to continuous time-transformations)
Note that Theorem 5 does not hold for discontinuous time-transformations, for example for Lévy subordinators. If there is a jump in the time transformation Λ, we do not observe the time-changed Brownian motion on the whole interval $[0, \Lambda_T]$, see also Figure 2.3. *Thus, the true barrier hitting probabilities in the case of a discontinuous time transformation are always lower than the expressions given in Theorem 5. To account for this issue of discontinuous time changes, Hurd [2009] introduces the term* **first-passage time of second kind** *that is in many applications also (economically) reasonable.*

[7] For $\mu = 0$, the first term in Equation (2.17) has to be replaced by $\lim_{\mu \to 0} \frac{\exp\left(-\frac{2\mu b}{\sigma^2}\right) - 1}{\exp\left(-\frac{2\mu b}{\sigma^2}\right) - \exp\left(-\frac{2\mu a}{\sigma^2}\right)} = -\frac{b}{a-b}$.

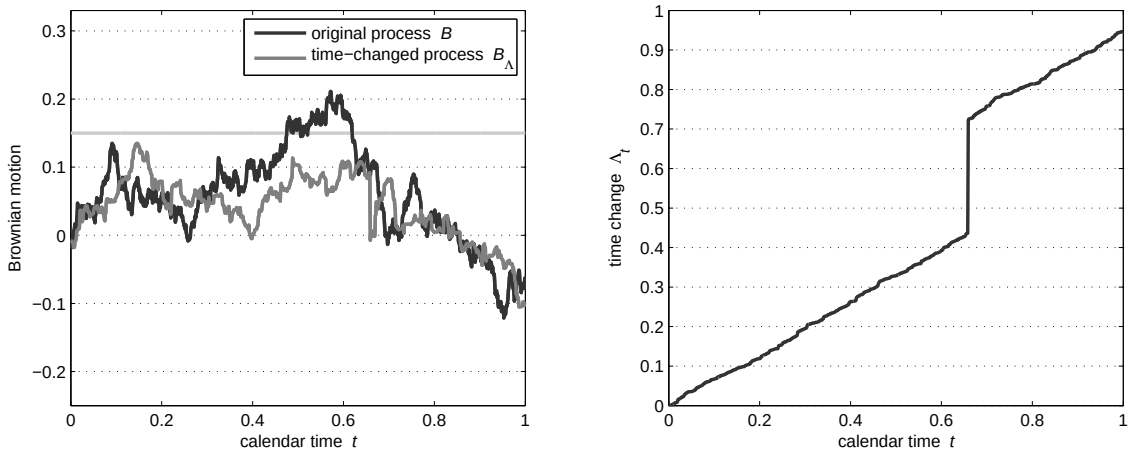

Figure 2.3: Example of a discontinuous time change. While the original process $\{B_t\}_{t\geq 0}$ (black) hits the barrier, the time-changed process $\{B_{\Lambda_t}\}_{t\geq 0}$ (grey) does not. This is not possible for continuous time changes; then barrier crossings are observed until time Λ_T.

2.4.2 Examples

Continuous time transformations can easily be constructed by integrating over a positive diffusion $\lambda = \{\lambda_t\}_{t\geq 0}$, i.e. $\Lambda_T := \int_0^T \lambda_t dt$, $T \geq 0$. Note that suitable models for the stochastic clock can also be constructed by combining two time changes $\Lambda_T^{(1)}$ and $\Lambda_T^{(2)}$, i.e. by addition $\Lambda_T^{(1)} + \Lambda_T^{(2)}$ or subordination $\Lambda^{(1)}_{\Lambda_T^{(2)}}$. We demonstrate the flexibility of this approach by four examples, including intensities of CIR-type (Example 1), OU-type (Example 2), shot-noise-type (Example 3), and regime-switching-type (Example 4).

Example 1 (CIR process)
A popular possibility to construct a continuous, stochastic time change is an integrated Cox-Ingersoll-Ross (CIR) process as introduced in, e.g., Duffie et al. [2000]. The CIR process is defined via the sde

$$d\lambda_t = \theta(\nu - \lambda_t)dt + \gamma\sqrt{\lambda_t}\, d\tilde{W}_t, \quad \lambda_0 > 0, \tag{2.19}$$

where θ, ν, and γ are non-negative constants, and $\{\tilde{W}_t\}_{t\geq 0}$ a one-dimensional Brownian motion. The Feller condition $2\theta\nu > \gamma^2$ guarantees that the process is almost surely positive, see Feller [1951]. The Laplace transform of $\Lambda_T := \int_0^T \lambda_t dt$ is given by (see, e.g., Cox et al. [1985], Dufresne [2001], Albrecher et al. [2007])

$$\vartheta_T^{CIR}(u) := \mathbb{E}\Big[\exp\Big(-u\int_0^T \lambda_t dt\Big)\Big] = \left(\frac{\exp(\theta T/2)}{\cosh(\varrho T)+\frac{\theta}{2\varrho}\sinh(\varrho T)}\right)^{\frac{2\theta\nu}{\gamma^2}} \exp\left(-\frac{\sinh(\varrho T)\,\lambda_0 u}{\varrho\cosh(\varrho T)+\frac{\theta}{2}\sinh(\varrho T)}\right), \quad (2.20)$$

where $\varrho := \frac{1}{2}\sqrt{\theta^2+2u\gamma^2}$. *Furthermore, there is an analytical expression for the average speed of the time change, i.e.*

$$\mathbb{E}[\Lambda_T] = \frac{\lambda_0}{\theta} - \frac{\nu}{\theta} + \nu T + \exp(-\theta T)\Big(-\frac{\lambda_0}{\theta}+\frac{\nu}{\theta}\Big). \quad (2.21)$$

As a generalization of the CIR process, λ *can be modeled as a basic affine process, see, e.g., Duffie et al. [2000]. This allows for an additional jump component of the intensity process. Note that the integrated intensity remains continuous in time and the Laplace transforms of the integrated intensity process are still known.*

Example 2 (OU process)
To guarantee the positiveness of λ, *we define an integrated Ornstein-Uhlenbeck (OU) process via* $\Lambda_T := \int_0^T \lambda_t dt$, $\lambda_t := \sigma_t^2$, *and*

$$d\sigma_t = \xi(\sigma_t - \varkappa)dt + k\,dW_t, \quad \sigma_0 > 0, \quad (2.22)$$

where ξ, $\varkappa$, *and* k *are positive constants;* $\{W_t\}_{t\geq 0}$ *a one-dimensional Brownian motion.* $\sigma = \{\sigma_t\}_{t\geq 0}$ *is an arithmetic Ornstein-Uhlenbeck process, with a tendency to revert back to a long-run average level of* $\varkappa$. *The Laplace transform of* $\Lambda_T := \int_0^T \lambda_t dt$ *is given by, see, e.g., Stein and Stein [1991]*

$$\vartheta_T^{OU}(u) := \mathbb{E}\Big[\exp\Big(-u\int_0^T \lambda_t dt\Big)\Big] = \exp\big(L(u)\lambda_0^2/2 + M(u)\lambda_0 + N(u)\big), \quad (2.23)$$

where the functions $L(u)$, $M(u)$, *and* $N(u)$ *are given in Appendix A.1. Furthermore*

$$\mathbb{E}[\Lambda_T] = \frac{1}{\xi}\Big[\big(\varkappa-\lambda_0\big)\big(1-\exp(-\theta T)\big) - \xi\varkappa T\Big]. \quad (2.24)$$

Example 3 (Shot-noise process)
Consider a shot-noise process[8] *as in Cox and Isham [1980], Dassios and Jang [2003]*

$$\lambda_t = \lambda_0\exp(-\delta t) + \sum_{s_i\leq t} M_i \exp\big(-\delta(t-s_i)\big),\ t\geq 0, \quad (2.25)$$

where $\lambda_0 > 0$ *is the initial intensity,* $\delta > 0$ *the exponential decay rate,* $\{s_i\}_{i\geq 1}$ *are the jump times of a time-homogeneous Poisson process with intensity* $\psi > 0$, *and* $M_i \sim Exp(\zeta)$ *are exponentially distributed jump sizes. The Laplace transform of the integrated process*

[8] Note that the presented model is not the most general definition of a shot-noise process. It is without difficulty possible to, for example, change the jump size distribution, see Dassios and Jang [2003].

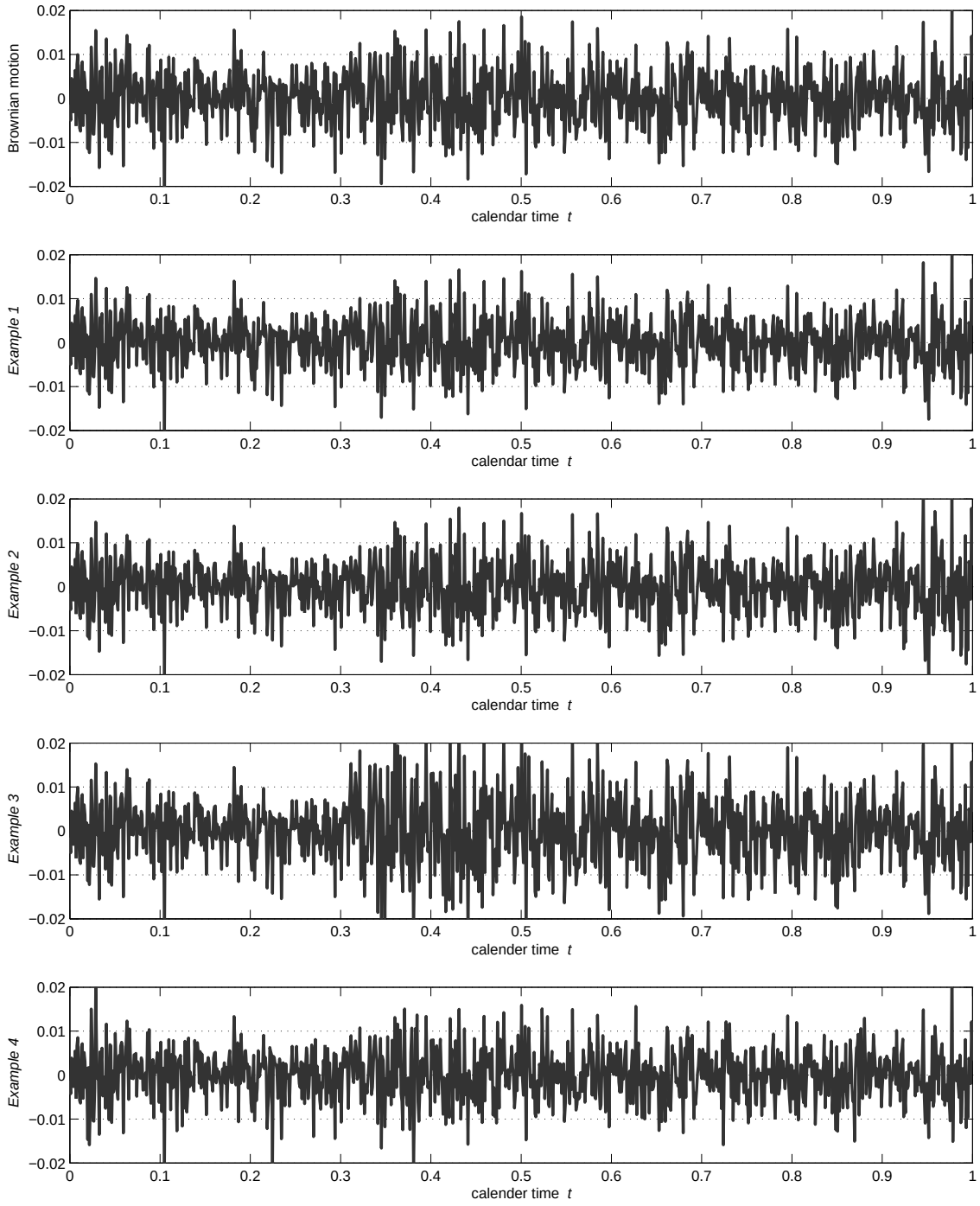

Figure 2.4: Sample innovations in the case of Brownian motion (above) compared to time-changed Brownian motion for a time change $\Lambda_T := \int_0^T \lambda_t dt$. *Intensities* λ *of CIR-type (second from above, Example 1), OU-type (third from above, Example 2), shot-noise-type (forth from above, Example 3), and Markov-switching-type (below, Example 4) are presented.*

$\Lambda_T := \int_0^T \lambda_t dt$ *is given by*[9]

$$\begin{aligned}\vartheta_T^{sn}(u) &:= \mathbb{E}\Big[\exp\Big(-u\int_0^T \lambda_t dt\Big)\Big] \\ &= \exp\left(-\frac{u\lambda_0}{\delta}\big(1-\exp(-\delta T)\big) - \psi T + \frac{\psi T + \frac{\psi}{\delta}\ln\Big(1+\frac{u}{\delta\zeta}\big(1-\exp(-\delta T)\big)\Big)}{1+\frac{u}{\delta\zeta}}\right). \quad (2.26)\end{aligned}$$

The average time change Λ_T *can be obtained as*

$$\mathbb{E}[\Lambda_T] = \Big(\frac{\lambda_0}{\delta} - \frac{\psi}{\delta^2\zeta}\Big)\big(1-\exp(-\delta T)\big) + \frac{\psi T}{\delta\zeta}\,. \quad (2.27)$$

Example 4 (Markov-switching model)
A very illustrative way to include stochastic volatility constitute so called Markov-switching models, proposed by Hamilton [1989]. Here, λ_t *is state dependent and can (only) take finitely many values. A continuous time Markov chain models the transition between those values. The continuous time change is then defined via* $\Lambda_T := \int_0^T \lambda_t dt$ *and*

$$\lambda_t = k_{Z_t}, \quad (2.28)$$

where $Z = \{Z_t\}_{t\geq 0}$, $Z_t \in \{1, 2, \ldots, M\}$, *is a time-homogeneous Markov chain. An intensity matrix* Q_0 *parameterizes the transition probabilities between the different states of the Markov chain and* $\pi := (\mathbb{P}(Z_0 = 1), \mathbb{P}(Z_0 = 2), \ldots)'$ *is the initial distribution on the states. Chapter 2.5 discusses those type of models in more detail. The Laplace transform of the time change is then given by (see, e.g., Buffington and Elliott [2002])*

$$\begin{aligned}\vartheta_T^{ms}(u) &:= \mathbb{E}\Big[\exp\Big(-u\int_0^T \lambda_t dt\Big)\Big] \\ &= \left\langle \exp\left(Q_0 T - u\begin{pmatrix} k_1^2 & 0 & 0 \\ 0 & k_2^2 & 0 \\ 0 & 0 & \ldots \end{pmatrix} T\right)\begin{pmatrix}\pi_1 \\ \pi_2 \\ \ldots\end{pmatrix}, \mathbf{1}\right\rangle. \quad (2.29)\end{aligned}$$

The average stochastic time change is

$$\mathbb{E}[\Lambda_T] = \left\langle \begin{pmatrix} k_1^2 & 0 & 0 \\ 0 & k_2^2 & 0 \\ 0 & 0 & \ldots \end{pmatrix} T\,\exp(Q_0 T)\begin{pmatrix}\pi_1 \\ \pi_2 \\ \ldots\end{pmatrix}, \mathbf{1}\right\rangle. \quad (2.30)$$

Figure 2.4 presents sample paths of return processes generated by time-changed Brownian motion $\{B_{\Lambda_t}\}_{t\geq 0}$. Innovations of Brownian motion (above) are compared to the different

[9] This Laplace transform can be obtained from Dassios and Jang [2003] by introducing exponential jump sizes $\hat{g}(u) = 1/(1+u/\zeta)$ in Equation (2.10), p. 79.

time change models (Examples 1–4). In the case of Brownian motion, return innovations are independent and identically distributed (i.i.d.), a feature of any Lévy model. In Examples 1–4, we are able to leave the class of Lévy models; return distributions are no longer i.i.d. but state-dependent. Here, one observes a stochastic volatility: Calm periods with a lower volatility alternate with more volatile periods.

There are many other examples of a continuous time change not covered in this thesis. Frequently used is the Hull-White model (see, e.g., Hull and White [1987]). This type of model also occurs as a continuous diffusion limit of GARCH models (see, e.g., Klüppelberg et al. [2004], Brockwell et al. [2006]). However, there is no explicit expression for the characteristic function.

Furthermore, rich volatility structures can be obtained by multi–factor models. An extension of Examples 1, 2, and 3 to multi–factor models is straightforward and will be considered in the application to option pricing, see *Section 3.1.1*.

2.4.3 Error bounds

To implement the probabilities in Lemma 2 and Theorem 5, the infinite series $K^{\infty}_{\Lambda_T}$ have to be approximated by finite series $K^{N}_{\Lambda_T}$. Theorem 6 presents corresponding error bounds if the Laplace transform of the time change is exponentially bounded, i.e. if $\vartheta_T(u) \leq J\exp(-Mu)$, where J, M are positive constants, and if the Laplace transform is bounded by $J^*\exp(-M^*\sqrt{u})$, where J^*, M^* are again positive constants. Then, it is possible to derive error bounds for all examples presented in *Section 2.4.2*.

Theorem 6 (Error bounds)
Define the (absolute) computation error of the first-exit time probability $\mathbb{P}(T_{ab} \leq T)$ by

$$\epsilon := \left| \mathbb{P}(T_{ab} \leq T) - \left(1 - \left(\exp\left(\frac{\mu b}{\sigma^2}\right) K^{N}_{\Lambda_T}(a) - \exp\left(\frac{\mu a}{\sigma^2}\right) K^{N}_{\Lambda_T}(b)\right)\right) \right|. \tag{2.31}$$

For a given precision $\epsilon > 0$, a lower bound for the summation index $N \in \mathbb{N}$ is required.

(a) If the Laplace transform of the time change is exponentially bounded, i.e. if $\vartheta_T(u) \leq J\exp(-Mu)$, where J, M are positive constants, we find that

$$N > \sqrt{-\frac{2(a-b)^2}{\pi^2\sigma^2 M}\left[\ln\left(\frac{\pi^3\sigma^2 M\epsilon}{4(a-b)^2 J}\right) - \frac{|\mu|\max\{|a|,|b|\}}{\sigma^2}\right]}. \tag{2.32}$$

(b) If $\vartheta_T(u) \leq J^*\exp(-M^*\sqrt{u})$, where $J^*, M^* > 0$ are positive constants, then

$$N > -\frac{\sqrt{2}(a-b)}{\pi\sigma M^*}\left[\ln\left(\frac{\pi^2\sigma M^*\epsilon}{4\sqrt{2}(a-b)J^*}\right) - \frac{|\mu|\max\{|a|,|b|\}}{\sigma^2}\right]. \tag{2.33}$$

Proof. For part (a), i.e. if $\vartheta_T(u) \leq J\exp(-Mu)$, where J, M are positive constants, we get from Equation (2.31)

$$\begin{aligned}
\epsilon &= \left|\exp\left(\frac{\mu b}{\sigma^2}\right)\left(K^{\infty}_{\Lambda_T}(a) - K^{N}_{\Lambda_T}(a)\right) - \exp\left(\frac{\mu a}{\sigma^2}\right)\left(K^{\infty}_{\Lambda_T}(b) - K^{N}_{\Lambda_T}(b)\right)\right| \\
&\overset{(*)}{\leq} \left|\left(\exp\left(\frac{\mu b}{\sigma^2}\right) + \exp\left(\frac{\mu a}{\sigma^2}\right)\right)\frac{\sigma^2\pi}{(a-b)^2}\sum_{n=N+1}^{\infty}\frac{n}{\frac{\sigma^2 n^2\pi^2}{2(a-b)^2}}\,\vartheta_T\left(\frac{\mu^2}{2\sigma^2} + \frac{\sigma^2 n^2\pi^2}{2(a-b)^2}\right)\right| \\
&\leq \left|\exp\left(\frac{|\mu|\max\{|a|,|b|\}}{\sigma^2}\right)\frac{4}{\pi}\sum_{n=N+1}^{\infty}\frac{1}{n}\,\vartheta_T\left(\frac{\sigma^2 n^2\pi^2}{2(a-b)^2}\right)\right| \\
&\leq \left|J\exp\left(\frac{|\mu|\max\{|a|,|b|\}}{\sigma^2}\right)\frac{4}{\pi}\int_N^{\infty}\frac{1}{n}\,\exp\left(-M\frac{\pi^2\sigma^2}{2(a-b)^2}n^2\right)dn\right| \\
&\leq \left|J\exp\left(\frac{|\mu|\max\{|a|,|b|\}}{\sigma^2}\right)\frac{4(a-b)^2}{\pi^3\sigma^2 M}\exp\left(-M\frac{\pi^2\sigma^2}{2(a-b)^2}N^2\right)\right|.
\end{aligned}$$

From this, a lower bound for the summation index N is obtained as

$$N > \sqrt{-\frac{2(a-b)^2}{\pi^2\sigma^2 M}\left[\ln\left(\frac{\pi^3\sigma^2 M\epsilon}{4(a-b)^2 J}\right) - \frac{|\mu|\max\{|a|,|b|\}}{\sigma^2}\right]}. \tag{2.34}$$

For part (b), if $\vartheta_T(u) \leq J^*\exp(-M^*\sqrt{u})$, where J^*, M^* are positive constants, we get analoguously

$$\begin{aligned}
\epsilon &\overset{(*)}{\leq} \left|J^*\exp\left(\frac{|\mu|\max\{|a|,|b|\}}{\sigma^2}\right)\frac{4}{\pi}\int_N^{\infty}\frac{1}{n}\,\exp\left(-M^*\frac{\pi\sigma}{\sqrt{2}(a-b)}n\right)dn\right| \\
&\leq \left|J^*\exp\left(\frac{|\mu|\max\{|a|,|b|\}}{\sigma^2}\right)\frac{4\sqrt{2}(a-b)}{\pi^2\sigma M^*}\exp\left(-M^*\frac{\pi\sigma}{\sqrt{2}(a-b)}N\right)\right|.
\end{aligned}$$

Then,

$$N > -\frac{\sqrt{2}(a-b)}{\pi\sigma M^*}\left[\ln\left(\frac{\pi^2\sigma M^*\epsilon}{4\sqrt{2}(a-b)J^*}\right) - \frac{|\mu|\max\{|a|,|b|\}}{\sigma^2}\right]. \tag{2.35}$$

The estimation $\overset{(*)}{\leq}$ is also an upper bound for the (absolute) computation error of the probabilities $\mathbb{P}(T^-_{ab} \leq T)$ and $\mathbb{P}(T^+_{ab} \leq T)$. Thus, the bounds in Equation (2.34), respectively Equation (2.35), can also be used to truncate the series representations of $\mathbb{P}(T^-_{ab} \leq T)$ and $\mathbb{P}(T^+_{ab} \leq T)$, see also Hieber and Scherer [2012]. □

Lemma 3 applies the results from Theorem 2.4.3 to the examples in *Section 2.4.2*, i.e. if the time change Λ is an integrated CIR process (Example 1), an integrated shot-noise process (Example 3), or an integrated regime-switching process (Example 4).

Lemma 3 (Truncating $K^{\infty}_{\Lambda_T}$)
Define the (absolute) computation error of $\mathbb{P}(T_{ab} \leq T)$ *by*

$$\epsilon := \left| \mathbb{P}(T_{ab} \leq T) - \left(1 - \left(\exp\left(\frac{\mu b}{\sigma^2}\right) K^N_{\Lambda_T}(a) - \exp\left(\frac{\mu a}{\sigma^2}\right) K^N_{\Lambda_T}(b) \right)\right) \right|. \tag{2.36}$$

To obtain a given precision $\epsilon > 0$*, a lower bound for the summation index* $N \in \mathbb{N}$ *is...*

(a) ...in the case of Brownian motion

$$N > \sqrt{-\frac{2(a-b)^2}{\pi^2\sigma^2 T}\left[\ln\left(\frac{\pi^3\sigma^2 T\epsilon}{4(a-b)^2}\right) - \frac{|\mu|\max\{|a|,|b|\}}{\sigma^2}\right]}. \tag{2.37}$$

(b) ...in Example 1, i.e. an integrated CIR process with parameters $(\theta, \nu, \gamma, \lambda_0)$

$$N > \frac{(a-b)}{\pi\sigma M^*}\left(\frac{|\mu|\max\{|a|,|b|\}}{\sigma^2} + \frac{\theta^2\nu T}{\gamma^2} - \ln\left(\frac{\epsilon\pi^2\sigma M^*}{4\sqrt{2}(a-b)}\right)\right), \tag{2.38}$$

where $M^* := \lambda_0\big(1 - \exp(-\sqrt{\theta^2 + 2\gamma^2}T)\big)/\sqrt{\theta^2 + 2\gamma^2}$.

(c) ...in Example 3, i.e. an integrated shot-noise process with parameters $(\delta, \zeta, \psi, \lambda_0)$

$$N > \sqrt{-\frac{2\delta(a-b)^2}{\pi^2\sigma^2\lambda_0 D^*}\left[\ln\left(\frac{\pi^3\sigma^2\lambda_0 D^*\epsilon}{4\delta(a-b)^2}\right) - \frac{|\mu|\max\{|a|,|b|\}}{\sigma^2}\right]}. \tag{2.39}$$

where $D^* := 1 - \exp(-\delta T)$.

(d) ...in Example 4, i.e. an integrated regime-switching process with parameters k_i*,* $i \in \{1, 2, \ldots, M\}$

$$N > \sqrt{-\frac{2(a-b)^2}{\pi^2\underline{\lambda}^2\sigma^2 T}\left[\ln\left(\frac{\pi^3\underline{\lambda}^2\sigma^2 T\epsilon}{4(a-b)^2}\right) - \frac{|\mu|\max\{|a|,|b|\}}{\sigma^2}\right]}. \tag{2.40}$$

where $\underline{\lambda} := \min_{i\in\{1,2,\ldots,M\}} k_i$.

The same lower bounds hold for the (absolute) computation error of $\mathbb{P}(T^+_{ab} \leq T)$ *and* $\mathbb{P}(T^-_{ab} \leq T)$.

Proof. Part (a): In the Gaussian case, i.e. $\Lambda_T = T$ and $\vartheta_T(u) = \exp(-uT)$, we set $M = T$, $J = 1$.

Part (b): If the time change is an integrated CIR process (Example 1), using that $\cosh(\varrho T/2) + \theta/\varrho \sinh(\varrho T/2) > \cosh(\varrho T/2) > 1$, $\exp(\varrho T/2) \geq \exp(-\varrho T/2)$, and $\theta/\varrho \leq 1$, we find that

$$\begin{aligned}
\vartheta_T^{CIR}(u) &= \left[\frac{\exp(\theta T/2)}{\cosh(\varrho T/2) + \frac{\theta}{\varrho}\sinh(\varrho T/2)}\right]^{\frac{2\theta\nu}{\gamma^2}} \exp\left(- u\frac{\lambda_0}{\varrho}\frac{2\sinh(\varrho T/2)}{\cosh(\varrho T/2) + \frac{\theta}{\varrho}\sinh(\varrho T/2)}\right) \\
&\leq \exp\left(\frac{\theta^2\nu T}{\gamma^2}\right) \exp\left(- u\frac{\lambda_0}{\sqrt{\theta^2 + 2u\gamma^2}}\big(1 - \exp\big(- \sqrt{\theta^2 + 2u\gamma^2}T\big)\big)\right) \\
&\leq \exp\left(\frac{\theta^2\nu T}{\gamma^2}\right) \exp\left(- \sqrt{u}\frac{\lambda_0}{\sqrt{\theta^2 + 2\gamma^2}}\big(1 - \exp\big(- \sqrt{\theta^2 + 2\gamma^2}T\big)\big)\right),
\end{aligned}$$

where the last inequality holds for $u \geq 1$. We can then apply Theorem 6(b) with $M^* = \lambda_0\big(1 - \exp(-\sqrt{\theta^2 + 2\gamma^2}T)\big)/\sqrt{\theta^2 + 2\gamma^2}$, $J^* = \exp\big(\theta^2\nu T/\gamma^2\big)$.

Part (c): If Λ is an integrated shot-noise process, we obtain

$$\vartheta_T^{sn}(u) \leq \exp\Big(- \frac{\lambda_0}{\delta}\big(1 - \exp(-\delta T)\big)u\Big),$$

since $\frac{\psi}{1+\frac{u}{\delta\zeta}}\Big(T + \frac{1}{\delta}\ln\big(1 + \frac{u}{\delta\zeta}\big(1 - \exp(-\delta T)\big)\big)\Big)$ is decreasing for $u \in [0, \infty)$. From this, we find that $M = \lambda_0\big(1 - \exp(-\delta T)\big)/\delta$, $J = 1$.

Part (d): For a regime switching volatility (Example 4), the Laplace transform of the time change Λ is bounded via

$$\begin{aligned}
\vartheta_T^{ms}(u) := \mathbb{E}\Big[\exp\Big(- u\int_0^T \lambda_t dt\Big)\Big] &\leq \exp\left(-u\int_0^T \min_{i\in\{1,2,\ldots,M\}} k_i^2\, dt\right) \\
&= \exp\left(-u \min_{i\in\{1,2,\ldots,M\}} k_i^2\, T\right).
\end{aligned}$$

□

2.5 Regime switching jump-diffusion model[10]

The advantage of the results in *Sections 2.3* and *2.4* is the fact that first-exit time probabilities can be computed analytically. The underlying model assumptions (i.e. continuous diffusion, independent increments) might, however, be unsatisfactory for many applications. In a structural credit risk model a continuous diffusion implies that firms cannot default unexpectedly (i.e. by surprise), see, e.g., Giesecke [2006]. If a company is not in distress, its short-term default probability is zero, therefore its short-term debt should have zero credit spreads. This assumption is questioned by empirical data: For example Jones et al. [1984] find that credit spreads on corporate bonds are generally too high to be matched by a structural credit risk model with continuous diffusion. Another questionable assumption are independent (and identically distributed) increments. On financial markets, one observes periods of distress with a persistently higher risk; subsequent daily returns tend to be dependent.

That is why, the quite general class of regime-switching jump diffusions is introduced in the following. Since analytical expressions in this general setting are unavailable, efficient and accurate numerical schemes to obtain the first-exit time probabilities are necessary. On the probability space $(\Omega, \mathcal{F}, \mathbb{P})$, regime-switching jump diffusions are defined via

$$dB_t = \mu_{Z_t}\, dt + \sigma_{Z_t}\, dW_t + Y_{N_t^{Z_t}}\, dN_t^{Z_t}, \tag{2.41}$$

where $Z = \{Z_t\}_{t\geq 0} \in \{1, 2, \ldots, M\}$ is a time-homogeneous Markov chain and $W = \{W_t\}_{t\geq 0}$ an independent standard Brownian motion. The parameters now depend on Z: Drift $\mu_{Z_t} \in \mathbb{R}$, volatility $\sigma_{Z_t} > 0$, and time in-homogeneous counting process $N^{Z_t} = \{N_t^{Z_t}\}_{t\geq 0}$, a Poisson process with intensity $\lambda_{Z_t} \geq 0$ at time t. The initial value is $B_0 = 0$; the jump-sizes $Y = \{Y_i\}_{i\geq 1}$ are independent and identically distributed (i.i.d.) with distribution $\mathbb{P}_Y$. All processes are mutually independent.

The Markov chain is described by an intensity matrix[11] Q_0. The entries $q_{ij} := Q_0(i, j)$ of this intensity matrix can easily be interpreted: The time spent in state i is exponentially distributed with intensity $-q_{ii} > 0$. If a state change from the current state i occurs, the probability of moving to state $j \neq i$ is $-q_{ij}/q_{ii} \geq 0$ (note that, since Q_0 is an intensity matrix, we have that $-\sum_{i\neq j} q_{ij} = q_{ii}$).

[10] Part of this section is based on the papers: Hieber, P. and Scherer, M. (2010): *Efficiently pricing barrier options in a Markov-switching framework*, Journal of Computational and Applied Mathematics, Vol. 235, pp. 679-685. and Fernández, L.; Hieber, P. and Scherer, M. (2013): *Double-barrier first-passage times of jump-diffusion processes*, Monte Carlo Methods and Applications, Vol. 19, No. 2, pp. 107–141.

[11] An intensity matrix has negative diagonal and non-negative off-diagonal entries. Each row sums up to zero.

In this type of model, it is usually difficult to derive analytical expressions for the first-exit time probability $\mathbb{P}\big(T_{ab} \leq T\big)$. In rare cases, however, at least a closed-form expression for the Laplace transform of the first-exit time, i.e.

$$\Psi_{ab}(u) := \mathbb{E}\left[\exp\big(-uT_{ab}\big)\right] \tag{2.42}$$

is available. This turned out to be possible in the case of exponential jump-diffusion models, i.e. if the jump-size distribution is either exponential or a mixture of exponential random variables. Examples include the Cramér-Lundberg model and single, double, and hyper-exponential jump-diffusion models (see, e.g., Mordecki [1999], Rogers [2000], Boyarchenko and Levendorskiĭ [2002], Mordecki [2002], Avram et al. [2003], Kou and Wang [2003], Asmussen et al. [2004], Lewis and Mordecki [2008], Cai [2009], Cai et al. [2009]). One explanation for the tractability of exponential jump-diffusions is the fact that exponential jumps can (up to a time change) be *embedded* in a continuous diffusion, namely a regime-switching model: Positive or negative exponential jumps are added as an additional state with zero volatility and positive, respectively negative, slope (a technique referred to as "*fluid embedding*", see, e.g., Asmussen et al. [2004], Jiang and Pistorius [2008]). Continuous diffusion models turn out to be more tractable than jump-diffusion models.

We present two popular examples where the Laplace transform of the first-exit time is still available, both are special cases of the regime-switching jump-diffusion model (2.41). First, Example 5 introduces the 2-state regime-switching model without jumps.

Example 5 (2-state regime-switching model without jumps)
In a 2-state world, i.e. $Z_t \in \{1, 2\}$ for all $t \geq 0$, the diffusion part of the process B is described by the intensity matrix Q_0 and two sets of parameters: (μ_1, σ_1) and (μ_2, σ_2), respectively. There are no jumps, i.e. the jump intensity λ is 0. One advantage of this simple extension of Brownian motion (where $Z_t \in \{1\}$ for all $t \geq 0$) is the fact that even a 2-state regime switching model can better capture empirically observed phenomena, see, for example, Timmermann [2000], Hardy [2001], Fuh et al. [2003]. The Laplace transform of the first-exit time in a 2-state regime switching model was originally derived by Guo [2001]; in a much more general setting a semi-analytical expression is presented by Jiang and Pistorius [2008].

Due to its tractability, the double-exponential jump-diffusion model is frequently used in academia. Example 6 introduces this model class together with the Laplace transform of the first-exit time as derived in Kou and Wang [2003], Kou et al. [2005]. In this type of model, mean μ_{Z_t} and volatility σ_{Z_t} are constant, i.e. $Z_t = 1$ for all $t \geq 0$.

Example 6 (Double-exponential jump-diffusion)
One popular possibility to model jump sizes is the double-exponential distribution, see, e.g., Kou and Wang [2003]:

$$\mathbb{P}_Y(dx) = p\,\alpha_\oplus e^{-\alpha_\oplus x}\,\mathbb{1}_{\{x\geq 0\}}dx + (1-p)\,\alpha_\ominus e^{\alpha_\ominus x}\,\mathbb{1}_{\{x<0\}}dx, \tag{2.43}$$

where $0 \leq p \leq 1$ is the probability that a jump has positive sign. Upward jumps are exponentially distributed with parameter $\alpha_\oplus > 1$, downward jumps are exponentially distributed with parameter $\alpha_\ominus > 0$. Figure 2.5 *gives one year of daily sample innovations in a double-exponential jump-diffusion model.*

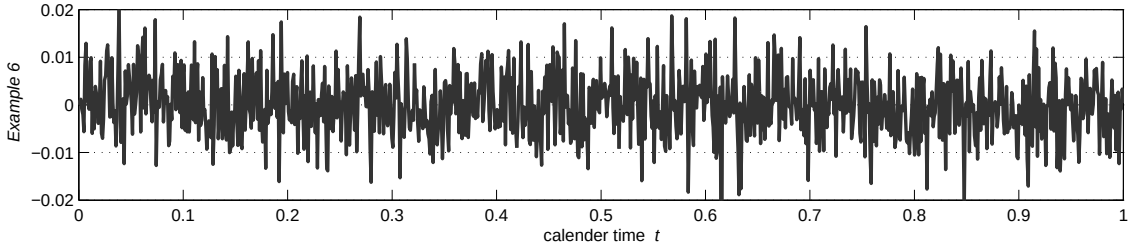

Figure 2.5: Sample innovations in a double-exponential jump-diffusion model.

The characteristic function of a double-exponential jump-diffusion model is given by (see, e.g., Kou and Wang [2003])

$$\varphi_T(u,0) := \mathbb{E}\left[\exp\left(iuB_T\right)\right] = \exp\left(\Upsilon(u)\,T\right), \tag{2.44}$$

where $\beta \neq \alpha_\oplus$, $\beta \neq \alpha_\ominus$, and

$$\Upsilon(\beta) := \mu_1\beta + \frac{1}{2}\sigma_1^2\beta^2 + \lambda\left(\frac{p\alpha_\oplus}{\alpha_\oplus - \beta} + \frac{(1-p)\alpha_\ominus}{\alpha_\ominus + \beta} - 1\right). \tag{2.45}$$

The Laplace transform of the first-exit time is given in Theorem 7.

Theorem 7 (First-exit time double-exponential jump-diffusion)
Denote the roots of $\Upsilon(\beta) = u$ by[12] *$\beta_{4,u} < -\alpha_\ominus < \beta_{3,u} < 0 < \beta_{1,u} < \alpha_\oplus < \beta_{2,u} < \infty$. The Laplace transform (see Equation (2.42)) of the first-exit time on an upper barrier $a > B_0 = 0$, respectively a lower barrier $b < B_0 = 0$, is given by*

$$\Psi_{a,-\infty}(u) = \frac{\beta_{2,u}}{\beta_{2,u}-\beta_{1,u}}\,\frac{\alpha_\oplus - \beta_{1,u}}{\alpha_\oplus}\,e^{-\beta_{1,u}a} + \frac{\beta_{1,u}}{\beta_{2,u}-\beta_{1,u}}\,\frac{\beta_{2,u}-\alpha_\oplus}{\alpha_\oplus}\,e^{-\beta_{2,u}a}, \tag{2.46}$$

$$\Psi_{\infty,b}(u) = \frac{\beta_{3,u}}{\beta_{3,u}-\beta_{4,u}}\,\frac{\alpha_\ominus + \beta_{4,u}}{\alpha_\ominus}\,e^{\beta_{4,u}b} - \frac{\beta_{4,u}}{\beta_{3,u}-\beta_{4,u}}\,\frac{\beta_{3,u}+\alpha_\ominus}{\alpha_\ominus}\,e^{\beta_{3,u}b}. \tag{2.47}$$

[12] Those roots can be derived in closed-form, see the Appendix of Kou et al. [2005].

Proof. See, e.g., Kou and Wang [2003], Kou et al. [2005]. □

If one writes

$$\Psi_{ab}^{\pm}(u) := \mathbb{E}\left[\exp\left(-uT_{ab}^{\pm}\right)\right], \tag{2.48}$$

this result can be extended to the double barrier case, see Theorem 8.

Theorem 8 (Double barrier first-exit time double-exponential jump-diffusion)
Denote the roots of $\Upsilon(\beta) = u$ *by* $\beta_{4,u} < -\alpha_{\ominus} < \beta_{3,u} < 0 < \beta_{1,u} < \alpha_{\oplus} < \beta_{2,u} < \infty$. *The Laplace transform (see Equation (2.48)) of the double barrier first-exit times on two barriers* $b < B_0 = 0 < a$ *is given by*

$$\Psi_{ab}^{+}(u) = \langle c^{+}, \mathbf{1}\rangle, \qquad \Psi_{ab}^{-}(u) = \langle c^{-}, \mathbf{1}\rangle, \tag{2.49}$$

where $\langle\,\cdot\,\rangle$ *denotes the scalar product and* $\mathbf{1}$ *a vector of ones of appropriate size. The vectors* c^{+} *and* c^{-} *are defined via* $M\,c^{+} = m^{+}$ *and* $M\,c^{-} = m^{-}$, *where*

$$M = \begin{pmatrix} \frac{\alpha_{\ominus}e^{\beta_{2,u}b}}{\beta_{2,u}+\alpha_{\ominus}} & \frac{\alpha_{\ominus}e^{\beta_{1,u}b}}{\beta_{1,u}+\alpha_{\ominus}} & \frac{\alpha_{\ominus}e^{\beta_{3,u}b}}{\beta_{3,u}+\alpha_{\ominus}} & \frac{\alpha_{\ominus}e^{\beta_{4,u}b}}{\beta_{4,u}+\alpha_{\ominus}} \\ e^{\beta_{2,u}b} & e^{\beta_{1,u}b} & e^{\beta_{3,u}b} & e^{\beta_{4,u}b} \\ e^{\beta_{2,u}a} & e^{\beta_{1,u}a} & e^{\beta_{3,u}a} & e^{\beta_{4,u}a} \\ \frac{\alpha_{\oplus}e^{\beta_{2,u}a}}{\beta_{2,u}-\alpha_{\oplus}} & \frac{\alpha_{\oplus}e^{\beta_{1,u}a}}{\beta_{1,u}-\alpha_{\oplus}} & \frac{\alpha_{\oplus}e^{\beta_{3,u}a}}{\beta_{3,u}-\alpha_{\oplus}} & \frac{\alpha_{\oplus}e^{\beta_{4,u}a}}{\beta_{4,u}-\alpha_{\oplus}} \end{pmatrix}, \quad m^{+} = \begin{pmatrix} 0 \\ 0 \\ 1 \\ -1 \end{pmatrix}, \text{ and } m^{-} = \begin{pmatrix} 1 \\ 1 \\ 0 \\ 0 \end{pmatrix}.$$

Proof. See, e.g., Sepp [2004]. □

The Laplace transforms in Theorems 7 and 8 have to be inverted to yield the first-exit time probabilities $\mathbb{P}(T_{ab}^{\pm} \le T)$. Many different algorithms are possible, for example the Gaver-Stehfest algorithm; a good overview of Laplace inversion algorithms is given in Abate and Whitt [2006]. Note, however, that some of those algorithms require high-precision arithmetic and can hardly be implemented using double-precision arithmetic. If double-precision arithmetic is used, reasonable results can be obtained by numerically evaluating the integral[13]

$$\mathbb{P}\big(T_{ab}^{\pm} \le T\big) = \frac{\Psi_{ab}^{\pm}(0)}{2} - \frac{1}{\pi}\int_0^{\infty} e^{-iuT}\,\frac{\Psi_{ab}^{\pm}(-iu)}{iu}\,du. \tag{2.50}$$

In the following, a Brownian bridge simulation scheme is introduced. This kind of algorithm was originally suggested by Metwally and Atiya [2002] for one barrier in a

[13] Note that the Laplace transforms $\Psi_{ab}^{\pm}(\,\cdot\,)$ have to be evaluated for purely imaginary numbers $-iu$. Thus, the roots $\beta_{i,u}$, for $i \in \{1,2,3,4\}$, are no longer real, but still form two groups: The real part of $\beta_{1,u}, \beta_{2,u}$ is negative while that of $\beta_{3,u}, \beta_{4,u}$ is positive. Then, the results in Theorems 7 and 8 hold; the order relation $\beta_{1,u} < \beta_{2,u}$ is unnecessary since the Laplace transforms are symmetric in $\beta_{1,u}$, $\beta_{2,u}$.

jump-diffusion setting. For extensions (i.e. two barriers, regime-dependent parameters) or improvements, see, among others, Gobet [2009], Hieber and Scherer [2010], Ross and Ghamami [2010], and Fernández et al. [2013]. The idea of this approach is based on a technique called *Conditional Monte–Carlo*: First, a skeleton of the process B immediately before and after regime changes and jumps is sampled. Between two successive gridpoints of this skeleton B is simply a Brownian motion. In this case, conditional exit probabilities (see the Brownian bridge probabilities in *Section 2.3*) are known analytically. In contrast to a brute-force Monte–Carlo simulation on a discrete grid, this approach is unbiased and (usually) faster.

Section 2.5.1 introduces an algorithm to sample the skeleton of the process immediately before and after regime changes and jumps. Then, *Section 2.5.2* proceeds with the Brownian bridge algorithm.

2.5.1 Skeleton

As a first step, we deal with a jump-diffusion model, i.e. we assume that there is only one regime ($M = 1$). Then, Algorithm 1 generates one realization of the path skeleton at jump instants.

Algorithm 1 (Process skeleton: Jump-diffusion process)
This algorithm generates one realization of jump instants (0, t_1, t_2,...,t_N, T) and path values (B_{t_0}, B_{t_1-}, B_{t_1}, B_{t_2-}, ..., B_{t_N-}, B_{t_N}, B_{T-}) (shortly) before and after the jumps.

(A) Simulate the number of jumps within $[0,T]$ as $N \sim Poi(\lambda T)$.

(B) Simulate the jump times $0 < t_1 < \ldots < t_N < T$. Conditional on N, these jumps are distributed as order statistics of i.i.d. $Uni[0,T]$ random variables, see, for example, Sato [1999], p. 17.

(C) Generate two independent series of random variables $b_1, \ldots, b_{N+1}$ and $y_1, \ldots, y_N$, independent of N:

$$b_i \sim \mathcal{N}\big(\mu(t_i - t_{i-1}), \sigma^2(t_i - t_{i-1})\big) \quad \text{and} \quad y_i \sim \mathbb{P}_Y.$$

(D) Simulate the asset path on the grid of the jump times (set $t_{N+1} = T$):

$$B_{t_0} = 0,\ B_{t_i-} = B_{t_{i-1}} + b_i, \quad \forall i \in \{1, \ldots, N+1\},$$
$$B_{t_i} = B_{t_i-} + y_i, \quad \forall i \in \{1, \ldots, N\}.$$

(E) Return the jump instants (0, t_1, t_2,...,t_N, T) together with (B_0, B_{t_1-}, B_{t_1}, B_{t_2-}, ..., B_{t_N-}, B_{t_N}, B_{T-}).

In the general case with multiple regimes ($M > 1$), we first sample the times of regime changes according to the intensity matrix Q_0 of the generating Markov chain. Within one regime, we are back in the situation covered by Algorithm 1. Algorithm 2 generates the skeleton in the general model framework (2.41).

Algorithm 2 (Process skeleton: Multi-regime case)
This algorithm generates one realization of the times of either jumps or regime changes (0, t_1, t_2,...,t_N, T) and path values (B_{t_0}, B_{t_1-}, B_{t_1}, B_{t_2-}, ..., B_{t_N-}, B_{t_N}, B_{T-}) (shortly) before and after those instants. It furthermore returns the states (Z_0, Z_{t_1}, Z_{t_2},...,Z_{t_N}, Z_T) adopted at those instants.

(A) Use the information provided by the intensity matrix Q_0 to generate one realization of the Markov chain $\{Z_t\}_{t\geq 0}$ (The time spent in state i is exponentially distributed with intensity $\lambda = -q_{ii} > 0$. If a state change from the current state i occurs, the probability of moving to state $j \neq i$ is $-q_{ij}/q_{ii} \geq 0$). The times of regime changes in the interval $[0, T]$ are denoted $\{\tau_1, \tau_2, \ldots, \tau_K\}$.

(B) Generate the jump instants iteratively in each interval $[\tau_{j-1}, \tau_j]$, for $j = 1, 2, \ldots, K+1$. Set $\tau_0 = 0$ and $\tau_{K+1} = T$ and apply Algorithm 1 *for each interval $[\tau_{j-1}, \tau_j]$. Inside the intervals, the diffusion has mean $\mu_{Z_{\tau_{j-1}}}$ and volatility $\sigma_{Z_{\tau_{j-1}}}$; the jumps have intensity $\lambda_{Z_{\tau_{j-1}}}$.*

(C) Arrange the times of regime changes $\{\tau_1, \tau_2, \ldots, \tau_K\}$ and all the jump instants obtained in Step (B) in ascending order and denote them by (t_1, t_2,..., t_N).

(D) Return the instants (0, t_1, t_2,...,t_N, T) together with (B_0, B_{t_1-}, B_{t_1}, B_{t_2-}, ..., B_{t_N-}, B_{t_N}, B_{T-}) and (Z_0, Z_{t_1}, Z_{t_2},...,Z_{t_N}, Z_T).

2.5.2 Brownian bridge algorithm

Being able to sample the skeleton of the process at jump instants and at times of regime changes, we are now able to introduce the idea of conditional Monte–Carlo. Brownian bridge algorithms first sample the skeleton by Algorithm 1 or 2, respectively. Conditional on the skeleton, the exit probability of this sample can be computed analytically using the Brownian bridge probabilities from Theorem 1. This procedure is also demonstrated in *Figure 2.6*. In the following, the Brownian bridge algorithm on a constant upper barrier a is presented (Algorithm 3). In Algorithm 4, those results are extended to two barriers.

One barrier

Algorithm 3 estimates the first-exit time probabilities $\mathbb{P}(T_{a,-\infty} \leq T)$ together with the process at time T, B_T. The original idea is by Metwally and Atiya [2002]; it was extended to regime switching models by Hieber and Scherer [2012].

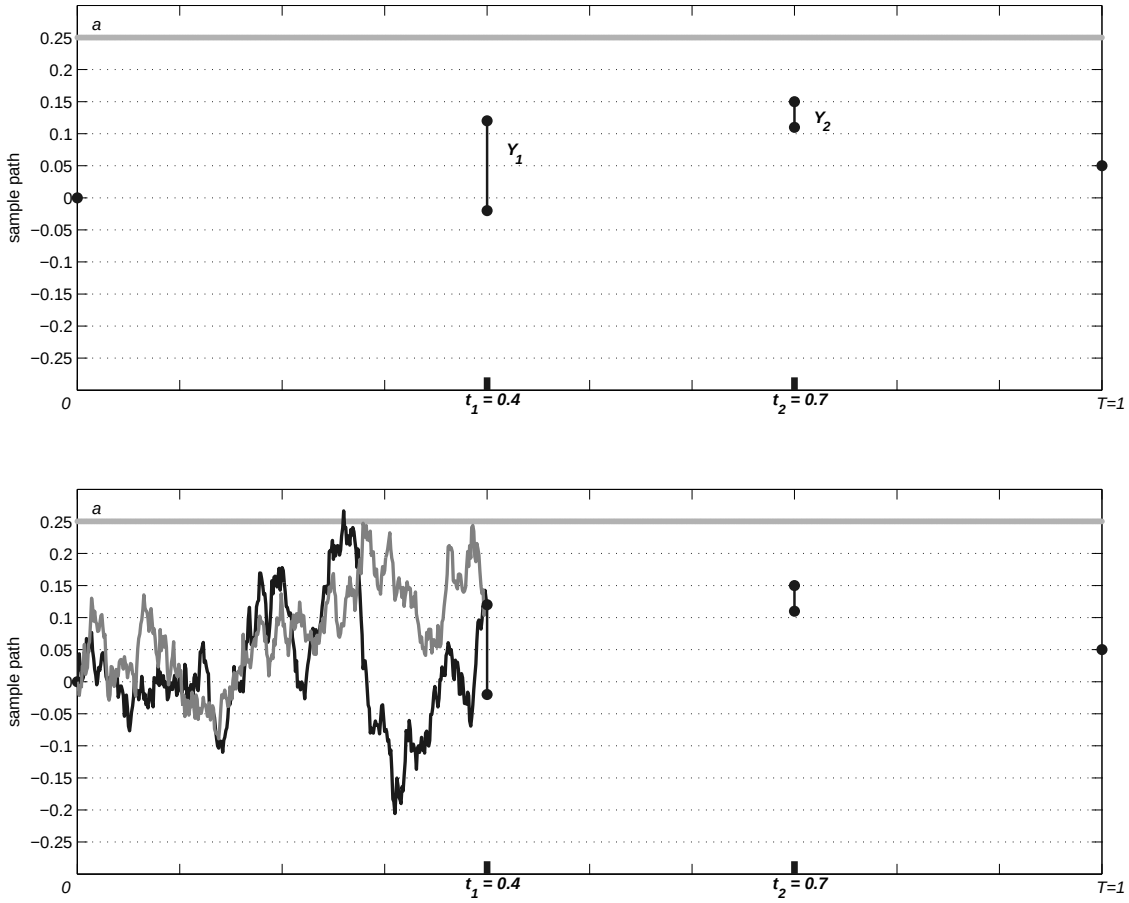

Figure 2.6: Visualization of the Brownian bridge algorithm. The upper graph shows the skeleton generated by Algorithm 2. Two jumps ($t_1 = 0.4$ and $t_2 = 0.7$) and no regime change occur in the considered time interval. Conditional on the skeleton, the Brownian bridge probabilities yield the barrier hitting probabilities.

Algorithm 3 (Brownian bridge technique 1)
This algorithm samples the first-exit time probability $\mathbb{P}(T_{a,-\infty} \leq T)$. *To this end, the number of simulation runs* K, *the constant upper barrier* $a > B_0$, *and the parameters that describe the process* B *are required. As a second output, the algorithm generates a* $K \times 2$ *matrix whose columns contain for each simulation run the conditional probability of hitting the barrier and the realized final path value.*

(1) Repeat Steps (A)–(C) for each simulation run $k \in \{1, \ldots, K\}$.

(A) Simulate the skeleton according to Algorithm 2.

(B) If either $B_{t_{i-1}}$ *or* B_{t_i-}, $i \in \{1, 2, \ldots, N+1\}$, *are above or equal to the barrier* a, *the process reaches the upper barrier and* $\mathcal{BB}(k) = 0$. *Return to Step (1) and increase the simulation run* k *by 1.*

(C) For $x_{i-1} := B_{t_{i-1}} < a$ *and* $x_i := B_{t_i-} < a$, *calculate the conditional exit probabilities*

$$\wp_i = \exp\Big(- \frac{2(a - x_{i-1})(a - x_i)}{\sigma^2 (t_i - t_{i-1})} \Big),\ i \in \{1, 2, \ldots, N+1\}.$$

Set $\mathcal{BB}(k) = \prod_{i=1}^{N+1} (1 - \wp_i)$. *Return to Step (1) and increase the simulation run* k *by 1.*

(2) Estimate the unconditional quantities in question via the sample mean of all conditional quantities over all runs, i.e.

$$\mathbb{P}(T_{a,-\infty} \leq T) \cong \frac{1}{K} \sum_{k=1}^{K} \mathcal{BB}(k),$$

and return a $K \times 2$ *matrix with rows* $\big(\mathcal{BB}(k),\, B_T(k)\big)$, $k \in \{1, \ldots, K\}$.

Algorithm 3 is unbiased and converges almost surely (a.s.) to the first-exit time probability $\mathbb{P}(T_{a,-\infty} \leq T)$ in a regime switching jump-diffusion model.

Theorem 9 (Unbiasedness and a.s. convergence)
Algorithm 3 generates unbiased first-exit time probabilities and converges almost surely to the first-exit time probability of a regime switching jump-diffusion model, i.e.

$$\frac{1}{K} \sum_{k=1}^{K} \mathcal{BB}(k) \ \xrightarrow{K \to \infty}\ \mathbb{P}(T_{a,-\infty} \leq T) \ (a.s.).$$

Proof. Using the tower property of conditional expectation, the first-exit time probability $\mathbb{P}(T_{a,-\infty} \leq T)$ can be expressed as the expectation of a conditional expectation. The inner conditional expectation is taken with respect to the skeleton sampled by Algorithm 2, i.e. we need (1) the time to maturity T and times of jumps or state changes $(t_1, t_2, \ldots, t_N)$, (2) the current state on this random grid $(Z_0, Z_{t_1}, Z_{t_2}, \ldots, Z_{t_N}, Z_T)$, and (3) the path values $(B_0, B_{t_1-}, B_{t_1}, B_{t_2-}, \ldots, B_{t_N-}, B_{t_N}, B_{T-})$. Combined:

$$\mathcal{F}^* := \sigma\big\{N; 0 < t_1 < \ldots < t_N < T; Z_{t_0}, \ldots, Z_{t_N}; B_0, b_1, \ldots, b_{N+1}, y_1, \ldots, y_N\big\},$$

where we denote $t_0 := 0$, $t_{N+1} := T$, and the evolution in the diffusion parts by $b_i := B_{t_i-} - B_{t_{i-1}}$, for $i \in \{1, 2, \ldots, N+1\}$ and in the jump parts by $y_i := B_{t_i} - B_{t_i-}$, for $i \in \{1, 2, \ldots, N\}$.

Integrating out the random variables in $\mathcal{F}^*$ and taking conditional expectations yields

$$\begin{aligned}\mathbb{P}(T_{a,-\infty} \leq T) &= \mathbb{E}\Big[\mathbb{E}\big[\mathbb{1}_{\{T_{a,-\infty} \leq T\}} \,\big|\, \mathcal{F}^*\big]\Big] \\ &= \sum_{n=0}^{\infty} \mathbb{Q}(N=n) \Bigg(\int\limits_{\substack{(t_1,\ldots,t_n) \\ \in (0,T)^n}} \int\limits_{\substack{(b_1,\ldots,b_{n+1}) \\ \in (-\infty,\infty)^{n+1}}} \int\limits_{\substack{(y_1,\ldots,y_n) \\ \in (-\infty,\infty)^n}} \mathbb{E}\big[\mathbb{1}_{\{T_{a,-\infty} \leq T\}} \,\big|\, \mathcal{F}^*\big] \prod_{i=1}^{n} \mathbb{P}(dy_i) \\ &\qquad \cdot \prod_{i=0}^{n} \varphi\big(b_{i+1}; \mu_{Z_{t_i}}(t_{i+1}-t_i), \sigma^2_{Z_{t_i}}(t_{i+1}-t_i)\big)\, db_{i+1}\; d\mathcal{G}_n(t_1, \ldots, t_n) \Bigg),\end{aligned}$$

where $\varphi(x; \mu, \sigma^2)$ denotes the probability density function of a normal distribution with mean μ and variance σ^2 and $\mathcal{G}_n$ is the (conditional) distribution of the location of jumps and state changes (given that $N = n$, i.e. the number of state changes and jumps totals n). The inner conditional expectation can be computed explicitly, i.e.

$$\mathbb{E}\big[\mathbb{1}_{\{T_{a,-\infty} \leq T\}} \,\big|\, \mathcal{F}^*\big] = \mathbb{1}_{\{I \neq 0\}} \prod_{i=0}^{I} (1 - \wp_i) = \mathcal{BB}(k),$$

where $I := \min(i \in \{0, \ldots, n+1\} : B_{t_i-} \geq a \text{ or } B_{t_i} \geq a)$, $\min(\emptyset) := 0$, denotes the index of the first barrier crossing during one of the state changes or jumps $\{t_0, \ldots, t_n, t_{n+1} = T\}$. The probability of defaulting within the interval (t_i, t_{i+1}) is given by $\wp_i$. In Step (1) of Algorithm 3, in each simulation run $k \in \{1, \ldots, K\}$, the value $\mathcal{BB}(k)$ is generated. This is achieved by simulating all random quantities defining $\mathcal{F}^*$. Then, the first-exit time probability is evaluated (without discretization bias) conditional on this information. Note that specific values for $\mathbb{Q}(N = n)$ and $\mathcal{G}_n$ are not required, as long as one can simulate the required random variables without bias (which is simple, see Algorithm 2). All simulation runs being independent, the generated realizations $\mathcal{BB}(k)$ are independent and identically distributed (i.i.d.).

Additionally, using the above results, it holds that

$$\mathbb{E}[\mathcal{BB}(k)] = \mathbb{E}\Big[\mathbb{E}\big[\mathbb{1}_{\{T_{a,-\infty}\leq T\}} \,\big|\, \mathcal{F}^*\big]\Big] = \mathbb{P}(T_{a,-\infty} \leq T),\ \forall k,$$
$$\mathrm{Var}\big(\mathcal{BB}(k)\big) \leq \mathbb{E}\big[\mathcal{BB}(k)^2\big] \leq 1 < \infty.$$

The stated convergence is then implied by the Law of Large Numbers. The same result was obtained in the case of jump-diffusion models by Ruf and Scherer [2011] and in the case of regime-switching models by Hieber and Scherer [2010]. □

Two barriers

Algorithm 3 can be extended to two barriers, i.e. we introduce in the following the Brownian bridge algorithms that allow to efficiently estimate two–sided exit probabilities of regime switching jump-diffusion processes. Again, the idea is to sample first the skeleton of the process immediately before and after regime changes and jumps (according to Algorithm 1 or 2, respectively). Between two successive instants, we have a Brownian motion; a process that allows us to get the (conditional) barrier hitting probabilities in closed-form (see the results in Theorem 1).

Algorithm 4 extends Algorithm 3 to two barriers and estimates $\mathbb{P}(T_{ab} \leq T)$, following Gobet [2009]. Note that the algorithm by Gobet [2009] does not distinguish which one of the two barriers is hit first.

Algorithm 4 (Brownian bridge technique 2)
This algorithm samples the first-exit time probability $\mathbb{P}(T_{ab} \leq T)$*. To this end, the number of simulation runs* K*, the constant barriers* $b < B_0 < a$*, and the parameters that describe the process* B *are required. As a second output, the algorithm generates a* $K \times 2$ *matrix whose columns contain for each simulation run the conditional probability of hitting the barriers and the realized final path value.*

(1) Repeat Steps (A)–(C) for each simulation run $k \in \{1, \ldots, K\}$*.*

(A) Simulate the skeleton according to Algorithm 2.

(B) If the skeleton $B_{t_{i-1}}$ *or* B_{t_i-}*,* $i \in \{1, 2, \ldots, N+1\}$*, does not stay withing the corridor* (b, a)*, we set* $\mathcal{BB}(k) = 0$*. Return to Step (1) and increase the simulation run* k *by 1.*

(C) For $x_{i-1} = B_{t_{i-1}}$ *and* $x_i = B_{t_i-}$*, calculate for* $i \in \{1, 2, \ldots, N+1\}$ *the conditional exit probabilities*

$$\wp_i = \sum_{n=-\infty}^{\infty} \left[\exp\left(-\frac{2n(a-b)}{\sigma^2(t_i - t_{i-1})}\big(x_{i-1} - x_i + n(a-b)\big)\right) + \exp\left(-\frac{2\big(x_i - na + (n-1)b\big)\big(x_{i-1} - na + (n-1)b\big)}{\sigma^2(t_i - t_{i-1})}\right)\right] - 1.$$

Set $\mathcal{BB}(k) = \prod_{i=1}^{N+1}(1 - \wp_i)$. *Return to Step (1) and increase the simulation run* k *by 1.*

(2) Estimate the unconditional quantities in question via the sample mean of all conditional quantities over all runs, i.e.

$$\mathbb{P}(T_{ab} \leq T) \cong \frac{1}{K}\sum_{k=1}^{K} \mathcal{BB}(k),$$

and return a $K \times 2$ *matrix with rows* $\big(\mathcal{BB}(k),\, B_T(k)\big)$, $k \in \{1, \ldots, K\}$.

Algorithm 4 is also unbiased; the results in Theorem 9 can easily be adapted to the case of two barriers.

Remark 2 (Stochastic volatility)
We can also combine the stochastic volatility results from Section 2.4 with the Brownian bridge algorithm, i.e. we can in the most general setting simulate the first-exit time probabilities of a regime switching jump-diffusion model with stochastic volatility introduced by a continuous time change Λ.

The main idea is the following: If the interval $[t_{i-1}, t_i]$ *is continuously transformed to* $[t_{i-1}, t_{i-1} + \Lambda_{t_i - t_{i-1}}]$, *Equation (2.11) in Theorem 1 is the Brownian bridge probability conditional on the time change* $t_i = t_{i-1} + \Lambda_{t_i - t_{i-1}}$. *This allows us to slightly modify the Brownian bridge algorithms: When generating the skeleton in Algorithm 1 or 2, in each time step we first sample from the distribution of the time change* $\Lambda_{t_i - t_{i-1}}$ *and then replace* t_i *by* $t_{i-1} + \Lambda_{t_i - t_{i-1}}$.

For continuously time-changed Brownian motion, the transition density function is known analytically, see, e.g., Escobar et al. [2013]. The transition density function describes the probability density that B *starts at* $x_{i-1} := B_{t_{i-1}}$, *survives until time* $t_i > t_{i-1}$, *and ends up in* $x_i := B_{t_i -}$. *In the Black–Scholes model, this density is given by (see, e.g., Cox and Miller [1965], Pelsser [2000])*

$$\frac{2e^{\frac{\mu}{2\sigma^2}x_{i-1}}}{a-b}\sum_{n=1}^{\infty} e^{-\left(\frac{\mu^2}{2\sigma^2} + \frac{n^2\pi^2}{2(a-b)^2}\right)(t_i - t_{i-1})}\, e^{\frac{\mu}{2\sigma^2}x_i} \sin\left(\frac{n\pi(x-b)}{a-b}\right)\sin\left(\frac{n\pi(y-b)}{a-b}\right). \quad (2.51)$$

If the interval $[t_{i-1}, t_i]$ *is continuously transformed to* $[t_{i-1}, t_{i-1} + \Lambda_{t_i - t_{i-1}}]$, *(2.51) is the transition density conditional on the time change* $t_i = t_{i-1} + \Lambda_{t_i - t_{i-1}}$. *If this time change has Laplace transform* $\vartheta_T(u) := \mathbb{E}[\exp(-u\Lambda_T)]$, $u \geq 0$, *we find that*

$$\mathbb{E}\Big[e^{-\left(\frac{\mu^2}{2\sigma^2}+\frac{n^2\pi^2}{2(a-b)^2}\right)(t_i - t_{i-1})} \;\Big|\; t_i = t_{i-1} + \Lambda_{t_i - t_{i-1}}\Big] = \vartheta_{t_i - t_{i-1}}\left(\frac{\mu^2}{2\sigma^2} + \frac{n^2\pi^2}{2(a-b)^2}\right)$$

and can obtain the transition density of continuously time-changed Brownian motion

$$\frac{2e^{\frac{\mu}{2\sigma^2}x_{i-1}}}{a-b}\sum_{n=1}^{\infty}\vartheta_{t_i - t_{i-1}}\left(\frac{\mu^2}{2\sigma^2} + \frac{n^2\pi^2}{2(a-b)^2}\right) e^{\frac{\mu}{2\sigma^2}x_i} \sin\left(\frac{n\pi(x-b)}{a-b}\right)\sin\left(\frac{n\pi(y-b)}{a-b}\right).$$

In many cases, however, one is also interested in the direction of the exit, i.e. in case of a barrier crossing in the question which barrier was hit first. Since the probability of hitting the upper (respectively the lower) barrier are obviously not independent (a path can hit both barriers in the interval $[0, T]$), this case is more complicated. For notational convenience, a simplified notation is necessary: We set $t_0 = 0$ and abbreviate the conditional exit probabilities in the time intervals (t_{i-1}, t_i), $i \in \mathbb{N}$, by $\mathcal{P}^+_{i-1,i}$ and $\mathcal{P}^-_{i-1,i}$ and the conditional survival probability by $\overline{\mathcal{P}_{i-1,i}}$, i.e.

$$\mathcal{P}^+_{i-1,i} := BB^+_{ab}(t_{i-1}, t_i, B_{t_{i-1}}, B_{t_i-}), \quad \mathcal{P}^-_{i-1,i} := BB^-_{ab}(t_{i-1}, t_i, B_{t_{i-1}}, B_{t_i-}), \tag{2.52}$$

$$\overline{\mathcal{P}_{i-1,i}} := 1 - \big(\mathcal{P}^+_{i-1,i} + \mathcal{P}^-_{i-1,i}\big). \tag{2.53}$$

We note from Theorem 1 that we define $\overline{\mathcal{P}_{i-1,i}} = 0$ if $B_{t_i-} \notin (b, a)$. The exit and survival probabilities sum up to one, i.e. $\mathcal{P}^+_{i-1,i} + \mathcal{P}^-_{i-1,i} + \overline{\mathcal{P}_{i-1,i}} = 1$. Further, denote on the interval $[0, t_i)$ the cumulated conditional probabilities

$$\overline{\mathcal{P}_i} := \prod_{k=1}^{i}\overline{\mathcal{P}_{k-1,k}}, \quad \mathcal{P}^+_i := \sum_{k=1}^{i}\overline{\mathcal{P}_{k-1}}\; BB^+_{ab}(t_{k-1}, t_k, B_{t_{k-1}}, B_{t_k-}). \tag{2.54}$$

Algorithm 5 proceeds iteratively on the intervals $(t_{i-1}, t_i]$, for $i \in \{1, 2, \ldots, N+1\}$. Step 1(B), part (a–c), returns the exit probability in the diffusion part (t_{i-1}, t_i). Then, part (d) verifies, whether there is a barrier crossing due to a jump at time t_i. The algorithm estimates the first-exit time probabilities $\mathbb{P}(T^+_{ab} \leq T)$, $\mathbb{P}(T_{ab} \leq T)$ together with the process at time T, B_T, following Fernández et al. [2013].

Algorithm 5 (Brownian bridge technique 3)
This algorithm estimates the first-exit time probabilities $\mathbb{P}(T_{ab}^{+} \leq T)$ *and* $\mathbb{P}(T_{ab} \leq T)$. *To this end, the number of simulation runs* K, *the barriers* a *and* b, *and the parameters that describe the process* B *are required. As a second output, the algorithm generates a* $K \times 3$ *matrix whose columns contain for each simulation run the conditional probability of hitting the upper barrier, the conditional probability that the path stays within the corridor* (b, a), *and the realized final path value.*

(1) Repeat Steps (A)–(C) for each simulation run $k \in \{1, \ldots, K\}$[14], *then continue with Step (2).*

(A) Simulate the skeleton according to Algorithm 2.

(B) Compute the conditional barrier crossing probabilities between the grid points. Set $\overline{\mathcal{P}_0} := 1$ *and repeat Steps (a)–(d) for each time step* $i \in \{1, \ldots, N+1\}$.

(a) Compute the probabilities

$$\mathcal{P}_{i-1,i}^{+} = BB_{ab}^{+}(t_{i-1}, t_i, B_{t_{i-1}}, B_{t_i-}),$$
$$\overline{\mathcal{P}_{i-1,i}} = 1 - \mathcal{P}_{i-1,i}^{+} - BB_{ab}^{-}(t_{i-1}, t_i, B_{t_{i-1}}, B_{t_i-}),$$

and obtain $\overline{\mathcal{P}_i} = \overline{\mathcal{P}_{i-1}}\,\overline{\mathcal{P}_{i-1,i}}$, $\mathcal{P}_i^{+} = \mathcal{P}_{i-1}^{+} + \overline{\mathcal{P}_{i-1}}\,\mathcal{P}_{i-1,i}^{+}$.

(b) ∗ *If* $B_{t_i-} \notin (b, a)$, *set* $\mathcal{BB}^{+}(k) = \mathcal{P}_i^{+}$, $\mathcal{BB}(k) = 0$ *and go to (C).*
∗ *If* $B_{t_i-} \in (b, a)$, *continue with Step (c).*

(c) If $i = N+1$, *set* $\mathcal{BB}^{+}(k) = \mathcal{P}_{N+1}^{+}$, $\mathcal{BB}(k) = \overline{\mathcal{P}_{N+1}}$ *and go to (C), else continue with Step (d).*

(d) Check whether a barrier crossing occurs due to a jump.
∗ *If* $B_{t_i} > a$, *set* $\mathcal{BB}^{+}(k) = \overline{\mathcal{P}_i} + \mathcal{P}_i^{+}$, $\mathcal{BB}(k) = 0$ *and go to (C).*
∗ *If* $B_{t_i} < b$, *set* $\mathcal{BB}^{+}(k) = \mathcal{P}_i^{+}$, $\mathcal{BB}(k) = 0$ *and go to (C).*
∗ *If* $B_{t_i} \in (b, a)$, *return to Step (B).*

(C) Set $B_T(k) = B_{t_{N+1}-}$, *return to Step (1), increase the simulation run* k *by 1.*

(2) Estimate the unconditional quantities in question via the sample mean of all conditional quantities over all runs, i.e.

$$\mathbb{P}(T_{ab}^{+} \leq T) \cong \frac{1}{K}\sum_{k=1}^{K} \mathcal{BB}^{+}(k), \quad \mathbb{P}(T_{ab}^{-} \leq T) \cong 1 - \frac{1}{K}\sum_{k=1}^{K} \mathcal{BB}^{+}(k) - \frac{1}{K}\sum_{k=1}^{K} \mathcal{BB}(k),$$

and return a $K \times 3$ *matrix with rows* $\big(\mathcal{BB}^{+}(k),\, \mathcal{BB}(k),\, B_T(k)\big)$, $k \in \{1, \ldots, K\}$.

[14] In the kth simulation run the quantities $\mathcal{BB}^{+}(k)$ (conditional probability of hitting the upper barrier) and $\mathcal{BB}(k)$ (conditional probability of surviving within the corridor (b, a)), and the final asset value $B_T(k)$ are sampled.

2.5.3 Functionals of the first-exit time

Algorithm 6 additionally estimates expectations of functionals of the first-exit time T_{ab}^{+}. This is an important requirement to, for example, price certain credit products that contain default risk and thus often depend on the time of default. Algorithm 6 works exemplary on an interval (t_{i-1}, t_i), where both $B_{t_{i-1}}$ and B_{t_i-} are known and $\{B_t\}_{t_{i-1}<t<t_i}$ is a Brownian motion. It is straightforward to include this idea into the Brownian bridge algorithms 3, 4, or 5 and sample expectations of functionals on the first-exit time of regime-switching jump-diffusions. As an input, the Brownian bridge probability $BB_{ab}^{+}(t_{i-1}, t_i, x_{i-1}, x_i)$ (see Equation (2.8) or (2.10)) and the first-exit time intensity $g_{ab}^{+}(t, x_{i-1}, x_i)$ (see Theorem 3) are needed. The estimation algorithm then proceeds as follows: It first draws the first-exit time uniformly on the interval (t_{i-1}, t_i). To account for the different likelihood of default over time (see, e.g., *Figure 2.2*), an importance sampling weight $p(k)$ is introduced that weights the sampled functionals according to the first-exit time intensities.

Algorithm 6 (Estimating functionals of the first-exit time)
This algorithm estimates $\mathbb{E}\big[h(T_{ab}^{+}) \,\big|\, t_{i-1} < T_{ab}^{+} < t_i,\, B_{t_{i-1}} = x_{i-1},\, B_{t_i-} = x_i\big]$ *for an integrable functional* $h(\,\cdot\,)$ *and a Brownian motion* $\{B_t\}_{t_{i-1}<t<t_i}$. *As an input the interval* (t_{i-1}, t_i) *as well as the process at endpoints* $x_{i-1} := B_{t_{i-1}}$ *and* $x_i := B_{t_i-}$ *are required.*

(1) Repeat Steps (A)–(B) for each simulation run $k \in \{1, \dots, K\}$.

(A) Draw a random variable $U \sim$ *Uni[0,1] and set* $w := BB_{ab}^{+}(t_{i-1}, t_i, x_{i-1}, x_i)$.

(B) Set

$$T_{ab}^{+}(k) = t_{i-1} + \big(t_i - t_{i-1}\big)\, U\,,$$
$$p(k) = g_{ab}^{+}\big(T_{ab}^{+}(k), x_{i-1}, x_i\big)\, \frac{t_i - t_{i-1}}{w}\,.$$

(2) Return the weighted mean over all samples in question, i.e.

$$\mathbb{E}\big[h(T_{ab}^{+}) \,\big|\, t_{i-1} < T_{ab}^{+} < t_i,\, B_{t_{i-1}} = x_{i-1},\, B_{t_i-} = x_i\big] \cong \frac{1}{K} \sum_{k=1}^{K} p(k)\, h\big(T_{ab}^{+}(k)\big)\,.$$

Algorithm 6 can also be integrated into the Brownian bridge algorithms 3, 4, and 5, see Fernández et al. [2013]. Algorithm 6 is unbiased, see Theorem 10.

Theorem 10 (Unbiasedness of Algorithm 6)
Consider an integrable functional $h(\,\cdot\,)$. Then, Algorithm 6 returns an unbiased estimate of $\mathbb{E}\big[h(T_{ab}^{+}) \,\big|\, t_{i-1} < T_{ab}^{+} < t_i,\, B_{t_{i-1}} = x_{i-1},\, B_{t_i-} = x_i\big]$.

Proof. For $U \sim \text{Uni}[0,1]$ and $w := BB_{ab}^{+}(t_{i-1}, t_i, x_{i-1}, x_i)$, we find that

$$\begin{aligned}
&\mathbb{E}\big[p(k)\, h\big(T_{ab}^{+}(k)\big)\big] \\
&\qquad = \int_0^1 \frac{\big(t_i - t_{i-1}\big) g_{ab}^{+}\Big(t_{i-1} + \big(t_i - t_{i-1}\big)u, x_{i-1}, x_i\Big)}{w}\, h\Big(t_{i-1} + \big(t_i - t_{i-1}\big)\, u\Big)\, du \\
&\qquad = \frac{1}{w} \int_{t_{i-1}}^{t_i} h(t)\, g_{ab}^{+}\big(t, x_{i-1}, x_i\big)\, dt \\
&\qquad = \mathbb{E}\big[h(T_{ab}^{+}) \,\big|\, t_{i-1} < T_{ab}^{+} < t_i,\, B_{t_{i-1}} = x_{i-1},\, B_{t_i-} = x_i\big]\,.
\end{aligned}$$

□

An alternative to the presented algorithm uses acceptance/rejection techniques to sample from the (conditional) first-exit time density, see, e.g., Ross and Ghamami [2010].

2.6 Numerical examples

In the following, we compare the different models and numerical techniques presented so far.

Time-changed Brownian motion

We consider a Brownian motion with zero drift and unit volatility, time–changed by an independent time change Λ, i.e. we consider the process

$$dB_t = dW_{\Lambda_t}. \tag{2.55}$$

To be able to compare different stochastic volatility models (see the parameterizations in Examples 1 to 4), *Table 2.1* presents parameter sets that are standardized, i.e. the average time change $\mathbb{E}[\Lambda_1]$ is identical.

First, we want to examine the effect of stochastic volatility. Therefore, *Table 2.2* presents survival probabilities $\mathbb{P}(T_{ab} > T)$ for different threshold levels (b, a) using the parameter sets in *Table 2.1*. To achieve highly accurate prices with an acceptable absolute error (ϵ = 1e–08), the rapidly converging series from Theorem 5 are truncated following the

model	$\{\lambda_t\}_{t\geq 0}$	**parameters**	$\sqrt{\mathbb{E}[\Lambda_1]}$
Brown. motion	$\lambda_t = \sigma^2 \in \mathbb{R}$	$\sigma = 21.0\%$	21.0%
Example 1	CIR	$(\theta, \nu, \gamma, \lambda_0) = (0.0050, 0.0441, 0.1000, 0.0441)$	21.0%
Example 2	OU	$(\xi, \varkappa, k, \lambda_0) = (0.2000, 0.0420, 0.100, 0.0484)$	21.0%
Example 3	shot-noise	$(\delta, \zeta, \psi, \lambda_0) = (0.3000, 4.7000, 0.1000, 0.0400)$	21.0%
Example 4	reg.-switching	$(k_1, k_2, \lambda_1, \lambda_2, Z_0) = (0.228, 0.050, 0.5, 1.0, 1)$	21.0%

Table 2.1: Exemplary parameter set used to compare the different models and techniques. The intensities $\{\lambda_t\}_{t\geq 0}$ define the time change $\Lambda_T := \int_0^T \lambda_t dt$ of a Brownian motion.

error bounds in *Section 2.4.3*. One of the series can be computed within fractions of seconds (i.e. 4ms). As we will see later on, this approach is significantly faster than alternatives, i.e. Fourier techniques (see *Section 3.1.4* for a detailed comparison).

	Brownian motion	**Time-changed Brownian motion**			
		Example 1	Example 2	Example 3	Example 4
$a = -b = 0.1$	0.55%	1.35%	3.27%	1.64%	3.92%
$a = -b = 0.2$	32.67%	34.88%	36.09%	40.97%	35.82%
$a = -b = 0.3$	69.38%	70.05%	67.30%	74.75%	69.66%
$a = -b = 0.5$	96.54%	96.03%	91.47%	96.03%	95.84%

Table 2.2: Survival probability $\mathbb{P}(T_{ab} > T)$ for different threshold levels (b, a) examining the effect of stochastic volatility. We compare Example 1 (Λ_T is integrated CIR process), Example 2 (Λ_T is integrated OU process), Example 3 (Λ_T is integrated shot-noise process), Example 4 (Λ_T is integrated regime-switching process). The parameters are taken from Table 2.1, the time horizon is $T = 1$.

From the results in *Table 2.2*, we observe that an increase in stochastic volatility does not necessarily decrease the survival probability. Surprisingly, we realize in this example that stochastic volatility tends to increase the survival probability.

As a second step, we want to compare the analytical results in Theorem 5 to its numerical alternatives. To this end, we use the time change model with a regime switching intensity (Example 4). This allows us to compare the results to the Brownian bridge algorithm (*Section 2.5.2*). Furthermore, a finite elements scheme is implemented (see, e.g.,

the guideline in the Appendix of Kim et al. [2008]). Last, we compare the results to a brute-force Monte–Carlo simulation on a grid. *Table 2.3* presents survival probabilities $\mathbb{P}(T_{ab} > T)$ for different threshold levels (b, a) using the parameter set in *Table 2.1*. The numerical algorithms are compared according to accuracy (Theorem 5 provides us with the true probabilities) and computation time. For the two simulation schemes (Brownian bridge algorithm and brute-force Monte–Carlo), 95% confidence intervals are in the range of 0.01%, therefore the unsystematic error is negligible.

	true value	**Brownian bridge**		**Finite elements**		**Monte–Carlo**	
		$\mathbb{P}(T_{ab} > T)$	time	$\mathbb{P}(T_{ab} > T)$	time	$\mathbb{P}(T_{ab} > T)$	time
$a = -b = 0.1$	3.92%	3.92%	9s	3.92%	0.1s	4.38%	1min
$a = -b = 0.2$	35.82%	35.81%	11s	35.80%	0.2s	37.45%	3min
$a = -b = 0.3$	69.66%	69.67%	13s	69.64%	0.3s	70.73%	4min
$a = -b = 0.5$	95.84%	95.84%	13s	95.84%	0.5s	96.06%	4min

Table 2.3: Survival probability $\mathbb{P}(T_{ab} > T)$ for different threshold levels (b, a) comparing the Brownian bridge algorithm (left) to a finite element scheme (middle, $\triangle t$ = 1e–03, $\triangle p$ = 1e–02), and a brute-force Monte–Carlo simulation (right, 10^6 simulation runs, mesh 1/250 years). The true value was computed using the time-change representation (see Example 4 and Theorem 5). The chosen parameters of the regime switching model are $(k_1, k_2, \lambda_1, \lambda_2) = (0.2280, 0.0500, 0.5, 1.0)$, $T = 1$, $\mathbb{P}(Z_0 = 1) = 1$, $B_0 = 0$. The given computation time was calculated using Matlab on a 2.4 GHz PC.

We observe that the brute-force Monte–Carlo suffers from a significant discretization bias. In contrast, the Brownian bridge algorithm is unbiased and – since one does not need to simulate on a fine grid – several times faster. By far the best technique are the closed–form results using the rapidly converging series from Theorem 5 (computed in fractions of seconds). However, one has to be aware that the model class of continuously time–changed Brownian motion covered by Theorem 5 is limited. If one wants to, for example, include jumps, one has to rely on numerical schemes. In this case, the Brownian bridge algorithm is the most flexible technique and can easily be adapted to different model classes. Finite elements schemes are equally flexible but can, especially if we are working on single barrier exit probabilities and jumps, become computationally more challenging. Furthermore, they suffer from a discretization bias.

Double exponential jump-diffusion

In *Tables 2.4* and *2.5*, we now compute the (upper) barrier first hitting time probabilities $\mathbb{P}(T_{a,-\infty} \leq T)$, respectively $\mathbb{P}(T_{ab}^{+} \leq T)$, for different threshold levels (b, a), this time using a double-exponential jump-diffusion model (see Example 6 for an introduction). The double-exponential jump-diffusion model has the advantage that one can compare the results to the analytical expression by Kou and Wang [2003] (*Table 2.4*, single barrier case) and Sepp [2004] (*Table 2.5*, double barrier case). If one wants to depart from the assumption of exponential jumps, for example to include heavy tailed jump size distributions, one usually has to rely on numerical schemes.

	Kou,Wang [2003]	**Brownian bridge**		**Monte–Carlo**	
	$\mathbb{P}(T_{a,-\infty} \leq T)$	$\mathbb{P}(T_{a,-\infty} \leq T)$	time	$\mathbb{P}(T_{a,-\infty} \leq T)$	time
$a = 0.1,\ b \to -\infty$	68.37%	68.37%	10s	66.68%	3min
$a = 0.2,\ b \to -\infty$	47.45%	47.46%	12s	46.26%	2min
$a = 0.3,\ b \to -\infty$	33.08%	33.08%	14s	32.29%	2min
$a = 0.5,\ b \to -\infty$	16.39%	16.40%	14s	16.04%	2min

Table 2.4: Upper barrier first-exit time probability $\mathbb{P}(T_{a,-\infty} \leq T)$ for different threshold levels a comparing the Brownian bridge algorithm (left) to the analytic expression by Kou and Wang [2003] (true value, see also Theorem 7), and a brute-force Monte–Carlo simulation (right, 10^6 simulation runs, mesh 1/250 years). The true value is given by the Kou and Wang [2003] results. The chosen parameters of the double-exponential jump-diffusion model are $(\lambda, \alpha_{\oplus}, \alpha_{\ominus}, \mu_1, \sigma_1) = (2, 5, 5, 0, 0.2)$, $T = 1$, $B_0 = 0$. The given computation time was calculated using Matlab on a 2.4 GHz PC.

Again, in both *Tables 2.4* and *2.5*, we observe that the brute-force Monte–Carlo simulation suffers from a discretization bias and is significantly slower than the Brownian bridge algorithm. The Brownian bridge algorithm is very accurate, already 10^6 simulation runs guarantee reliable probabilities on the first 3–4 digits. The computation time can be further accelerated: First, a parallelization of Monte–Carlo simulations can very easily be implemented. Secondly, there are variance reduction techniques to further (significantly) accelerate the algorithm (see, e.g., Joshi and Leung [2007], DiCesare and McLeish [2008], Ross and Ghamami [2010] on the single barrier algorithm).

To summarize the results on the comparison of the different numerical techniques to estimate first-exit time probabilities, *Table 2.6* presents the main advantages and

	Sepp [2004]	**Brownian bridge**		**Monte–Carlo**	
	$\mathbb{P}(T_{ab}^{+} \leq T)$	$\mathbb{P}(T_{ab}^{+} \leq T)$	time	$\mathbb{P}(T_{ab}^{+} \leq T)$	time
$a = -b = 0.1$	49.89%	49.89%	13s	49.80%	4min
$a = -b = 0.2$	42.92%	42.92%	14s	42.02%	3min
$a = -b = 0.3$	31.85%	31.85%	15s	31.10%	3min
$a = -b = 0.5$	16.25%	16.25%	15s	15.92%	2min

Table 2.5: Upper barrier first-exit time probability $\mathbb{P}(T_{ab}^{+} \leq T)$ for different threshold levels (b, a) comparing the Brownian bridge algorithm (left) to a brute-force Monte–Carlo simulation (right, 10^6 simulation runs, mesh 1/250 years). The true value is given by the Sepp [2004] results (see also Theorem 8). The chosen parameters of the double-exponential jump-diffusion model are $(\lambda, \alpha_{\oplus}, \alpha_{\ominus}, \mu_1, \sigma_1) = (2, 5, 5, 0, 0.2)$, $T = 1$, $B_0 = 0$. The given computation time was calculated using Matlab on a 2.4 GHz PC.

disadvantages. The techniques considered are

MC: Brute-force Monte–Carlo.
BB: Brownian bridge algorithm.
FE: Finite elements, PIDE technique.
TC: Time change representation.
LI: Laplace inversion (e.g. Kou,Wang [2003], Sepp [2004]).

First, one major advantage of the Monte–Carlo simulations and the finite elements scheme (**MC, BB, FE**) is their flexibility to adapt to different jump size distributions or to, for example, state-dependent or stochastic volatility. For the two analytical techniques (**TC, LI**) this is only possible up to a certain degree. Yet, the latter two methods are usually significantly faster than the Monte–Carlo simulations or the finite elements scheme. One big disadvantage of the brute-force Monte–Carlo simulation (**MC**) and the finite elements scheme (**FE**) is an often significant discretization bias.

As a final remark, it is important to stress that there is not one uniformly superior technique; depending on the model and on the specific problem (i.e. non-constant barriers, state-dependent volatility), an apparently inefficient technique might be more suitable.

MC	$\oplus$ Very flexible; easy to implement. $\ominus$ Very slow. $\ominus$ Leads to a discretization error.
BB	$\oplus$ Very flexible; easy to implement. $\oplus$ Fast for reasonably small jump intensities. $\oplus$ Unbiased.
FE	$\oplus$ Very flexible; easy to implement. $\oplus$ Usually fast. $\ominus$ Leads to a discretization error.
TC	$\oplus$ Very easy to implement. $\oplus$ Extremely fast; very high accuracy. $\oplus$ Unbiased. $\ominus$ Only applicable for (continuously) time-changed Brownian motion.
LI	$\oplus$ Very fast. $\ominus$ Only available for specific jump size distributions. $\ominus$ Implementation can be challenging, as Laplace inversion is known to be an ill-posed problem.

Table 2.6: Summary of advantages and disadvantages of the most frequently used techniques to obtain first-exit time probabilities.

Chapter 3

Default–linked contracts in Finance and Insurance

The aim of this chapter is to show how the theoretical results from *Chapter 2* can be used for the pricing and risk management of default–linked contracts in Finance and Insurance.

Section 3.1 introduces to the field of option pricing which has earned a lot of attention since the seminal paper of Black and Scholes [1973]. For this result, Myron Scholes was awarded the Nobel Prize in Economics (*The Sveriges Riksbank Prize in Economic Sciences in Memory of Alfred Nobel*) in 1997. The focus of this section is on barrier contracts, i.e. contracts that depend on whether or not a stock price stays within certain boundaries. This allows us to use the first-exit time results from *Chapter 2*.

The second part of this chapter (*Section 3.2*) deals with the usually very risky asset class Private Equity (PE). Since the term "Private" stands for investments that are not listed on stock exchanges, the main issue of this asset class is the scarcity of available data. Calculating risk indicators for PE-sponsored companies is considerably more difficult compared to publicly listed, and therefore continuously or at least frequently valued, companies. This leads to serious difficulties if one wants to quantify the risks inherent in PE transactions. We provide a valuation model that explicitly accounts for the characteristics of PE (i.e. high leverage, high default risk, scarcity of data,...) and allows us to obtain implied risk measures. Within a cooperation with the *Center for Entrepreneurial and Financial Studies*, Technische Universität München (Prof. Dr. Dr. A.-K. Achleitner), we were able to test our results empirically on a unique PE database. This allowed us to examine the risk of PE transactions over time and to identify factors that determine the riskiness of a PE transaction.

Finally, *Section 3.3* gives a short note on applications of first-exit times in the insurance industry. Here, any insurance company has to ensure that its risk reserves are sufficient to cover the claims of all its policyholders. In the worst case, negative risk reserves lead to a default of the insurance company.

3.1 Pricing barrier derivatives

The simplest and most popular financial model, named Black–Scholes model (see Black and Scholes [1973]) assumes that the stock price process evolves as a geometric Brownian motion. Risk-free interest rate $r_t = r \in \mathbb{R}$ and volatility $\sigma > 0$ do not vary over time, i.e. the stock price process $S = \{S_t\}_{t\geq 0}$ is given by the stochastic differential equation (sde)

$$\frac{dS_t}{S_t} = r\,dt + \sigma\,dW_t, \quad S_0 > 0\,. \tag{3.1}$$

Apart from the stock, one can invest in a risk-free bank account $\mathcal{B}_t := \exp(rt)$. Note that (by an application of a standard theorem in Mathematical Finance – Itô's Lemma) the stock price process S can also be written as an exponential of a Brownian motion with drift $\mu = r - \sigma^2/2$ and volatility σ, i.e. $S_t = S_0 \exp(B_t)$. This provides us with the connection to all the results in *Chapter 2*: We are now able to apply first-exit times to the pricing of financial contracts.

In model (3.1), many financial contracts can be priced analytically, a fact that is rare at least for complex (i.e. path-dependent) payoff schemes. The most frequently and liquidly traded options on exchanges are *(vanilla) call options*. If the stock price at maturity T stays above a given strike $K_T := K_0 \exp(\int_0^T r_t dt)$, the option holder receives $(S_T - K_T)$, otherwise the option expires worthless. Under the risk-neutral measure $\mathbb{Q}$, this option is priced as

$$C_K(S_0, T) := \frac{1}{\mathcal{B}_T}\,\mathbb{E}_{\mathbb{Q},S_0}\big[\max(S_T - K_T, 0)\big],$$

where we denote $\mathbb{E}_{\mathbb{Q},x}[\,\cdot\,] := \mathbb{E}_{\mathbb{Q}}[\,\cdot \mid S_0 = x]$. In the Black–Scholes model, (vanilla) call options with strike K_T were first priced by the seminal paper Black and Scholes [1973] as

$$C_K(S_0, T) = S_0\,\Phi\big(d_1\big) - K_0\,\Phi\big(d_1 - \sigma\sqrt{T}\big),$$

where $d_1 := \big(\ln(S_0/K_0) + \sigma^2 T/2\big)/\big(\sigma\sqrt{T}\big)$. Due to their popularity and liquidity, call options are often used to calibrate financial models (see, e.g., *Section 3.1.3*).

In *Section 3.1.1*, we expand the Black–Scholes model to stochastic volatility by introducing a (continuous) stochastic time change. If this time change is independent of W, we are still able to price many complex derivatives.

Barrier derivatives are among the most liquidly traded over-the-counter (OTC) products. Their payout depends on whether the underlying crosses some prespecified level(s) until the maturity of the contract. If the final payoff depends on an upper and a lower threshold (contracts termed "double barrier derivatives"), barrier products constitute a simple possibility to obtain a long/short position in volatility.

Closed-form prices for barrier derivatives were first obtained in the Black–Scholes model; the single barrier pricing formulas can be referred to, for example, Black and Cox [1976] or Reiner and Rubinstein [1991]. Later, those results were extended to (stochastic and local) volatility models that fulfill certain symmetry conditions in the return distribution (see, e.g., Derman et al. [1994], Carr et al. [1998], Dupont [2002], Carr and Lee [2009], Carr et al. [2011]). Related to this work, several authors price barrier derivatives analytically (for example by fast Fourier techniques (FFT)) for special cases of the stochastic volatility models of Heston (see, e.g., [Lipton, 2001, p. 235], Carr et al. [2003], Sepp [2006], Kammer [2007], Escobar et al. [2011]) and Stein–Stein (see, e.g., Götz [2011]). Those extensions allow to include important stylized facts that are criticized in the Black–Scholes model: (1) volatility varies over time (stochastic volatility) and (2) implied volatility depends on the strike price (smile feature).

The contribution of this section is as follows:

- We review existing results on the pricing and risk management of double barrier derivatives under stochastic volatility and present an alternative and simple proof for the price of double barrier derivatives based on the reflection principle. We aim at providing a reader friendly recipe on pricing and statistically hedging double barrier derivatives under stochastic volatility. We provide a toolbox of (single and multi-factor) stochastic volatility models that allow to price barrier derivatives in closed-form, an aspect that has not been the prime focus of earlier works. Examples include single and multi-factor CIR-type stochastic volatility (which is the type of volatility used in Heston [1993], Schöbel and Zhu [1999], Christoffersen et al. [2009]), or the Stein and Stein [1991] model. Jump processes for the volatility are also discussed, an idea that was applied in the Barndorff-Nielsen and Shephard [2001] model.
- We show that the existing results based on fast Fourier pricing (FFT) techniques can significantly be improved in terms of computational efficiency. Double barrier derivatives can (in the same stochastic volatility setting) be priced by rapidly con-

verging infinite series, following the ideas presented in *Section 2.4*. In contrast to Fourier techniques, this result avoids the integration over contours of the complex plane and is (in all examples we considered) faster than FFT.

Increasingly popular and numerically demanding tasks like the pricing and risk management of large portfolios of barrier derivatives or their calibration to over-the-counter prices (see, e.g., Carr and Crosby [2010] and Kilin [2011]) have flagged the need for fast and reliable numerical techniques. Closed-form prices for barrier derivatives in (special cases of) several well-known models can be used as a benchmark to assess the performance of other numerical techniques or as a control variate for variance reduction in Monte–Carlo simulations.

3.1.1 Stochastic volatility model

On the probability space $(\Omega, \mathcal{F}, \mathbb{Q})$, we consider – as an extension of the Black–Scholes model in Equation (3.1) – the stock price process

$$\frac{dS_t}{S_t} = r_t\,dt + \sigma_t\,dW_t, \quad S_0 > 0, \tag{3.2}$$

where $W = \{W_t\}_{t\geq 0}$ is a standard Brownian motion, $\{\sigma_t\}_{t\geq 0} > 0$ the (stochastic) volatility, independent of W, and $\{r_t\}_{t\geq 0}$ the (deterministic) risk-less interest rate[1]. The processes satisfy the regularity conditions $\int_0^t |r_s|\,ds < \infty$ and $\mathbb{E}_{\mathbb{Q}}\big[\int_0^t \sigma_s^2\,ds\big] < \infty$ for all $t \geq 0$. We define a (lower) barrier $D_t = D_0 \exp(\int_0^t r_s ds)$ and an (upper) barrier $P_t = P_0 \exp(\int_0^t r_s ds)$, where $D_0 < S_0 < P_0$.

Still, one can invest in a bank account $\mathcal{B}_t := \exp(\int_0^t r_s\,ds)$. Similar to *Chapter 2*, the first-exit time is denoted by[2]

$$T_{P,D} := \inf\big\{t \geq 0 \,|\, S_t \notin (D_t, P_t)\big\}, \tag{3.3}$$

where $\inf\{\emptyset\}=\infty$. Besides, $T^+_{P,D} := T_{P,D}$, $T^-_{P,D} := \infty$ if $S_{T_{P,D}} = P_{T_{P,D}}$ and $T^-_{P,D} := T_{P,D}$, $T^+_{P,D} := \infty$ if $S_{T_{P,D}} = D_{T_{P,D}}$, i.e. if the upper barrier is hit first, we set $T^+_{P,D} := T_{P,D}$; if the lower barrier is hit first, we set $T^-_{P,D} := T_{P,D}$.

For a given maturity T, we want to price financial contracts, for example call, digital, and barrier options or exotic derivatives like bonus certificates.

[1] A comment on generalizations to stochastic interest rates is given in Remark 3.

[2] In contrast to *Chapter 2*, we are now working with a geometric Brownian motion S instead of the Brownian motion B. The relation to *Chapter 2* is simple: The first-exit time $T_{P,D}$ is the same as the first-exit time T_{ab} from *Chapter 2* if one works on the process $B := \{\ln(S_t/S_0)\}_{t\geq 0}$ with barriers $a := \ln(P/S_0)$ and $b := \ln(D/S_0)$.

- *Digital options* depend on the whole path of the underlying security S. For a strike $K_T \in [D_T, P_T]$, the holder receives $\mathbb{1}_{\{S_T > K_T\}}$ at maturity T, if the underlying stays above a given barrier $D = \{D_t\}_{t\geq 0}$ (single barrier contract) or within a given corridor (D_t, P_t) (double barrier contract) until maturity T, and 0 otherwise. They are not publicly traded but range amongst the most liquidly traded over-the-counter (OTC) derivatives (see, e.g., Carr and Crosby [2010]). Single, respectively double, barrier contracts are priced as

$$I_K\big(S_0; D, T\big) := \frac{1}{\mathcal{B}_T}\,\mathbb{E}_{\mathbb{Q},S_0}\big[\mathbb{1}_{\{T_{\infty,D}>T\}}\big], \quad I_K\big(S_0; D, P, T\big) := \frac{1}{\mathcal{B}_T}\,\mathbb{E}_{\mathbb{Q},S_0}\big[\mathbb{1}_{\{T_{P,D}>T\}}\big].$$

- *Barrier options* are another popular path-dependent exotic option. If the underlying stays above a given barrier $D = \{D_t\}_{t\geq 0}$ (single barrier contract) or within a given corridor (D_t, P_t) (double barrier contract) until maturity T, the holder receives the payoff of a (vanilla) call option. Else, the option expires worthless. Due to this additional feature, barrier options are cheaper than (vanilla) call options. They can be priced as

$$\begin{aligned} DOC_K\big(S_0; D, T\big) &:= \frac{1}{\mathcal{B}_T}\,\mathbb{E}_{\mathbb{Q},S_0}\big[\mathbb{1}_{\{T_{\infty,D}>T\}}\,\max(S_T - K_T, 0)\big], \\ DOC_K\big(S_0; D, P, T\big) &:= \frac{1}{\mathcal{B}_T}\,\mathbb{E}_{\mathbb{Q},S_0}\big[\mathbb{1}_{\{T_{P,D}>T\}}\,\max(S_T - K_T, 0)\big]. \end{aligned}$$

- *Bonus certificates* constitute one example of a rather exotic derivative that is rarely traded on exchanges. It is, however, possible to hedge this kind of derivative by a portfolio of some of the aforementioned standard products. For a given bonus level $L_T := L_0\,\exp(\int_0^T r_t dt) \geq D_T$, the holder receives the maximum of this bonus level and the stock price at maturity S_T if the stock price stays above a given barrier $D = \{D_t\}_{t\geq 0}$ until maturity T. If the barrier is hit, the payoff at time T equals the stock price S_T. Its (risk-neutral) price is written as

$$BO_L(S_0; D, T) := \frac{1}{\mathcal{B}_T}\,\mathbb{E}_{\mathbb{Q},S_0}\big[\mathbb{1}_{\{T_{\infty,D}>T\}}\,\max(S_T, L_T) + \mathbb{1}_{\{T_{\infty,D}\leq T\}}\,S_T\big].$$

This is, of course, not a complete list of available contracts. However, many complex derivatives can (similar to the example on bonus certificates) be replicated by call, digital, or barrier options. In the following, we want to concentrate on so-called barrier contracts, i.e. derivatives that depend on whether or not $\{S_t\}_{t\geq 0}$ crosses the thresholds $D = \{D_t\}_{t\geq 0}$ or $P = \{P_t\}_{t\geq 0}$ (we have that the initial stock price $S_0 \in (D_0, P_0)$). Examples include the aforementioned *digital options*, *barrier options*, and *bonus certificates*.

We consider contracts $X_{D,P}^{g(S_T)}(S_0)$ whose payoff is $g(S_T)$ (where $\mathbb{E}_{\mathbb{Q}}[g(S_T)] < \infty$) if none of the barriers D or P is hit until maturity T (and 0 otherwise). The price of those contracts is in the double barrier version given by

$$X_{D,P}^{g(S_T)}(S_0) := \frac{1}{\mathcal{B}_T}\,\mathbb{E}_{\mathbb{Q},S_0}\big[\mathbb{1}_{\{T_{P,D}>T\}}\,g(S_T)\big]. \tag{3.4}$$

A special case are single barrier contracts, i.e.

$$X_{D,\infty}^{g(S_T)}(S_0) := \frac{1}{\mathcal{B}_T}\,\mathbb{E}_{\mathbb{Q},S_0}\big[\mathbb{1}_{\{T_{\infty,D}>T\}}\,g(S_T)\big]. \tag{3.5}$$

Black–Scholes model

In the Black–Scholes model, we obtain a closed-form pricing formula for (single) digital options (see, e.g., Schrödinger [1915], Black and Cox [1976], Folks and Chhikara [1978])

$$I_K\big(S_0;D,T\big) = \frac{1}{\mathcal{B}_T}\left[\Phi\Big(\frac{\ln(S_0/K_0)-\sigma^2T/2}{\sigma\sqrt{T}}\Big) - \frac{S_0}{D_0}\,\Phi\Big(\frac{\ln(D_0^2/(S_0K_0))-\sigma^2T/2}{\sigma\sqrt{T}}\Big)\right].$$

Further, (single) barrier options are priced as (see, e.g., Reiner and Rubinstein [1991])

$$DOC_K(S_0;D,T) = C_K\big(S_0,T\big) - \frac{S_0}{D_0}\,C_K\big(D_0^2/S_0,T\big).$$

Remarkably, the path dependent barrier options can be replicated by a portfolio of (vanilla) call options. This is also possible for more complex payoffs like double barrier options or bonus certificates, see the following.

Stochastic clock

There are many ways to parameterize the stochastic volatility model (3.2). This section discusses some of the most famous examples that are used by both practitioners and academics. These include the CIR-type stochastic volatility, which is the type of volatility used in the Heston [1993] or Christoffersen et al. [2009] model. If the volatility follows an Ornstein–Uhlenbeck (OU) process, this results in the Stein and Stein [1991] model. Jump processes for the volatility are discussed, an idea that was applied in the Barndorff-Nielsen and Shephard [2001] model. Finally, we consider a regime-switching volatility, i.e. the volatility jumps between a finite set of discrete values.

We explicitly discuss richer volatility structures including multiple risk factors. Multi-factor models have become very popular in modeling short rates where it is widely accepted

that one factor is not sufficient to capture the time and cross-sectional variation in the term structure; however, their application has only recently reached the area of option pricing (see, e.g., Christoffersen et al. [2009]).

Example 7 first presents the Heston-type stochastic volatility model.

Example 7 (Heston-type stochastic volatility)
The Heston [1993] model has been introduced as

$$\begin{aligned} \frac{dS_t}{S_t} &= r_t\,dt + \sqrt{v_t}\,dW_t, \quad S_0 > 0, \\ dv_t &= \theta(\nu - v_t)dt + \gamma\sqrt{v_t}\,d\tilde{W}_t, \quad v_0 > 0, \end{aligned} \tag{3.6}$$

where θ, ν, and γ are non-negative constants; $\{\tilde{W}_t\}_{t\geq 0}$ and $\{W_t\}_{t\geq 0}$ one-dimensional Brownian motions with correlation ρ. The Feller condition, see Feller [1951], $2\theta\nu > \gamma^2$ guarantees that the process is almost surely positive. The characteristic function of the log-asset price of the Heston model is given by, see Heston [1993], Albrecher et al. [2007], Rollin et al. [2011]

$$\begin{aligned} \varphi_T(u, S_0) = \mathbb{E}\big[e^{iu\ln(S_T)}\big] &= \exp\left(iu\ln(S_0) + iu\int_0^T r_t\,dt\right) \\ &\cdot \left(\frac{\exp(\theta T/2)}{\cosh(\varrho T/2) + \frac{\xi}{\varrho}\sinh(\varrho T/2)}\right)^{\frac{2\theta\nu}{\gamma^2}} \exp\left(-\frac{v_0}{\varrho}\,\frac{(iu+u^2)\sinh(\varrho T/2)}{\cosh(\varrho T/2) + \frac{\xi}{\varrho}\sinh(\varrho T/2)}\right), \end{aligned} \tag{3.7}$$

where $\varrho := \sqrt{(\theta - \gamma\rho iu)^2 + \gamma^2(iu+u^2)}$ and $\xi := \theta - \gamma\rho ui$. The special case $\rho = 0$ is considered in, e.g., Ball and Roma [1994], [Lipton, 2001, p. 235], Carr et al. [2003], Sepp [2006], Kammer [2007], Escobar et al. [2011], and Pistorius and Stolte [2012].

It is possible to model the variance as a linear combination of several independent CIR processes. The two factor case is considered, in, e.g., Götz [2011], Kiesel and Lutz [2011], Escobar and Götz [2012], see also *Section 4.1.*

If the volatility is of OU-type, we obtain the Stein and Stein [1991] stochastic volatility model (later extended by Schöbel and Zhu [1999]), see Example 8.

Example 8 (Stein–Stein model)
Stein and Stein [1991] introduce the following stochastic volatility model

$$\begin{aligned} \frac{dS_t}{S_t} &= r_t\,dt + \sigma_t\,dW_t, \quad S_0 > 0, \\ d\sigma_t &= \xi(\sigma_t - \varkappa)dt + k\,d\tilde{W}_t, \quad \sigma_0 > 0, \end{aligned} \tag{3.8}$$

where ξ, $\varkappa$, and k are positive constants; $\{\tilde{W}_t\}_{t\geq 0}$ and $\{W_t\}_{t\geq 0}$ independent one-dimensional Brownian motions. In this model, the volatility is governed by an arithmetic Ornstein–Uhlenbeck process with a tendency to revert back to a long-run average level of $\varkappa$. The characteristic function of the log-asset price is given by, see, for example, Stein and Stein [1991]

$$\begin{aligned} \varphi_T(u) = \mathbb{E}\big[e^{iu\ln(S_T)}\big] &= \exp\left(iu\ln(S_0) + iu\int_0^T r_t\,dt\right) \\ &\cdot \exp\Big(L\big((iu+u^2)/2\big)\sigma_0^2/2 + M\big((iu+u^2)/2\big)\sigma_0 + N\big((iu+u^2)/2\big)\Big), \end{aligned} \tag{3.9}$$

where the functions $L(u)$, $M(u)$, and $N(u)$ are defined in Appendix A.1.

Similar to the Heston model, Exercise 8 can be extended to several risk factors, allowing for richer volatility structures.

Jumps in the volatility process have also become stylized facts, see – among many others – Naik [1993], Barndorff-Nielsen and Shephard [2001], and Eraker et al. [2003]. While a jump in returns has no impact on the future distribution of returns, jumps in volatility are highly persistent. Barndorff-Nielsen and Shephard [2001] assume that (external) shocks lead to a sudden increase in volatility. Then, volatility gradually returns to its original level (see Example 9). Those kind of processes are also popular in insurance applications, see, for example, Dassios and Jang [2003].

Example 9 (Jumps in the volatility)
Barndorff-Nielsen and Shephard [2001] propose a stochastic volatility model with jumps in the volatility process:

$$\begin{aligned} \frac{dS_t}{S_t} &= r_t\,dt + \sqrt{v_t}\,dW_t, \quad S_0 > 0, \\ v_t &= v_0\exp(-\delta t) + \sum_{s_i\leq t} M_i \exp\big(-\delta(t-s_i)\big), \end{aligned} \tag{3.10}$$

where $v_0 > 0$ is the initial variance, $\delta > 0$ the exponential decay rate, $\{s_i\}_{i=1}^{\infty}$ are the jump times of a time-homogeneous Poisson process with intensity $\psi > 0$, and M_i are the jump

sizes with distribution $G(y)$, $y > 0$. The characteristic function of the log-asset price is given by, see, for example, Dassios and Jang [2003]

$$\varphi_T(u, S_0) = \mathbb{E}\big[e^{iu\ln(S_T)}\big] = \exp\left(iu\ln(S_0) + iu\int_0^T r_t\,dt - \frac{(iu+u^2)v_0}{2\delta}\big(1-\exp(-\delta T)\big)\right)$$
$$\cdot\exp\left(-\psi\int_0^T\left[1-\hat{g}\left(\frac{(iu+u^2)}{2\delta}\big(1-\exp(\delta(T-t))\big)\right)\right]dt\right), \tag{3.11}$$

where $\hat{g}(u) := \int_0^\infty \exp(-uy)\,dG(y)$ is the Laplace transform of the jump size distribution $G(y)$, $y > 0$. Special cases include, for example, Exp(ζ)-distributed jumps for a parameter $\zeta > 0$, i.e. $\hat{g}(u) = 1/(1+u/\zeta)$. For applications in insurance or finance see, for example, Cox and Isham [1980], Dassios and Jang [2003].

Another simple parameterization of model (3.2) is a regime switching volatility. In Example 10, the volatility jumps between finitely many states.

Example 10 (Regime switching volatility)
A very simple way to include stochastic volatility are so-called Markov-switching models, proposed by Hamilton [1989]. Then, the volatility σ is state dependent and can (only) take finitely many values. A Markov chain models the transition between those values. We set

$$\frac{dS_t}{S_t} = r_t\,dt + \sigma_{Z_t}\,dW_t, \quad S_0 > 0, \tag{3.12}$$

where $Z = \{Z_t\}_{t\geq 0}$, $Z_t \in \mathbb{N}_0 \in \{1, 2, \ldots, M\}$ is a time-homogeneous Markov chain. An intensity matrix Q_0 models the transition between the different states of the Markov chain. The characteristic function of the log-asset price is then given by

$$\varphi_T(u, S_0) := \mathbb{E}\big[e^{iu\ln(S_T)}\big] = \exp\left(iu\ln(S_0) + iu\int_0^T r_t\,dt\right)$$
$$\cdot\left\langle\exp\left(Q_0T - \begin{pmatrix}\frac{1}{2}\sigma_1^2u^2 & 0 & \ldots\\ 0 & \frac{1}{2}\sigma_2^2u^2 & \ldots\\ \ldots & \ldots & \ldots\end{pmatrix}T\right)\pi,\,\mathbf{1}\right\rangle, \tag{3.13}$$

where $\pi := (\mathbb{Q}(Z_0 = 0), \mathbb{Q}(Z_0 = 1), \ldots)'$ is the initial distribution on the states, $\langle\,\cdot\,\rangle$ denotes the scalar product, and $\exp(\,\cdot\,)$ the matrix exponential.

In the following, closed-form prices for barrier contracts in the stochastic volatility framework (3.2) are presented. To obtain those results, the assumption of independence between return and volatility observations is vital. Only this assumption allows us to derive prices that do not depend on the whole path of the underlying security. In more general settings, one has to rely on (possibly computationally challenging) numerical algorithms (see, e.g.,

Griebsch and Wystup [2011] or *Section 2.5*). In the following sections, we provide two approaches to price the single and double barrier contracts:

- *Fourier pricing*: According to Carr et al. [1998], Carr and Madan [1999], and Raible [2000] digital and call options can efficiently be priced by fast Fourier transform (FFT) methods. Barrier contracts can in framework (3.2) (often) be replicated by portfolios of (vanilla) call and digital options (see, e.g., Carr and Lee [2009]).
- *Time-change representation*: The model class (3.2) can be represented as a time-changed Brownian motion. Following the ideas in *Section 2.4*, this allows us to price double barrier contracts by rapidly converging infinite series.

Fourier pricing

Before considering the more complicated case of barrier contracts, the concept of fast Fourier pricing – as developed in Carr and Madan [1999] and Raible [2000] – is introduced. If the characteristic function of the log-asset price $\varphi_T(u, S_0) := \mathbb{E}\big[e^{iu\ln(S_T)}\big]$ is known, for a given strike $K_T := K_0 \exp(\int_0^T r_t\,dt)$, closed-form expressions for (1) the price of a (vanilla) call option $C_K(S_0, T)$ and (2) the probability of exceeding the strike price at maturity $\mathbb{Q}_{S_0}(S_T > K_T)$ are available (see Lemma 4). The presented integrals can efficiently be evaluated using fast Fourier techniques (see, e.g., Carr and Madan [1999] and Raible [2000]).

Lemma 4 (Fast Fourier pricing (FFT))
Consider the stochastic volatility model (3.2). The price of a (vanilla) call option is given by

$$C_K(S_0,T) = \frac{1}{\mathcal{B}_T}\frac{e^{-\alpha\ln(K_T)}}{\pi}\int_0^\infty \mathrm{Re}\left[e^{-iu\ln(K_T)}\,\frac{\varphi_T\big(u-(1+\alpha)i, S_0\big)}{\alpha^2+\alpha-u^2+i(2\alpha+1)u}\right]du, \tag{3.14}$$

where $\mathrm{Re}(x+iy) = x$ *denotes the real part of a complex number* $x+iy$*, where* $x, y \in \mathbb{R}$*.* $\varphi_T(u, S_0) = \mathbb{E}\big[e^{iu\ln(S_T)}\big]$ *is the characteristic function of* $\ln(S_T)$*. The damping factor* $\alpha > 0$ *is usually chosen in the interval* $[1, 2]$*; for a more detailed discussion, we refer to Carr and Madan [1999]. The probability of exceeding the strike price at maturity is*

$$\mathbb{Q}_{S_0}(S_T > K_T) = \frac{1}{2} + \frac{1}{\pi}\int_0^\infty \mathrm{Re}\left[\frac{e^{-iu\ln(K_T/S_0)}\,\varphi_T\big(u-i, S_0\big)}{iu\,\varphi_T(-i, S_0)}\right]du, \tag{3.15}$$

where $\mathbb{Q}_x(\,\cdot\,) := \mathbb{Q}(\,\cdot \mid S_0 = x)$*.*

Theorem 11 presents the price of a barrier contract in the stochastic volatility model (3.2). We provide an intuitive proof in the Appendix showing that Girsanov's theorem and the

reflection principle can still be applied in the present framework. Using slightly more general assumptions, this result is given in Carr and Lee [2009].

Theorem 11 (Barrier contracts I)
In model (3.2), consider a lower barrier $D = \{D_t\}_{t\geq 0}$ and an upper barrier $P = \{P_t\}_{t\geq 0}$ with $D_0 < S_0 < P_0$. In this setting, derivatives with payoff $\mathbb{1}_{\{T_{P,D}>T\}}\, g(S_T)$ (where $\mathbb{E}_{\mathbb{Q}}[g(S_T)] < \infty$) can be priced.

(a) In the single barrier case this price is given by

$$X_{D,\infty}^{g(S_T)}(S_0) = \frac{1}{\mathcal{B}_T}\left(\mathbb{E}_{\mathbb{Q},S_0}\Big[\mathbb{1}_{\{S_T>D_T\}}\, g(S_T)\Big] - \frac{S_0}{D_0}\,\mathbb{E}_{\mathbb{Q},D_0^2/S_0}\Big[\mathbb{1}_{\{S_T>D_T\}}\, g\left(S_T\right)\Big]\right). \quad (3.16)$$

(b) In the double barrier case this price is given by

$$X_{D,P}^{g(S_T)}(S_0) = \frac{1}{\mathcal{B}_T}\sum_{n=-\infty}^{\infty}\frac{D_0^n}{P_0^n}\left(\mathbb{E}_{\mathbb{Q},S_0^{(2n)}}\Big[\mathbb{1}_{\{S_T\in(D_T,P_T)\}}\, g(S_T)\Big] - \frac{S_0}{D_0}\,\mathbb{E}_{\mathbb{Q},S_0^{(2n-1)}}\Big[\mathbb{1}_{\{S_T\in(D_T,P_T)\}}\, g(S_T)\Big]\right), \quad (3.17)$$

where $S_0^{(2n)} := S_0 P_0^{2n}/D_0^{2n}$ and $S_0^{(2n-1)} := P_0^{2n}/(D_0^{2n-2}S_0)$, $n \in \mathbb{Z}$.

Note that the expectations do not depend on the whole path $\{S_t\}_{t\geq 0}$ of the security, but on the integrated quantities $S_T = S_0 \exp\big(\int_0^T (r_t - \sigma_t^2/2)\,dt + \int_0^T \sigma_t\, dW_t\big)$, $D_T = D_0 \exp(\int_0^T r_t\, dt)$, and $P_T = P_0 \exp(\int_0^T r_t\, dt)$.

Proof. See, for example, Carr and Lee [2009]. An alternative proof using the reflection principle is presented in *Appendix A.2.* □

We now give some explicit payoffs $g(S_T)$ to apply the results of Theorem 11. Example 11 deals with (double) digital options, Example 12 with (double) barrier options, and, finally, Example 13 with bonus certificates.

Example 11 ((Double) digital options)
Consider the stochastic volatility model (3.2). Recall that a digital option with strike $K_T := K_0 \exp(\int_0^T r_t\, dt) \in [D_T, P_T]$ pays $\mathbb{1}_{\{S_T>K_T\}}$ at maturity T if the security stays within the corridor (D_t, P_t) until T. In the single barrier case (i.e. $P_0 \to \infty$, $g(S_T) = \mathbb{1}_{\{S_T>K_T\}}$), Theorem 11(a) yields

$$I_K(S_0; D, T) = \frac{1}{\mathcal{B}_T}\Big[\mathbb{Q}_{S_0}\big(S_T > K_T\big) - \frac{S_0}{D_0}\,\mathbb{Q}_{D_0^2/S_0}\big(S_T > K_T\big)\Big]. \quad (3.18)$$

In the general case, we obtain from Theorem 11(b) that

$$I_K(S_0;D,P,T)=\frac{1}{\mathcal{B}_T}\sum_{n=-\infty}^{\infty}\frac{D_0^n}{P_0^n}\Big(\mathbb{Q}_{S_0^{(2n)}}\big(S_T\in(K_T,P_T)\big)-\frac{S_0}{D_0}\,\mathbb{Q}_{S_0^{(2n-1)}}\big(S_T\in(K_T,P_T)\big)\Big),$$

where $S_0^{(2n)}:=S_0P_0^{2n}/D_0^{2n}$ *and* $S_0^{(2n-1)}:=P_0^{2n}/(D_0^{2n-2}S_0)$, $n\in\mathbb{Z}$. *The probabilities* $\mathbb{Q}_\cdot(\,\cdot\,)$ *can be evaluated using FFT, see Lemma 4. In the Black–Scholes model (which is the special case* $r_t\equiv r\in\mathbb{R}$, $\sigma_t\equiv\sigma>0$, *for all* $t\geq 0$*), digital options were priced by, for example, Schrödinger [1915], Darling and Siegert [1953], Black and Cox [1976], Folks and Chhikara [1978], Geman and Yor [1996], Lin [1999].*

Example 12 ((Double) barrier options)
Consider the stochastic volatility model (3.2). Recall that a barrier option with strike $K_T:=K_0\,\exp(\int_0^T r_t\,dt)\in[D_T,P_T]$ *pays* $\max(S_T-K_T,0)$ *(call option) or* $\max(K_T-S_T,0)$ *(put option) at maturity* T *if the security stays within the corridor* (D_t,P_t) *until* T. *In the single barrier case (i.e.* $P_0\to\infty$*), we distinguish barrier call options (payoff function* $g(S_T)=\max(S_T-K_T,0)$*) and barrier put options (*$g(S_T)=\max(K_T-S_T,0)$*).*
Theorem 11(a) then yields

$$DOC_K(S_0;D,T)=C_K\big(S_0,T\big)-\frac{S_0}{D_0}\,C_K\big(D_0^2/S_0,T\big), \tag{3.19}$$

$$\begin{aligned}DOP_K(S_0;D,T)&=P_K\big(S_0,T\big)-\frac{S_0}{D_0}\,P_K\big(D_0^2/S_0,T\big)\\&=DOC_K(S_0;D,T)+(K_0-S_0)-\frac{S_0}{D_0}(K_0-S_0),\end{aligned} \tag{3.20}$$

where $P_K(S_0,T):=C_K(S_0,T)-S_0+K_0$. *Call options are priced by FFT, see Lemma 4. The case* $0\leq K_0\leq D_0$ *can be treated similarly. The price of double barrier options with conditional payoff function* $g(S_T)=\max(S_T-K_T,0)$ *in Theorem 11(b), is*

$$\begin{aligned}DOC_K(S_0;D,P,T)=\frac{D_0^n}{P_0^n}\sum_{n=-\infty}^{\infty}\Big[&C_K\big(S_0^{(2n)},T\big)-C_P\big(S_0^{(2n)},T\big)+(P_0-K_0)\,I_P\big(S_0^{(2n)};P,T\big)\\&-\frac{S_0}{D_0}\,\Big(C_K\big(S_0^{(2n-1)},T\big)-C_P\big(S_0^{(2n-1)},T\big)+(P_0-K_0)\,I_P\big(S_0^{(2n-1)};P,T\big)\Big)\Big],\end{aligned}$$

where $S_0^{(2n)}:=S_0P_0^{2n}/D_0^{2n}$ *and* $S_0^{(2n-1)}:=P_0^{2n}/(D_0^{2n-2}S_0)$, $n\in\mathbb{Z}$. *In the Black–Scholes model, prices for double barrier options have – for different parameterizations – been presented in the literature (see, e.g., Geman and Yor [1996], Lin [1999], Pelsser [2000]). The presented equations, however, often tend to be rather complicated and usually lack the intuitive (and for replication very convenient) interpretation as a portfolio of infinitely many call options.*

Example 13 (Bonus certificates)
Consider the stochastic volatility model (3.2). For a barrier $D = \{D_t\}_{t\geq 0}$ and a given bonus level $L_T := L_0 \exp(\int_0^T r_t\,dt) \geq D_T$, the payoff at maturity T is given by

$$\text{payoff}(T) = \begin{cases} \max(S_T, L_T), & T_{\infty,D} > T, \\ S_T, & \textit{else.} \end{cases} \tag{3.21}$$

Bonus certificates are an example of a rather exotic derivative, nevertheless, they are (especially in Germany) frequently traded. Remarkably, most of these exotic products with complicated payoff features can be replicated by (vanilla) call, digital, or barrier options. In the present case, we find that

$$\begin{aligned} BO_L(S_0; D, T) &= \frac{1}{\mathcal{B}_T}\,\mathbb{E}_{\mathbb{Q},S_0}\Big[\mathbb{1}_{\{T_{\infty,D}>T\}}\max(S_T, L_T) + \mathbb{1}_{\{T_{\infty,D}\leq T\}}S_T\Big] \\ &= \frac{1}{\mathcal{B}_T}\,\mathbb{E}_{\mathbb{Q},S_0}\Big[\mathbb{1}_{\{T_{\infty,D}>T\}}\max(0, L_T - S_T) + S_T\Big] \\ &= \frac{1}{\mathcal{B}_T}\,\mathbb{E}_{\mathbb{Q},S_0}\big[S_T\big] + X_{D,\infty}^{\max(0,L_T-S_T)}(S_0) = S_0 + DOP_L(S_0; D, T). \end{aligned}$$

Since we are able to price call options (see, e.g., Lemma 4) and barrier put options (see, e.g., Example 12) by FFT, this result allows us to price bonus certificates.

Time change representation

For the discounted stock price process $\tilde{S} = \{\tilde{S}_t\}_{t\geq 0} := \{S_t/\mathcal{B}_t\}_{t\geq 0}$, representations as a time-changed Brownian motion are available. The time-change representations are interesting from a numerical point of view: They allow for fast converging infinite series (instead of Laplace or Fourier inversions) for the prices of barrier contracts.
We represent $\tilde{S}$ as a time-changed geometric Brownian motion G_{Λ_t}, i.e.

$$\frac{dG_t}{G_t} = dW_t, \quad G_0 := S_0 > 0\,. \tag{3.22}$$

The time change $\Lambda = \{\Lambda_t\}_{t\geq 0}$ is a (pathwise) continuous and increasing stochastic process with $\Lambda_0 = 0$ and $\lim_{t\to\infty}\Lambda_t = \infty$ $\mathbb{Q}$-a.s., independent of G. If the Laplace transform of Λ_T is known, it is denoted by $\vartheta_T(u) := \mathbb{E}\big[\exp\big(-u\Lambda_T\big)\big]$. Then, the characteristic function of $\ln(\tilde{S}_t)$ $\big(=\ln(G_{\Lambda_t})\big)$ is given by $\tilde{\varphi_T}(u, S_0) = \exp(iu\ln(S_0)) \cdot \vartheta_T\big((iu + u^2)/2\big)$ (see, e.g., Equation (2.3) in Hurd [2009]).

Now, barrier contracts can be priced by rapidly converging infinite series. In contrast to Theorem 11 where one had to compute two Fourier integrals per term, Theorem 12 presents infinite series where each term is just a single evaluation of the Laplace transform

of the time change. This allows for a faster computation and an easier control of the truncation error (error bounds for digital options are given in, for example, Section 2.4 or Hieber and Scherer [2012]). Theorem 12 presents prices for barrier contracts that pay $g(S_T)$ at maturity T if the security stays within the corridor (D_t, P_t) until T.

Theorem 12 (Barrier contracts II)
Consider a time-changed geometric Brownian motion G_{Λ_t} with a (pathwise) continuous time-change Λ, independent of G. Denote by $\vartheta_T(u) := \mathbb{E}[\exp(-u\Lambda_T)]$, $u \geq 0$, the Laplace transform of Λ_T. Then, the price of a derivative with payoff $\mathbb{1}_{\{T_{P,D}>T\}}\, g(S_T)$ (where $\mathbb{E}_{\mathbb{Q}}[g(S_T)] < \infty$) is given by

$$X_{D,P}^{g(S_T)}(S_0) = \frac{1}{\mathcal{B}_T}\frac{2e^{\frac{x}{2}}}{a-b}\sum_{n=1}^{\infty}\vartheta_T\left(\frac{1}{8}+\frac{n^2\pi^2}{2(a-b)^2}\right)\sin\left(\frac{n\pi(x-b)}{a-b}\right)Z_n^{g(S_T)}, \tag{3.23}$$

with $Z_n^{g(S_T)} := \int_b^a e^{-\frac{y}{2}}\sin\left(\frac{n\pi(y-b)}{a-b}\right)g(e^y)dy$, $x := \ln(S_0)$, $a := \ln(P_0)$, and $b := \ln(D_0)$.

Proof. The transition density function $f_{ab}(T, y)$ describes the probability density that the logarithmic stock price process $\{\ln(S_t)\}_{t\geq 0}$ starts at $x := \ln(S_0)$, survives until time T, and ends up in $y := \ln(S_T)$. In the Black–Scholes model, this density is given by (see, e.g., Cox and Miller [1965], Pelsser [2000])[3]

$$f_{ab}(T,y) = \frac{2e^{\frac{x}{2}}}{a-b}\sum_{n=1}^{\infty}e^{-\left(\frac{1}{8}+\frac{n^2\pi^2}{2(a-b)^2}\right)T}e^{-\frac{y}{2}}\sin\left(\frac{n\pi(x-b)}{a-b}\right)\sin\left(\frac{n\pi(y-b)}{a-b}\right).$$

In the Black–Scholes model, we then find that the price of a barrier contract with payoff $\mathbb{1}_{\{T_{P,D}>T\}}\, g(S_T)$ at maturity T is given by

$$\begin{aligned} BS_{D,P}^{g(S_T)}(S_0) &:= \frac{1}{\mathcal{B}_T}\int_b^a f_{ab}(T,y)\, g(e^y)\, dy \\ &= \frac{1}{\mathcal{B}_T}\frac{2e^{\frac{x}{2}}}{a-b}\sum_{n=1}^{\infty}e^{-\left(\frac{1}{8}+\frac{n^2\pi^2}{2(a-b)^2}\right)T}\sin\left(\frac{n\pi(x-b)}{a-b}\right)\left(\int_b^a e^{-\frac{y}{2}}\sin\left(\frac{n\pi(y-b)}{a-b}\right)g(e^y)dy\right). \end{aligned}$$

If the interval $[0, T]$ is continuously transformed to $[0, \Lambda_T]$, the latter expression is the price of a barrier contract conditional on the time change $T = \Lambda_T$. If this time-change has Laplace transform $\vartheta_T(u) := \mathbb{E}[\exp(-u\Lambda_T)]$, $u \geq 0$, we can conclude that

$$\mathbb{E}\left[\mathbb{E}\left[e^{-\left(\frac{1}{8}+\frac{n^2\pi^2}{2(a-b)^2}\right)T}\,\middle|\, T=\Lambda_T\right]\right] = \vartheta_T\left(\frac{1}{8}+\frac{n^2\pi^2}{2(a-b)^2}\right)$$

[3]Note that $\{\ln(G_t)\}_{t\geq 0}$ is a Brownian motion with drift $-1/2$ and unit volatility. The density function $f_{ab}(T, y)$ is an application of Equation (2) in Pelsser [2000] using that $\mu = -1/2$ and $\sigma = 1$.

and then obtain the price of barrier contracts on time-changed geometric Brownian motion

$$X_{D,P}^{g(S_T)}(S_0) = \frac{1}{\mathcal{B}_T}\frac{2e^{\frac{x}{2}}}{a-b}\sum_{n=1}^{\infty}\vartheta_T\left(\frac{1}{8}+\frac{n^2\pi^2}{2(a-b)^2}\right)\sin\left(\frac{n\pi(x-b)}{a-b}\right) \cdot\left(\int_b^a e^{-\frac{y}{2}}\sin\left(\frac{n\pi(y-b)}{a-b}\right)g(e^y)dy\right).$$

□

The result in Theorem 12 can also be used to price options on one barrier. Therefore, the upper barrier is set to a very high value (i.e. $P_0 = 100 \cdot S_0$) that guarantees that the probability of hitting the upper barrier is negligible (i.e. smaller than 1e–16). In our numerical examples (see *Section 3.1.4*), this approach is still significantly faster than FFT techniques.

Theorem 13 is a first application of Theorem 12 to price (double) digital options.

Theorem 13 (Double digital options II)
Consider a time-changed geometric Brownian motion G_{Λ_t} with a (pathwise) continuous time change Λ, independent of G. Denote by $\vartheta_T(u) := \mathbb{E}[\exp(-u\Lambda_T)]$, $u \geq 0$, the Laplace transform of Λ_T . If the strike price is written as $K_T := K_0\exp(\int_0^T r_t\,dt) \in [D_T, P_T]$, the price of a double digital option with payoff $\mathbb{1}_{\{T_{P,D}>T;\,S_T>K_T\}}$ at maturity T is given by

$$I_K\big(S_0; D, P, T\big) = \frac{1}{\mathcal{B}_T}\frac{2e^{\frac{x}{2}}}{a-b}\sum_{n=1}^{\infty}\vartheta_T\left(\frac{1}{8}+\frac{n^2\pi^2}{2(a-b)^2}\right)\sin\left(\frac{n\pi(x-b)}{a-b}\right)Z_n^{g(S_T)},$$

where

$$Z_n^{g(S_T)} = \frac{e^{-\frac{a}{2}}\frac{n\pi(-1)^{n+1}}{a-b} + e^{-\frac{k}{2}}\left(\frac{1}{2}\sin\left(\frac{n\pi(k-b)}{a-b}\right)+\frac{n\pi}{a-b}\cos\left(\frac{n\pi(k-b)}{a-b}\right)\right)}{\frac{1}{4}+\frac{n^2\pi^2}{(a-b)^2}},$$

$x := \ln(S_0)$, $k := \ln(K_0)$, $a := \ln(P_0)$, *and* $b := \ln(D_0)$.

Proof. From Theorem 12, we can conclude that

$$\begin{aligned} Z_n^{g(S_T)} &= \int_b^a e^{-\frac{y}{2}}\sin\left(\frac{n\pi(y-b)}{a-b}\right)g(e^y)dy = \int_k^a e^{-\frac{y}{2}}\sin\left(\frac{n\pi(y-b)}{a-b}\right)dy \\ &= \frac{e^{-\frac{y}{2}}}{\frac{1}{4}+\frac{n^2\pi^2}{(a-b)^2}}\left(-\frac{1}{2}\sin\left(\frac{n\pi(y-b)}{a-b}\right)-\frac{n\pi}{a-b}\cos\left(\frac{n\pi(y-b)}{a-b}\right)\right)\Bigg|_k^a \\ &= \frac{e^{-\frac{a}{2}}\frac{n\pi(-1)^{n+1}}{a-b} + e^{-\frac{k}{2}}\left(\frac{1}{2}\sin\left(\frac{n\pi(k-b)}{a-b}\right)+\frac{n\pi}{a-b}\cos\left(\frac{n\pi(k-b)}{a-b}\right)\right)}{\frac{1}{4}+\frac{n^2\pi^2}{(a-b)^2}}. \end{aligned}$$

In the special case $k = b$, this is a result derived in Hieber and Scherer [2012][4], i.e.

$$Z_n^{g(S_T)} = \frac{e^{-\frac{a}{2}} \frac{n\pi(-1)^{n+1}}{a-b} + e^{-\frac{k}{2}} \frac{n\pi}{a-b}}{\frac{1}{4} + \frac{n^2\pi^2}{(a-b)^2}}.$$

□

The same idea can now be used to price (double) barrier options. Theorem 14 builds on a representation of the Black–Scholes price of a double barrier option that is rarely used in the literature, see, for example, Pelsser [2000].

Theorem 14 (Double barrier options II)
Consider a time-changed Brownian motion G_{Λ_t} with a (pathwise) continuous time change Λ, independent of G. Denote the Laplace transform of Λ_T by $\vartheta_T(u) := \mathbb{E}[\exp(-u\Lambda_T)]$, $u \geq 0$. If the strike price is denoted $K_T := K_0 \exp(\int_0^T r_t\, dt) \in [D_T, P_T]$, the price of a double barrier option with payoff $\mathbb{1}_{\{T_{P,D}>T\}}(S_T - K_T)^+$ is given by

$$DOC_K(S_0; D, P, T) = \frac{2e^{\frac{x}{2}}}{a-b} \sum_{n=1}^{\infty} \vartheta_T\left(\frac{1}{8} + \frac{n^2\pi^2}{2(a-b)^2}\right) \sin\left(\frac{n\pi(x-b)}{a-b}\right) Z_n^{g(S_T)}, \quad (3.24)$$

where

$$Z_n^{g(S_T)} = \frac{\frac{2n\pi}{a-b}(-1)^{n+1} \sinh\left(\frac{a-k}{2}\right) - \sin\left(\frac{n\pi(k-b)}{a-b}\right)}{e^{-\frac{k}{2}}\left(\frac{1}{4} + \frac{n^2\pi^2}{(a-b)^2}\right)},\ x := \ln(S_0),\ k := \ln(K_0),\ a := \ln(P_0),$$

and $b := \ln(D_0)$.

Proof. Applying the results from Theorem 12, we obtain

$$\begin{aligned}
Z_n^{g(S_T)} &= \int_b^a e^{-\frac{y}{2}} \sin\left(\frac{n\pi(y-b)}{a-b}\right) g(e^y)dy = \int_k^a e^{-\frac{y}{2}} \sin\left(\frac{n\pi(y-b)}{a-b}\right) (e^y - e^k)dy \\
&= \frac{\frac{e^{\frac{y}{2}}+e^{k-\frac{y}{2}}}{2} \sin\left(\frac{n\pi(y-b)}{a-b}\right) - \frac{n\pi\left(e^{\frac{y}{2}}-e^{k-\frac{y}{2}}\right)}{a-b} \cos\left(\frac{n\pi(y-b)}{a-b}\right)}{\frac{1}{4} + \frac{n^2\pi^2}{(a-b)^2}} \Bigg|_k^a \\
&= \frac{\frac{n\pi(-1)^{n+1}}{a-b}\left(e^{\frac{a}{2}} + e^{k-\frac{a}{2}}\right) - e^{\frac{k}{2}} \sin\left(\frac{n\pi(k-b)}{a-b}\right)}{\frac{1}{4} + \frac{n^2\pi^2}{(a-b)^2}} \\
&= \frac{\frac{2n\pi(-1)^{n+1}}{a-b} \sinh\left(\frac{a-k}{2}\right) - \sin\left(\frac{n\pi(k-b)}{a-b}\right)}{e^{-\frac{k}{2}}\left(\frac{1}{4} + \frac{n^2\pi^2}{(a-b)^2}\right)}.
\end{aligned}$$

[4]Using that $\sin\left(\frac{n\pi(x-b)}{a-b}\right) = (-1)^n \sin\left(\frac{n\pi(x-a)}{a-b}\right)$, one obtains the results in Hieber and Scherer [2012], Theorem 2 ($\mu = -1/2$, $\sigma = 1$, a generalization to $\mu \in \mathbb{R}$ and $\sigma > 0$ is straightforward).

In the case of Brownian motion ($\Lambda_T = T$) this pricing result is given in, for example, Pelsser [2000]. □

Remark 3 (Stochastic interest rates)
If necessary, it is possible to include stochastic interest rates in the model framework (3.2) while still keeping the analytical tractability. If $\{r_t\}_{t\geq 0}$ *is independent of* $W = \{W_t\}_{t\geq 0}$ *and* $\{\sigma_t\}_{t\geq 0}$*, this is straightforward:* $1/\mathcal{B}_T$ *must simply be replaced by* $\mathbb{E}_{\mathbb{Q}}[1/\mathcal{B}_T]$*. Dependence between* $\{r_t\}_{t\geq 0}$ *and* $\{\sigma_t\}_{t\geq 0}$ *can be introduced as follows:* $r_t := \gamma_t - \rho_* \sigma_t^2$*, where* $\{\gamma_t\}_{t\geq 0}$ *is independent of* $W = \{W_t\}_{t\geq 0}$ *and* $\{\sigma_t\}_{t\geq 0}$*. The correlation parameter* $\rho_* \in \mathbb{R}$ *can be used to include either a positive or a negative dependence between volatility and interest rates. The results in Theorems 13 and 14 can rather easily be modified;* $\vartheta_T\big(\frac{1}{8} + \frac{n^2\pi^2}{2(a-b)^2}\big)$ *then changes to* $\vartheta_T\big(\frac{1}{8} + \frac{n^2\pi^2}{2(a-b)^2} + \rho_*\big)$*. The Fourier pricing results can also easily be adapted.*

Remark 4 (Error bounds)
Similar to Section 2.4.3, one can derive error bounds to truncate the infinite series in Theorems 11 and 12. The interested reader is referred to Escobar et al. [2013].

3.1.2 Regime switching jump-diffusion model

In *Section 2.5*, we have worked with first-exit times of Brownian motion with jumps. This process, however, allows for negative values and is thus not a reasonable model for a stock price process. For $t \geq 0$, we assume that there exists a risk-neutral measure $\mathbb{Q}$ and write the stock price process (under the risk-neutral measure $\mathbb{Q}$) as the exponential of a jump-diffusion process, i.e.

$$S_t := S_0 \exp(B_t) = S_0 \exp\Big(\int_0^t r_s ds - \delta t - \frac{1}{2}\int_0^t \sigma_{Z_s}^2 \, ds + \int_0^t \sigma_{Z_s} \, dW_s + \sum_{i=1}^{N_t^{Z_t}} Y_i \Big), \quad (3.25)$$

where $\{r_t\}_{t\geq 0}$ denotes the risk-free interest rate and δ_{Z_t} the expected relative price change due to the jumps given by $\delta_{Z_t} := \lambda_{Z_t}\big(\mathbb{E}_{\mathbb{Q}}[\exp(Y_1)] - 1\big)$. The other parameters and processes are defined as in *Section 2.5*, i.e. $Z = \{Z_t\}_{t\geq 0} \in \{1, 2, \ldots, M\}$ is a time-homogeneous Markov chain, $W = \{W_t\}_{t\geq 0}$ a standard Brownian motion. Some parameters now depend on Z: volatility $\sigma_{Z_t} > 0$, and time in-homogeneous counting process $N^{Z_t} = \{N_t^{Z_t}\}_{t\geq 0}$, a Poisson process with intensity $\lambda_{Z_t} \geq 0$ at time t. The initial value is $S_0 > 0$. The jump-sizes $Y = \{Y_i\}_{i\geq 1}$ are i.i.d. with distribution $\mathbb{P}_Y$. All processes are mutually independent.

Examples of popular jump size distributions are given in Examples 14 and 15.

Example 14 (Normal jump-diffusion)
The simplest jump size distribution is a normally distributed jump size, a model suggested by Merton [1976] and thus also referred to as Merton jump-diffusion model. Jump sizes Y_i in this specification of model (3.25) are normally distributed, i.e. $Y_i \sim \mathcal{N}(\beta, \gamma^2)$ for $\beta \in \mathbb{R}$ and $\gamma > 0$. Then, the drift adjustment due to the jumps is given by $\delta = \exp(\beta + \gamma^2/2) - 1$.

Example 15 (Double-exponential jump-diffusion)
One popular possibility to model jump sizes is the double-exponential distribution, see, for example, Kou and Wang [2003]:

$$\mathbb{P}_Y(dx) = p\,\alpha_\oplus e^{-\alpha_\oplus x}\mathbb{1}_{\{x\geq 0\}}dx + (1-p)\,\alpha_\ominus e^{\alpha_\ominus x}\mathbb{1}_{\{x<0\}}dx, \tag{3.26}$$

where $0 \leq p \leq 1$ is the probability that jumps have positive sign. Upward jumps are exponentially distributed with parameter $\alpha_\oplus > 1$, downward jumps are exponentially distributed with parameter $\alpha_\ominus > 0$. In this model, we find that $\delta := \lambda\big(\mathbb{E}_\mathbb{Q}[\exp(Y_1)] - 1\big)$ $= \lambda\big(p\alpha_\oplus/(\alpha_\oplus - 1) + (1-p)\alpha_\ominus/(\alpha_\ominus + 1) - 1\big)$.

3.1.3 Model calibration[5]

This section discusses the calibration of the stock price models to vanilla call option prices. Call options are the most liquidly traded derivatives; that is why one is able to obtain reliable prices for various underlyings, strikes, and maturities. In the following, we use a call option data set on the German stock index DAX obtained on 06/02/2012[6]. The evolution of the stock index until that date is displayed in *Figure 3.1*; June 2012 corresponds to calm and slightly rising stock markets with a rather low stock price volatility.

The dataset consists of 658 call option prices $C_K(S_0, T)$ together with the corresponding strike K_T, maturity T, and LIBOR rate r_T. Some statistics are presented in *Table 3.1*.

In *Section 3.1*, Theorem 4, we showed that the price of a call option can efficiently be obtained from the characteristic function $\varphi_T(u, S_0)$ of its log-asset price via fast Fourier Pricing (see, e.g., Carr and Madan [1999], Raible [2000]), i.e.

$$\hat{C}_K(S_0, T) = \frac{1}{\mathcal{B}_T}\,\frac{e^{-\alpha\ln(K_T)}}{\pi}\int_0^\infty \mathrm{Re}\left[e^{-iu\ln(K_T)}\,\frac{\varphi_T\big(u-(1+\alpha)i, S_0\big)}{\alpha^2+\alpha-u^2+i(2\alpha+1)u}\right]du,$$

where $\mathrm{Re}(x+iy) = x$ denotes the real part of a complex number $x+iy$, for x, $y \in \mathbb{R}$. The damping factor $\alpha > 0$ is usually chosen in the interval $[1, 2]$. To calibrate the model, we use an error functional to compare the model prices $\hat{C}_K^{(i)}(S_0, T)$ to the dataset $C_K^{(i)}(S_0, T)$

[5] I want to thank Wim Schoutens (KU Leuven) for fruitful discussions on model calibration during his lecture *Recent Developments in Financial Engineering* (TUM, 2012/13).
[6] Data source: *Reuters*.

Figure 3.1: Evolution of the German stock index DAX from 01/01/2000 to 06/02/2012. *(Data source:* Reuters.*)*

	minimum	average	maximum
maturity T (in years)	0.11	1.19	4.86
strike K_T	2 200	6 109	12 000
LIBOR rate r_T	0.684%	1.330%	2.409%
call price $C_K(S_0, T)$	0.20	1 340.65	4 820.71

Table 3.1: Description of the call option dataset $C_K^{(i)}(S_0, T)$, for $i = 1, 2, \ldots, 658$. The data set consists of vanilla calls on DAX obtained on 06/02/2012 (on that day DAX closed at $S_0 = 6\,764.83$). *(Data source:* Reuters.*)*

(for $i = 1, 2, \ldots, 658$) described in *Table 3.1*. There are many possible choices for this error functional, we choose the *relative mean squared error*, i.e.

$$\epsilon := \sqrt{\mathbb{E}\left[\left(\frac{\hat{C}_K(S_0,T) - C_K(S_0,T)}{C_K(S_0,T)}\right)^2\right]}. \tag{3.27}$$

For our dataset, this error functional is estimated as

$$\epsilon \approx \sqrt{\frac{1}{658}\sum_{i=1}^{658}\left(\frac{\hat{C}_K^{(i)}(S_0,T) - C_K^{(i)}(S_0,T)}{C_K^{(i)}(S_0,T)}\right)^2}.$$

Table 3.2 summarizes the calibration results together with the relative mean squared error ϵ for different models, i.e. the Black–Scholes model, the stochastic volatility models of Heston, Stein–Stein, Barndorff-Nielsen-Shephard (BNS), and regime-switching-type (see Examples 7–10), and the double-exponential jump-diffusion model (D.–Exp.).

model	**parameters**	ϵ
B.–S.	$\sigma = 20.7330\%$	0.06238
Heston ($\rho = 0$)	$(\theta, \nu, \gamma, v_0) = (31.8692, 0.0436, 2.3695, 0.0449)$	0.06193
Heston ($\rho < 0$)	$(\theta, \nu, \gamma, \rho, v_0) = (13.7270, 0.0441, 1.1438, -0.9813, 0.0476)$	0.04191
Stein–Stein	$(\xi, k, \varkappa, \sigma_0) = (0.0428, 0.3379, 0.0010, 0.0866)$	0.06532
BNS	$(\delta, \zeta, \psi, v_0) = (0.0071, 1.5423, 0.0164, 0.0419)$	0.05248
Reg.–sw.	$(k_1, k_2, \lambda_1, \lambda_2, Z_0) = (0.2185, 0.1764, 0.2601, 0.0262, 1)$	0.06073
D.–Exp.	$(\sigma, \lambda, p, \alpha_\ominus, \alpha_\oplus) = (0.2015, 0.0528, \approx 0, 6.5296, \approx 1)$	0.06049

Table 3.2: Calibration results of different models using the parameter set described in Table 3.1. *The examples include the Black–Scholes model (B.–S.), the stochastic volatility models of Heston, Stein–Stein, Barndorff-Nielsen-Shephard (BNS), and regime-switching-type (see Examples 7–10), and the double-exponential jump-diffusion model (D.–Exp.). The relative mean squared error ϵ of the calibrated parameter set is given.*

The best calibration results and a significant improvement relative to the Black–Scholes model (B.–S.) were obtained by the Heston stochastic volatility model. For the double-exponential jump-diffusion model, the calibration results indicate that positive jumps are not significant. This reduces the number of parameters by 2 ($\alpha_\ominus$ and p are no longer necessary) and we are back in the (single) exponential jump-diffusion model. *Figures 3.2* and *3.3* further visualize the calibration performance. A representative sample of call option prices (denoted by "$\circ$") is compared to the model prices (denoted by "+"). On the given data set one observes that – compared to the Black–Scholes model ($\epsilon = 0.06238$) – the exponential jump-diffusion model ($\epsilon = 0.06049$) and the BNS model ($\epsilon = 0.05248$) do only lead to hardly visuable, minor improvements in the calibration performance. However – as one can see in *Figure 3.3* – the Heston model ($\epsilon = 0.04191$) provides a significantly better fit, especially for the long-dated contracts. The Heston model is – in contrast to any Lévy model – flexible enough to fit a term structure of option prices. This is even more important in turbulent periods of rapidly changing economic conditions. Although the Black–Scholes model seems to perform pretty well on this data set, one has to be aware that call options are not path-dependent: The effects of jumps or stochastic volatility tend to diminish over time. Those effects, however, come into play if one is interested in the pricing or risk management of, for example, barrier derivatives or Asian options, where path behavior significantly influences the option price.

In the following, we are examining this effect on the prices of barrier derivatives. Having

calibrated different stock price models to the same dataset allows us to assess the effect of stochastic volatility and jumps on exotic option prices.

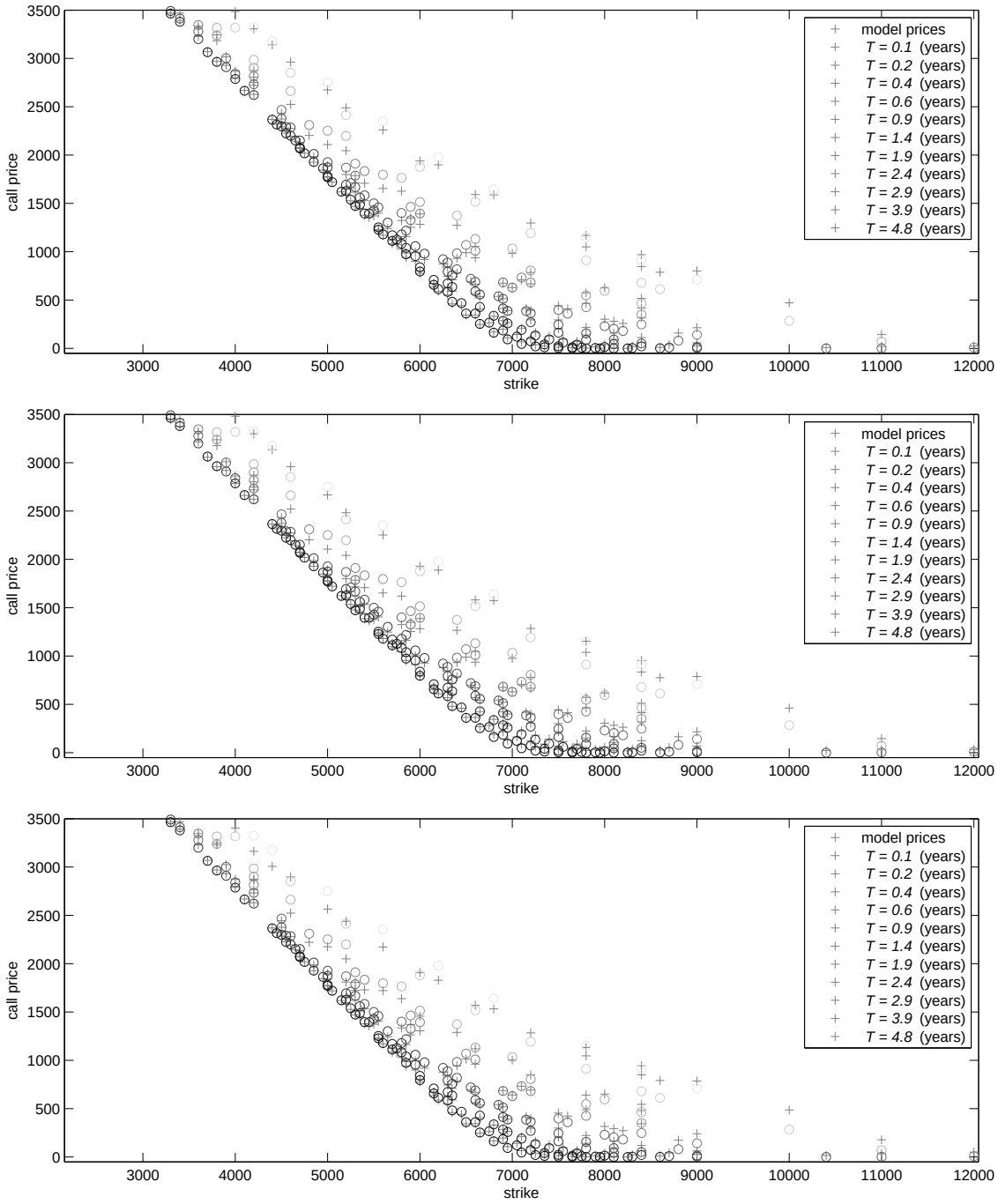

Figure 3.2: Calibration results for the Black–Scholes (top), the double-exponential jump diffusion model (Example 7, middle), and the Barndorff-Nielsen-Shephard model (Example 9, below). Observed market data is denoted by a "∘", model prices by a "+".

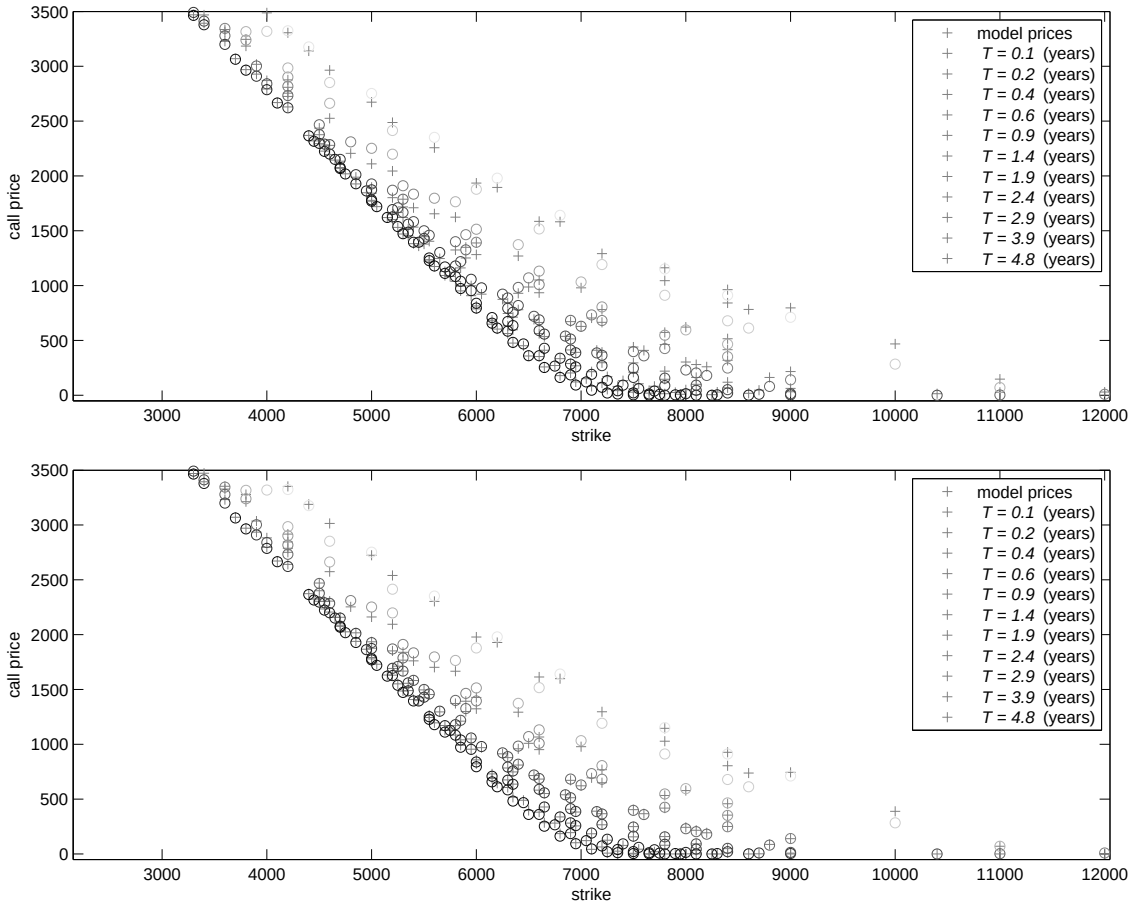

Figure 3.3: Calibration results for the Heston model (Example 7). Observed market data is denoted by a "∘", model prices by a "+". Compared are the calibration results if the correlation between stock price process and volatility is $\rho = 0$ (above) and $\rho < 0$ (below).

3.1.4 Numerical examples

This section uses the parameters calibrated in *Section 3.1.3* to price several financial contracts. We consider both stochastic volatility models and the regime switching jump-diffusion model.

Stochastic volatility model

In this section, we give a numerical example comparing the FFT technique to the analytical expressions using the time change representation of the different models. We compare the results of the one-factor stochastic volatility models, i.e. the Heston and Stein–Stein model, with regard to accuracy and computation time. First, we price digital options. The corresponding pricing formulas are to be found in Example 11 (FFT technique) and Theorem 13 (time change representation). To apply the double barrier result presented in Theorem 13, the upper barrier $a := \ln(P_0)$ is set to $10\sigma\sqrt{T}$, a value that guarantees that the probability of hitting the upper barrier is negligible, i.e. it is smaller than 1e–16. Apart from that, the infinite series has to be truncated. Error bounds for this truncation are easy to obtain, see, for example, *Section 2.4.3* in *Chapter 2* or Hieber and Scherer [2012]. In our parameter sets, $N = 90$ terms turned out to be enough to obtain an acceptable relative pricing error.

Table 3.3 gives the results for different parameter sets in the Black–Scholes, the Heston, and the Stein–Stein model. We aim at relative pricing errors below 1e–04. If the time change representation is used, a higher accuracy of 1e–12 comes at almost no additional computational cost. In the stochastic volatility models, the true value is computed using the time change representation with $a = 20\sigma\sqrt{T}$ and $N = 200$. The Black–Scholes model is also displayed, since in this model the more convenient closed-form expression allows us to assess the numerical results. If we aim at an accuracy of at least 1e–04 – in all models and over all the considered parameter sets – we find that the time change representation is about 30–40 times faster than FFT. This is mainly due to the fact that the Laplace transform of the time change has to be evaluated only $N = 90$ times for the time-change representation, whereas a reasonably small error in the FFT technique requires several thousand evaluations of the characteristic function. This explains why the benefit of the time-change representation is even higher if more complex or multi-factor stochastic volatility models are used.

For double digital options, the pricing formulas are presented in Example 11 (FFT technique) and in Theorem 13 (time-change representation). The advantage of the FFT technique is the fact that call and digital options with different strikes can be evaluated simultaneously (see, e.g., Carr and Madan [1999]); a fact that is very convenient when evaluating

Black–Scholes	**analytic expression**			**FFT**			**true value**
	$\hat{I_K}(S_0;D,T)$	rel. err.	time	$\hat{I_K}(S_0;D,T)$	rel. err.	time	$I_K(S_0;D,T)$
$D_0 = 70$	85.4538614262	1e–16	0.21ms	85.4540057263	4e–06	16.1ms	85.4538614262
$D_0 = 80$	65.2422276006	1e–16	0.23ms	65.2419573588	2e–06	28.8ms	65.2422276006
$D_0 = 85$	50.5441995528	1e–16	0.17ms	50.5440955283	7e–06	16.7ms	50.5441995528
$D_0 = 90$	33.9336338323	1e–16	0.16ms	33.9338704798	7e–06	18.6ms	33.9336338323

Heston	**analytic expression**			**FFT**			**true value**
	$\hat{I_K}(S_0;D,T)$	rel. err.	time	$\hat{I_K}(S_0;D,T)$	rel. err.	time	$I_K(S_0;D,T)$
$D_0 = 70$	83.4866936948	3e–12	0.32ms	83.4868068129	4e–06	19.2ms	83.4866936948
$D_0 = 80$	63.5749107489	2e–12	0.23ms	63.5746700119	2e–06	15.3ms	63.5749107489
$D_0 = 85$	49.3197017223	2e–12	0.19ms	49.3196000374	7e–06	15.5ms	49.3197017223
$D_0 = 90$	33.1719456729	2e–12	0.19ms	33.1721774368	8e–06	15.3ms	33.1719456729

Stein–Stein	**analytic expression**			**FFT**			**true value**
	$\hat{I_K}(S_0;D,T)$	rel. err.	time	$\hat{I_K}(S_0;D,T)$	rel. err.	time	$I_K(S_0;D,T)$
$D_0 = 70$	80.9824899941	1e–08	1.06ms	80.9861054076	4e–06	36.5ms	80.9824899941
$D_0 = 80$	66.3518973059	1e–08	1.58ms	66.3550405414	2e–06	33.8ms	66.3518973059
$D_0 = 85$	54.7171462441	2e–08	2.15ms	54.7199452215	8e–06	33.2ms	54.7171462441
$D_0 = 90$	39.3047684487	3e–08	3.30ms	39.3074778522	8e–06	33.2ms	39.3047684487

Table 3.3: Prices $\hat{I_K}(S_0;D,T)$ of digital options in the Black–Scholes model (top, $\sigma = 20.7330\%$), the Heston model (middle, $v_0 = 0.0449$, $\theta = 31.8692$, $\nu = 0.0436$, $\gamma = 2.3695$, $\rho = 0$), and the Stein–Stein model (below, $\sigma_0 = 0.0866$, $\xi = 0.0428$, $k = 0.3379$, $\varkappa = 0.0010$) calculated by the analytic expression (left column, $N = 90$, $P_0 = \exp(10\sigma\sqrt{T})$, see Theorem 13) and by FFT (middle column, see Example 11). The true value $I_K(S_0;D,T)$ (right column) was calculated using $N = 200$ and $P_0 = \exp(20\sigma\sqrt{T})$ in the analytic expression. The remaining parameters are $S_0 = 100$, $K_0 = D_0$, $r_t = 5\%$, and $T = 1$. Relative errors of both approaches are given. The computation time was calculated using Matlab on a 2.4 GHz PC.

Black–Scholes	**analytic expression**			**FFT**			**true value**
	$\hat{I_K}(S_0;D,P,T)$	rel. err.	time	$\hat{I_K}(S_0;D,P,T)$	rel. err.	time	$I_K(S_0;D,P,T)$
$D_0 = S_0^2/P_0 = 70$	78.6855519230	1e–16	0.05ms	78.6852820842	9e–07	9.4ms	78.6855519230
$D_0 = S_0^2/P_0 = 80$	41.5744313561	1e–16	0.05ms	41.5739282389	5e–06	9.4ms	41.5744313561
$D_0 = S_0^2/P_0 = 85$	16.1877599654	1e–16	0.05ms	16.1876865090	6e–06	9.3ms	16.1877599654
$D_0 = S_0^2/P_0 = 90$	1.0147035461	1e–16	0.05ms	1.0148621094	2e–02	7.5ms	1.0147035460

Heston	**analytic expression**			**FFT**			**true value**
	$\hat{I_K}(S_0;D,P,T)$	rel. err.	time	$\hat{I_K}(S_0;D,P,T)$	rel. err.	time	$I_K(S_0;D,P,T)$
$D_0 = S_0^2/P_0 = 70$	75.3471981471	1e–16	0.22ms	75.3468975875	6e–06	14.5ms	75.3471981471
$D_0 = S_0^2/P_0 = 80$	39.1239528894	1e–16	0.18ms	39.1235007244	5e–06	19.8ms	39.1239528894
$D_0 = S_0^2/P_0 = 85$	15.8845258917	1e–16	0.22ms	15.8844268925	6e–06	21.1ms	15.8845258917
$D_0 = S_0^2/P_0 = 90$	1.5861960239	1e–16	0.25ms	1.5864097410	9e–04	20.0ms	1.5861960239

Stein–Stein	**analytic expression**			**FFT**			**true value**
	$\hat{I_K}(S_0;D,P,T)$	rel. err.	time	$\hat{I_K}(S_0;D,P,T)$	rel. err.	time	$I_K(S_0;D,P,T)$
$D_0 = S_0^2/P_0 = 70$	71.6800212987	1e–16	0.88ms	71.6805943479	6e–06	34.6ms	71.6800212987
$D_0 = S_0^2/P_0 = 80$	47.3929219824	1e–16	0.97ms	47.3926883220	5e–06	37.1ms	47.3929219824
$D_0 = S_0^2/P_0 = 85$	30.1576540576	1e–16	0.94ms	30.1574472013	6e–06	35.4ms	30.1576540576
$D_0 = S_0^2/P_0 = 90$	11.8689869073	1e–16	0.84ms	11.8696009918	1e–03	37.3ms	11.8689869073

Table 3.4: Prices $\hat{I_K}(S_0;D,P,T)$ of double digital options in the Black–Scholes model (top, $\sigma = 20.7330\%$), the Heston model (middle, $v_0 = 0.0449$, $\theta = 31.8692$, $\nu = 0.0436$, $\gamma = 2.3695$, $\rho = 0$), and the Stein–Stein model (below, $\sigma_0 = 0.0866$, $\xi = 0.0428$, $k = 0.3379$, $\varkappa = 0.0010$) calculated by the analytic expression (left column, $N = 20$, see Theorem 13) and by FFT (middle column, $N = 20$, see Example 11). The true value $I_K(S_0;D,P,T)$ (right column) was calculated using $N = 200$ in the analytic expression. The remaining parameters are chosen as $S_0 = 100$, $K_0 = D_0$, $r_t = 5\%$, and $T = 1$. Relative errors of both approaches are given. The computation time was calculated using Matlab on a 2.4 GHz PC.

Black–Scholes	**analytic expression**			**FFT**			**true value**
	$D\hat{O}C_K(S_0;\cdot)$	rel. err.	time	$D\hat{O}C_K(S_0;\cdot)$	rel. err.	time	$DOC_K(S_0;\cdot)$
$D_0 = S_0^2/P_0 = 70$	23.6056655769	1e–16	0.06ms	23.6057715409	3e–06	5.83ms	23.6056655769
$D_0 = S_0^2/P_0 = 80$	8.3148862712	1e–16	0.05ms	8.3146985451	9e–06	5.16ms	8.3148862712
$D_0 = S_0^2/P_0 = 85$	2.4281639948	1e–16	0.04ms	2.4281272887	3e–05	4.79ms	2.4281639948
$D_0 = S_0^2/P_0 = 90$	0.1014703546	1e–16	0.03ms	0.1015431731	2e–07	4.81ms	0.1014703546

Heston	**analytic expression**			**FFT**			**true value**
	$D\hat{O}C_K(S_0;\cdot)$	rel. err.	time	$D\hat{O}C_K(S_0;\cdot)$	rel. err.	time	$DOC_K(S_0;\cdot)$
$D_0 = S_0^2/P_0 = 70$	22.6041594441	1e–16	0.20ms	22.6042456846	6e–08	12.9ms	22.6041594441
$D_0 = S_0^2/P_0 = 80$	7.8247905779	1e–16	0.11ms	7.8246194160	9e–07	13.4ms	7.8247905779
$D_0 = S_0^2/P_0 = 85$	2.3826788838	1e–16	0.10ms	2.3826396395	2e–05	13.1ms	2.3826788838
$D_0 = S_0^2/P_0 = 90$	0.1586196024	1e–16	0.10ms	0.1586977412	3e–03	13.1ms	0.1586196024

Stein–Stein	**analytic expression**			**FFT**			**true value**
	$D\hat{O}C_K(S_0;\cdot)$	rel. err.	time	$D\hat{O}C_K(S_0;\cdot)$	rel. err.	time	$DOC_K(S_0;\cdot)$
$D_0 = S_0^2/P_0 = 70$	21.5040063896	1e–16	0.79ms	21.5040360517	5e–06	32.7ms	21.5040063896
$D_0 = S_0^2/P_0 = 80$	9.4785843965	1e–16	0.66ms	9.4784818990	9e–06	32.7ms	9.4785843965
$D_0 = S_0^2/P_0 = 85$	4.5236481086	1e–16	0.73ms	4.5235861827	6e–06	32.8ms	4.5236481086
$D_0 = S_0^2/P_0 = 90$	1.1868986907	1e–16	0.70ms	1.1870464365	2e–02	35.8ms	1.1868986907

Table 3.5: Prices $D\hat{O}C_K(S_0;D,P,T)$ of double barrier options in the Black–Scholes model (top, $\sigma = 20.7330\%$), the Heston model (middle, $v_0 = 0.0449$, $\theta = 31.8692$, $\nu = 0.0436$, $\gamma = 2.3695$, $\rho = 0$), and the Stein–Stein model (below, $\sigma_0 = 0.0866$, $\xi = 0.0428$, $k = 0.3379$, $\varkappa = 0.0010$) calculated by the analytic expression (left column, $N = 20$, see Theorem 14) and by FFT (middle column, see Example 12). The true value $I_K(S_0;D,P,T)$ (right column) was calculated using $N = 200$ in the analytic expression. The remaining parameters are chosen as $S_0 = 100$, $K_0 = D_0$, $r_t = 5\%$, and $T = 1$. Relative errors of both approaches are given. Computation time was calculated using Matlab on a 2.4 GHz PC.

the series from Example 11. *Table 3.4* presents the price estimates together with both computation time and relative error in the Black–Scholes model (top), the Heston model (middle), and the Stein–Stein model (below). Again, we aim at an accuracy (in terms of the relative error) of 1e–04. In the two barrier case, the advantage of the time change representation is more significant than in the single barrier case. Since the upper barrier is not set to infinity, $N = 20$ terms in the series representation (Theorem 13) are sufficient to obtain a very high accuracy. The results in *Table 3.4* show that the computation time for the time change representation is now 50–100 times faster than the FFT technique. Although the FFT technique is now also an infinite series of call options (truncated at $N = 20$), its computation time is about the same as in the single barrier case since digital options with different strikes can be computed simultaneously.

The same holds for double barrier options. The pricing formulas are given in Example 12 (FFT technique) and Theorem 14 (time change representation). *Table 3.5* presents the pricing results together with both computation time and relative error in the Black–Scholes model (top), the Heston model (middle), respectively the Stein–Stein model (below). Aiming at a relative pricing error of less than 1e-04, the analytic expression resulting from the time change representation turns out to be superior to the FFT technique, this time being about 100 times faster. A higher precision in the time change representation – which is, for example, important for at the money barriers – comes at almost no additional computational cost.

Regime switching jump-diffusion model

Having analyzed the effect of stochastic volatility on digital and barrier option prices, we can now do the same in jump-diffusion models. Here, we concentrate on numerical schemes instead of analytic expressions, i.e. we further analyze the Brownian bridge algorithms from *Chapter 2*. Apart from the greater flexibility in our stock price model (i.e. we can include jumps), the Brownian bridge technique has another big advantage: The algorithms can easily be adapted to exotic payoff structures and can thus be used to price, for example, *(step) double barrier options* or *(corridor) bonus certificates*. The calibration to a single call option dataset in *Section 3.1.3* allows us to compare the option prices in models with and without jumps.

Digital first-touch options

First, we again deal with *digital first-touch options*. Options of this form provide a building block for more complex derivatives; for more details see, for example, *Section 3.1.1* or Boyarchenko and Levendorskiĭ [2002].

As before, *digital first-touch options* pay 1 at maturity T if the stock price crosses (a) specific threshold(s). The owner of an *up-and-in* (respectively *down-and-in*) contract receives 1 if the upper barrier $P = \{P_t\}_{t\geq 0}$ (respectively lower barrier $D = \{D_t\}_{t\geq 0}$) is hit first. If the underlying remains within the corridor (D_t, P_t), the option expires worthless.

Under the risk-neutral measure $\mathbb{Q}$, the *up-and-in* option can be priced as

$$I_K^+(S_0; D, P, T) := \exp\left(-\int_0^T r_t dt\right) \mathbb{Q}(T_{P,D}^+ \leq T)\,. \tag{3.28}$$

Similarly, the price of a *down-and-in* option is given by

$$I_K^-(S_0; D, P, T) := \exp\left(-\int_0^T r_t dt\right) \mathbb{Q}(T_{P,D}^- \leq T)\,. \tag{3.29}$$

Example 16 (Digital first-touch options)
First, in order to compare the results to the stochastic volatility models (i.e. Table 3.4*)* Table 3.6 *compares the prices $I_K(S_0; D, P, T)$ of digital first-touch options in a double-exponential jump-diffusion model obtained by the standard Monte–Carlo simulation on a discrete grid to the Brownian bridge algorithm (Algorithm 1). Then,* Table 3.7 *examines the similar case of (upper barrier) first-touch option prices $I_K^+(S_0; D, P, T)$. The parameters considered in the simulations are: $r_t = 5\%$, $\sigma = 20.15\%$, $p = 0$, $\alpha_\ominus = 6.5296$, and $T = 1$ (expiration date of the contract). Furthermore, we set $D_0 = 90$, $S_0 = 100$, and $P_0 = S_0^2/D_0$.*

In the standard Monte–Carlo algorithm, we use 250, respectively 1000, discretization steps. According to the expected number of jumps per year λ, we consider the scenarios "Black-Scholes" ($\lambda = 0$), "Low" ($\lambda = 0.1$), "Middle" ($\lambda = 0.2$), and "High" ($\lambda = 0.5$). We chose double-exponential jump diffusions as this allows us to compare the results to the Laplace transforms of the first-exit time as presented in Kou and Wang [2003], Sepp [2004]. Note that it is very easy to change the jump-size distribution in a Brownian bridge algorithm, whereas it often requires new theoretical results if one is interested in analytical solutions for the Laplace transform of the first-exit times.

From Table 3.7*, we conclude that the Brownian bridge algorithm is significantly faster than the brute–force Monte–Carlo simulation on a discrete grid. Furthermore, the Brownian bridge algorithm is unbiased and thus leads to prices that are close to the exact prices by Sepp [2004]. There are ways to further accelerate this algorithm: First, a parallelization of Monte–Carlo simulations can very easily be implemented. Secondly, there are many variance reduction techniques to accelerate the algorithm (see, e.g., Joshi and Leung [2007], DiCesare and McLeish [2008], Ross and Ghamami [2010] on the single barrier algorithm).*

Black–Scholes	$\triangle t = 1/250$			$\triangle t = 1/1000$			**true value**
	$\hat{I_K}(S_0; D, P, T)$	rel. err.	time	$\hat{I_K}(S_0; D, P, T)$	rel. err.	time	$I_K(S_0; D, P, T)$
$D_0 = S_0^2/P_0 = 70$	78.69 ± 0.01	3e–04	2.2s	78.68 ± 0.00	7e–05	18.2s	78.6856
$D_0 = S_0^2/P_0 = 80$	41.57 ± 0.01	1e–04	2.2s	41.57 ± 0.00	1e–04	17.9s	41.5744
$D_0 = S_0^2/P_0 = 85$	16.18 ± 0.01	5e–04	2.2s	16.21 ± 0.00	1e–04	17.8s	16.1878
$D_0 = S_0^2/P_0 = 90$	1.01 ± 0.01	5e–03	2.2s	1.01 ± 0.00	1e–04	17.5s	1.0147

D.–Exp. ($\lambda = 0.1$)	$\triangle t = 1/250$			$\triangle t = 1/1000$			**true value**
	$\hat{I_K}(S_0; D, P, T)$	rel. err.	time	$\hat{I_K}(S_0; D, P, T)$	rel. err.	time	$I_K(S_0; D, P, T)$
$D_0 = S_0^2/P_0 = 70$	72.68 ± 0.05	7e–04	2.5s	72.62 ± 0.01	7e–05	19.1s	72.6253
$D_0 = S_0^2/P_0 = 80$	36.68 ± 0.05	6e–04	2.5s	36.65 ± 0.01	1e–04	18.8s	36.6552
$D_0 = S_0^2/P_0 = 85$	13.99 ± 0.05	7e–03	2.5s	14.02 ± 0.01	1e–04	18.8s	14.0238
$D_0 = S_0^2/P_0 = 90$	0.87 ± 0.05	8e–03	2.5s	0.86 ± 0.01	1e–03	18.3s	0.8630

D.–Exp. ($\lambda = 0.5$)	$\triangle t = 1/250$			$\triangle t = 1/1000$			**true value**
	$\hat{I_K}(S_0; D, P, T)$	rel. err.	time	$\hat{I_K}(S_0; D, P, T)$	rel. err.	time	$I_K(S_0; D, P, T)$
$D_0 = S_0^2/P_0 = 70$	23.16 ± 0.05	2e–03	3.0s	23.22 ± 0.02	5e–04	23.2s	23.2082
$D_0 = S_0^2/P_0 = 80$	7.03 ± 0.05	7e–03	3.0s	7.08 ± 0.02	7e–05	22.7s	7.0805
$D_0 = S_0^2/P_0 = 85$	2.24 ± 0.05	2e–03	3.0s	2.28 ± 0.02	1e–04	22.6s	2.2831
$D_0 = S_0^2/P_0 = 90$	0.12 ± 0.05	1e–03	3.0s	0.12 ± 0.02	1e–03	22.3s	0.1224

Table 3.6: Prices $\hat{I_K}(S_0; D, P, T)$ of double digital options in the Black–Scholes model (top, $\sigma = 20.7330\%$), the Double-exponential jump diffusion model D.–Exp. (middle, $\sigma = 20.15\%$, $p = 0$, $\alpha_\ominus = 6.5296$) estimated using the Brownian bridge algorithm. The true value $I_K(S_0; D, P, T)$ (right column) was calculated using 10^8 simulation runs. The remaining parameters are chosen as $S_0 = 100$, $K_0 = D_0$, $r_t = 5\%$, and $T = 1$. Relative errors of both approaches are given. The computation time was calculated using Matlab on a 3.1 GHz PC.

		Black-Scholes	Jump-diffusion		
		$\lambda = 0$	Low ($\lambda = 0.1$)	Middle ($\lambda = 0.2$)	High ($\lambda = 0.5$)
StdMC($\triangle = 1/250$)	$\hat{I_K^+}(S_0; D, P, T)$	42.37 ± 0.08	33.58 ± 0.08	25.83 ± 0.08	9.86 ± 0.08
	rel. bias	4.6%	3.8%	1.7%	0.3%
	runtime	47.2s	46.1s	45.0s	41.7s
StdMC($\triangle = 1/1000$)	$\hat{I_K^+}(S_0; D, P, T)$	43.43 ± 0.03	34.28 ± 0.03	25.98 ± 0.08	9.87 ± 0.04
	rel. bias	2.2%	1.8%	1.3%	0.2%
	runtime	185.6s	183.8s	179.4s	161.7s
Brownian Bridge	$\hat{I_K^+}(S_0; D, P, T)$	44.41 ± 0.02	34.91 ± 0.02	26.45 ± 0.03	9.89 ± 0.03
	rel. bias	0.0%	0.0%	0.0%	0.0%
	runtime	18.1s	19.3s	14.3s	30.1s
	$I_K^+(S_0; D, P, T)$	44.43	34.87	26.45	9.88

Table 3.7: Prices $I_K^+(S_0; D, P, T)$ and confidence intervals at the confidence level $\alpha = 90\%$ of (upper barrier) digital first-touch options for different jump intensities λ. We compare the standard Monte–Carlo simulation on a discrete grid with mesh 1/250, respectively 1/1000, to the Brownian bridge algorithm (Algorithm 5) using 10^6 simulation runs. The exact value of the option was estimated by inverting the Laplace transforms presented by, for example, Sepp [2004]. The table additionally presents the bias and runtime for each algorithm. The relative bias is the relative difference between the expected simulated value $\mathbb{E}[\hat{I_K^+}(S_0; D, P, T)]$ divided by the true value $I_K^+(S_0; D, P, T)$ of the option. The computation time was calculated using Matlab 2012a on a 3.1 GHz PC.

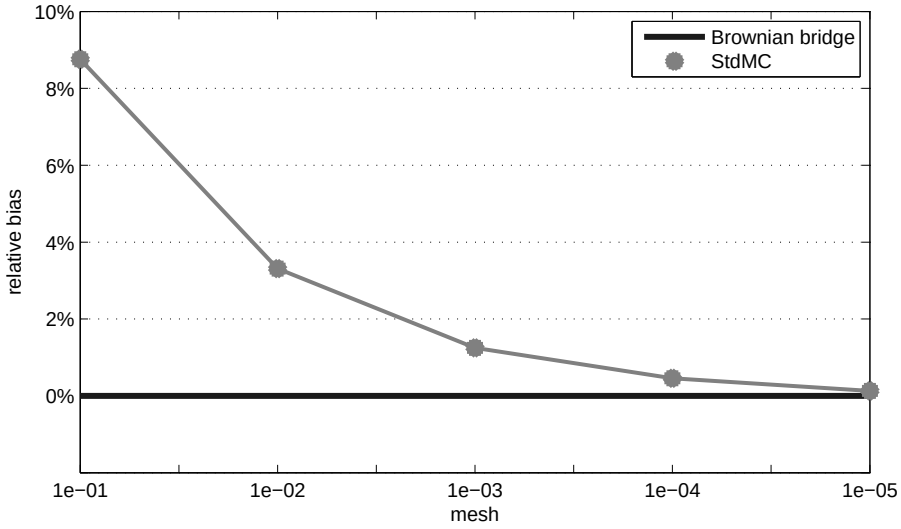

Figure 3.4: Bias of (upper barrier) digital first-touch option prices $I_K^+(S_0; D, P, T)$. *We compare the standard Monte–Carlo simulation on a discrete grid with mesh* $\triangle t \in \{$1e–01, 1e–02, 1e–03, 1e–04, 1e–05$\}$ *to the Brownian bridge algorithm (Algorithm 5) using* 10^6 *simulation runs. The jump intensity is* $\lambda = 2$*; the same parameters as in* Table 3.7 *are used. The relative bias is the relative difference between the expected simulated value* $\mathbb{E}\big[\hat{I_K^+}(S_0; D, P, T)\big]$ *divided by the true value* $I_K^+(S_0; D, P, T)$ *of the option.*

Figure 3.4 *further examines the discretization bias of the two algorithms. Note that the discretization bias in the standard Monte–Carlo simulation is still considerably high even for 1000 discretization steps ($\triangle t$ = 1e–03). The Brownian bridge technique returns unbiased price estimates.*

Furthermore, we can now assess the effect of stochastic volatility and jumps on barrier option prices. Already a jump intensity of $\lambda = 0.1$ (which corresponds to a one-year jump probability of $1 - \exp(0.1) \approx 9.5\%$) leads to about 10% lower barrier option prices (see *Table 3.6*). The effect of stochastic volatility is smaller; it affects option prices by – on average – 5% (see *Table 3.4*). The advantage of the Brownian bridge simulation is its flexibility – not only regarding to the stock price model – but also with respect to payoff streams of financial contracts. The Brownian bridge algorithm can easily be adapted to price exotic derivatives like *step double barrier options* or *corridor bonus certificates*.

(Step) Double barrier options

Double barrier options are very popular over-the-counter (OTC) derivatives and are frequently embedded in a variety of structured products. The holder receives the payoff of a standard call or put option if the stock price stays within a corridor (D_t, P_t) over the lifetime of the option (and receives 0 otherwise). For an investor, this standard contract is often not suitable: Following his risk aversion, his hedging requirements, or his market views, the investor might want to change the barrier level over time. For instance, he/she might want to widen the corridor (D_t, P_t) over time (a contract often referred to as "expanding tunnel"). A large range of exotic products aim at providing this additional flexibility, i.e. step double barrier options (the barriers are piecewise constant) or window double barrier options (the barriers can only be observed during certain time intervals). Many different names were created for those type of contracts, i.e. "hot-dog-option", "wedding cakes", or "onion options", for a more detailed review of traded contracts, we refer to Guillaume [2003, 2010]. Analytical pricing formulas for such products tend to become extremely complicated (this is already true for simple examples in the Black–Scholes model, see, e.g., the Appendix of Guillaume [2010]) and are not flexible enough to adapt to many exotic payoff streams.

In the following, we introduce step double barrier options formally. For certain observation points $t_0 = 0 < t_1 < \ldots < t_n = T$, the barrier of an n-step double barrier option is constant over the intervals $[t_{i-1}, t_i]$, for $i = 1, 2, \ldots, n$. Denoting those ranges by $[D_t^{(i)}, P_t^{(i)}]$, a step double barrier option has the same payoff as a standard call or put if the underlying asset has stayed within the thresholds $(D_t^{(i)}, P_t^{(i)})$ until the maturity of the contract.

		Black-Scholes	Jump-diffusion		
		$\lambda = 0$	Low ($\lambda = 0.1$)	Middle ($\lambda = 0.2$)	High ($\lambda = 0.5$)
StdMC($\triangle = 1/250$)	$\hat{DOC}_K(S_0; D, P, T)$	20.33 ± 0.02	14.77 ± 0.02	8.61 ± 0.01	0.46 ± 0.05
	rel. bias	3.4%	2.3%	2.1%	1.4%
	runtime	43.0s	42.4s	40.0s	36.1s
StdMC($\triangle = 1/1000$)	$\hat{DOC}_K(S_0; D, P, T)$	19.97 ± 0.01	14.59 ± 0.01	8.54 ± 0.01	0.47 ± 0.04
	rel. bias	1.6%	1.0%	0.9%	0.6%
	runtime	171.1s	169.2s	159.5s	144.2s
Brownian Bridge	$\hat{DOC}_K(S_0; D, P, T)$	19.65 ± 0.01	14.42 ± 0.01	8.48 ± 0.01	0.47 ± 0.02
	rel. bias	0.0%	0.0%	0.0%	0.0%
	runtime	27.4s	30.7s	33.5s	32.3s
	$DOC_K(S_0; D, P, T)$	19.65	14.41	8.46	0.47

Table 3.8: Prices $\hat{DOC}_K(S_0; D, P, T)$ and confidence intervals at the confidence level $\alpha = 90\%$ of two-step double barrier options for different jump intensities λ. We compare the standard Monte–Carlo simulation on a discrete grid with mesh 1/250, respectively 1/1000, to the Brownian bridge algorithm (Algorithm 5) using 10^6 simulation runs. The exact value of the option is considered to be the one obtained by 10^8 simulation runs using the Brownian bridge pricing algorithm. The table additionally presents the bias and runtime for each algorithm. The bias is the (relative) difference between the expected simulated value $\mathbb{E}[\hat{DOC}_K(S_0; D, P, T)]$ and the true value $DOC_K(S_0; D, P, T)$ of the option. The computation time was calculated using Matlab 2012a on a 3.1 GHz PC.

Example 17 (Step double barrier options)
We consider a two-step double barrier option, i.e. an "expanding tunnel" with $t_1 = 1$, $[D_0^{(1)}, P_0^{(1)}] = [60, 140]$ *and* $[D_0^{(2)}, P_0^{(2)}] = [50, 150]$. *The strike price at* $T = t_2 = 2$ *is* $K_0 = 70$. *The other parameters are chosen as in Example 16, i.e.* $r_t = 5\%$, $\sigma = 20.15\%$ *and* $S_0 = 100$. *Again, we use a double-exponential jump-diffusion model with* $p = 0$ *and* $\alpha_{\ominus} = 6.5296$. *According to the expected number of jumps per year* λ, *we consider the scenarios "Black-Scholes"* ($\lambda = 0$), *"Low"* ($\lambda = 0.1$), *"Middle"* ($\lambda = 0.2$), *and "High"* ($\lambda = 0.5$). Table 3.8 *compares the prices of two-step double barrier options obtained by the standard Monte–Carlo simulation on a discrete grid and the Brownian bridge algorithm (Algorithm 5). Pricing this type of exotic options analytically tends – even for the case of a double-exponential jump size distribution – to be very tedious and also computationally challenging. In the Black–Scholes model, closed-form prices for two-step double barrier options are available (see the Appendix of Guillaume [2010]). The advantage of both Monte–Carlo algorithms presented in* Table 3.8 *is the fact that they are very flexible, easy to implement, and can easily be adapted to different payoff streams or jump-size distributions. The Brownian bridge algorithm is moreover both unbiased and faster than the standard Monte–Carlo simulation.*

Corridor bonus certificates

Corridor bonus certificates provide the largest payoff if the stock price stays within a given corridor (D_t, P_t) during the lifetime of the contract and thus offer the possibility to bet on sideways markets. On different underlying assets, they are emitted by all major banks[7].

The payoff of a *corridor bonus certificate* depends on the market value of the underlying at the expiration date T, the first-exit time events on the two barriers D and P, and on an initially specified "fixed amount" $F_T = F_0 \exp(\int_0^T r_t dt)$. One distinguishes the following two cases:

- If the stock prices stays within the corridor (D_t, P_t), then the owner of the certificate receives the fixed amount F_T at maturity T.
- If the stock price reaches one of the barriers, the payoff depends on the stock price S_T at the expiration date of the certificate.

[7] Note that there exist different kinds of *corridor bonus certificates* with slightly different payoff structures. As an example, Société Générale emitted several certificates (e.g. ISIN: DE000SG12BS9).

More precisely, we get the following payoff:

$$\text{payoff}(T) = \begin{cases} F_T & \text{if } T_{P,D} > T, \\ \min(S_T, F_T) & \text{if } T^-_{P,D} \le T, \\ \max\big(\min(2S_0 - S_T, F_T), 0\big) & \text{if } T^+_{P,D} \le T. \end{cases}$$

Note that if the upper barrier is hit, the certificate converts into a short position in the underlying S. In most standard contract specifications the resulting loss is bounded by the initial investment. Under the risk-neutral measure $\mathbb{Q}$, the price of *corridor bonus certificates* conditional on $T^-_{P,D}$, $T^+_{P,D}$, and S_T is given by

$$\begin{aligned} B_F(S_0; D, P, T) &:= \exp\left(-\int_0^T r_t dt\right) \mathbb{E}_{\mathbb{Q}}\big[\text{payoff}(T)\big] \\ &= \exp\left(-\int_0^T r_t dt\right) \mathbb{E}_{\mathbb{Q}}\Big[\mathbb{E}_{\mathbb{Q}}\big[\text{payoff}(T) \,\big|\, T^-_{P,D},\, T^+_{P,D},\, S_T\big]\Big] \\ &= \exp\left(-\int_0^T r_t dt\right) \mathbb{E}_{\mathbb{Q}}\Big[F_T\big(1 - \mathbb{1}_{\{T^+_{P,D}\le T\}} - \mathbb{1}_{\{T^-_{P,D}\le T\}}\big) \\ &\qquad + \mathbb{1}_{\{T^+_{P,D}\le T\}} \max(\min(2S_0 - S_T, F_T), 0) + \mathbb{1}_{\{T^-_{P,D}\le T\}} \min(S_T, F_T)\Big]. \end{aligned} \tag{3.30}$$

This can be estimated using the triplets $\big(\mathcal{BB}^+(k),\, \mathcal{BB}(k),\, B_T(k)\big)$ from Algorithm 5.

Example 18 (Corridor bonus certificates)
Table 3.9 *estimates the prices of corridor bonus certificates using Algorithm 5.*

	Black-Scholes	Jump-diffusion		
	$\lambda = 0$	Low ($\lambda = 0.1$)	Middle ($\lambda = 0.2$)	High ($\lambda = 0.5$)
$D_0 = S_0^2/P_0 = 70$	105.98 ± 0.00	104.97 ± 0.02	103.97 ± 0.04	101.02 ± 0.07
$D_0 = S_0^2/P_0 = 80$	92.61 ± 0.00	91.76 ± 0.01	90.90 ± 0.03	88.45 ± 0.07
$D_0 = S_0^2/P_0 = 85$	86.20 ± 0.00	85.65 ± 0.02	85.12 ± 0.04	83.94 ± 0.07
$D_0 = S_0^2/P_0 = 90$	85.23 ± 0.00	84.96 ± 0.02	84.70 ± 0.04	83.57 ± 0.07

Table 3.9: Prices of corridor bonus certificates $\hat{B}_F(S_0; D, P, T)$ using Algorithm 5 for different jump size distributions (parameters $\alpha_\oplus = 6.5296$ and $p = 0$) and jump size intensities λ. We choose $S_0 = 100$, $r_t = 5\%$, $T = 1$, $\sigma = 20.15\%$, and $F_0 = 120$. The results have been obtained in a simulation with 10^6 trajectories. 90% confidence intervals are given.

Credit risk

Another frequent application of first-exit times are *structural credit risk models*. The idea behind those models is to define default as a consequence of insufficient asset values, with the result that bonds can be priced as an option on the company's assets S. One considers two possibilities that the bond spread payments cease: First, the company defaults as soon as S falls below some prespecified level $D = \{D_t\}_{t\geq 0}$. Second, due to, for example, the company's desire to upgrade its credit rating or due to an initial public offering (IPO), the bond might be repaid earlier. This event is triggered as soon as S crosses an upper barrier $P = \{P_t\}_{t\geq 0}$, see, for example, Downing et al. [2005], Gabaix et al. [2007], Dobránszky and Schoutens [2008].

The price of a defaultable bond with nominal value 1 and maturity T that pays (continuous) interest at a rate d and can (at any time) be recalled by the bond holder is then priced as

$$\text{Bond Price} = \text{Nominal} + \text{Interest}, \tag{3.31}$$

$$\begin{aligned}
\text{Nominal} &= \exp\Big(-\int_0^T r_t dt\Big)\,\mathbb{Q}(T_{P,D} > T) \\
&\quad + \mathbb{E}_{\mathbb{Q}}\Big[R\,\exp\Big(-\int_0^{T^-_{P,D}} r_t dt\Big)\,\mathbb{1}_{\{T^-_{P,D}\leq T\}} + \exp\Big(-\int_0^{T^+_{P,D}} r_r dt\Big)\,\mathbb{1}_{\{T^+_{P,D}\leq T\}}\Big], \\
\text{Interest} &= \mathbb{E}_{\mathbb{Q}}\Big[\int_0^{\min(T_{P,D},T)} d\,\exp\Big(-\int_0^t r_s ds\Big)\,dt\Big] \\
&= \frac{d}{r}\Big(1-\exp\Big(-\int_0^T r_t dt\Big)\Big)\,\mathbb{Q}(T_{P,D} > T) \\
&\quad + \underbrace{\mathbb{E}_{\mathbb{Q}}\Big[\int_0^{T^+_{P,D}} d\,\exp\Big(-\int_0^t r_s ds\Big)\,dt\;\mathbb{1}_{\{T^+_{P,D}\leq T\}}\Big]}_{\text{early repayment in } T^+_{P,D}} \\
&\quad + \underbrace{\mathbb{E}_{\mathbb{Q}}\Big[\int_0^{T^-_{P,D}} d\,\exp\Big(-\int_0^t r_s ds\Big)\,dt\;\mathbb{1}_{\{T^-_{P,D}\leq T\}}\Big]}_{\text{default in } T^-_{P,D}},
\end{aligned}$$

where $\{r_t\}_{t\geq 0}$ is the risk-free interest rate and $R \in [0,1]$ the recovery rate in case of default.

This price depends on the first-exit times $T^+_{P,D}$, $T^-_{P,D}$ and can thus be computed using Algorithm 6. This concept of structural credit risk models is also applied in the following *Section 3.2* in an empirical study on the asset class Private Equity (PE).

3.2 The risk appetite of Private Equity (PE) sponsors[8]

Investments that belong to the asset class Private Equity (PE) are equity holdings on operating companies that are not publicly traded on a stock exchange. In this section, we want to empirically investigate the risks inherent in PE transactions and identify key determinants of deal-level risks chosen.

Due to the illiquidity and opaqueness of the PE business (see, among many others, Ljungqvist and Richardson [2003]), the main problem in PE risk management lies in the scarcity of available data. Market valuations of enterprise and equity values can hardly be observed or appropriately calculated over the holding period of the PE sponsor (i.e. the time span between purchasing and selling the target company). However, the (observable) fluctuation in a value is fundamental to the calculation of risk – for example measured via the standard deviation. Consequently, calculating risk indicators for PE-sponsored companies is considerably more difficult compared to for publicly listed companies.

In contrast to most previous studies focusing on systematic risks excluding unsystematic risk factors (see, e.g., Franzoni et al. [2012], Groh and Gottschalg [2009]), we want to explicitly measure idiosyncratic (transaction level) risk. Both systematic and unsystematic risks are obviously inherent in single PE investments as it is usually impossible to fully diversify PE funds that often embrace less than 20 investments (see, e.g., Lossen [2006]).

In this context, Axelson et al. [2009] propose the convincing theoretical argument that the typical compensation structure of PE funds gives PE firms an incentive to undertake risky but unprofitable investments. The basic idea of their theory is that PE sponsors as general partners (GPs) participate in the success of transactions through their compensation scheme. Their downside risk in case of failure, however, is limited and mainly borne by the investors of their fund, the so called limited partners (LPs). This situation resembles a call option for the PE firm as it faces a strong upside potential if the investment turns out to be successful, but the lion's share of downside risk is borne by their investors.

This call option-like valuation is in the literature referred to as a *structural model* or a *real option valuation* (see also the *Introduction* of this thesis). The option-like valuation for highly leveraged firms is empirically supported (see, e.g., Green [1984], Arzac [1996]). One example – the Merton model – assumes constant debt and allows for no default during

[8] This section is joint work with Prof. Dr. Reiner Braun and Dr. Nico Engel from the *Center for Entrepreneurial and Financial Studies, Technische Universität München* (Prof. Dr. Dr. Ann-Kristin Achleitner) and Prof. Dr. Rudi Zagst and is based on the paper: Braun, R.; Engel, N.; Hieber, P. and Zagst, R. (2011): *The Risk Appetite of Private Equity Sponsors*, Journal of Empirical Finance, Vol. 18, No. 5, pp. 815-832. The empirical analyses were carried out by Dr. Nico Engel.

the lifetime of the transaction. This is, however, a too simplistic model for buyouts. Buyouts are characterized by substantial debt redemptions after the transaction entry and a continuous default risk (see, e.g., Groh et al. [2008]). There are several extensions of the Merton model that allow for more realistic assumptions:

- Ho and Singer [1984] present a two-step extension that allows for two redemption payments during the lifetime of the PE transaction. Groh et al. [2008] apply this model to price leveraged buyouts (LBOs).
- Black and Cox [1976], Geske [1979] as well as Brockman and Turtle [2003] see equity as a (path dependent) option that allows for continuous default.

Both approaches still do not incorporate the central characteristics of the PE business model mentioned above. The first one does not allow for continuous default while the second one usually either assumes constant debt or neglects the fact that debt usually does not decrease to zero at the end of the investment horizon. Groh et al. [2008] is one of the rare studies explicitly dealing with unsystematic risks associated with buyout investments. We capitalize on the basic ideas of Groh et al. [2008] and combine them with the continuous default assumption of, for example, Black and Cox [1976], Geske [1979], and Brockman and Turtle [2003]. We think that this is more adequate in the context of PE as it allows for continuous default and redemption payments during the holding period. Based on our model, we calculate deal-specific implied asset and equity risk. These risks represent the ex-ante assumptions (i.e. at investment entry) of the PE sponsor regarding the expected volatility of the company/enterprise value (asset risk) and equity value (equity risk). The latter represents the risk appetite of a PE sponsor since it can be interpreted as the intentionally chosen risk level from the perspective of the PE sponsor, given a certain willingness of banks to provide leverage.

The remainder of this section is organized as follows: In *Section 3.2.1*, we introduce the *structural model* to value PE transactions. After a data description in *Section 3.2.2*, we show how the structural model can be used to obtain an implied volatility as a measure of the risk inherent in a single PE transaction. The empirical results on a PE database are discussed in *Section 3.2.3*. The aim of this study is to identify risk factors of PE transactions. For more details, we also refer to Braun et al. [2011].

3.2.1 Structural default model

This section presents the structural default model for pricing PE transactions. With the help of this model, one is able to calculate an implied volatility, using deal specific

information on time horizon, debt and equity prices, average recovery rates, and on quoted risk-free rates and bond spreads.

We follow Ho and Singer [1984] and use the following assumptions for a firm value model listed below:

(1) The firm's capital structure consists of a single equity and a single debt layer.

(2) The yield curve is flat and non-stochastic.

(3) Until the maturity of the debt, the firm's investment decisions are known.

(4) The firm does not pay dividends and does not make any other contributions to shareholders.

(5) Amortization payments are fixed in the indentures.

(6) Amortization payments are financed with new equity.

(7) Default occurs when the firm (enterprise) value S falls below the face value of debt D. In this case, the debt holders have the right to take control over the firm and the shareholders need to forfeit the buyout company's assets to the lenders costlessly.

As in *Section 3.1*, Equation (3.1), the firm's assets $S = \{S_t\}_{t\geq 0}$ are modeled as a geometric Brownian motion (GBM) with drift $r \in \mathbb{R}$ and volatility $\sigma > 0$. While it is mathematically possible to relax most of the given assumptions, the limited availability and level of detail of PE data makes it practically difficult (if not impossible) to calibrate more complicated models with many parameters. The resulting use of standard deviation as a risk measure turned out to be sufficient in the context of highly leveraged investments. In the related case of hedge funds, Eling and Schuhmacher [2005, 2007] show that the use of different risk-adjusted performance measures (with changing assumptions with regard to the underlying return distribution) does not change the ranking between different investments. This even holds true if the return distribution significantly deviates from a normal distribution. For those reasons we stay at this level of simplification.

The face value of debt $D = \{D_t\}_{t\geq 0}$ bears continuous interest at a rate of c. The debt holders receive a continuous rate λ that consists of (part of) the interest payments plus a potential amortization payment. Both c and λ are assumed to be constant over time. Thus, the face value of debt at time t is given by

$$D_t = D_0\, e^{(c-\lambda)t},\ D_0 > 0\,. \tag{3.32}$$

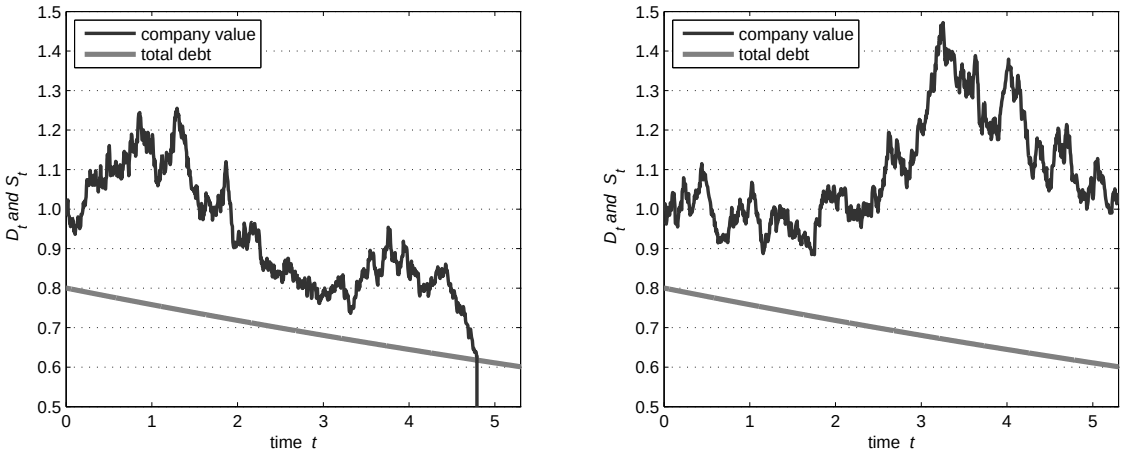

Figure 3.5: A sample private equity transaction with parameters $S_0 = 1.0$, $D_0 = 0.8$, $T = 5.3$, $\sigma = 18.2\%$, $r = 5.0\%$, $c = 8.0\%$, $\lambda = 13.4\%$. *Two samples of the firm value path (*black line*) were generated using Monte–Carlo simulation. The company defaults as soon as its value hits the current face vale of debt (*grey line*).*

As in *Chapter 2*, the first-exit time is written as

$$T_{\infty,D} := \inf\{t \geq 0 : S_t \leq D_t\}\,. \tag{3.33}$$

Figure 3.5 displays the two possible outcomes of a sample PE transaction[9]. While on the right-hand side, the company value (*black line*) stays above the face value of debt (*grey line*) until maturity T, the black path on the left-hand side hits the face value of debt and the company defaults. The default time is the first-exit time $T_{\infty,D}$ as defined in Equation (3.33).

As already mentioned, the debt holders receive the redemption payments of the continuous rate λ until the company either defaults or matures in T. Apart from those redemption payments, the debt holders demand the remaining debt as soon as the transaction is terminated. If the company defaults, they receive $D_{T_{\infty,D}}$ times a recovery rate $R \in [0,1]$ at time $T_{\infty,D}$, else the remaining debt D_T in T. *Figure 3.6* displays the payments to the debt holders for the two possible cases of default (*left*) and no default (*right*) and using the same sample transaction as in *Figure 3.5*.

A well-known result is the continuous barrier hitting probability in the presented continuous setting, see also Equation (2.2) in *Chapter 2*. Lemma 5 summarizes the main finding.

[9]We randomly picked one transaction from our data set.

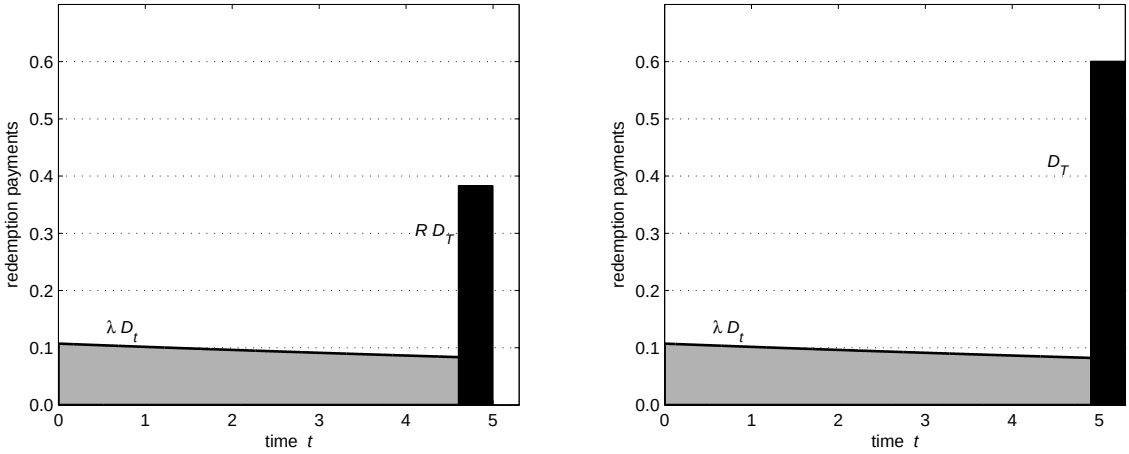

*Figure 3.6: Payments to the debt holders in case of default (*left*) and no default (*right*). The chosen parameters are the same as in Figure 3.5, the recovery rate R is 62%.*

Lemma 5 (Barrier hitting probability GBM)
Let S denote a geometric Brownian motion (GBM) with drift $r \in \mathbb{R}$ and volatility $\sigma > 0$, starting at $S_0 > D_0$. The barrier level is $D_t = D_0\, e^{(c-\lambda)t}$, $d := \ln(D_0/S_0)$ is the logarithm of the initial leverage ratio. The survival probability

$$\mathbb{Q}(T_{\infty,D} > T) = \mathbb{Q}\big(S_t > D_t,\ \textit{for all } t \in [0,T]\big),$$

abbreviated by $\Phi_{d,\mu,\sigma}(T)$, simplifies to

$$\Phi_{d,\mu,\sigma}(T) := \Phi\!\left(\frac{-d+\mu T}{\sigma\sqrt{T}}\right) - \exp\left(\frac{2\mu d}{\sigma^2}\right)\,\Phi\!\left(\frac{d+\mu T}{\sigma\sqrt{T}}\right), \tag{3.34}$$

where $\mu := r - c + \lambda - \sigma^2/2$, $\Phi(\,\cdot\,)$ denotes the standard normal cumulative distribution function, and $\ln(\,\cdot\,)$ the natural logarithm.

Proof. Lemma 1 in *Chapter 2* displays the upper barrier default probability. The lower barrier survival probability is a straightforward corollary to this result. □

If we continuously test for default, the total value of debt $V_D(0)$ can be priced using results on structural credit risk models. For an introduction and more details see, for example, Schönbucher [2003]. $V_D(0)$ is seen as a coupon bond with initial face value D_0

and continuous redemption payments $\lambda D_t dt$. Then[10],

$$V_D(0) = \left[\int_0^T e^{-rt}\lambda D_t\, dt + e^{-rT} D_T\right] \mathbb{Q}(T_{\infty,D} > T) + \int_0^T \left[\int_0^s e^{-rt}\lambda D_t\, dt + R e^{-rs} D_s\right] d\mathbb{Q}(T_{\infty,D} \leq s)\,, \tag{3.35}$$

where $d\mathbb{Q}(T_{\infty,D} \leq s)$ is the first-exit time density (see Lemma 5). Equation (3.35) implies that default can occur at any time during the holding period $[0, T]$. Equation (3.35) consists of the survived (*first term*) and defaulted (*second term*) firm value paths. Those terms contain the discounted redemption payments $\int_0^{\min(T_{\infty,D};T)} e^{-rt}\lambda D_t dt$ plus the discounted remaining debt value at maturity ($e^{-rT} D_T$) or at default ($R e^{-rT_{\infty,D}} D_{T_{\infty,D}}$).

Theorem 15 gives an analytic expression for the bond in Equation (3.35).

Theorem 15 (Pricing the face value of debt)
The total value of debt $V_D(0)$ can, under the risk-neutral measure $\mathbb{Q}$ with the risk-free interest rate r, be priced as

$$V_D(0) = -D_0 \frac{\lambda}{c-r-\lambda} + D_0\, e^{(c-r-\lambda)T} \frac{c-r}{c-r-\lambda}\, \Phi_{d,\mu,\sigma}(T) + D_0\, e^{-\frac{d(\tilde{\mu}-\mu)}{\sigma^2}} \left(R + \frac{\lambda}{c-r-\lambda}\right)\big(1 - \Phi_{d,\tilde{\mu},\sigma}(T)\big), \tag{3.36}$$

where the notation is the same as in Lemma 5, $\mu := r - c + \lambda - \sigma^2/2$, $d := \ln(D_0/S_0)$, $\tilde{\mu} := \sqrt{\mu + 2(c-r-\lambda)\sigma^2}$, and $\lambda \neq c - r$.

Proof. It holds that

$$\int_0^{\min(T_{\infty,D};T)} e^{-rt}\lambda D_t\, dt = D_0 \int_0^{\min(T_{\infty,D};T)} e^{(c-r-\lambda)t}\lambda\, dt = D_0 \frac{\lambda}{c-r-\lambda}\big(e^{(c-r-\lambda)\min(T_{\infty,D};T)} - 1\big)\,.$$

Equation (3.35) can then be written as

$$V_D(0) = \left[D_0 \frac{\lambda}{c-r-\lambda}\big(e^{(c-r-\lambda)T} - 1\big) + e^{-rT} D_T\right] \mathbb{Q}(T_{\infty,D} > T) + \int_0^T \left[D_0 \frac{\lambda}{c-r-\lambda}\big(e^{(c-r-\lambda)s} - 1\big) + R e^{-rs} D_s\right] d\mathbb{Q}(T_{\infty,D} \leq s)$$

[10] $V_D(0)$ is the general formula for the market price of defaultable debt. Note that in the case of $\lambda > c$, the face value of debt increases over time, while it decreases for $\lambda < c$. Also note that the spread c is a par spread; at the closing of the transaction it is set such that $D_0 = V_D(0)$.

$$
\begin{aligned}
= &- D_0 \frac{\lambda}{c-r-\lambda} + D_0\, e^{(c-r-\lambda)T} \frac{c-r}{c-r-\lambda}\, \mathbb{Q}(T_{\infty,D} > T) \\
&+ D_0 \left(R + \frac{\lambda}{c-r-\lambda} \right) \int_0^T e^{(c-r-\lambda)s}\, d\mathbb{Q}(T_{\infty,D} \leq s)\,.
\end{aligned}
$$

The latter integral is solved using Theorem 3.3 in Scherer and Zagst [2010]

$$
\int_0^T e^{(c-r-\lambda)s} d\mathbb{Q}(T_{\infty,D} \leq s) = e^{-\frac{d(\tilde{\mu}-\mu)}{\sigma^2}} \left(1 - \Phi_{d,\tilde{\mu},\sigma}(T)\right),
$$

with the notation of Lemma 5, $\mu := r - c + \lambda - \sigma^2/2$, and $\tilde{\mu} := \sqrt{\mu^2 + 2(c-r-\lambda)\sigma^2}$. Then,

$$
\begin{aligned}
V_D(0) = &- D_0 \frac{\lambda}{c-r-\lambda} + D_0\, e^{(c-r-\lambda)T} \frac{c-r}{c-r-\lambda}\, \Phi_{d,\mu,\sigma}(T) \\
&+ D_0\, e^{-\frac{d(\tilde{\mu}-\mu)}{\sigma^2}} \left(R + \frac{\lambda}{c-r-\lambda} \right) \left(1 - \Phi_{d,\tilde{\mu},\sigma}(T)\right).
\end{aligned}
$$

□

Theorem 15 can be applied to obtain an implied asset volatility σ using data on d, T, r, c, λ, and R. Therefore one has to use a root search algorithm, for example Newton's method.

The following results in Theorem 6 can then be used to retrieve an equity volatility σ_E from the asset volatility σ. The proof is an application of Itô's Lemma and can be found in, for example, Schönbucher [2003], p. 276.

Lemma 6 (Equity volatility)
With the notation of Lemma 5, it holds that

$$
\sigma_E = \sigma \frac{\partial V_E(0)}{\partial S_0} \frac{S_0}{V_E(0)}\,, \tag{3.37}
$$

where $V_E(0)$ denotes the initial equity value of the firm[11].

Using the results of this section, we are able to calculate deal-specific asset and equity volatilities. The application to a large PE data set is carried out in the following two sections.

[11] For the calculation of $V_E(0)$ and $\partial V_E(0)/\partial S_0$, see the Appendix.

3.2.2 Data description: PE database

Our initial sample of 1 290 buyout transactions initiated between 1990 and 2005 is drawn from proprietary databases of two international PE funds-of-funds. When considering investing into a PE fund, these investors request detailed information on historical transactions managed by the PE sponsor. This information is a key element of their fund due diligence process. The PE funds-of-funds grant us access to all information they possess (in anonymous form), irrespective of their final investment decision. This means we have information on deals sponsored by a variety of PE firms and the investment pattern exhibited by the PE funds-of-funds is not a source of sample selection. Nevertheless, as these investors are more likely to collaborate with previously successful PE sponsors, there is likely to be a bias in our sample towards deals from more successful funds.

While all of the buyouts included in our initial sample are realized, i.e. the PE sponsor has already sold the company, a substantial share of these transactions does not meet the data requirements as imposed by our quantitative model. We remove all transactions with missing values for variables which are relevant for our model (581 transactions). Because we do not consider "quick flips", i.e. short-termed investments in which PE sponsors do not realize the value potential of the buyout firms, to be PE (Kaplan and Strömberg [2009]), we also delete all transactions for which the reported holding period, i.e. the time span between acquisition and exit, is six months or shorter (11 transactions). Finally, for some transactions, the final debt levels reported in the databases exceed the compounded initial debt. In these cases, the companies were apparently financed with further external capital within the holding period. As our model does not allow for such additional financing rounds (if not anticipated at investment entry) we discard these 168 deals. In addition, we have to remove 70 deals for which certain deal-related data is not available (e.g. industry affiliation of the target company, PE sponsor characteristics etc.), ending up with 460 transactions.

We identify the 5-Year US Treasury Notes at the date of transaction as proxy for the risk-free interest rate r. We decide for this maturity as it is closest to holding periods said to be characteristic for buyouts (e.g. six years as reported by Strömberg [2008]) and similar to those observed in our sample. The default spread consists of an interbank rate and a deal-specific spread. In order to obtain information on these loan characteristics, we use Reuters' LPC DealScan database (DealScan)[12]. DealScan reports comprehensive information on syndicated loan deals sponsored by PE firms. We are able to match 95 of our total 460 transactions in the final sample. For these deals DealScan provided

[12]Data from DealScan was retrieved while Reiner Braun was a visiting researcher at Said Business School, Oxford University.

information on the interbank rate underlying the loans and the size and spread of each debt tranche. The spreads were all based on the London Interbank Offered Rate (LIBOR) or the Euro Interbank Offered Rate (EURIBOR). Historical data is publicly available for both rates and we retrieved them from the European Central Bank[13]. We calculate the corresponding historical rate for each of the 95 matched deals in our sample by using the geometric mean of all monthly interbank rates during the holding period of the transaction. Further, we compute the tranche size weighted average spread for each matched deal. By adding up the interbank base rate and the weighted total spread for each of the matched deals we obtained the total cost of debt c.

We fill the missing values of default spread for the other 365 deals we are unable to find in DealScan by imputation. Imputation is a procedure which has been shown to be superior to ad-hoc filling of missing data in finance research (Kofman and Sharpe [2003]) and is common among other researchers in the field (see, e.g., Bernstein et al. [2010]). We impute missing default spreads by constructing fitted values from a regression of default spreads on deal size, the ratio of net debt to equity, the ratio of net debt to EBITDA, the yield spread on corporate bonds (Moody's BAA bond index) on the risk-free rate over time, a dummy variable distinguishing European and North American deals, and industry variables.

Further, since our model allows for default during the holding period of the PE sponsor, we have to make assumptions about the debt recovery rate R in case of default. In line with Wilson et al. [2010] we assume a recovery rate of 62% throughout the paper. With regard to the calculation of λ, i.e. the continuous rate the debt holders receive (including interest and debt redemption payments), we calibrate λ using the equation $D_T = D_0\, e^{(c-\lambda)t}$ and D_0, D_T from our database. In other words, since all transactions used in our analyses are already realized we can resort to the actual value of debt at investment exit in order to make assumptions about λ.

In addition, in order to calculate variables on the PE sponsor experience at the time of each transaction we use Thomson Venture Economics (TVE). First, we count the number of transactions the respective PE firm had historically sponsored before the deal at hand as reported in TVE. Second, we calculate the total assets under management of the PE sponsor accumulated in the five years before each transaction. Finally, in order to account for the volatility in public equity markets we use the MSCI website[14] to obtain data on the MSCI World index. For descriptive statistics and sample characteristics of the PE dataset, we refer to Braun et al. [2011].

[13]The data can be obtained from `http://sdw.ecb.europa.eu`.
[14]The data can be obtained from `http://www.mscibarra.com`.

3.2.3 Risk factors of PE investments

Now, we analyze the risk appetite of PE sponsors reflected in deal-level equity volatilities. The first part deals with patterns of PE sponsors' risk appetite over time, i.e. in different cycles of the PE market. In the second part, we report the results of cross-sectional analyses to assess the role of several drivers explaining equity volatility variation among PE transactions. We put a particular emphasis on factors related to the PE sponsor.

Time Trends

Table 3.9 shows summary statistics on the equity volatilities (i.e. the standard deviations resulting from our model) grouped by PE market cycles according to Strömberg [2008]. These volatilities represent the annual implied equity volatilities for the individual transactions and are calculated with the model introduced in *Section 3.2.1*. The mean and median values in the entire final sample are 80% and 72%, respectively. This is considerably higher than the average firm equity volatility of 51.3% p.a. and the median firm equity volatility of 43.6% p.a. reported by Choi and Richardson [2008] who calculate the implied equity volatility for over 150 000 public companies. However, given that in general PE-backed firms have higher leverage ratios (which, ceteris paribus, increases equity risk) this result is intuitive (see, e.g., Guo et al. [2011]). This finding confirms the general feeling that PE deals are particularly risky, at least from the perspective of equity investors. In line with this argument, Cochrane [2005] reports an annualized standard deviation of equity returns of 89% for a sample of venture capital (VC)-backed firms. Taking into consideration that Cochrane [2005] analyses VC investments, which are thought to be even more risky than buyout transactions, this finding is intuitive.

Our equity risk numbers reflect the risk appetite of a PE sponsor in the sense that they are mainly determined by the buyout target's asset volatility and its specific financing structure. Both factors can be influenced by the PE sponsor. Even if one argues that the financing structure is mainly determined by the willingness of banks to provide debt (the PE sponsor always takes as much debt as possible) it is still the choice of a PE sponsor to choose a company with a relatively high or low asset volatility. As *Table 3.10* shows, banks do not always offset investments in companies with high asset volatilities by providing less debt. Significant rank sum tests indicate considerable fluctuations of equity risk levels over time. Overall, our results imply that it is reasonable to assume that the PE sponsor can significantly influence this process, especially during boom periods when banks have a relatively pronounced risk appetite.

Table 3.10 shows additionally the mean and median asset volatility and net debt to equity ratio grouped by the PE market cycles. Interestingly, our mean and median asset

	#	Asset risk		Equity risk		Debt to equity		Default risk	
		Mean	Median	Mean	Median	Mean	Median	Mean	Median
1990–1994	48	34%	27%	79%	68%	2.61	1.59	4.35%	3.03%
1995–1999	203	31%	27%	84%	73%	2.59	1.82	4.92%	4.52%
2000–2002	118	29%	25%	68%	64%	1.83	1.56	2.38%	1.91%
2003–2005	91	38%	32%	89%	82%	2.56	1.62	5.59%	5.41%
Total	460	32%	27%	80%	72%	2.39	1.64	4.34%	3.53%

Table 3.10: Mean and median values of deal-level asset/equity risk and the net debt to equity ratio according to private equity (PE) market cycles based on Strömberg [2008]. Asset and equity risk for each transaction is calculated based on the model introduced in this section. The reported net debt to equity ratios of the buyout companies are those at entry, i.e. when the PE sponsor acquired the company.

volatility of 32% and 27%, respectively, is considerably lower than the mean and median asset volatility of 40% and 31% reported by Choi and Richardson [2008]. This finding supports the assumption that appropriate buyout targets are companies with low inherent asset volatilities. However, given the relatively high equity risks of buyout transactions, PE sponsors obviously offset the low asset volatilities by deploying high leverage ratios. In this context, *Table 3.10* reveals another interesting observation. The relatively high mean asset risk of 38% for deals conducted in the 2003–2005 period is very close to the result by Choi and Richardson [2008] which indicates that during boom periods, which in general are accompanied by increasing fundraising activity, higher investment pressure might induce PE sponsors to invest in less appropriate companies, i.e. companies with more volatile cash flows and consequently higher asset risk. This could be due to the fact that elevated supply of capital meets a relatively inflexible demand, i.e. a somewhat given pool of appropriate buyout companies. This is an intuitive assumption as there are only a limited number of appropriate buyout companies, i.e. firms that produce stable and predictable cash flows allowing the forecasting of interest payment and debt repayment schemes over any given holding period (Opler and Titman [1993]). This finding is in line with the over-investment problem described by Axelson et al. [2009].

Another intuitive and interesting observation from *Table 3.10* are the high average equity volatilities in the periods 1995–1999 and 2003–2005. The period after 1994 was a period with increasing deal activity after the burst of the first leverage buyout bubble around 1990 (Guo et al. [2011]). Similarly, the period beginning after 2003 is considered to be a boom period in the PE market (see, e.g., Axelson et al. [2010]) with increasing deal

activity, decreasing costs of debt and, consequently, high leverage levels. This situation emerged out of the bust period between 2000 and 2002 after the bursting of the dot.-com bubble. This can be seen in a sharp decline of deals observed in our sample and the considerably lower equity risk compared to the late 1990s[15]. The patterns of risk appetite of PE sponsors shown in *Table 3.10* are intuitively in line with the market cycles of the PE market.

We argue that these findings result from agency problems inherent in the PE business in combination with loose debt market conditions. PE funds are limited partnerships with the PE sponsor acting as the GP who manages the fund. Institutional or other investors are LPs and provide most of the capital. In turn, PE sponsors only provide a relatively small amount of the capital (typically about 1 percent) (Kaplan and Strömberg [2009]). PE sponsors as fund managers are (at least) compensated through management fees and a share of the profits of the fund (carried interest).

We observe an increasing risk appetite from 2003 onwards, a result that can mainly be explained by two aspects: First, in times of favorable debt market conditions PE sponsors are able to use more debt to finance a transaction as banks probably demand a lower equity stake from a PE sponsor. Given their asymmetric payoff profile they use as much debt as possible. Second, as Axelson et al. [2010] and Demiroglu and James [2010] show, the overall debt financing terms for PE sponsors improved considerably after 2003. If costs of debt are not priced adequately due to overheating debt markets it might be rational for any investor to use more inadequately priced debt since the costs for higher probabilities of default are not reflected in the interest rates. This means in the present context that equity volatility in PE market boom periods increases. Furthermore, in addition to the increased use of leverage, PE sponsors also invest in companies with higher asset volatilities (see *Table 3.10*). Apparently, both factors explain the significant increase in equity risk.

Table 3.10 shows that the increased risk appetite of PE sponsors during PE market boom periods also has a downside as default risk increases. The assumed ex-ante median probability that a PE company will default within the first year after the buyout increased from about 2% in 2000-2002 to more than 5% in 2003-2005. The average and median default rates for the whole sample are 4.3% and 3.5% respectively. This supports the notion of an incentive conflict between the PE sponsor on the one side and LPs as well as

[15]The most recent period 2003–2005 contains relatively few deals considering that it is a boom period of the PE market. This is a direct result from our sampling requirement since we can only use realized deals for calculating equity risk. Hence, at the time the fund-of-fund investors obtained information on these deals, fewer deals entered in the most recent period were realized, even though deal activity was relatively high.

other stakeholders of the company, e.g. employees and creditors, on the other side, as PE sponsors try to shift risks from themselves to others.

With regard to the explanatory power of our model, a comparison with other studies delivers encouraging results. Given that the probability of default in our model is at a maximum in the first year after the PE sponsor acquired a company (due to high interest and redemption payments) this number is comparable to the average annual default rates of 1.2% and 2.8% per year in Strömberg [2008] and Jason [2010], respectively, neither of whom account for the fact that the probability of default is not equally distributed over the holding period[16].

Now, we conduct multiple regression analyses using equity volatility as dependent variable.

Regression analysis[17]

In our analyses of drivers of deal-level risk appetite, we focus on buyout company size, PE sponsor experience and equity risk exposure, public market volatility, and, finally, the PE market cycles.

To begin with, larger buyout companies are assumed to have a higher lending capacity as they are less risky (Nikoskelainen and Wright [2007], Halpern et al. [2009]) and less exposed to asymmetrical information (Chen [1983] and Chan et al. [1985]). In addition, larger companies are assumed to be more diversified and consequently less exposed to industry shocks. According to this argument, we would expect larger companies to have lower asset volatilities, which, ceteris paribus, would result in lower equity volatilities. However, the lower asset risk of larger companies might be offset or even outweighed by more leverage deployed by the PE sponsor. If this holds, we would rather expect larger buyout companies to have higher equity volatilities. Since there are arguments in both directions, it remains an empirical question. We address this question by including the *logarithmized enterprise value of the buyout company* at investment entry in our regressions.

Regarding PE sponsor characteristics, more experienced PE sponsors are thought to be more reputable (Gompers and Lerner [2000], Kaplan and Schoar [2005]). As reputation can be an important competitive advantage, for example in terms of lending capacity (Demiroglu and James [2010], Ivashina and Kovner [2011]), more reputed PE sponsors

[16] For example, our median default rate of 3.5% is not an annualized default rate over the holding period, but the probability that a firm defaults within the first year after the buyout. In year two, three, etc. the probability of default decreases.

[17] I want to thank Dr. Nico Engel for carrying out the regression analysis.

would not risk their reputation by taking excessive risks (Diamond [1989]). Therefore, we expect a negative relation between PE sponsor reputation and equity risk. In order to assess this relationship we include the *logarithmized number of previously completed deals* by the respective PE sponsor at investment entry as proxy for PE sponsor reputation (Demiroglu and James [2010]). As the measures of PE sponsor experience are controversially discussed in the literature (e.g. Gompers and Lerner [1999]) we also use the *logarithmized total assets under management* of the PE sponsor accumulated in the five years before investment entry as proxy for PE sponsor experience (Gompers and Lerner [1999], Kaplan and Schoar [2005]).

Another PE sponsor characteristic is its *ownership stake in the company* which can be interpreted as the equity risk exposure. While in a typical buyout transaction, the PE sponsor purchases majority control (Kaplan and Strömberg [2009]), the ownership stake, and accordingly the equity risk exposure, varies. The intuition behind this is that if a PE sponsor owns a large part of the equity value, the willingness to take excessive risks might be reduced. This argument fits into the concept of equity stakes as call options on firm values (Axelson et al. [2009]). If the PE sponsor provides a higher share of the enterprise's equity value, the downside risk, ceteris paribus, increases. We expect a negative relation between PE sponsor ownership and equity risk. Accordingly, we include the total capital invested by the PE sponsor divided by the total equity value at investment entry in our regressions.

Apart from company- and PE sponsor-related characteristics, it is reasonable to assume that the conditions of public equity markets also have an influence on the chosen deal-level equity risk. Very volatile public equity markets may indicate a relatively high uncertainty with regard to future economic development which could lead to a reduced risk appetite among all participants in both public and private equity markets. In order to test for these more general market effects we assign the *volatility of the MSCI World Index* in the last twelve months (LTM) before the entry date of a specific PE transaction to each deal. Considering that we have a regionally diverse sample of European and North American transactions, the MSCI World Index may be the best measure to account for worldwide market volatility and is consequently the best proxy for the level of uncertainty about future economic developments. As a result, we expect a negative relationship between LTM public market volatility and deal-level equity risk.

In order to account for the effects of PE market cycles, we include *time dummies* to control for systematic time patterns in the buyout market. Again, we resort to the PE market cycle time categories introduced by Strömberg [2008].

Furthermore, there are some other standard factors we include in our analysis: First, to control for significant systematic differences between European and North American deals, a *region dummy* is used which adopts a value of 1 if the PE transaction took place in Europe and a value of 0 if the deal took place in North America. Second, we include eight *ICB industry dummies* to control for industry specific risks.

Table 3.11 shows the regression results on our final sample of 460 buyout transactions using as a dependent variable the equity volatility resulting from our model. We use the logarithmized value in our regression analysis since equity volatility can only take non-negative numbers. In our first specification, which only includes the 12-month historical volatility of the MSCI World Stock Market Index before the transaction, our PE market cycles and control variables, we find that deals conducted in a relatively bullish economic environment (i.e. the periods between 1995-1999 and 2003-2005) are riskier than those carried out during the relatively bust period during the years 2000-2002 that we use as reference category. For instance, buyout transactions entered between 2003 and 2005 have a 26% higher equity risk compared to the deals entered during the period 2000-2002. The coefficients for the boom periods of the PE market are highly significant throughout all specifications and strongly support our findings concerning time patterns reported earlier.

Throughout all specifications we find a significantly (5% and 1% level) negative relation between the volatility of the MSCI World Index and deal-level equity risk. Higher volatility in public markets represents a strong uncertainty with regard to the economic outlook. Apparently, this situation also reduces the risk appetite of PE sponsors who craft less risky deal structures in such an environment.

The highly significant (1% level) negative coefficient of buyout company size in specification (2) confirms the argument that larger deals are less risky. Apparently, PE sponsors do not use excessive leverage in order to offset the lower asset volatility of larger companies.

Our findings show that PE sponsor reputation measured by the logarithm of historical deals is significantly (1% level) negatively related to deal-level equity risk (see specification (3)). Similar results hold if the logarithm of assets under management is used as proxy for PE sponsor reputation (specification (4)). While this estimated coefficient is significant at the 1% level, the relationship decreases in statistical and practical significance when including deal size in specification (5). We think that this finding is intuitive as larger PE funds conduct larger deals. Hence, there is a strong positive correlation between assets under management and deal size which has a moderating effect on the relationship between PE sponsor experience and equity risk. In addition, some very experienced and

Specification	(1)	(2)	(3)	(4)	(5)
Variables	ln(*equity volatility*)	ln(*equity volatility*)	ln(*equity volatility*)	ln(*equity volatility*)	ln(*equity volatility*)
ln(*enterprise value*)		-0.045***	-0.045***		-0.033**
ln(*number of deals*)			-0.026***		
ln(*ownership*)				-0.018*	-0.017*
ln(*assets under management*)				-0.050***	-0.031**
ln(*MSCI world volatility*)	-0.127***	-0.118**	-0.131***	-0.131***	-0.123**
1990–1994	0.046	0.010	-0.038	-0.040	0.036
1995–1999	0.164***	0.162***	0.138***	0.094***	0.106**
2003–2005	0.233***	0.249***	0.273***	0.201***	0.202***
Industry dummies	Yes	Yes	Yes	Yes	Yes
Region dummy	Yes	Yes	Yes	Yes	Yes
Observations	458	458	458	416	416
R-squared	0.096	0.121	0.133	0.126	0.137

*Table 3.11: Equity Risk as Dependent Variable. We present the results of ordinary least squares regressions on the determinants of equity risk using our final sample of 460 leveraged buyouts acquired between 1990 and 2005. The dependent variable is the logarithmized equity risk volatility as computed in our model. In order to account for temporal effects, a value of 1 is assigned to all buyouts that, for example, were initiated between 1990 and 1994 and 0 otherwise. Again, these categories represent different cycles of the PE market based on Strömberg [2008]. We have chosen the period between 2000 and 2002 as the base category. In addition, we include eight ICB industry category dummies accounting for industry effects. We also include the logarithmized value of the average volatility in the last twelve months (LTM) prior to the investment entry date of the respective PE transaction of the MSCI World Stock Index to account for public market volatility. Finally, the region dummy obtains a value of 1 if the buyout target company's headquarter is in Europe and 0 if it is located in North America. *, ** and *** indicate p-values of 10%, 5%, and 1% significance level, respectively.*

We use an ordinary least squares regression with heteroscedasticity-consistent standard errors. Our data fulfills the standard assumptions necessary to perform a linear regression (e.g. normality of residuals and linearity).

highly reputed PE sponsors deliberately restrict their maximum fund size in order to avoid putting their fund-level performance at risk. As the assets under management proxy would indicate low PE sponsor experience, we believe that our first reputation proxy is a superior proxy in this context. Thus, we argue that more experienced and higher reputed PE sponsors exhibit less risk appetite because they fear losing their reputation and its corresponding competitive advantage.

Our specifications (4) and (5) consistently show a negative relationship between the ownership stake at investment entry and equity risk. Our results are in line with viewing PE investors' equity stakes as call options. As higher equity stakes go along with reduced risk appetite, lower stakes in the total equity values could trigger "gambling for resurrection" behavior (Axelson et al. [2009], Axelson et al. [2010]).

3.2.4 Summary and Conclusion

During the last two decades, PE has become an important source of capital for companies and considerable amounts of money have flown into these funds from investors around the globe. While academic work has made significant progress, evidence on the risks associated with PE investing is still relatively scarce. The main reasons for this situation are the conceptual problems to compute risks for these illiquid investments as well as the limited availability of appropriate data sets. Using a proprietary data set of 460 realized European and North American buyouts entered between 1990 and 2005, we analyzed time patterns and determinants of the risk appetite of PE sponsors.
We started by developing a quantitative model to calculate deal-level implied asset and equity volatilities including both systematic and idiosyncratic risk. Our model allows for continuous interest and redemption payments as well as for continuous default. We think that the implied deal-level asset and equity risks resulting from our model represent good indications of the PE sponsors' assumptions about the development of the asset and equity risk over the holding period at investment entry.

We then calculated the deal-level equity volatilities for our transactions in order to analyze the risk appetite of PE sponsors over time. We have found that the risk appetite of PE sponsors fluctuates remarkably over time indicating that these investors adjust their attitude towards risk according to the economic environment. In this context we have found that PE sponsors take more risk during boom periods which explains (or can be explained by) boom and bust cycles in the buyout market. It is important to note that it is not only banks issuing cheap debt in times of economic upturns which causes overheating buyout markets but also the increasing risk appetite of PE sponsors. PE sponsors could use more equity to finance a transaction and not accept all supplied debt or offset higher

leverage ratios by choosing companies with lower asset risk.

In this context, we have also found high volatility in public equity markets prior to the investment entry of a PE sponsor (i.e. in the twelve months before the PE sponsor buys a company) has a negative influence on deal-level equity risk. Obviously, high uncertainty with regard to future economic development leads to reduced risk appetite of PE sponsors and/or a reduced willingness by banks to provide debt to finance a transaction.

In a next step, we have taken a detailed look at the determinants of PE sponsors' risk appetite. We find that larger buyouts exhibit lower equity risks. This finding indicates that PE sponsors do not use excessive leverage in order to offset the lower asset volatility of larger companies. If they were to do so, the equity risk increases through heightened leverage would outweigh the effect of low asset risk embraced in the company. Further, we find that buyouts initiated by more experienced and higher reputed PE sponsors are less risky. We attribute this reduced risk appetite to their fear of damaging their reputation and its corresponding competitive advantage in the PE context (Achleitner et al. [2012], Demiroglu and James [2010], Ivashina and Kovner [2011]). Finally, we have found that an increasing ownership stake by the PE sponsor is related to a decreasing risk appetite. This finding is in line with viewing the PE investors' equity stake as a call option. If the price the PE sponsor has to pay for his option rises, the risk appetite decreases. Since we have found that equity volatilities increase during boom periods and that reputation (as well as ownership stake) is negatively related to equity risk, we argue that PE sponsors do not always act in the interest of LPs when they deploy a certain debt to equity ratio on a buyout target, but take excessive risks. This is further support for agency conflicts between GPs and LPs which can (at least partially) be solved through reputation.

3.3 Insurance risk

As a third example, we discuss applications of first-exit times in insurance. Consider an insurance company that, for example, issues fire insurance policies. The insurance company receives premiums regularly and, in return, has to pay the claims of the policyholders. Since size and arrival time of insurance claims are random, the insurance company has to ensure that it is able to fulfill its obligations to the policyholders. Therefore, the total assets of the insurance company – called *risk reserve* – has to stay positive. This risk reserve $B := \{B_t\}_{t\geq 0}$ is usually modeled as (see, e.g., Asmussen and Albrecher [2010])

$$B_t = B_0 + \mu t - C_{N_t}\,, \tag{3.38}$$

where $B_0 > 0$ is the initial reserve, $\mu > 0$ the continuously paid premiums per unit of time, $N_t \in \mathbb{N}_0$ the number of claims, and C_{N_t} the cumulated loss of the policies. One assumes that individual claim sizes Y_i are independent and identically distributed (i.i.d.) with expectation $\mathbb{E}[Y_i] = \zeta > 0$ and that $C_j := Y_1 + Y_2 + \ldots + Y_j$. The process C_{N_t} can be any renewal-type process; it does not necessarily have to be a compound Poisson process. A special case is the classical compound-Poisson risk model, known as Cramér-Lundberg model (see, e.g., Cramér [1969]). An example of a claim size distribution is given in Example 19.

The insurance company defaults as soon as the risk reserve turns negative. As in Equation (2.1) in *Chapter 2*, we define the first-exit time

$$T_{\infty,-B_0} := \inf\big\{t \geq 0 \,:\, B_t < 0\big\}, \tag{3.39}$$

where we use the convention $\inf\{\emptyset\}=\infty$. The objective of this chapter is to find approximations for the first-exit time distribution by applying the central limit theory.

Example 19 (Pareto distribution)
For the distribution of the claim sizes, a generalized Pareto distribution is often used. A Pareto(k, θ, σ) distribution is for $x \geq \theta$ (if $k \geq 0$), respectively $\theta \leq x \leq \theta - \sigma/k$ (if $k < 0$), defined via the probability density function (pdf)

$$f(x) = \frac{1}{\sigma}\left(1 + \frac{k(x-\theta)}{\sigma}\right)^{-\frac{1}{k}-1}\,,$$

where $k \in \mathbb{R}$, $\theta \in \mathbb{R}$, and $\sigma > 0$. If $Y_i \sim$Pareto(k, θ, σ), then we can derive the first two moments as $\mathbb{E}[Y_i] = \theta + \sigma/(1-k)$ (if $k < 1$) and $Var(Y_i) = \sigma^2/\big((1-k)^2(1-2k)\big)$ (if $k < 1/2$).

Equation (3.38) has extensively been treated in the literature, we refer to Asmussen and Albrecher [2010] for a detailed and recent overview. In this section, we

want to discuss an idea that relates this problem to the earlier results in this thesis: It is often possible to approximate the risk reserve by a diffusion (see, e.g., Iglehart [1969]). The idea behind this approximation is that if the number of claims is large, we can take advantage of the central limit theorem and deduce that $C_n/\sqrt{n}$ converges for $n \to \infty$ to a normal distribution[18]. As one can see in *Figure 3.7*, this approximation seems to already be acceptable if the number of claims is around 40.

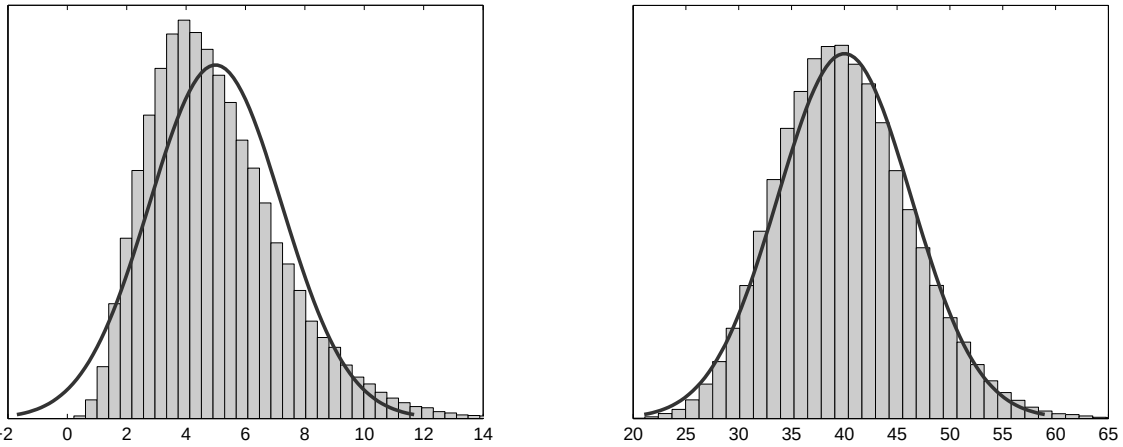

Figure 3.7: Distribution of C_5 (left) and C_{40} (right) together with a normal approximation. The claims Y_i follow a Pareto(k, θ, σ) distribution with parameters $k = 0$, $\theta = 0.8$, and $\sigma = 0.2$.

The general idea is now to construct a sequence of risk reserve processes $B_t^{(n)}$, $Y_i^{(n)}$, and $C_j^{(n)} := Y_1^{(n)} + Y_2^{(n)} + \ldots + Y_j^{(n)}$ that – for a large number n of claims per unit of time – serves as an approximation for the original process B_t. Therefore, we take advantage of central limit theorem results, for example by Prokhorov [1956]. Take an expected claim size $\mathbb{E}[Y_i^{(n)}] = 0$ with $\mathrm{Var}(Y_i^{(n)}) = \sigma_n^2 \xrightarrow{n\to\infty} \sigma^2$ and assume that $\mathbb{E}\big[\big(Y_i^{(n)}\big)^{2+\epsilon}\big] < \infty$ for some $\epsilon > 0$. Then, according to Prokhorov [1956], we find that

$$\frac{C_{\lfloor nt \rfloor}^{(n)}}{\sqrt{n}\,\sigma} \tag{3.40}$$

converges in distribution to a standard normal distribution (hereby $\lfloor x \rfloor$ returns the smallest integer less than or equal to x).

In our setting (3.38) not only the claim sizes but also the number of claims is random. That is why, we define equidistant arrival times $(0 <) t_1 < t_2 < \ldots$, where the waiting

[18] This convergence is "in distribution". The terms "convergence in distribution" and "weak convergence" are frequently used in this section. We refer the unfamiliar reader to, i.e., Billingsley [2008].

times $\triangle t_i := t_i - t_{i-1}$, for $i = 1, 2, \ldots$, are i.i.d. and positive. The number of claims that occur up to time t is then written as

$$N_t := \max\left\{n : \sum_{i=1}^{n} \triangle t_i \leq t\right\}.$$

By weak convergence we can conclude that (see, e.g., Iglehart [1969])

$$\frac{N_{nt}}{n} \xrightarrow{n\to\infty} \lambda t\,, \tag{3.41}$$

where λ can be interpreted as the average number of claims per unit of time. Following Iglehart [1969] (see also Equations (3.40) and (3.41)), we can conclude that the defined sequence $B_t^{(n)}$ for $n \to \infty$ converges weakly to a Brownian motion, i.e. to

$$B_t = B_0 + (\mu - \lambda\zeta)t + \sigma\sqrt{\lambda t}\, W_1\,, \tag{3.42}$$

where W_1 is a standard Brownian motion (see Iglehart [1969] for a proof). Central limit theorems can not only be applied on the process itself, but also on a large class of functionals of the process. That is why, we define a sequence of stopping times

$$T^{(n)}_{\infty,-B_0} := \inf\{t \geq 0 \,:\, B_t^{(n)} < 0\},$$

that allows us to conclude that $\lim_{n\to\infty} \mathbb{P}(T^{(n)}_{\infty,-B_0} \leq T) = \mathbb{P}(T_{\infty,-B_0} \leq T)$.

An approximation of the probability of a negative risk reserve and thus a default of the insurance company is then given by (see also Equation (2.2) in *Chapter 2*)

$$\begin{aligned}\mathbb{P}(T_{\infty,-B_0} \leq T) = \Phi\left(\frac{-B_0 - (\mu-\lambda\zeta)T}{\sigma\sqrt{\lambda T}}\right) \\ + \exp\left(\frac{-2(\mu-\lambda\zeta)B_0}{\sigma^2}\right)\Phi\left(\frac{-B_0 + (\mu-\lambda\zeta)T}{\sigma\sqrt{\lambda T}}\right),\end{aligned} \tag{3.43}$$

where $\Phi(\,\cdot\,)$ denotes the standard normal cumulative distribution function.

To summarize this section: Using the central limit theorem, we showed that for a large number n of claims per unit of time, the risk reserve process B_t is approximately a Brownian motion. This allows us to use the first-exit time results from *Chapter 2* and derive the default probability of, for example, a fire insurance company.

For rigorous mathematical proofs, we refer to Iglehart [1969].

Chapter 4

Multivariate extensions[1]

The aim of this chapter is to extend the univariate results of *Chapter 2* to higher dimensions. This can be used to, for example, examine the default distribution of a credit portfolio. For an individual portfolio constituent, we consider the two exit events $\oplus$ and $\ominus$, corresponding to the hitting of an upper ($\oplus$) or a lower barrier ($\ominus$) in *Chapter 2*. For d components, we now define exit times $T_{ab}^{+}(i)$ and $T_{ab}^{-}(i)$ for $i = 1, 2, \ldots, d$. In the following, we present suitable models where one is able to determine joint exit probabilities, for example the probability that (until time T) two components jointly exit to $\oplus$, i.e.

$$\mathbb{Q}\big(T_{ab}^{+}(1) \leq T;\, T_{ab}^{+}(2) \leq T\big),$$

or to $\ominus$, i.e.

$$\mathbb{Q}\big(T_{ab}^{-}(1) \leq T;\, T_{ab}^{-}(2) \leq T\big).$$

Therefore, it is necessary to adequately model the dependence between the portfolio components while still being analytically tractable. Note that this is not an easy task since in finance or insurance we typically have to deal with large portfolios (i.e. $d = 100$ or $d = 125$). In the literature, two approaches are frequently used:

- *Structural approach* (*Section 4.1*): The idea behind the structural approach is that an exit event is triggered as soon as a certain quantity exceeds (a) prespecified threshold(s). In the multivariate extension, one considers correlated "trigger" processes and their joint exit times. This is the most natural extension of the univariate case, however, it lacks the analytical tractability as already the bivariate case leads to ex-

[1] This chapter is based on the paper: Hieber, P. and Scherer, M. (2013): *Modeling credit portfolio derivatives, including both a default and a prepayment feature*, Applied Stochastic Models in Business and Industry, Vol. 19, No. 5, pp. 479–495.

tremely complicated expressions for the first-exit time distribution. More than two dimensions cannot be treated analytically, yet one has to rely on numerical schemes.

- *Copula approach* (*Section 4.2*): Another idea is to link the univariate first-exit time probabilities by means of a copula (see, e.g., Schönbucher and Schubert [2001]). The advantage of such an approach is the fact that one can treat the univariate exit probabilities and their dependence structure separately. Thus, this approach is analytically tractable and can rather easily be calibrated to market data.

In the following, we discuss the structural approach (*Section 4.1*) and the copula approach (*Section 4.2*) in more detail.

4.1 Structural approach

The structural approach is a natural extension of the univariate case in Equation (2.1) to d dependent processes $B^{(i)} = \{B_t^{(i)}\}_{t\geq 0}$, for $i = 1, 2, \ldots, d$. If those processes are Brownian motions, the dynamics read as

$$dB_t^{(i)} = \mu^{(i)}dt + \sigma^{(i)}dW_t^{(i)}, \quad B_0^{(i)} = 0,$$

where $\mu^{(i)} \in \mathbb{R}$, $\sigma^{(i)} > 0$, and $W^{(i)} = \{W_t^{(i)}\}_{t\geq 0}$, for $i = 1, 2, \ldots, d$, are correlated standard Brownian motions. Similar to *Chapter 2*, individual first-exit times can be defined via

$$T_{ab}(i) := \inf\{t \geq 0 \,:\, B_t^{(i)} \notin (b_i, a_i)\}\,, \tag{4.1}$$

where the corridors are defined such that $b_i < B_0^{(i)} = 0 < a_i$. Again – as in the univariate case – upper (and lower) barrier first-exit times $T_{ab}^{+}(i)$ (and $T_{ab}^{-}(i)$) can be defined.

In the bivariate case, there are still analytical expressions for the joint single-barrier first-exit times (see, e.g., He et al. [1998], Zhou [2001b]). However, those expressions are already numerically challenging and involve integrals and infinite series of Bessel functions. Further extensions to two-sided barriers or to the d-dimensional case are to the author's knowledge not available in (semi) closed-form. Here, one has to rely on numerical schemes.

The result by He et al. [1998] and Zhou [2001b] on Brownian motion can – similarly to our results on the univariate case in *Section 2.4* – be extended to stochastic volatility by introducing a (joint) continuous stochastic clock $\Lambda = \{\Lambda_t\}_{t\geq 0}$, independent of the $B^{(i)}$. In financial applications, this includes, for example, the following bivariate model with a Heston-type stochastic volatility:

$$\frac{dS_t^{(1)}}{S_t^{(1)}} = r\,dt + \sqrt{v_t}\,dW_t^{(1)}, \quad S_0^{(1)} > 0, \tag{4.2}$$

$$\frac{dS_t^{(2)}}{S_t^{(2)}} = r\,dt + \sqrt{v_t}\,dW_t^{(2)}, \quad S_0^{(2)} > 0, \tag{4.3}$$

$$dv_t = \theta(\nu - v_t)dt + \gamma\sqrt{v_t}\,d\tilde{W}_t, \quad v_0 > 0, \tag{4.4}$$

where r is the risk-free interest rate and θ, ν, and γ are non-negative constants fulfilling the Feller condition $2\theta\nu > \gamma^2$ that guarantees that the variance process $\{v_t\}_{t\geq 0}$ is almost surely positive (see Feller [1951]). The one-dimensional Brownian motions $\{W_t^{(1)}\}_{t\geq 0}$ and $\{W_t^{(2)}\}_{t\geq 0}$ have correlation ρ and are independent of $\{\tilde{W}_t\}_{t\geq 0}$. For a detailed discussion and more examples we refer to, for example, Kammer [2007], Götz [2011]. The latter example is one of the few bivariate models that are analytically tractable, even for payoffs like barrier (see, e.g., Götz [2011]) or spread options (see, e.g., Kiesel and Lutz [2011]).

If one wants to depart from the unsatisfactory assumption of continuous diffusion one has to rely on numerical techniques. The Brownian bridge algorithm from *Section 2.5* can (for one barrier) be extended to the bivariate case (see, e.g., Zhang and Melnik [2009]). This extension builds on the fact that analytical expressions for the bivariate Brownian bridge probabilities are available (see, e.g., He et al. [1998], Zhou [2001b]).

However, if one is interested in analytically tractable models, the copula approach in the subsequent section might be more useful. The disadvantage of this approach is the fact that those kind of models work for fixed time horizons T, yet they are not dynamic in time.

4.2 Copula approach

In *Chapter 2*, the univariate case deals with two exit events, denoted by $\oplus$ (the upper barrier is hit) and $\ominus$ (the lower barrier is hit). In credit risk applications, those exits can refer to default ($\ominus$) and an early repayment of debt ($\oplus$). Other examples like insurance portfolios can be treated similarly.

In the following, we again consider d components (which might refer to obligors or companies in a credit risk context). The univariate exit times of component i (for $i = 1, 2, \ldots, d$) are still denoted by $T_{ab}(i)$, $T_{ab}^{+}(i)$, and $T_{ab}^{-}(i)$. As mentioned earlier, we are now interested in joint exit probabilities, for example in the probability that two components simultaneously exit to $\oplus$ (until time T), i.e.

$$\mathbb{Q}\big(T_{ab}^{+}(1) \leq T;\, T_{ab}^{+}(2) \leq T\big),$$

or the probability that component 1 and 2 exit to $\ominus$ while component 3 is still active, i.e.

$$\mathbb{Q}\big(T_{ab}^{-}(1) \leq T;\, T_{ab}^{-}(2) \leq T;\, T_{ab}(3) > T\big).$$

There are many ways to model such a joint probability, for an overview see Nelsen [2006] or Mai and Scherer [2012]. In this thesis the focus is on an analytically tractable class called Archimedean copulas. To be able to work with this class, some basic concepts of copula theory are in the following recalled and applied to our specific framework. First, marginal risk-neutral exit probabilities are for $t \geq 0$ abbreviated as

$$q_i(t) := \mathbb{Q}\big(T_{ab}^{+}(i) \leq t\big), \qquad p_i(t) := \mathbb{Q}\big(T_{ab}^{-}(i) \leq t\big). \tag{4.5}$$

The functions $t \mapsto p_i(t)$ and $t \mapsto q_i(t)$ are right continuous, increasing functions with $p_i(0) = q_i(0) = 0$ and $\lim_{t\to\infty}\big(p_i(t) + q_i(t)\big) = 1$. In the copula approach we do not further discuss those marginal exit probabilities (therefore we refer to *Chapter 2*); instead these marginal probabilities are considered as model input. The aim of this chapter is to adequately model the dependence structure, i.e. to link the marginal exit probabilities to account for their dependence.

At a fixed time $T > 0$, we now decide on the fate of component i by drawing one standard uniform random variable U_i. To preserve (4.5), i.e. the marginal exit probabilities $p_i(T)$ and $q_i(T)$, we write for $i = 1, 2, \ldots, d$

$$\mathbb{Q}\big(T_{ab}^{+}(i) \leq T\big) := \mathbb{Q}\big(U_i \leq p_i(T)\big), \text{ and} \tag{4.6}$$

$$\mathbb{Q}\big(T_{ab}^{-}(i) \leq T\big) := \mathbb{Q}\big(U_i \geq 1 - q_i(T)\big)\,. \tag{4.7}$$

It is important to stress that the latter two probabilities are defined via the same standard uniform random variable U_i to account for the dependence between the two events $\oplus$ and $\ominus$. Note that in this setting, $\oplus$ and $\ominus$ are exclusive events. The previously specified marginal probabilities $p_i(t)$ and $q_i(t)$ are obviously preserved.

Figure 4.1 gives one example of $d = 4$ homogeneous components. The black, respectively gray, line corresponds to the marginal probabilities $p(t) := p_i(t)$, respectively $1 - q(t) := 1 - q_i(t)$, for the components $i = 1, 2, 3, 4$. Following the construction (4.6)–(4.7), standard uniform random variables U_1, U_2, U_3, U_4 are drawn. For $T = 5$, we find that $U_4 \leq p_4(T)$ (exit event $\ominus$ for component 4) and $U_1 \geq 1 - q_1(T)$ (exit event $\oplus$ for component 1).

Apart from dependence between the two exit events $\oplus$ and $\ominus$, the construction (4.6)–(4.7) also allows to include dependence between the components by coupling the random variables $(U_1, U_2, \ldots, U_d)$. This coupling is in the following achieved by means of a copula, see Definition 1 and, for example, Mai and Scherer [2012].

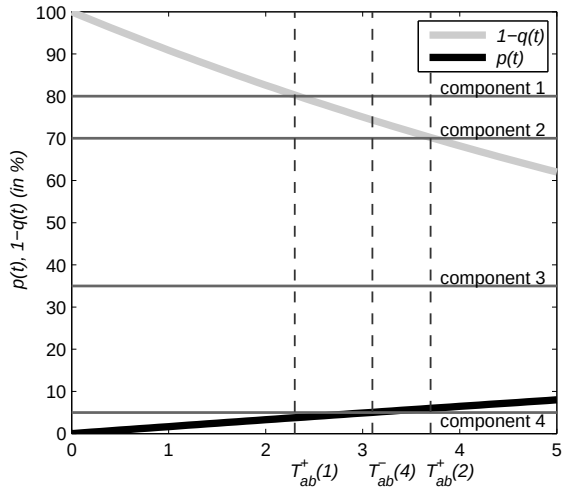

Figure 4.1: Exit events in a portfolio of $d = 4$ homogeneous components. The gray line corresponds to $1 - q(t)$, i.e. 1 minus the exit distribution for $\oplus$; the black line to $p(t)$, i.e. the exit distribution for $\ominus$.

Definition 1 (Copula)
A function $C : [0,1]^d \longrightarrow [0,1]$ is called a d-dimensional copula, if there exists a probability space $(\Omega, \mathcal{F}, \mathbb{Q})$ supporting a random vector $(U_1, U_2, \ldots, U_d)$ such that $U_i \sim U(0,1)$ for all $i = 1, 2, \ldots, d$ and

$$C(u_1, u_2, \ldots, u_d) := \mathbb{Q}(U_1 \leq u_1, U_2 \leq u_2, \ldots, U_d \leq u_d), \quad u_1, \ldots, u_d \in [0,1].$$

Using this definition in our example, we can obtain the marginal distribution $p_1(T)$ as

$$C\big(p_1(T), 1, \ldots, 1\big) = \mathbb{Q}\big(U_1 \leq p_1(T), U_2 \leq 1, \ldots, U_d \leq 1\big) = \mathbb{Q}\big(U_1 \leq p_1(T)\big).$$

There are many examples of copulas C: Well known and frequently used (but also criticized for missing tail dependence and radial symmetry) is, for example, the Gaussian copula. In this chapter, we want to concentrate on the class of Archimedean copulas that allows for flexible dependence structures while still being analytically tractable. An Archimedean copula is defined via its generator φ fulfilling the properties of Definition 2.

Definition 2 (Archimedean generator)
A function $\varphi : [0, \infty) \mapsto [0, 1]$ is called an Archimedean generator if it fulfills the properties:

(a) $\varphi(0) = 1$, $\lim_{u\to\infty} \varphi(u) = 0$,

(b) φ *is continuous,*

(c) φ *is decreasing on* $[0, \infty)$ *and strictly decreasing on* $[0, \inf\{u > 0 : \varphi(u) = 0\}]$, *where* $\inf \emptyset := \infty$.

We restrict our analysis to completely monotone generators, i.e. generators where the j-order derivatives $\varphi^{(j)}$ of φ have alternating signs: $(-1)^j \varphi^{(j)}(u) \geq 0$, for all $u > 0$ and $j \in \mathbb{N}_0$.

A possibility to construct random variables with Archimedean dependence structure is presented in Marshall and Olkin [1988], for extensions see McNeil and Nešhlová [2009]. In this construction, a common factor $Y > 0$ is introduced. Conditional on this factor, the components $(U_1, U_2, \ldots, U_d)$ are assumed to be independent. Following Bernstein's theorem (originally in Bernstein [1929], see also [Feller, 1966, p. 439]), the positive random variable Y has a (completely monotone) Laplace transform $\varphi(u) := \mathbb{E}[\exp(-uY)]$. Thus, there is a one-to-one relationship between Laplace transforms of positive random variables and completely monotone Archimedean generators (see, e.g., Kimberling [1974]). For various examples see Nelsen [2006] or Mai and Scherer [2012].

For any Archimedean generator, the joint distribution of the U_i is defined as

$$\mathbb{Q}(U_1 \leq u_1, \ldots, U_d \leq u_d) = C_\varphi(u_1, \ldots, u_d) := \varphi\Big(\varphi^{-1}(u_1) + \ldots + \varphi^{-1}(u_d)\Big). \tag{4.8}$$

Note that the inverse $\varphi^{-1}(\,\cdot\,)$ exists for completely monotone generators φ. In some cases, there exists a closed-form expression for both φ and its inverse φ^{-1}. Thus, (4.8) can easily be evaluated. Furthermore, the correspondence to positive random variables Y allows us to construct a straightforward sampling algorithm for the vector $(U_1, U_2, \ldots, U_d)$, using that

$$(U_1, \ldots, U_d) := \left(\varphi\left(\frac{\epsilon_1}{Y}\right), \ldots, \varphi\left(\frac{\epsilon_d}{Y}\right)\right) \sim C_\varphi, \tag{4.9}$$

where $\{\epsilon_i\}_{i=1}^d$ are independent exponential random variables with mean 1. The fact that construction (4.9) leads to an Archimedean dependence structure can be seen as follows: The univariate marginal distributions are standard uniform, i.e. for $i = 1, 2, \ldots, d$, we have that $\mathbb{Q}(U_i \leq u_i) = \mathbb{Q}(\varphi(\epsilon_i/Y) \leq u_i) = \mathbb{E}[1 - \exp(-Y\varphi^{-1}(u_i))] = 1 - u_i$. Furthermore, the dependence structure is of Archimedean kind, since

$$\mathbb{Q}(U_1 \leq u_1, \ldots, U_d \leq u_d) = \mathbb{E}\big[\,\mathbb{E}[\,\mathbb{1}_{\{\varphi(\epsilon_1/Y)\leq u_1\}} \cdots \mathbb{1}_{\{\varphi(\epsilon_d/Y)\leq u_d\}} \,|\, Y]\,\big]$$

$$= \mathbb{E}\Big[\exp\big(- Y(\varphi^{-1}(u_1) + \ldots + \varphi^{-1}(u_d)) \big)\Big]$$
$$= \varphi\Big(\varphi^{-1}(u_1) + \ldots + \varphi^{-1}(u_d)\Big).$$

This leads to Algorithm 7 which is originally by Marshall and Olkin [1988], see also Mai and Scherer [2012]. Algorithm 7 samples random variables $(U_1, U_2, \ldots, U_d)$ whose dependence structure is Archimedean.

Algorithm 7 (Sampling Archimedean Copulas)
This algorithm returns a realization $(U_1, U_2, \ldots, U_d)$ of the Archimedean copula C_φ.

(1) Sample i.i.d. $\epsilon_1, \epsilon_2, \ldots, \epsilon_d$, where $\epsilon_i \sim Exp(1)$ for $i = 1, 2, \ldots, d$.

(2) Sample a positive random variable Y with Laplace transform φ.

(3) Return $(U_1, U_2, \ldots, U_d)$, where $U_i := \varphi(\epsilon_i / Y)$ for $i = 1, 2, \ldots, d$.

The advantage of relying on a simulation is the possibility to generalize the presented model, for example, by including a hierarchical dependence structure, see Remark 5.

Remark 5 (Hierarchical Dependence Structure)
A hierarchical model is constructed as follows: First, we define some reasonable economic criterion (for example the geographic region, the affiliation to a certain group,...) that is known to influence the likelihood of the exit event. According to this criterion, we partition our portfolio in J groups. Each group contains d_j components ($j = 1, 2, \ldots, J$), where $d_1 + d_2 + \ldots + d_J = d$. Our motivation is to design a model where the dependence of the exit times within one group is stronger than between different groups. This can be achieved by means of a generalization of the original model that relies on J independent subordinators $\Lambda^{(j)} = \{\Lambda_t^{(j)}\}_{t \geq 0}$, $j = 1, \ldots, J$ that determine the dependence within each group. The dependence between those subordinators is modeled by a common random time V. For the i-th firm in group j ($i = 1, 2, \ldots, d_j$) we define the trigger variate $U_{ji} := \varphi^{(j)}\big(\epsilon_{ji} / \Lambda_V^{(j)}\big)$, where the ϵ_{ji} are independent exponential random variables with mean 1 and $\varphi^{(j)}(u) := \mathbb{E}[\exp(-u\Lambda_V^{(j)}(u))]$. Following Hering et al. [2010], it can be shown that the vector $(U_{11}, \ldots, U_{Jd_J})$ is distributed according to the hierarchical Archimedean copula, i.e.

$$(U_{11}, \ldots, U_{Jd_J}) \sim C_\psi\big(C_{\varphi^{(1)}}(u_{11}, \ldots, u_{1d_1}), \ldots, C_{\varphi^{(J)}}(u_{J1}, \ldots, u_{Jd_J})\big), \tag{4.10}$$

where the "global" Archimedean copula is defined via the common time V with Laplace transform $\psi(u)$ and the group specific "inner" copulas via the composition of V and the subordinators $\Lambda^{(j)}$. This composition has Laplace transform $\varphi^{(j)}(u) := \mathbb{E}\big[\exp\big(-u\Lambda_V^{(j)}(u)\big)\big] =$

$\mathbb{E}[\exp(-V\xi^{(j)}(u))] = \psi\big(\xi^{(j)}(u)\big)$ *where* $\xi^{(j)}$ *is the Laplace exponent of* $\Lambda^{(j)}$*. One then observes that the pairwise dependence within a group is indeed stronger than between two different groups.*

The common factor Y regulates the dependence between the portfolio components, i.e. the probabilities of joint exits. From construction (4.9), it is possible to imply conditional exit probabilities. If the common factor Y takes the value y, we find that

$$p_i^y(t) := \mathbb{Q}\big(T_{ab}^-(i) \le t \,\big|\, Y = y\big) = \exp\big(-y\varphi^{-1}\big(p_i(t)\big)\big)\,, \tag{4.11}$$

$$q_i^y(t) := \mathbb{Q}\big(T_{ab}^+(i) \le t \,\big|\, Y = y\big) = 1 - \exp\big(-y\varphi^{-1}\big(1 - q_i(t)\big)\big)\,. \tag{4.12}$$

An example with $d = 4$ homogeneous components ($p(t) := p_i(t)$, $q(t) := q_i(t)$, for $i = 1, 2, 3, 4$) is illustrated in *Figure 4.2*. A high value of Y corresponds to a high probability of the exit event $\oplus$ and a low probability of the exit event $\ominus$, whereas a low value of Y increases the likelihood of $\ominus$ and decreases the likelihood of $\oplus$.

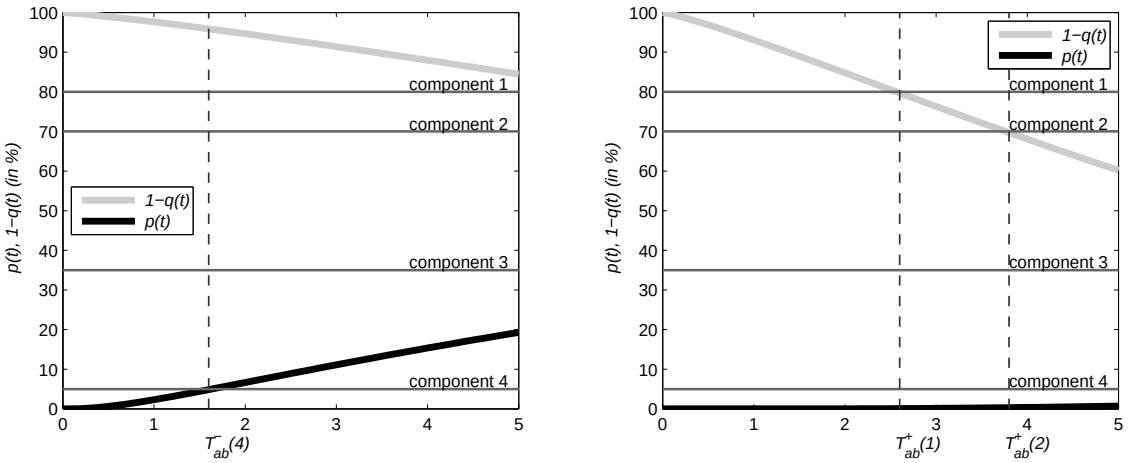

Figure 4.2: Exit events in a "recession" (left, $Y = 2$*) and in a "boom" period (right,* $Y = 6$*). In the recession (*$p^{Y=2}(5) = 19\%$*,* $q^{Y=2}(5) = 16\%$*) we observe one exit to* $\oplus$*, while in the boom period (*$p^{Y=6}(5) = 1\%$*,* $q^{Y=6}(5) = 40\%$*) we observe two exits to* $\ominus$*.*

The so described portfolio model allows for applications, for example, in the modeling and risk management of credit or (life) insurance portfolios.

4.2.1 Dependence measurement

Up to now, we have described a dependence model. This section presents some possibilities on how to measure this dependence. Since, for example, in credit risk management it is vital to adequately account for extreme events (i.e. clusters of joint exits), we introduce

the *tail dependence coefficients* and *Kendall's* τ. In contrast to, for example, a Gaussian correlation coefficient, both characteristics allow us to measure dependence in the tails of the distribution.

In the following, we focus on a portfolio with homogeneous components ($p(t) := p_i(t)$, $q(t) := q_i(t)$ for all $i = 1, \dots, d$). The results can rather easily be generalized to the case of inhomogeneous marginal exit probabilities. However, the resulting expressions are rather unhandy and do not provide a deeper understanding of the model.

Definition 3 introduces the *tail dependence coefficients* and *Kendall's* τ. The *tail dependence coefficients* (see, e.g., [Schönbucher, 2003, p. 332]) measure the dependence in the lower, respectively upper, tail of a distribution. A positive coefficient of upper (lower) tail dependence of C_φ increases the likelihood of joint exits within small amounts of time. Dependence structures that allow for a positive tail dependence tend to better fit empirical observations (for portfolio credit derivatives, see, e.g., Hofert and Scherer [2011]). *Kendall's* τ (see, e.g., [Schönbucher, 2003, p. 355], [Embrechts et al., 2005, p. 207]) is a measure of the overall dependence structure that is often used to calibrate Archimedean copulas to empirical data via moment matching.

Definition 3 (Tail dependence and Kendall's τ)
Consider an Archimedean copula with generator φ.

(a) The copula C_φ *has upper tail dependence (given the limit exists)*

$$\lambda_U := \lim_{u \to 1} \frac{1 + C_\varphi(u,u) - 2u}{1-u} = 2 - 2 \lim_{x \to 0} \frac{\varphi'(2x)}{\varphi'(x)}, \tag{4.13}$$

and lower tail dependence

$$\lambda_L := \lim_{u \to 0} \frac{C_\varphi(u,u)}{u} = 2 \lim_{x \to \infty} \frac{\varphi'(2x)}{\varphi'(x)}, \tag{4.14}$$

where $\varphi^{-1}(u) := x$ *is used.*

(b) Kendall's τ *of* $(U_1, U_2) \sim C_\varphi(u_1, u_2)$ *is given by*

$$\begin{aligned} \tau :=& \mathbb{E}\Big[\operatorname{sign}\Big((U_1 - \tilde{U}_1)(U_2 - \tilde{U}_2) \Big) \Big] = 4 \int_0^1 \int_0^1 C_\varphi(u_1, u_2) \; dC_\varphi(u_1, u_2) - 1 \\ =& 1 + 4 \int_0^1 \frac{\varphi^{-1}(u)}{(\varphi^{-1}(u))'} \, du, \end{aligned} \tag{4.15}$$

where $(\tilde{U}_1, \tilde{U}_2)$ *is an independent copy of* (U_1, U_2) *and* $\operatorname{sign}(x)$ *returns 1 for* $x \in \mathbb{R}^+$, *-1 for* $x \in \mathbb{R}^-$, *and 0 otherwise.*

A proof of part (b) is to be found in [Embrechts et al., 2005, p. 207 and p. 222].

Theorem 16 presents the correlation between exit events (in the sense of Lucas [1995]). To get an impression of the behavior for short time horizons, furthermore the limiting correlations for $(t \to 0)$ are derived. A non–zero limit is important to adequately model dependence for short time horizons. If the limiting correlation is zero, exit events behave almost as independent for short time horizons.

Theorem 16 (Exit correlation)
Consider a portfolio with d components having marginal default probability $p(t)$ and prepayment probability $q(t)$, where $p(t)+q(t) \leq 1$. Dependence is modeled by the Archimedean copula C_φ via construction (4.8)–(4.9).

(a) Exit correlations (for each bivariate margin) are given by

$$\operatorname{Corr}\big(\mathbb{1}_{\{T^-_{ab}(1)\leq t\}}, \mathbb{1}_{\{T^-_{ab}(2)\leq t\}}\big) = \frac{\varphi\big(2\varphi^{-1}\big(p(t)\big)\big) - p(t)^2}{p(t)(1-p(t))},$$
$$\operatorname{Corr}\big(\mathbb{1}_{\{T^+_{ab}(1)\leq t\}}, \mathbb{1}_{\{T^+_{ab}(2)\leq t\}}\big) = \frac{\varphi\big(2\varphi^{-1}\big(1-q(t)\big)\big) - \big(1-q(t)\big)^2}{q(t)(1-q(t))}.$$

(b) The correlation between the exits $\oplus$ and $\ominus$ is non–positive and given by

$$\operatorname{Corr}\big(\mathbb{1}_{\{T^-_{ab}(1)\leq t\}}, \mathbb{1}_{\{T^+_{ab}(2)\leq t\}}\big) = -\frac{\varphi\big(\varphi^{-1}\big(p(t)\big) + \varphi^{-1}\big(1-q(t)\big)\big) - p(t)(1-q(t))}{\sqrt{p(t)(1-p(t))}\sqrt{q(t)(1-q(t))}}.$$

(c) In the limit $(t \to 0)$, one gets $\lim_{t\to 0} \operatorname{Corr}(\mathbb{1}_{\{T^-_{ab}(1)\leq t\}}, \mathbb{1}_{\{T^-_{ab}(2)\leq t\}}) = \lambda_L$, $\lim_{t\to 0} \operatorname{Corr}(\mathbb{1}_{\{T^+_{ab}(1)\leq t\}}, \mathbb{1}_{\{T^+_{ab}(2)\leq t\}}) = \lambda_U$, $\lim_{t\to 0} \operatorname{Corr}(\mathbb{1}_{\{T^-_{ab}(1)\leq t\}}, \mathbb{1}_{\{T^+_{ab}(2)\leq t\}}) = 0$.

Proof. Part (a):

$$\operatorname{Corr}\big(\mathbb{1}_{\{T^-_{ab}(1)\leq t\}}, \mathbb{1}_{\{T^-_{ab}(2)\leq t\}}\big) = \frac{C_\varphi\big(p(t), p(t)\big) - p(t)^2}{p(t)(1-p(t))} = \frac{\varphi\big(2\varphi^{-1}\big(p(t)\big)\big) - p(t)^2}{p(t)(1-p(t))}.$$

A similar argument leads to

$$\operatorname{Corr}\big(\mathbb{1}_{\{T^+_{ab}(1)\leq t\}}, \mathbb{1}_{\{T^+_{ab}(2)\leq t\}}\big) = \frac{2q(t) - 1 + C_\varphi\big(1-q(t), 1-q(t)\big) - q(t)^2}{q(t)(1-q(t))}.$$

Part (b):

$$\operatorname{Corr}\big(\mathbb{1}_{\{T^-_{ab}(1)\leq t\}}, \mathbb{1}_{\{T^+_{ab}(2)\leq t\}}\big) = \frac{p(t) - \varphi\Big(\varphi^{-1}\big(p(t)\big) + \varphi^{-1}\big(1-q(t)\big)\Big) - p(t)q(t)}{\sqrt{p(t)(1-p(t))}\sqrt{q(t)(1-q(t))}}.$$

The relation $C_\varphi(p(t), 1-q(t)) \geq p(t)(1-q(t))$ holds for Archimedean copulas with completely monotone generator due to their positive quadrant dependence property (PQD),

see, e.g., [Nelsen, 2006, p. 141]. Those are precisely the kind of copulas constructed in (4.9). Thus, $\mathrm{Corr}(\mathbb{1}_{\{T^-_{ab}(1)\le t\}}, \mathbb{1}_{\{T^+_{ab}(2)\le t\}}) \le 0$.

Part (c):
From Definition 3, we conclude that $\lim_{t\to 0} \mathrm{Corr}(\mathbb{1}_{\{T^-_{ab}(1)\le t\}}, \mathbb{1}_{\{T^-_{ab}(2)\le t\}}) = \lambda_L$. A similar argument leads to $\lim_{t\to 0} \mathrm{Corr}(\mathbb{1}_{\{T^+_{ab}(1)\le t\}}, \mathbb{1}_{\{T^+_{ab}(2)\le t\}}) = \lambda_U$. In the limit $t \to 0$, the last term in the denominator of Equation (4.16) cancels out; furthermore $\varphi^{-1}(1-q(t)) \to 0$ $(t \to 0)$. Thus, $\lim_{t\to 0} \mathrm{Corr}(\mathbb{1}_{\{T^-_{ab}(1)\le t\}}, \mathbb{1}_{\{T^+_{ab}(2)\le t\}}) = 0$. □

We now need a parametric model with both positive lower and upper tail dependence to obtain the desirable model features discussed earlier. The positive tail dependence parameters allow to include the possibility for exit clusters. Furthermore, the exit correlation is positive for $t \to 0$, allowing for dependence for short time horizons. Theorem 16 has additionally shown that the correlation between the exits $\oplus$ and $\ominus$ is less than or equal to zero if the Archimedean generator φ is completely monotone. A possible choice for the copula C_φ, respectively the common factor Y, is presented in the next section.

4.2.2 Numerical example

A suitable Archimedean copula C_φ should allow us to obtain clusters of joint exits in the two exit possibilities $\oplus$ and $\ominus$. A possible choice is the generator

$$\varphi_{\alpha,\theta}(u) := (1+u^\alpha)^{-\frac{1}{\theta}}, \tag{4.16}$$

where $0 < \alpha \le 1$ and $\theta > 0$. In Joe [1997], p. 376, this generator is referred to as *LTE*; the resulting Archimedean copula as *BB1*.

Lemma 7 (Archimedean generator *LTE*)
The generator $\varphi_{\alpha,\theta}(u) := (1+u^\alpha)^{-\frac{1}{\theta}}$ defines a (completely monotone) Archimedean generator, i.e.

(a) According to Definition 2, $\varphi_{\alpha,\theta}$ is an Archimedean generator.

(b) The generator $\varphi_{\alpha,\theta}$ is completely monotone.

Furthermore, the resulting copula C_φ has upper tail dependence $\lambda_U = 2 - 2^\alpha$, lower tail dependence $\lambda_L = 2^{-\frac{\alpha}{\theta}}$, and Kendall's $\tau = 1 - 2\alpha/(\theta+2)$.

Proof. The continuity, $\varphi_{\alpha,\theta}(0) = 1$, and $\lim_{u\to\infty}\varphi_{\alpha,\theta}(u) = 0$ are obvious. The generator $\varphi_{\alpha,\theta}(u)$ belongs to the so-called "outer power family" and thus still defines an Archimedean

copula (see, e.g., Nelsen [2006], p. 141, or Mai and Scherer [2012], p. 69). Later on, we show that the resulting market factor Y is positive and can be sampled easily.

For the dependence characteristics, we use Definition 3 to get

$$\lambda_L = \lim_{u\to\infty} \frac{\varphi_{\alpha,\theta}(2u)}{\varphi_{\alpha,\theta}(u)} = \lim_{u\to\infty} \frac{(1+(2u)^\alpha)^{-\frac{1}{\theta}}}{(1+u^\alpha)^{-\frac{1}{\theta}}} = \lim_{u\to\infty} \frac{(1/u^\alpha+2^\alpha)^{-\frac{1}{\theta}}}{(1/u^\alpha+1)^{-\frac{1}{\theta}}} = 2^{-\frac{\alpha}{\theta}},$$

$$\begin{aligned}\lambda_U &= 2 - \lim_{u\to 0} \frac{1-\varphi_{\alpha,\theta}(2u)}{1-\varphi_{\alpha,\theta}(u)} = 2 - \lim_{u\to 0} \frac{1-(1+(2u)^\alpha)^{-\frac{1}{\theta}}}{1-(1+u^\alpha)^{-\frac{1}{\theta}}} \\ &= 2 - \lim_{u\to 0} 2^\alpha \left(\frac{1+(2u)^\alpha}{1+u^\alpha}\right)^{-\frac{1}{\theta}-1} = 2-2^\alpha,\end{aligned}$$

$$\begin{aligned}\tau &= 1 + 4\int_0^1 \frac{\varphi_{\alpha,\theta}^{-1}(u)}{(\varphi_{\alpha,\theta}^{-1}(u))'}\,du = 1 + 4\int_0^1 \frac{(u^{-\theta}-1)^{\frac{1}{\alpha}}}{\frac{1}{\alpha}(u^{-\theta}-1)^{\frac{1}{\alpha}-1}(-\theta)u^{-\theta-1}}\,du \\ &= 1 + 4\int_0^1 \frac{-\alpha}{\theta}(u-u^{\theta+1})\,du = 1 - 4\frac{\alpha}{\theta}\left[\frac{u^2}{2} - \frac{u^{\theta+2}}{\theta+2}\right]_0^1 = 1 - \frac{2\alpha}{\theta+2}.\end{aligned}$$

□

Again, we want to take advantage of the one-to-one relationship between Archimedean generators and Laplace transforms of positive random variables. First, we observe that $\varphi_{1,\theta}(u)$ is, for $u > 1/\theta$, the Laplace transform of a $\Gamma(1/\theta, 1)$-distributed random variable. The Laplace exponent $u^\alpha = -\log\big(\mathbb{E}[\exp(-u\Lambda(\alpha))]\big)$ corresponds to a special form of an alpha-stable random variable[2] $\Lambda(\alpha)$.

The common factor Y in construction (4.9) is then an α-stable Lévy subordinator $\Lambda = \{\Lambda_t(\alpha)\}_{t\geq 0}$ stopped at time $V \sim \Gamma(1/\theta, 1)$. Then,

$$\begin{aligned}\mathbb{E}\big[\exp\big(-u\Lambda_V(\alpha)\big)\big] &= \mathbb{E}\Big[\mathbb{E}\big[\exp\big(-u\Lambda_V(\alpha)\big)\,\big|\,V\big]\Big] \\ &= \mathbb{E}\Big[\exp\big(-Vu^\alpha\big)\Big] = \varphi_{1,\theta}(u^\alpha) = (1+u^\alpha)^{-\frac{1}{\theta}} =: \varphi_{\alpha,\theta}(u).\end{aligned}$$

To sample Archimedean copulas using Algorithm 7, one can then sample the common factor $Y = \Lambda_V$ as $V^{\frac{1}{\alpha}}W$, where $W \sim \Lambda(\alpha)$.

[2] α-stable random variables, see, e.g., Nolan [2010], are parameterized as $S^1(\alpha,\beta,\gamma,\delta)$, where $0 < \alpha \leq 2$, $-1 \leq \beta \leq 1$, $0 < \gamma < \infty$, $\delta \in \mathbb{R}$, and are defined by their characteristic function

$$\phi(u) = \exp\Big(iu\delta - |\gamma u|^\alpha\Big(1 - i\beta\,\mathrm{sign}(u)\tan\frac{\pi\alpha}{2}\Big)\Big). \tag{4.17}$$

A special form is $\Lambda(\alpha) \sim S^1\Big(\alpha, 1, \big(\cos\big(\frac{\pi\alpha}{2}\big)\big)^{\frac{1}{\alpha}}, \mathbb{1}_{\{\alpha=1\}}\Big)$. Using Euler's formula, the Laplace transform of $\Lambda(\alpha)$ can be obtained as $\phi_\alpha(u) = \exp(-u^\alpha)$. Details of this calculation can be found in Hofert [2010].

Note that this parameterization is special: The generator LTE is one of the rare Archimedean generators that allows for both positive upper tail dependence $\lambda_U = 2 - 2^{\alpha}$ and positive lower tail dependence $\lambda_L = 2^{-\frac{\alpha}{\theta}}$.

Additionally, the two parameters α and θ allow to calibrate exit correlation for the two exit events $\oplus$ and $\ominus$ separately. In the bivariate case, the dependence structure of (U_1, U_2) can be visualized by a scatterplot. *Figure 4.3* gives examples for different parameter choices. A rather strong clustering in the lower left corner of the scatterplot is evidence for positive lower tail dependence and thus a high likelihood of joint exits to $\ominus$. A clustering in the upper right corner is a sign for positive upper tail dependence and, thus, a high likelihood of joint exits to $\oplus$. The flexibility of the model to fit different magnitudes of exit clusters is crucial.

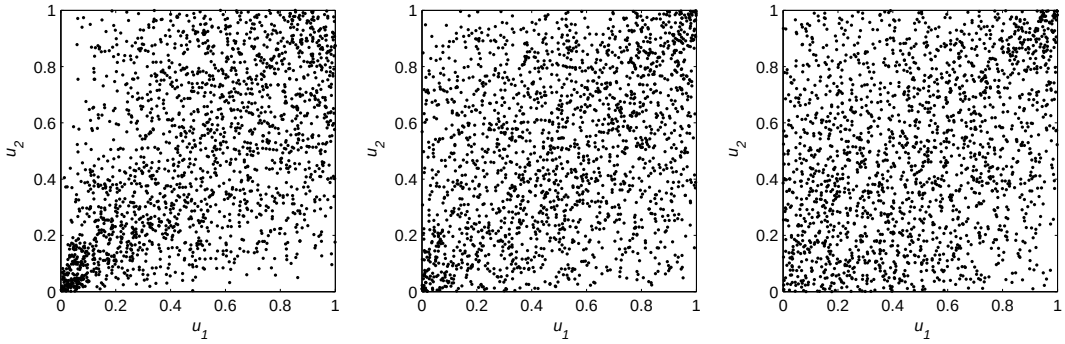

Figure 4.3: Bivariate scatterplots of the Archimedean copula C_φ. Clusters in the lower left and the upper right corner provide evidence for tail dependence. Copulas with solely lower (left, $\alpha = 1.00$, $\theta = 0.91$), upper and lower tail dependence (middle, $\alpha = 0.84$, $\theta = 0.24$), and mostly upper (right, $\alpha = 0.80$, $\theta = 1000.0$) tail depencence are presented.

A special case of the presented Archimedean dependence structure $C_{\varphi_{\alpha,\theta}}$ is, for $\alpha = 1$, the Clayton copula. The limit $\theta \to \infty$ corresponds to the comonotonicity copula; the limit $\theta \to 0$, $\alpha = 1$ is the independence copula. In this sense, C_φ interpolates between independence and perfect comonotonicity.

4.3 Credit risk management: Prepayment risk

Default risk for (portfolios of) mortgages, loans, and bonds is a well-studied phenomenon. Fewer attention is put on the borrower's option of early contract termination. For instance, mortgagors in the US are allowed to pay back their mortgages at any time at the price of the outstanding notional. Loans and bonds can be equipped with similar characteristics. Related is the case of mortality risk (or longevity risk) for life insurance contracts and the option that such contracts can be canceled by the policy holders. This flexibility introduces a cash-flow uncertainty called prepayment risk.

With \$13.1 trillion[3] in total mortgage debt outstanding, mortgage-backed securities (MBS) are one of the most important asset classes in the US. Prepayment risk is one of the key determinants for the pricing of MBS (see, e.g., Deng et al. [2000], Chow et al. [2000], Maxam and Lacour-Little [2001]). Several empirical studies, for example Brown [1999] and Gabaix et al. [2007], find evidence that this risk is priced in the MBS market. Due to various reasons for early contract termination, modeling prepayment risk has turned out to be difficult. Apart from borrower-specific factors like, for example, divorce or unemployment, the literature has identified four major risk factors affecting all borrowers. First, mortgagors tend to refinance if the prevailing mortgage rate is lower than the coupon rate (see, e.g., Hakim [1992], Schwartz and Torous [1993], Gabaix et al. [2007]). Second, a high loan-to-value (LTV) ratio leads to a faster repayment (Schwartz and Torous [1993], Deng et al. [2000], Downing et al. [2005]). Third, rising house prices result in an increased activity in the housing market and thus in increased prepayment rates (Monsen [1992], Caplin et al. [1997], Downing et al. [2005], Gabaix et al. [2007]). Last, the age of the mortgage is an important determinant of the prepayment behavior: Prepayment rates tend to increase during the first 8–10 years of the mortgage and decrease after that (see, e.g., Schwartz and Torous [1993], Maxam and Lacour-Little [2001], Goncharov [2006]). The reported percentage of prepaid mortgages varies widely: In a portfolio of single family mortgage loans originated between 1968 and 1973, Deng et al. [2000] estimate a 5-year prepayment rate of 19.0%, while Coffey [2007] – using a different sample – finds a 5-year prepayment rate of 38.0%. Chow et al. [2000] estimate a yearly prepayment rate of above 20.0% in the Hong Kong housing market. However, there is vast agreement that banks must not neglect this risk. First, due to the high costs of acquiring a mortgage, the funds need to remain on the books for several years in order to be profitable. Second, in case of prepayment, banks have to find alternative use for the funds and thus face reinvestment risk. As prepayments tend to occur when interest rates are low, banks often have to relend

[3] According to the Federal Reserve Statistical Release, December 2012 (`http://www.federalreserve.gov/econresdata/releases/mortoutstand/mortoutstand2013.htm`).

the funds at a loss.

This motivates why managing both default and prepayment risk is important. To compute the Value–at–Risk (VaR) of a mortgage portfolio for regulatory or internal purposes, it is necessary to estimate quantiles of the portfolio loss distribution. Thus, an accordant model must appropriately specify the interdependence between the different obligors. At the same time, the computational burden associated with the MBS valuation technique – especially on a portfolio level – has to remain feasible. During daily business, possibly large portfolios of MBS have to be revaluated frequently under different scenarios. A model relying on time expensive numerical schemes might be unsuitable for most real–world applications (see, e.g., Collin-Dufresne and Harding [1999], Sharp et al. [2007]). Another feature of mortgage and loan portfolios is the joint occurrence of defaults and prepayments. Defaults/prepayments tend to occur in clusters (see, e.g., Dobránszky and Schoutens [2008]). On the markets, times of prospering economy with an increased prepayment activity and few defaults as well as times of recession with a high probability of joint defaults are observed. Therefore, it is necessary to model both tails of the portfolio distribution adequately. As correlations of prepayments and of defaults tend to be different (see, e.g., Dobránszky and Schoutens [2009]), fitting default and prepayment correlation separately is important. Gaussian (and other elliptical) copulas – being radially symmetric – do not allow for this flexibility. Furthermore, the Gaussian dependence structure leads to unrealistic prices for short time horizons as defaults and, respectively, prepayments under a Gaussian dependence assumption are almost independent for short maturities. Last, a default and prepayment model has to consider the interdependence between defaults and prepayments. Estimating both risks separately leads to serious pricing errors, as pointed out in Deng et al. [2000]. Households are more likely to prepay in good states of the economy than in bad states (see, e.g., Gabaix et al. [2007]). Furthermore, there is evidence that the value of a prepayment option rises if the value of the corresponding default option falls (see, e.g., Deng et al. [2000], Downing et al. [2005]). Thus, it is largely accepted in the literature to assume a negative association between prepayments and defaults (see, e.g., Dobránszky and Schoutens [2009], Jönsson et al. [2009], Liang and Zhou [2010]).

There are two main strands of literature on the joint modeling of default and prepayment. The first one is intensity-based: Default and prepayment intensities are correlated, by, for example, a factor model construction (see, e.g., Liang [2009], Jönsson et al. [2009], Schoutens and Cariboni [2009], and Liang and Zhou [2010]). The second one is a structural approach using both a default and a prepayment barrier. The obligor defaults, respectively prepays, if a certain process falls below a given level, respectively exceeds a given level. The two levels are either calibrated to default and prepayment probabil-

ities (see, e.g., Kau et al. [1987], Dobránszky and Schoutens [2009]), credit spreads (see, e.g., Breeden and Gilkeson [1997]) or directly linked to house prices and some interest rate level (see, e.g., Gabaix et al. [2007]). As discussed above, modeling the dependence between different obligors is vital to adequately account for portfolio risk. Only few papers tackle this problem in a joint default and prepayment model: Jönsson et al. [2009], Schoutens and Cariboni [2009], and Dobránszky and Schoutens [2009] use a skewed Lévy copula that allows for both default and prepayment clusters. For the related case of CDO pricing, see also Albrecher et al. [2007].

In the remaining part of this chapter, a related model is presented, the dependence structure, however, is of Archimedean kind and, hence, (a) flexible, (b) explicitly given in terms of a copula representation, and (c) well studied. Technically speaking, obligors are assumed to be independent conditional on a positive common factor Y. This common factor models the current state of the economy: A low value of Y increases the likelihood of joint defaults while a high value of Y increases the probability of joint prepayment. Our construction, which is in the spirit of the stochastic representation of extendible Archimedean copulas, see Marshall and Olkin [1988], is both flexible enough to allow for the features necessary for a realistic joint default and prepayment model and at the same time analytically tractable to obtain accurate results in little time.

In *Section 4.2*, we showed how to model dependence in a portfolio of d components. We now apply those results to portfolio credit risk in a portfolio of d obligors. Therefore, we define the two exit events default ($\ominus$) and early repayment of debt ($\oplus$). We now derive expressions for the loss and notional of an according credit portfolio. This can be achieved by means of an iterative procedure or through Monte–Carlo simulation.

4.3.1 Distribution of the portfolio loss and notional

Equations (4.11) and (4.12) in *Section 4.2* provide the marginal probabilities of default conditional on a realization $Y = y$ of the common factor. In a portfolio with d obligors, an important quantity is the joint probability of prepayments and defaults, i.e. the probabilities

$$\mathbb{Q}(\text{“}b \text{ defaults and } l \text{ prepayments until } t\text{”} \,|\, Y = y) =: \Pi^{y,d}_{b,l}(t), \tag{4.18}$$

where $b, l \in \mathbb{N}_0$ and obviously $0 \leq b + l \leq d$ (otherwise $\Pi^{y,d}_{b,l}(t)$ is set to zero). These probabilities can be obtained by extending the classical recursive loss formula to default and prepayment risk, see Dobránszky and Schoutens [2009]:

$$\Pi^{y,i}_{b,l}(t) = \Big(1 - p^y_i(t) - q^y_i(t)\Big)\, \Pi^{y,i-1}_{b,l}(t) + p^y_i(t)\, \Pi^{y,i-1}_{b-1,l}(t) + q^y_i(t)\, \Pi^{y,i-1}_{b,l-1}(t), \tag{4.19}$$

where one uses as initial conditions that

$$\Pi_{b,l}^{y,-1}(t) = \Pi_{-1,l}^{y,d}(t) = \Pi_{b,-1}^{y,d}(t) := 0,\ \Pi_{0,0}^{y,0}(t) = 1, \tag{4.20}$$

for all $i = 0, \ldots, d$. The explanation of this iterative procedure is rather easy: If an additional obligor is added to the portfolio, it can either default ($b \mapsto b+1$), prepay ($l \mapsto l+1$), or survive. The procedure results in a triangular matrix containing the probabilities of b defaults and l prepayments conditional on a realization $Y = y$ of the common factor. Integrating out the common factor Y yields the unconditional default and prepayment probabilities

$$\Pi_{b,l}^{d}(t) := \int_0^\infty \Pi_{b,l}^{y,d}(t)\ dF_Y(y), \tag{4.21}$$

where F_Y denotes the cumulative distribution function of Y. The marginal distribution

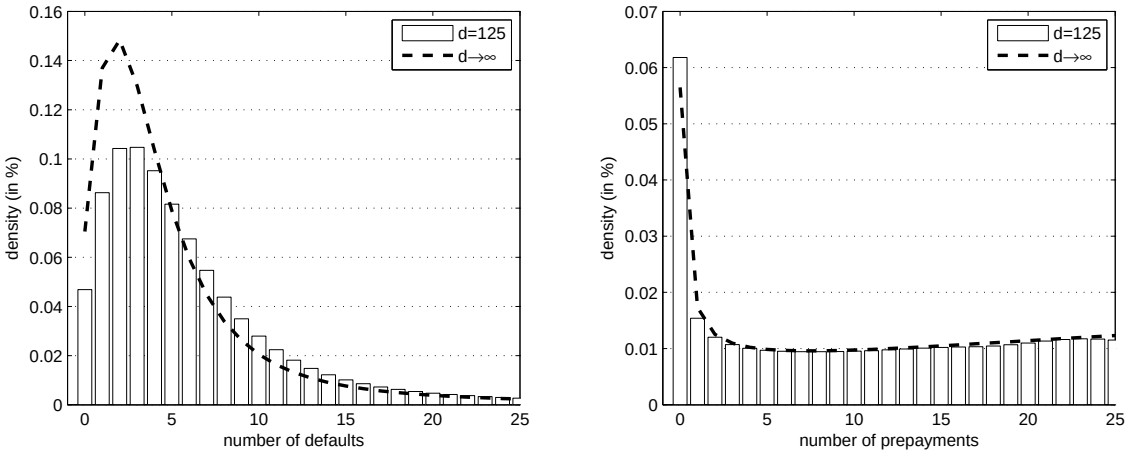

Figure 4.4: Distributions $\mathbb{Q}$("b defaults until t") (left) and $\mathbb{Q}$("l prepayments until t") (right). The bar graph shows the distribution for $d = 125$ obligors and is compared to a large homogeneous portfolio approximation (dotted line). The x-axis is either the number of defaulted, respectively prepaid, firms ($d = 125$) or the percentage of defaulted, respectively prepaid, firms ($d \to \infty$). For a better visual representation, we display the distribution for $0 \le b \le 25$, $0 \le l \le 25$ only.

of the probability of multiple defaults, conditional on $Y = y$, can be obtained as

$$\mathbb{Q}(\text{“}b \text{ defaults until } t\text{”} \mid Y = y) = \sum_{l=0}^{d-b} \Pi_{b,l}^{y,d}(t), \tag{4.22}$$

or iteratively using the procedure (4.19), setting $q_i^y(t) = 0$. *Figure 4.4* (left hand side) gives an example in a portfolio with $d = 125$ loans.

In case of default, we might additionally assume that the loan is liquidated at a recovery rate $R \in [0,1]$. Then, loss $L^d(t)$ and notional $N^d(t)$ in a portfolio with d obligors are discrete random variables with distribution

$$\mathbb{Q}\left(L^d(t) \leq (1-R)\frac{j}{d}\right) = \sum_{b=0}^{j}\sum_{l=0}^{d-b}\Pi_{b,l}^d(t), \qquad \text{for } 0 \leq j \leq d, \tag{4.23}$$

$$\mathbb{Q}\left(N^d(t) < 1 - \frac{j}{d}\right) = 1 - \sum_{b=0}^{\lfloor j/R \rfloor}\sum_{l=0}^{\lfloor j-Rb \rfloor}\Pi_{b,l}^d(t), \qquad \text{for } 0 \leq j \leq d, \tag{4.24}$$

where $\lfloor x \rfloor$ returns the smallest integer less than or equal to x.

What remains is a specification of the dependence structure and the common factor Y. A detailed discussion of dependence modeling via the common factor Y and its relation to Archimedean copulas was given in *Section 4.2*. We use the Archimedean generator LTE (see Lemma 7 in *Section 4.2* for an introduction and some important quantities) since it allows for both lower and upper tail dependence; a feature that allows us to model both default and prepayment clusters.

Apart from an integration over the distribution of the common factor (see, for example, Equation (4.21)), the distribution of portfolio loss and notional can efficiently be estimated by Monte–Carlo simulation. The algorithm requires samples of α-stable and gamma-distributed random variables as input. As demonstrated in *Section 4.2.2*, the common factor Y is sampled as $V^{\frac{1}{\alpha}}W$, where $V \sim \Gamma(1/\theta, 1)$ and $W \sim \Lambda(\alpha)$. Using Algorithm 7 from *Section 4.2*, Algorithm 8 is an efficient sampling algorithm from which the portfolio loss and notional distribution can be estimated.

Algorithm 8 (Sampling $(L^d(t), N^d(t))$)
This algorithm samples one realization of the portfolio loss $L^d(t)$ and notional $N^d(t)$. As an input the marginal default and prepayment probabilities $p_i(t)$ and $q_i(t)$, for $i = 1, 2, \ldots, d$, and the parameterization of the common factor Y are needed.

1. *Get a realization of $(U_1, U_2, \ldots, U_d)$ using Algorithm 7 in* Section 4.2. *The common factor Y is thereby sampled as $V^{\frac{1}{\alpha}}W$, where $V \sim \Gamma(1/\theta, 1)$ and $W \sim \Lambda(\alpha)$.*

2. *Return a realization of the portfolio loss $L^d(t)$ and notional $N^d(t)$ by* $\left(L^d(t), N^d(t)\right) = \left(\frac{1-R}{d}\sum_{i=1}^{d}\mathbb{1}_{\{p_i(t)\geq U_i\}}, \frac{1}{d}\sum_{i=1}^{d}\mathbb{1}_{\{p_i(t)<U_i<1-q_i(t)\}} + R\,\mathbb{1}_{\{p_i(t)\geq U_i\}}\right)$.

Let us summarize the findings of this section: We found two ways to compute the joint distribution of loss and notional $L^d(t), N^d(t)$ of a credit portfolio with d obligors: One via Monte–Carlo simulation and Algorithm 8; another analytically via Equations (4.23) and (4.24).

4.3.2 Pricing loan-credit-default-swaps (LCDS)

One possible application of the presented model is the pricing of LCDS contracts (see, e.g., Dobránszky and Schoutens [2008], Dobránszky and Schoutens [2009], and Liang and Zhou [2010]). LCDS is buying or selling protection on an issuer's loan. Buyers of protection pay a fixed amount and receive compensation on the principal if the reference entity of the contract defaults. Payments cease if the loan is either in default or fully repaid. There are two differences between LCDS and the (better–established) credit-default-swaps (CDS): First, the underlying reference obligation of LCDS is a secured loan, leading in general to higher recovery rates. Second, LCDS contracts are cancellable, thus prepayment risk is priced in those contracts. The risk-less interest rate is in the following denoted by r.

LCDS contracts are traded in tranches $[K_{j-1}; K_j]$, for $j = 1, \ldots, \#\text{tranches}$. These are typically $[0\%; 5\%]$, $[5\%; 8\%]$, $[8\%; 12\%]$, $[12\%; 15\%]$, and $[15\%; 100\%]$ of the reference portfolio notional. In respective contracts (see ISDA [2010] for standardized contract specifications), the junior-most tranche is the first to be hit by a loss; the senior-most tranche is the first to be reduced by a decrease in notional. The random variables tranche loss $L_{[K_{j-1};K_j]}(L^d(t), t)$ and tranche notional $N_{[K_{j-1};K_j]}\big(N^d(t), t\big)$ are thus defined as

$$L_{[K_{j-1};K_j]}\big(L^d(t), t\big) := \frac{\min(L^d(t), K_j) - \min(L^d(t), K_{j-1})}{K_j - K_{j-1}},$$
$$N_{[K_{j-1};K_j]}\big(N^d(t), t\big) := \frac{\min(N^d(t), K_j) - \min(N^d(t), K_{j-1})}{K_j - K_{j-1}} - L_{[K_{j-1};K_j]}\big(L^d(t), t\big).$$

In standard LCDS contracts, spread payments at the rate $s_{[K_{j-1};K_j]}$ occur in n quarterly periods at times $(t_0 = 0 <)\ t_1 < t_2 < \ldots < t_n$. The present value per unit notional of all losses in tranche $[K_{j-1}; K_j]$ is then

$$PV^{loss}_{[K_{j-1};K_j]} := \sum_{i=1}^{n} \mathbb{E}\Big[\exp(-rt_i)\ \Big(L_{[K_{j-1};K_j]}\big(L^d(t_i), t_i\big) - L_{[K_{j-1};K_j]}\big(L^d(t_{i-1}), t_{i-1}\big)\Big)\Big].$$

For simplicity, we assume that default is only possible at times $t_1, t_2, \ldots, t_n$. The present value per unit notional of all spread payments is then

$$PV^{fee}_{[K_{j-1};K_j]} := s_{[K_{j-1};K_j]} \sum_{i=1}^{n} \mathbb{E}\Big[\exp(-rt_i)\ \Big(N_{[K_{j-1};K_j]}(N^d\big(t_i\big), t_i)\triangle t_i + AccC_i\Big)\Big],$$

where $\triangle t_i := t_i - t_{i-1}$ and $AccC_i$ is the interest that has accumulated in the time interval $[t_{i-1}, t_i]$. Then, $s_{[K_{j-1};K_j]}$ is chosen such that

$$PV^{loss}_{[K_{j-1};K_j]} = PV^{fee}_{[K_{j-1};K_j]}.$$

For large (e.g. $d = 125$) and homogeneous portfolios often Assumption 1 is meaningful (see, e.g., Schönbucher [2003]).

Assumption 1 (Large Homogeneous Portfolio Approximation)
The credit portfolio consists of a large $d \to \infty$ number of homogeneous obligors. Then, at a time $t > 0$, denote by $L^\infty(t)$ (respectively $N^\infty(t)$), the fraction of defaulted securities (respectively notional) of the credit portfolio.

Theorem 17 derives expected loss and notional in a finite portfolio with d obligors and in a large homogeneous portfolio approximation (Assumption 1). This can be used to calculate portfolio tranche loss $PV^{loss}_{[K_{j-1};K_j]}$ and notional $PV^{fee}_{[K_{j-1};K_j]}$ and then the LCDS tranche spreads $s_{[K_{j-1};K_j]}$.

Theorem 17 (Expected tranche loss and notional)
The expectations required to calculate a tranche spread in a LCDS can

(a) in a finite portfolio be obtained as

$$\mathbb{E}\Big[L_{[K_{j-1};K_j]}\big(L^d(t),t\big)\Big] = \sum_{b=0}^{d}\sum_{l=0}^{d-b} L_{[K_{j-1};K_j]}\Big((1-R)b/d,t\Big)\,\Pi^d_{b,l}(t),$$
$$\mathbb{E}\Big[N_{[K_{j-1};K_j]}\big(N^d(t),t\big)\Big] = \sum_{b=0}^{d}\sum_{l=0}^{d-b} N_{[K_{j-1};K_j]}\Big(1-(Rb+l)/d,t\Big)\,\Pi^d_{b,l}(t),$$

(b) in a large homogeneous portfolio approximation be obtained as

$$\mathbb{E}\Big[L_{[K_{j-1};K_j]}\big(L^\infty(t),t\big)\Big] = \int_0^\infty L_{[K_{j-1};K_j]}\Big((1-R)p^y(t),t\Big)\,dF_Y(y),$$
$$\mathbb{E}\Big[N_{[K_{j-1};K_j]}\big(N^\infty(t),t\big)\Big] = \int_0^\infty N_{[K_{j-1};K_j]}\Big(1-(Rp^y(t)+q^y(t)),t\Big)\,dF_Y(y).$$

Proof. Part (a): Both results are expectations of functions of random variables with known distribution. The corresponding probabilities are displayed in *Section 4.3.1.*

Part (b): If Assumption 1 holds, the share of defaulted obligors conditional on the common factor Y is by the strong law of large numbers equal to the default probability $p^y(t)$. Similarly, the conditional share of obligors that repay their debt early is $q^y(t)$. Assuming a unit notional, the amount of $(1-R)p^y(t)$ is lost due to default. Due to defaults and prepayments, the portfolio notional reduces to $1-(Rp^y(t)+q^y(t))$. Individual tranche losses and tranche notional are then obtained applying the monotone functions $L_{[K_{j-1};K_j]}(\,\cdot\,)$ and $N_{[K_{j-1};K_j]}(\,\cdot\,)$. Integrating out the common factor yields the

desired expression for the expected portfolio loss and notional. For a formal and more detailed proof, we refer to Hieber and Scherer [2013].

□

Remark 6

As obligors are more likely to refinance their loan when interest rates are low, interest rates tend to be negatively correlated to prepayment rates. For the sake of simplicity, this observation is not included in the latter model, instead interest rates have to be modeled stochastically. A possibility to do so is presented in Hieber and Scherer [2013].

Furthermore, empirical observations suggest an inverse relationship between recovery rates and default rates. In times of a crisis, recovery rates tend to be lower. This fact can be included in the presented model modifying the idea presented in Andersen et al. [2003] and Andersen and Sidenius [2004]. However, in such an extension, the loss distribution is no longer independent of the dependence structure, which might cause difficulties in model calibration.

4.3.3 Numerical example

This section uses reasonable parameters to finally price LCDS tranches in order to demonstrate the practical value of the model. The parameters α, θ, $p(t)$, $q(t)$, and R are set as follows: In Hofert and Scherer [2011], the lower tail dependence is calibrated (to CDO tranches) as $\lambda_L \approx 0.089$. As correlation in prepayments tends to be higher, $\mathrm{Corr}(\mathbb{1}_{\{T_{ab}^+(1)\leq t\}}, \mathbb{1}_{\{T_{ab}^+(2)\leq t\}}) = \lambda_U$ is set to 0.200. Thus, $\alpha = \ln(2-\lambda_U)/\ln(2) \approx 0.84$ and $\theta = -\alpha \ln(2)/\ln(\lambda_L) \approx 0.24$. According to Coffey [2007], about 38% of all obligors prepay within 5 years. The five year probability of default is set to 8%. The recovery rate for secured bonds is set to $R = 70\%$, following Dobránszky and Schoutens [2009]. The time to maturity is 5 years; spread payments occur in quarterly intervals. LCDS tranches are quoted as $[0\%, 5\%]$, $[5\%, 8\%]$, $[8\%, 12\%]$, $[12\%, 15\%]$, and $[15\%, 100\%]$ of the reference portfolio notional. The risk-less interest rate is set to $r = 5\%$.

Now, we compute LCDS tranche spreads and evaluate the effect of both prepayment risk and the dependence structure. This section compares the iterative procedure (Equation (4.19)) to a Monte–Carlo simulation and a large homogeneous portfolio approximation. Increased default and prepayment clusters are examined.

	$d = 125$						$(d \to \infty)$		
	iteration			simulation			analytic limit		
	$q(t) > 0$	$q(t) = 0$	ct	$q(t) > 0$	$q(t) = 0$	ct	$q(t) > 0$	$q(t) = 0$	ct
$[0\%; 5\%]$	1135bp	1134bp	2.9s	1135bp	1135bp	9.1s	1135bp	1135bp	1.8s
$[5\%; 8\%]$	140bp	139bp	2.9s	140bp	140bp	9.1s	140bp	140bp	1.8s
$[8\%; 12\%]$	77bp	76bp	2.9s	77bp	76bp	9.1s	77bp	76bp	1.8s
$[12\%; 15\%]$	51bp	50bp	2.9s	51bp	50bp	9.1s	51bp	50bp	1.8s
$[15\%; 100\%]$	8bp	4bp	2.9s	8bp	4bp	9.1s	9bp	4bp	18s
$[0\%; 100\%]$	89bp	52bp	2.9s	89bp	52bp	9.1s	89bp	52bp	1.8s

Table 4.1: LCDS spreads in a portfolio with $d = 125$ obligors (left) and a large homogeneous portfolio approximation (right). In the case of a finite portfolio, the iterative procedure (4.19) is compared to a Monte–Carlo simulation with 500 000 runs. Spreads including prepayment risk ($q(t) > 0$) are compared to spreads with zero prepayment risk ($q(t) = 0$). All parameters are chosen as in Section 4.3.3. The respective third column contains the computation time (ct) in seconds on a standard PC with 2.4GHz.

Impact of prepayment risk

Table 4.1 presents LCDS tranche spreads in both a portfolio with $d = 125$ obligors and a large homogeneous portfolio approximation. These spreads are compared to spreads that neglect prepayment risk. Spreads computed without prepayment risk ($q(t) = 0$) are lower than spreads that consider prepayment risk ($q(t) > 0$). This effect is especially visible for the senior-most tranche ($[15\%; 100\%]$). Those results are in line with several empirical studies that point out the relevance of prepayment risk in pricing MBS (see, e.g., Brown [1999] and Gabaix et al. [2007]). The large homogeneous portfolio approximation yields almost the same results as a finite portfolio with $d = 125$ obligors.

Tail dependence

High upper (UTD), respectively lower (LTD), tail dependence coefficients increase the probability of prepayment, respectively default, clusters. *Table 4.2* examines the effect of an increased upper, respectively lower, tail dependence coefficient. We observe that an increased upper tail dependence coefficient significantly increases the spread in the senior-most tranche ($[15\%; 100\%]$) that is mostly affected by prepayment risk. Increasing LTD produces more joint defaults but also more scenarios with few default events. The result is a smaller spread of the equity tranche ($[0\%; 5\%]$) and higher spreads for the more senior tranches.

	increased LTD $\lambda_L = 0.400$, $\lambda_U = 0.200$		base case $\lambda_L = 0.089$, $\lambda_U = 0.200$		increased UTD $\lambda_L = 0.089$, $\lambda_U = 0.400$	
	$q(t) > 0$	$q(t) = 0$	$q(t) > 0$	$q(t) = 0$	$q(t) > 0$	$q(t) = 0$
$[0\%; 5\%]$	1092bp	1073bp	1135bp	1135bp	758bp	756bp
$[5\%; 8\%]$	171bp	165bp	140bp	140bp	195bp	193bp
$[8\%; 12\%]$	90bp	85bp	77bp	76bp	132bp	129bp
$[12\%; 15\%]$	59bp	54bp	51bp	50bp	99bp	95bp
$[15\%; 100\%]$	9bp	5bp	8bp	4bp	18bp	10bp
$[0\%; 100\%]$	89bp	52bp	89bp	52bp	89bp	52bp

Table 4.2: Effect of increased lower tail dependence (LTD) and thus more default clusters (left column) and increased upper tail dependence (UTD) and thus more prepayment clusters (right column). Spreads including prepayment risk ($q(t) > 0$) are compared to spreads with zero prepayment risk ($q(t) = 0$). All parameters are chosen as in Section 4.3.3.

4.3.4 Summary and Conclusion

This section introduced a tractable and realistic joint default and prepayment portfolio model. This is, to the best of our knowledge, the first portfolio model that incorporates the empirically observed features regarding prepayment risk on a portfolio level: Reasonable prices for contracts with short maturities, default as well as prepayment clusters, distinct default and prepayment correlation, and negative association between default and prepayment. We provide an iterative procedure and a Monte–Carlo simulation to obtain the distribution of portfolio loss and notional in a finite portfolio of d obligors. Using realistic parameters in a case study on the pricing of LCDS, we found that including prepayment risk leads to a significantly higher spread of $89bp$ ($[0\%, 100\%]$ tranche), compared to $52bp$ when only default risk is considered. This is in line with empirical studies that confirm that prepayment risk is one of the key components pricing MBS (see, e.g., Brown [1999], Deng et al. [2000], Maxam and Lacour-Little [2001], and Gabaix et al. [2007]).

Chapter 5

Conclusion

In this thesis, we have extended results on one-sided first-exit time probabilities of (continuously) time-changed Brownian motion (see, e.g., Hurd [2009]) to two barriers and have shown that those probabilities can conveniently be represented by rapidly converging infinite series. This avoids Fourier integrals and allows for an easy error control. Even in the single barrier case, the infinite series have turned out to be an efficient and close approximation of the Fourier integrals by Hurd [2009]. In a second step, we worked on regime switching jump-diffusions. This model class is a lot more general and thus more suitable when incorporating empirical observed features of financial time series. However, analytical expressions for the first-exit time probabilities are available in special cases only. Here, we have extended an efficient and unbiased Brownian bridge algorithm by Metwally and Atiya [2002] to regime switching parameters and two barriers. The advantage of this approach is its speed, unbiasedness, and its flexibility to adapt to different jump size distributions and payoff streams. This has later allowed us to easily price exotic derivatives like (step) double barrier options and corridor bonus certificates. We have discussed the implementation of the presented methods and in a numerical case study compared them to its numerical alternatives (for example finite elements schemes or brute-force Monte–Carlo simulations on a grid).

First-exit time problems have a wide range of applications in finance, engineering, and physics, but also in more exotic disciplines like hydrology. In this thesis we have focused on applications in finance and insurance. First, we have shown how the results in *Chapter 2* can be used to price a large range of financial derivatives. While a time change has a quiet convenient interpretation as a "measure of activity" in the economy and is analytically tractable, regime switching jump-diffusions often calibrate better to empirical data and lead to more reasonable prices for short-dated contracts. Secondly, we have dealt with the asset class private equity (PE), where the scarcity of data makes it hard to quan-

tify the risk inherent in the PE transactions. We have presented a *structural credit risk model*, which allows us to determine an implied equity volatility that serves as an indicator for the deal-level equity risk. We have applied this model to a unique PE database to determine the drivers of PE sponsors' risk appetite. We have found that the risk appetite of PE sponsors fluctuates remarkably over time indicating that these investors adjust their attitude towards risk according to the economic environment: Due to an increased risk appetite and cheap debt, PE sponsors tend to take more risk during boom periods. We have taken a closer look at the determinants of this risk appetite. We have found that larger buyouts exhibit lower equity risks. Further, we find that buyouts initiated by more experienced and higher reputed PE sponsors are less risky. We have attributed this reduced risk appetite to their fear of damaging their reputation and its corresponding competitive advantage. Finally, we have found that an increasing ownership stake by the PE sponsor is related to a decreasing risk appetite. At the end of *Chapter 3*, we have shortly discussed first-exit times in insurance applications, where usually premium payments compensate for (stochastic) insurance claims. An insurance company has to ensure that it stays solvent, i.e. that its total assets stay positive.

In *Chapter 4*, we have then dealt with multivariate extensions of the afore-mentioned results. One of today's pressing problems in the financial industry is the interactiveness of companies or obligors especially in the banking and insurance sector. In the past, tail events (for example the probability that several mortgagors in a credit portfolio default simultaneously) have significantly been underestimated. The reason for this underestimation has in most cases been a too simple dependence model, relying for example on a Gaussian copula. In this chapter, we present several alternatives based on more general dependence concepts like Archimedean copulas. We have discussed those models with respect to their analytical tractability and their ability to well describe many empirical phenomena (for example strong dependence in the tails, dependence being dynamic in time, or asymmetric marginal distributions). In a numerical case study we have shown how those considerations can be used to price loan-credit-default-swaps (LCDS) – an extension of credit-default-swaps (CDS) where the borrower is allowed to redeem the debt at any point in time.

Overall, this thesis presented how to compute first-exit time probabilities for a large class of stochastic processes. Depending on the specific problem, one has to carefully choose the most appropriate specification and dependence structure. An inadequate risk management is an important competitive advantage for any company. Quoting Moody's[1]

> *"Default risk can be reduced and managed through diversification* [...]. *The rewards for bearing it will [...] be owned by those who can diversify it best."*

[1] See the publication *Portfolio Management of Default Risk*, KMV, 2001, p. 1.

Appendix A

Proofs and formulas

A.1 Parameters of the Stein–Stein model

The functions $L(u)$, $M(u)$, and $N(u)$ in the characteristic function are defined as

$$
\begin{aligned}
&A := -\frac{\xi}{k^2}, \quad B := \frac{\varkappa\xi}{k^2}, \quad C_u := -\frac{u}{k^2 T}, \quad a_u := \sqrt{A^2 - 2C_u}, \quad b_u = -\frac{A}{a_u}, \\
&L(u) := -A - a_u \left(\frac{\sinh(a_u k^2 T) + b_u \cosh(a_u k^2 T)}{\cosh(a_u k^2 T) + b_u \sinh(a_u k^2 T)} \right), \\
&M(u) := B \left(\frac{b_u \sinh(a_u k^2 T) + b_u^2 \cosh(a_u k^2 T) + 1 - b_u^2}{\cosh(a_u k^2 T) + b_u \sinh(a_u k^2 T)} - 1 \right), \\
&N(u) := \frac{a_u - A}{2a_u^2} \left(a_u^2 - AB^2 - B^2 a_u \right) k^2 T \\
&\quad + \frac{B^2(A^2 - a_u^2)}{2a_u^3} \left(\frac{(2A + a_u) + (2A - a_u) e^{2a_u k^2 T}}{A + a_u + (a_u - A) e^{2a_u k^2 T}} \right) \\
&\quad + \frac{2AB^2(a_u^2 - A^2) e^{a_u k^2 T}}{a_u^3 \big(A + a_u + (a_u - A) e^{2a_u k^2 T} \big)} - \frac{1}{2} \ln \left(\frac{1}{2} \left(\frac{A}{a_u} + 1 \right) + \frac{1}{2} \left(1 - \frac{A}{a_u} \right) e^{2a_u k^2 T} \right).
\end{aligned}
$$

From (3.8), we find that

$$
\lambda_T - \lambda_0 = \xi \int_0^T \lambda_t \, dt + \xi \varkappa t + k \, W_T,
$$

which leads to

$$
\begin{aligned}
\mathbb{E}\left[\int_0^T \lambda_t \, dt \right] &= \frac{1}{\xi} \mathbb{E}\big[\lambda_T - \lambda_0 - \xi \varkappa T - k \, W_T \big] = \frac{1}{\xi} \big(\mathbb{E}[\lambda_T] - \lambda_0 - \xi \varkappa T \big) \\
&= \frac{1}{\xi} \Big[\big(\varkappa - \lambda_0 \big) \big(1 - \exp(-\theta T) \big) - \xi \varkappa T \Big],
\end{aligned}
$$

where we used that $\mathbb{E}[\lambda_T] = \lambda_0 \exp(-\theta T) + \varkappa \big(1 - \exp(-\theta T) \big)$.

A.2 Proof of Theorem 11

Part (a):
Using the reflection principle (see, e.g., Bingham and Kiesel [2004], Billingsley [2008]), we prove the results in Theorem 11. First note that if we are only interested in the barrier hitting probabilities, it suffices to work with the discounted values, i.e. D_0, P_0, K_0, and $\tilde{S}_t := S_t/\mathcal{B}_t$, for all $t \geq 0$. Then

$$\begin{aligned} X_{D,\infty}^{g(S_T)}(S_0) &= \frac{1}{\mathcal{B}_T}\,\mathbb{E}_{\mathbb{Q},S_0}\Big[\mathbb{1}_{\{T_{\infty,D}>T\}}\,g(S_T)\Big] \\ &= \frac{1}{\mathcal{B}_T}\Big(\mathbb{E}_{\mathbb{Q},S_0}\big[\mathbb{1}_{\{\tilde{S_T}>D_0\}}\,g(S_T)\big] - \mathbb{E}_{\mathbb{Q},S_0}\big[\mathbb{1}_{\{\tilde{S_T}>D_0,\,T_{\infty,D}\leq T\}}\,g(S_T)\big]\Big). \end{aligned}$$

The path-independence in the latter expectation is now removed. Therefore, we consider the logarithmized path $\{s_t\}_{t\geq 0} := \{\ln \tilde{S}_t\}_{t\geq 0}$. After changing to a measure $\mathbb{P}$ where $\{s_t\}_{t\geq 0}$ has zero drift, we reflect the paths $\{s_T > \ln(D_0),\, T_{\infty,D} \leq T\}$ from $t = 0$ up to the first hitting time $T_{\infty,D}$ at the (lower) barrier $b := \ln(D_0)$. Since $\{s_t\}_{t\geq 0}$ has zero drift under $\mathbb{P}$, this reflected path obeys the same dynamics under $\mathbb{P}$, however, it starts at a different initial value $\tilde{s}_0 = 2b - s_0$. That is why, as illustrated in *Figure A.1*, we find that the

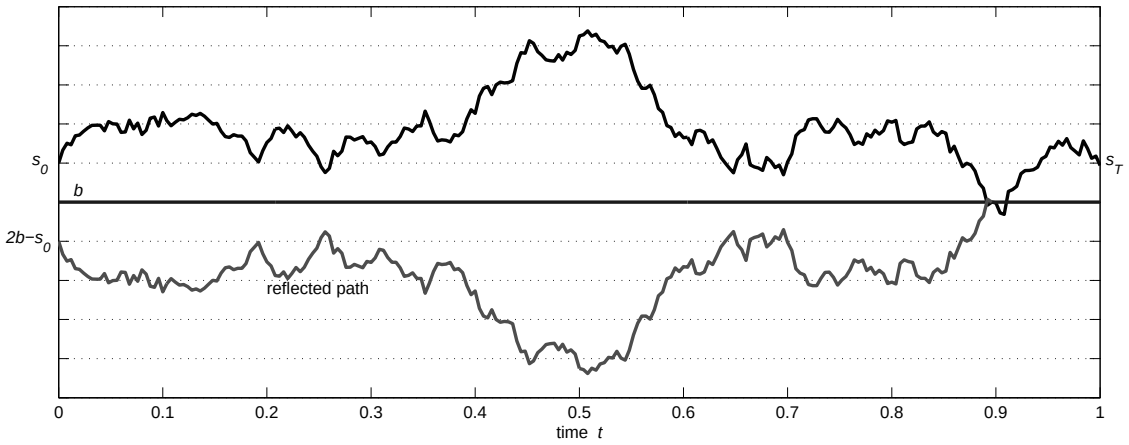

Figure A.1: Illustration of the reflection principle on a lower barrier $b < s_0$. The (logarithmized) process $\{s_t\}_{0\leq t\leq 1}$ (darkest path) is reflected up to its first-hitting time. Thereby s_0 is transformed into $\tilde{s}_0 = 2b - s_0$.

probability of $\{s_t\}_{t\geq 0}$ hitting b over the interval $[0, T]$ is the same as the probability of $\tilde{s}_T$ exceeding b. In more detail

$$\begin{aligned} &\mathbb{E}_{\mathbb{Q},S_0}\Big[\mathbb{1}_{\{T_{\infty,D}\leq T,\,\tilde{S_T}>D_0\}}\,g(S_T)\Big] \\ &\quad= \mathbb{E}_{\mathbb{P},S_0}\left[\mathbb{1}_{\{T_{\infty,D}\leq T,\,s_T>b\}}\,g(S_T)\,\exp\left((s_T - s_0)/2 - \int_0^T \sigma_t^2\,dt/8\right)\right] \end{aligned}$$

$$= \mathbb{E}_{\mathbb{P},D_0^2/S_0}\left[\mathbb{1}_{\{s_T>b\}}\, g\big(S_T\big)\, \exp\left(\big(s_T-(2b-s_0)\big)/2 - \int_0^T \sigma_t^2\, dt/8\right)\right]$$
$$= \frac{S_0}{D_0}\, \mathbb{E}_{\mathbb{Q},D_0^2/S_0}\Big[\mathbb{1}_{\{\tilde{S_T}>D_0\}}\, g\big(S_T\big)\Big],$$

where the second equality holds because of the independence of $\{W_t\}_{t\geq 0}$ and $\{\sigma_t\}_{t\geq 0}$. We finally obtain

$$X_{D,\infty}^{g(S_T)}(S_0) = \frac{1}{\mathcal{B}_T}\Big(\mathbb{E}_{\mathbb{Q},S_0}\big[\mathbb{1}_{\{S_T>D_T\}}\, g(S_T)\big] - \frac{S_0}{D_0}\, \mathbb{E}_{\mathbb{Q},D^2/S_0}\big[\mathbb{1}_{\{S_T>D_T\}}\, g\left(S_T\right)\big]\Big).$$

Part (b):
Similar to the single barrier result, we use the reflection principle to show the results in Theorem 11(b). First note that, again, if we are only interested in the barrier hitting probabilities, it suffices to work with the discounted values, i.e. D_0, P_0, K_0, and $\tilde{S}_t := S_t/\mathcal{B}_t$, for all $t \geq 0$. Then

$$X_{D,P}^{g(S_T)}(S_0) = \frac{1}{\mathcal{B}_T}\, \mathbb{E}_{\mathbb{Q},S_0}\Big[\mathbb{1}_{\{T_{P,D}>T\}}\, g(S_T)\Big]$$
$$= \frac{1}{\mathcal{B}_T}\, \Big(\mathbb{E}_{\mathbb{Q},S_0}\big[\mathbb{1}_{\{\tilde{S_T}\in(D_0,P_0)\}}\, g(S_T)\big] - \mathbb{E}_{\mathbb{Q},S_0}\big[\mathbb{1}_{\{T_{P,D}\leq T,\, \tilde{S_T}\in(D_0,P_0)\}}\, g(S_T)\big]\Big).$$

As in the single barrier case, we work on the logarithmized process $\{s_t\}_{t\geq 0} := \{\ln(\tilde{S}_t)\}_{t\geq 0}$. We denote $a := \ln(P_0)$, $b := \ln(D_0)$. We again try to remove the path-dependence of the barrier derivative by reflections at the two barriers. If $T_{P,D}^- \leq T$, respectively $T_{P,D}^+ \leq T$, we allow reflections ...

(1) ... at the lower barrier $D_0 < S_0$. The path is reflected at the barrier D_0 from $t = 0$ until its first hitting time $T_{P,D}^-$. This yields[1]

$$\mathbb{E}_{\mathbb{Q},S_0}\Big[\mathbb{1}_{\{S_{T_{P,D}^-}=D_0,\,...,\,\tilde{S_T}\in(D_0,P_0)\}}\, g(S_T)\Big] = \frac{S_0}{D_0}\, \mathbb{E}_{\mathbb{Q},D_0^2/S_0}\Big[\mathbb{1}_{\{...,\,\tilde{S_T}\in(D_0,P_0)\}}\, g\big(S_T\big)\Big]. \tag{A.1}$$

(2) ... at the upper barrier $P_0 > S_0$. Similarly, the path is reflected at the barrier P_0 from $t = 0$ until its first hitting time $T_{P,D}^+$. This yields[1]

$$\mathbb{E}_{\mathbb{Q},S_0}\Big[\mathbb{1}_{\{S_{T_{P,D}^+}=P_0,\,...,\,\tilde{S_T}\in(D_0,P_0)\}}\, g(S_T)\Big] = \frac{S_0}{P_0}\, \mathbb{E}_{\mathbb{Q},P_0^2/S_0}\Big[\mathbb{1}_{\{...,\,\tilde{S_T}\in(D_0,P_0)\}}\, g\big(S_T\big)\Big]. \tag{A.2}$$

[1] See the single barrier case for details.

We now divide the sets of paths according to the number of times it switches between the upper and lower barrier, i.e. the number of times it hits the upper (respectively lower) barrier after hitting the lower (respectively upper) barrier.

$$
\begin{aligned}
&\mathcal{A}_0 = \big\{s_T \in (b,a)\big\},\\
&\mathcal{A}_1 = \big\{\{s_t\}_{0\le t\le T} \text{ rises above } a,\, s_T \in (b,a)\big\},\\
&\mathcal{A}_2 = \big\{\{s_t\}_{0\le t\le T} \text{ rises above } a, \text{ then falls below } b,\, s_T \in (b,a)\big\},\\
&\mathcal{A}_3 = \big\{\{s_t\}_{0\le t\le T} \text{ rises above } a, \text{ then falls below } b, \text{ then rises above } a,\, s_T \in (b,a)\big\},\\
&\dots\\
&\mathcal{B}_0 = \big\{s_T \in (b,a)\big\},\\
&\mathcal{B}_1 = \big\{\{s_t\}_{0\le t\le T} \text{ falls below } b,\, s_T \in (b,a)\big\},\\
&\mathcal{B}_2 = \big\{\{s_t\}_{0\le t\le T} \text{ falls below } b, \text{ then rises above } a,\, s_T \in (b,a)\big\},\\
&\mathcal{B}_3 = \big\{\{s_t\}_{0\le t\le T} \text{ falls below } b, \text{ then rises above } a, \text{ then falls below } b,\, s_T \in (b,a)\big\},\\
&\dots
\end{aligned}
$$

The probability of first hitting the upper, respectively lower, barrier and $s_T \in (b,a)$ can then be represented as

$$
\begin{aligned}
\{T^+_{P,D} \le T,\, s_T \in (b,a)\} &= (\mathcal{A}_1 \backslash \mathcal{B}_2) \cup (\mathcal{A}_3 \backslash \mathcal{B}_4) \cup (\mathcal{A}_5 \backslash \mathcal{B}_6) \cup \dots\\
\{T^-_{P,D} \le T,\, s_T \in (b,a)\} &= (\mathcal{B}_1 \backslash \mathcal{A}_2) \cup (\mathcal{B}_3 \backslash \mathcal{A}_4) \cup (\mathcal{B}_5 \backslash \mathcal{A}_6) \cup \dots.
\end{aligned}
$$

Using that $\mathcal{A}_{2n} \subset \mathcal{B}_{2n-1}$ and $\mathcal{B}_{2n} \subset \mathcal{A}_{2n-1}$, $n \in \mathbb{N}$, we can rewrite

$$
\begin{aligned}
&\mathbb{E}_{\mathbb{Q},S_0}\big[\mathbb{1}_{\{T_{P,D}\le T,\, s_T\in(b,a)\}}\, g(S_T)\big]\\
&\qquad = \mathbb{E}_{\mathbb{Q},S_0}\big[\mathbb{1}_{\{T^+_{P,D}\le T,\, s_T\in(b,a)\}}\, g(S_T) + \mathbb{1}_{\{T^-_{P,D}\le T,\, s_T\in(b,a)\}}\, g(S_T)\big]\\
&\qquad = \sum_{n=1}^{\infty} \mathbb{E}_{\mathbb{Q},S_0}\Big[\big(\mathbb{1}_{\{\mathcal{A}_{2n-1}\}} - \mathbb{1}_{\{\mathcal{B}_{2n}\}} + \mathbb{1}_{\{\mathcal{B}_{2n-1}\}} - \mathbb{1}_{\{\mathcal{A}_{2n}\}}\big)\, g(S_T)\Big]. \qquad \text{(A.3)}
\end{aligned}
$$

The idea is now to remove the path dependence in the latter expression by applying reflections (1) and (2) iteratively. The procedure is demonstrated in *Figure A.2*. We apply the concept exemplary on the first term in Equation (A.3). Here, we first apply (1), then (2), then (1), then (2), until we reach $\mathcal{B}_0$ (which is path independent). We get

$$
\begin{aligned}
&\mathbb{E}_{\mathbb{Q},S_0}\Big[\mathbb{1}_{\{\mathcal{A}_{2n-1}\}}\, g(S_T)\Big] \overset{(1)}{=} \frac{S_0}{P_0}\, \mathbb{E}_{\mathbb{Q},\frac{P_0^2}{S_0}}\Big[\mathbb{1}_{\{\mathcal{B}_{2n-2}\}}\, g(S_T)\Big]\\
&\quad \overset{(2)}{=} \frac{S_0}{P_0}\, \frac{\frac{P_0^2}{S_0}}{D_0}\, \mathbb{E}_{\mathbb{Q},\frac{S_0 D_0^2}{P_0^2}}\Big[\mathbb{1}_{\{\mathcal{A}_{2n-3}\}}\, g(S_T)\Big] \overset{(1)}{=} \dots \overset{(1)}{=} \frac{S_0}{P_0}\, \frac{D_0^{n-1}}{P_0^{n-1}}\, \mathbb{E}_{\mathbb{Q},\frac{P_0^{2n}}{S_0 D_0^{2n-2}}}\Big[\mathbb{1}_{\{\mathcal{B}_0\}}\, g(S_T)\Big].
\end{aligned}
$$

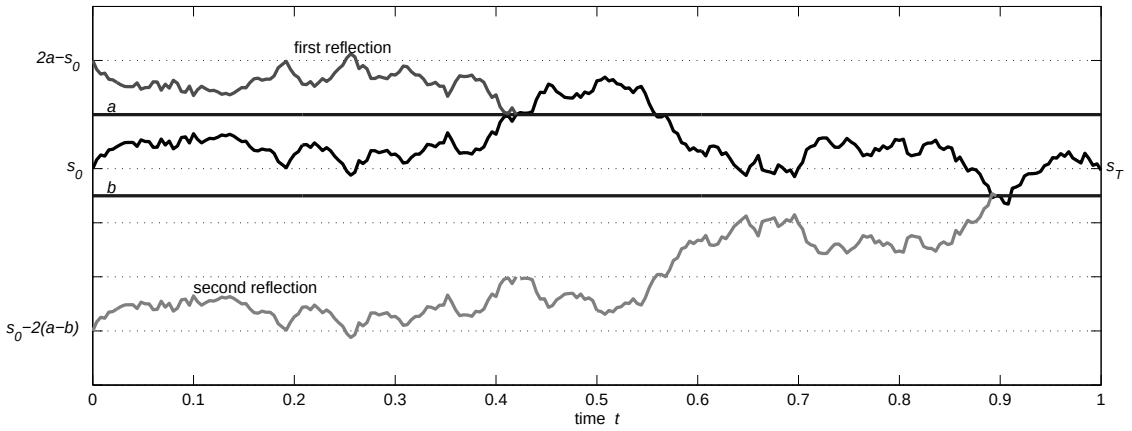

Figure A.2: Illustration of the reflection principle on two barriers $b < s_0 < a$. We apply (2), then (1) on the (logarithmized) process $\{s_t\}_{0\le t\le 1}$ (darkest path). Thereby s_0 is transformed into $s_0 - 2(a-b)$.

Applying the same arguments on the remaining three terms in Equation (A.3), we finally obtain

$$
\begin{aligned}
X_{D,P}^{g(S_T)}(S_0) = \frac{1}{\mathcal{B}_T} \Bigg[& \mathbb{E}_{\mathbb{Q},S_0}\left[\mathbb{1}_{\{\tilde{S_T}\in(D_0,P_0)\}}\, g(S_T)\right] \\
& - \sum_{n=1}^{\infty} \Bigg(\frac{S_0}{P_0}\,\frac{D_0^{n-1}}{P_0^{n-1}}\,\mathbb{E}_{\mathbb{Q},\frac{P_0^{2n}}{S_0 D_0^{2n-2}}}\left[\mathbb{1}_{\{s_T\in(b,a)\}}\, g(S_T)\right] - \frac{P_0^n}{D_0^n}\,\mathbb{E}_{\mathbb{Q},\frac{S_0 D_0^{2n}}{P_0^{2n}}}\left[\mathbb{1}_{\{s_T\in(b,a)\}}\, g(S_T)\right] \\
& \quad + \frac{S_0}{D_0}\,\frac{P_0^{n-1}}{D_0^{n-1}}\,\mathbb{E}_{\mathbb{Q},\frac{D_0^{2n}}{S_0 P_0^{2n-2}}}\left[\mathbb{1}_{\{s_T\in(b,a)\}}\, g(S_T)\right] - \frac{D_0^n}{P_0^n}\,\mathbb{E}_{\mathbb{Q},\frac{S_0 P_0^{2n}}{D_0^{2n}}}\left[\mathbb{1}_{\{s_T\in(b,a)\}}\, g(S_T)\right] \Bigg) \Bigg] \\
= \frac{1}{\mathcal{B}_T} & \sum_{n=-\infty}^{\infty} \frac{D_0^n}{P_0^n}\,\mathbb{E}_{\mathbb{Q},\frac{S_0 P_0^{2n}}{D_0^{2n}}}\left[\mathbb{1}_{\{s_T\in(b,a)\}}\, g(S_T)\right] - \frac{S_0}{D_0}\,\frac{D_0^n}{P_0^n}\,\mathbb{E}_{\mathbb{Q},\frac{P_0^{2n}}{S_0 D_0^{2n-2}}}\left[\mathbb{1}_{\{s_T\in(b,a)\}}\, g(S_T)\right] \\
= \frac{1}{\mathcal{B}_T} & \sum_{n=-\infty}^{\infty} \frac{D_0^n}{P_0^n}\left(\mathbb{E}_{\mathbb{Q},S_0^{(2n)}}\left[\mathbb{1}_{\{s_T\in(b,a)\}}\, g(S_T)\right] - \frac{S_0}{D_0}\,\mathbb{E}_{\mathbb{Q},S_0^{(2n-1)}}\left[\mathbb{1}_{\{s_T\in(b,a)\}}\, g(S_T)\right]\right),
\end{aligned}
$$

where we abbreviate

$$
S_0^{(2n)} = S_0\,\frac{P_0^{2n}}{D_0^{2n}},\ \text{and}\ S_0^{(2n-1)} = \frac{P_0^{2n}}{D_0^{2n}}\,\frac{D_0^2}{S_0},\quad n\in\mathbb{Z}\,.
$$

A.3 $V_E(0)$ and $\partial V_E(0)/\partial S_0$ in Theorem 6

This section derives an expression for $\partial V_E(0)/\partial S_0$. A *Down-and-out call option* (*DOC*) guarantees the holder a payoff of 0 in case of default ($T_{\infty,D} < T$) and a final payoff $\max(S_T - D_T, 0)$, where D_T denotes the strike price at maturity and D_t the time-varying default barrier. The price of such an option, $DOC^{GBM}_{d,\mu,\sigma}(S_0, D_0, T)$, is presented in the following Lemma 8 and can be found in, for example, *Section 3.1.*

Lemma 8 (Down-and-out call option (*DOC*))
Let S_t be the value of the firm's assets at time t. The time to maturity is T, r the risk-free interest rate, and D_0 the strike and knock-out barrier. Then, the value of a DOC option is given by

$$DOC^{GBM}_{d,\mu,\sigma}(S_0, D_0, T) = S_0\, \Phi_{d,\mu+\sigma^2,\sigma}(T) - e^{-rT} D_0\, \Phi_{d,\mu,\sigma}(T)\,,$$

where $\Phi_{d,\mu,\sigma}$ was introduced in Lemma 5.

Theorem 18 (Equity value $V_E(0)$)
The equity price $V_E(0)$ in the presented model is given by

$$\begin{aligned} V_E(0) = {} & S_0\, e^{(c-\lambda)T}\, \Phi_{d,\mu+\sigma^2,\sigma}(T) + D_0\, \frac{\lambda}{c-r-\lambda} - D_0\, e^{(c-r-\lambda)T}\, \frac{c-r}{c-r-\lambda}\, \Phi_{d,\mu,\sigma}(T) \\ & - D_0\, e^{-\frac{d(\tilde{\mu}-\mu)}{\sigma^2}}\, \frac{\lambda}{c-r-\lambda} \left(1 - \Phi_{d,\tilde{\mu},\sigma}(T)\right). \end{aligned} \tag{A.4}$$

Proof. The equity holders have to pay redemption payments at a continuous rate λ until the company either defaults or matures in T. They receive $S_T - D_T$ if the company survives until T, else they receive nothing. Thus

$$\begin{aligned} V_E(0) = {} & \mathbb{E}\big[e^{-rT}\, \mathbb{1}_{\{T_{\infty,D} > T\}} \max(S_T - D_T, 0)\big] \\ & - \left[\int_0^T e^{-rt} \lambda D_t dt\right] \mathbb{Q}(T_{\infty,D} > T) - \int_0^T \left[\int_0^s e^{-rt} \lambda D_t dt\right] d\mathbb{Q}(T_{\infty,D} \le s) \\ = {} & e^{(c-\lambda)T}\, DOC^{GBM}_{d,\mu,\sigma}(S_0, D_0, T) - \left[D_0\, \frac{\lambda}{c-r-\lambda}\big(e^{(c-r-\lambda)T} - 1\big)\right] \mathbb{Q}(T_{\infty,D} > T) \\ & - \int_0^T \left[D_0\, \frac{\lambda}{c-r-\lambda}\big(e^{(c-r-\lambda)s} - 1\big)\right] d\mathbb{Q}(T_{\infty,D} \le s) \\ = {} & e^{(c-\lambda)T} \left(S_0\, \Phi_{d,\mu+\sigma^2,\sigma}(T) - e^{-rT} D_0\, \Phi_{d,\mu,\sigma}(T)\right) + D_0\, \frac{\lambda}{c-r-\lambda} \\ & - D_0\, e^{(c-r-\lambda)T}\, \frac{\lambda}{c-r-\lambda}\, \Phi_{d,\mu,\sigma}(T) - D_0\, e^{-\frac{d(\tilde{\mu}-\mu)}{\sigma^2}}\, \frac{\lambda}{c-r-\lambda} \left(1 - \Phi_{d,\tilde{\mu},\sigma}(T)\right) \end{aligned}$$

$$= S_0\, e^{(c-\lambda)T}\, \Phi_{d,\mu+\sigma^2,\sigma}(T) + D_0\, \frac{\lambda}{c-r-\lambda} - D_0\, e^{(c-r-\lambda)T}\, \frac{c-r}{c-r-\lambda}\, \Phi_{d,\mu,\sigma}(T)$$
$$- D_0\, e^{-\frac{d(\tilde{\mu}-\mu)}{\sigma^2}}\, \frac{\lambda}{c-r-\lambda}\, \big(1 - \Phi_{d,\tilde{\mu},\sigma}(T)\big),$$

using the results from Lemma 8. □

Lemma 9 (The derivative $\partial\Phi_{d,\mu,\sigma}(T)/\partial S_0$)
The derivative of the default probability $\Phi_{d,\mu,\sigma}(T)$ (see Lemma 5) with respect to S_0 is given by

$$\triangle_{d,\mu,\sigma}(T) := \frac{\partial\Phi_{d,\mu,\sigma}(T)}{\partial S_0}$$
$$= \frac{2}{S_0\sigma\sqrt{T}}\, \phi\left(\frac{-d+\mu T}{\sigma\sqrt{T}}\right) + \frac{2\mu}{\sigma^2 S_0}\, e^{\frac{2\mu d}{\sigma^2}}\, \Phi\left(\frac{d+\mu T}{\sigma\sqrt{T}}\right),$$

where $\Phi(\,\cdot\,)$, respectively $\phi(\,\cdot\,)$, denote the standard normal cumulative distribution function, respectively the standard normal density function.

Proof.

$$\frac{\partial\Phi_{d,\mu,\sigma}(T)}{\partial S_0} = \frac{1}{S_0\sigma\sqrt{T}}\, \phi\left(\frac{-d+\mu T}{\sigma\sqrt{T}}\right) + \frac{1}{S_0\sigma\sqrt{T}}\, e^{\frac{2\mu d}{\sigma^2}}\, \phi\left(\frac{d+\mu T}{\sigma\sqrt{T}}\right) + \frac{2\mu}{\sigma^2 S_0}\, e^{\frac{2\mu d}{\sigma^2}}\, \Phi\left(\frac{d+\mu T}{\sigma\sqrt{T}}\right)$$

$$= \frac{2}{S_0\sigma\sqrt{T}}\, \phi\left(\frac{-d+\mu T}{\sigma\sqrt{T}}\right) + \frac{2\mu}{\sigma^2 S_0}\, e^{\frac{2\mu d}{\sigma^2}}\, \Phi\left(\frac{d+\mu T}{\sigma\sqrt{T}}\right).$$

□

Using the results from Theorem 18 and Lemma 9, Theorem 19 gives the derivative $\partial V_E(0)/\partial S_0$. The result is a straight forward application of the product rule on Equation (A.4).

Theorem 19 (The derivative $\partial V_E(0)/\partial S_0$)
The derivative of the equity value $V_E(0)$ with respect to S_0 is

$$\frac{\partial V_E(0)}{\partial S_0} = S_0\, e^{(c-\lambda)T}\, \triangle_{d,\mu+\sigma^2,\sigma}(T) - D_0\, e^{(c-r-\lambda)T}\, \frac{c-r}{c-r-\lambda}\, \triangle_{d,\mu,\sigma}(T)$$
$$+ e^{(c-\lambda)T}\, \Phi_{d,\mu+\sigma^2,\sigma}(T) - \frac{D_0}{S_0}\, \frac{\tilde{\mu}-\mu}{\sigma^2}\, e^{-\frac{d(\tilde{\mu}-\mu)}{\sigma^2}}\, \frac{\lambda}{c-r-\lambda}\, \big(1 - \Phi_{d,\tilde{\mu},\sigma}(T)\big)$$
$$- D_0\, e^{-\frac{d(\tilde{\mu}-\mu)}{\sigma^2}}\, \frac{\lambda}{c-r-\lambda}\, \triangle_{d,\tilde{\mu},\sigma}(T).$$

Bibliography

J. Abate and W. Whitt. A unified framework for numerically inverting Laplace transforms. *INFORMS Journal on Computing*, Vol. 18, No. 4:pp. 408–421, 2006.

A.-K. Achleitner, R. Braun, B. Hinterramskogler, and F. Tappeiner. The structure and determinants of financial covenants in leveraged buyouts. *Review of Finance*, Vol. 16, No. 3:pp. 647–684, 2012.

H. Albrecher, P. Mayer, W. Schoutens, and J. Tistaert. The little Heston trap. *Wilmott Magazine*, January:pp. 83–92, 2007.

L. Andersen and J. Sidenius. Extensions to the Gaussian copula: random recovery and random factor loadings. *Journal of Credit Risk*, Vol. 11:pp. 29–69, 2004.

L. Andersen, J. Sidenius, and S. Basu. All your hedges in one basket. *Risk Magazine*, pages 67–72, 2003.

T. W. Anderson. A modification of the sequential probability ratio test to reduce the sample size. *The Annals of Mathematical Statistics*, Vol. 31, No. 1:pp. 165–197, 1960.

E. Arzac. Valuation of highly leveraged firms. *Financial Analysts Journal*, Vol. 52, No. 4: pp. 42–50, 1996.

S. Asmussen and H. Albrecher. *Ruin probabilities*. Advanced Series on Statistical Science & Applied Probability, Vol. 14, 2010.

S. Asmussen, F. Avram, and M. Pistorius. Russian and American put options under exponential Lévy models. *Stochastic Processes and their Applications*, Vol. 109, No. 1: pp. 79–111, 2004.

F. Avram, M. Pistorius, and M. Usabel. The two barriers ruin problem vie a Wiener Hopf decomposition approach. *Annals of University of Craiova*, Vol. 30:pp. 38–44, 2003.

U. Axelson, P. Strömberg, and M. S. Weisbach. Why are buyouts levered? The financial structure of private equity funds. *Journal of Finance*, Vol. 64, No. 4:pp. 1549–1582, 2009.

U. Axelson, T. Jenkinson, P. Strömberg, and M. Weisbach. Leverage and pricing in buyouts: An empirical analysis. *EFA 2009 Bergen Meetings Paper*, 2010.

C. A. Ball and A. Roma. Stochastic volatility option pricing. *Journal of Financial and Quantitative Analysis*, Vol. 29:pp. 589–607, 1994.

O. Barndorff-Nielsen and N. Shephard. Non-Gaussian Ornstein-Uhlenbeck based models and some of their uses in financial economics. *Journal of the Royal Statistical Society: Series B*, Vol. 63, No. 2:pp. 167–241, 2001.

S. Bernstein. Sur les fonctions absolument monotones. *Acta Mathematica*, Vol. 52, No. 1: pp. 1–66, 1929.

S. Bernstein, J. Lerner, M. Sorensen, and P. Strömberg. Private equity and industry performance. *Harvard Business School Working Papers*, 2010.

J. Bertoin. *Lévy Processes*. Cambridge University Press, 1998.

P. Billingsley. *Probability and Measure*. Wiley Series in Probability, 2008.

N. Bingham and R. Kiesel. *Risk-neutral valuation*. Springer, 2004.

F. Black and J. C. Cox. Valuing corporate securities: Some effects of bond indenture provisions. *Journal of Finance*, Vol. 31, No. 2:pp. 351–367, 1976.

F. Black and M. Scholes. The pricing of options and corporate liabilities. *The Journal of Political Economy*, Vol. 81, No. 3:pp. 637–654, 1973.

S. Boyarchenko and S. Levendorskiĭ. Barrier options and touch-and-out options under regular Lévy processes of exponential type. *Annals of Applied Probability*, Vol. 12, No. 4:pp. 1261–1298, 2002.

S. Boyarchenko and S. Levendorskiĭ. Valuation of continuously monitored double barrier options and related securities. *Mathematical Finance*, Vol. 22, No. 3:pp. 419–444, 2012.

R. Braun, N. Engel, P. Hieber, and R. Zagst. The risk appetite of private equity sponsors. *Journal of Empirical Finance*, Vol. 18, No. 5:pp. 815–832, 2011.

D. Breeden and H. Gilkeson. A path-dependent approach to security valuation with application to interest rate contingent claims. *Journal of Banking & Finance*, Vol. 21: pp. 541–562, 1997.

P. Brockman and H. Turtle. A barrier option framework for corporate security valuation. *Journal of Financial Economics*, Vol. 67, No. 3:pp. 511–529, 2003.

P. Brockwell, E. Chadraa, and A. Lindner. Continuous-time GARCH processes. *The Annals of Applied Probability*, Vol. 16, No. 2:pp. 790–826, 2006.

D. T. Brown. The determinants of expected returns on mortgage-backed securities: An empirical analysis of option-adjusted spreads. *Journal of Fixed Income*, Vol. 9, No. 2: pp. 8–18, 1999.

J. Buffington and R. J. Elliott. American options with regime switching. *International Journal of Theoretical and Applied Finance*, Vol. 5:pp. 497–514, 2002.

N. Cai. On first passage times of a hyper-exponential jump diffusion process. *Operations Research Letters*, Vol. 37:pp. 127–134, 2009.

N. Cai, N. Chen, and X. Wan. Pricing double-barrier options under a flexible jump diffusion model. *Operations Research Letters*, Vol. 37:pp. 163–167, 2009.

A. Caplin, C. Freeman, and J. Tracy. Collateral damage: Refinancing constraints and regional recessions. *Journal of Money, Credit, and Banking*, Vol. 29, No. 4:pp. 496–516, 1997.

P. Carr and J. Crosby. A class of Lévy process models with almost exact calibration to both barrier and vanilla FX options. *Journal of Quantitative Finance*, Vol. 10, No. 10: pp. 1115–1136, 2010.

P. Carr and R. Lee. Put-call symmetry: Extensions and applications. *Mathematical Finance*, Vol. 19, No. 4:pp. 523–560, 2009.

P. Carr and D. B. Madan. Option valuation using the fast Fourier transform. *Journal of Computational Finance*, Vol. 2:pp. 61–73, 1999.

P. Carr and L. Wu. Time-changed Lévy processes and option pricing. *Journal of Financial Economics*, Vol. 17:pp. 113–141, 2004.

P. Carr, K. Ellis, and V. Gupta. Static heding of exotic derivatives. *Journal of Finance*, Vol. 53, No. 3:pp. 1165–1190, 1998.

P. Carr, H. Geman, D. Madan, and M. Yor. Stochastic volatility for Lévy processes. *Mathematical Finance*, Vol. 13, No. 3:pp. 345–382, 2003.

P. Carr, H. Geman, D. Madan, and M. Yor. Self-decomposability and option pricing. *Mathematical Finance*, Vol. 17, No. 1:pp. 31–57, 2007.

P. Carr, H. Zhang, and O. Hadjiliadis. Maximum drawdown insurance. *International Journal of Theoretical and Applied Finance*, Vol. 14, No. 8:pp. 1195–1230, 2011.

M. Chahal and J. Wang. A jump diffusion process and emerging bond and stock markets: An investigation using daily data. *Multinational Finance Journal*, Vol. 1, No. 3:pp. 169–197, 1997.

K. C. Chan, N.-F. Chen, and D. A. Hsieh. An exploratory investigation of the firm size effect. *Journal of Financial Economics*, Vol. 14, No. 3(3):pp. 451–471, 1985.

N.-F. Chen. Some empirical tests of the theory of arbitrage pricing. *Journal of Finance*, Vol. 38, No. 5(5):pp. 1393–1414, 1983.

J. Choi and M. Richardson. The volatility of the firm's assets. *Working paper*, 2008.

Y. Chow, C. Huang, and M. Liu. Valuation of adjustable rate mortgages with automatic stretching maturity. *Journal of Banking & Finance*, Vol. 24:pp. 1809–1829, 2000.

P. Christoffersen, S. Heston, and K. Jacobs. The shape and term structure of the index option smirk: Why multifactor stochastic volatility models work so well. *Management Science*, Vol. 55:pp. 1914–1932, 2009.

P. Clark. A subordinated stochastic process with finite variance for speculative prices. *Econometrica*, Vol. 41:pp. 135–155, 1973.

J. H. Cochrane. The risk and return of venture capital. *Journal of Financial Economics*, Vol. 75, No. 1:pp. 3–52, 2005.

M. Coffey. LCDS and loan spreads. *LPC Gold Sheets*, Vol. 21, No. 11:pp. 1–24, 2007.

P. Collin-Dufresne and J. P. Harding. A closed form formula for valuing mortgages. *Journal of Real Estate Finance and Economics*, Vol. 19, No. 2:pp. 133–146, 1999.

R. Cont and P. Tankov. *Financial Modelling with Jump Processes*. Chapman & Hall/CRC Financial Mathematics Series, 2003.

R. Cont and E. Voltchkova. Integro-differential equations for option prices in exponential Lévy models. *Finance and Stochastics*, Vol. 9:pp. 299–325, 2005.

D. Cox and V. Isham. *Monographs on Applied Probability and Statistics: Point Processes*. Chapman & Hall, 1980.

D. Cox and H. Miller. *Theory of Stochastic Processes*. Chapman & Hall, 1965.

J. Cox, J. Ingersoll, and S. Ross. A theory of the term structure of interest rates. *Econometrica*, Vol. 53:pp. 187–201, 1985.

H. Cramér. Historical review of Filip Lundberg's works on risk theory. *Scandinavian Actuarial Journal*, Vol. 3:pp. 6–12, 1969.

D. Darling and A. Siegert. The first passage problem for a continuous Markov process. *The Annals of Mathematical Statistics*, Vol. 24, No. 4:pp. 624–639, 1953.

S. R. Das. The surprise element: Jumps in interest rates. *Journal of Econometrics*, Vol. 106:pp. 27–65, 2002.

A. Dassios and J.-W. Jang. Pricing of catastrophe reinsurance and derivatives using the Cox process with shot noise intensity. *Finance and Stochastics*, Vol. 7:pp. 73–95, 2003.

C. Demiroglu and C. James. The role of private equity group reputation in LBO financing. *Journal of Financial Economics*, Vol. 96, No. 4:pp. 306–330, 2010.

Y. Deng, J. M. John M. Quigley, and R. van Order. Mortgage terminations, heterogeneity and the exercise of mortgage options. *Econometrica*, Vol. 68, No. 2:pp. 275–307, 2000.

E. Derman, D. Ergener, and I. Kani. Forever hedged. *Risk*, Vol. 7:pp. 139–145, 1994.

D. W. Diamond. Reputation acquisition in debt markets. *Journal of Political Economy*, Vol. 97, No. 4:pp. 828–862, 1989.

J. DiCesare and D. McLeish. Simulation of jump diffusions and the pricing of options. *Insurance: Mathematics and Economics*, Vol. 43:pp. 316–326, 2008.

P. Dobránszky and W. Schoutens. Generic Lévy one-factor models for the joint modelling of prepayment and default: Modelling LCDX. Technical report 08-03, Section of Statistics, K.U. Leuven, 2008.

P. Dobránszky and W. Schoutens. Do not forget the cancellation. Technical report 09-01, Section of Statistics, K.U. Leuven, 2009.

M. Dominé. First passage time distribution of a Wiener process with drift concerning two elastic barriers. *Journal of Applied Probability*, Vol. 33:pp. 164–175, 1996.

C. Downing, R. Stanton, and N. Wallace. An empirical test of a two-factor mortgage valuation model: How much do house prices matter? *Real Estate Economics*, Vol. 4: pp. 681–710, 2005.

D. Duffie, J. Pan, and K. Singleton. Transform analysis and asset pricing for affine jump-diffusions. *Econometrica*, Vol. 68:pp. 1343–1376, 2000.

D. Dufresne. The integrated square-root process. *Working paper, University of Montreal*, 2001.

D. Dupont. Hedging barrier options: Current methods and alternatives. *Working paper*, 2002.

M. Eling and F. Schuhmacher. *Performance Measurement of Hedge Fund Indices – Does the Measure Matter?* Springer, Berlin, 2005.

M. Eling and F. Schuhmacher. Does the choice of performance measure influence the evaluation of hedge funds? *Journal of Banking & Finance*, Vol. 31, No. 9:pp. 2632–2647, 2007.

P. Embrechts, R. Frey, and A. McNeil. *Quantitative Risk Management: Concepts, Techniques and Tools*. Princeton University Press, 2005.

B. Eraker, M. Johannes, and N. Polson. The impact of jumps in volatility and returns. *Journal of Finance*, Vol. 58, No. 3:pp. 1269–1300, 2003.

M. Escobar and B. Götz. Two asset-barrier option within stochastic volatility models. *Working paper*, 2012.

M. Escobar, T. Friederich, L. Seco, and R. Zagst. A general structural approach for credit modeling under stochastic volatility. *Journal of Financial Transformation*, Vol. 32:pp. 123–132, 2011.

M. Escobar, P. Hieber, and M. Scherer. Efficiently pricing barrier derivatives in stochastic volatility models. *Review of Derivatives Research*, in press, 2013.

W. Feller. Two singular diffusion problems. *The Annals of Mathematics*, Vol. 54, No. 1: pp. 173–182, 1951.

W. Feller. *An introduction to probability theory and its applications*. John Wiley Finance Series, 1966.

L. Fernández, P. Hieber, and M. Scherer. Double-barrier first-passage times of jump-diffusion processes. *Monte Carlo Methods and Applications*, Vol. 19, No. 2:pp. 107–141, 2013.

J. Figueroa-López and P. Tankov. Small-time asymptotics of stopped Lévy bridges and simulation schemes with controlled bias. *Working paper*, http://arxiv.org/pdf/1203.2355.pdf, 2012.

J. Folks and R. Chhikara. The inverse Gaussian distribution and its statistical application – a review. *Journal of the Royal Statistical Society. Series B*, Vol. 40, No. 3:pp. 263–289, 1978.

F. Franzoni, E. Nowak, and L. Phalippou. Private equity performance and liquidity risk. *Journal of Finance*, Vol. 67, No. 6:pp. 2341–2373, 2012.

C.-D. Fuh, I. Hub, and S. Lin. Empirical performance and asset pricing in hidden Markov models. *Communications in Statistics - Theory and Methods*, Vol. 32, No. 12:pp. 2477–2512, 2003.

X. Gabaix, A. Krishnamurthy, and O. Vigneron. Limits of arbitrage: Theory and evidence from the mortgage-backed securities market. *Journal of Finance*, Vol. 52, No. 2:pp. 557–595, 2007.

H. Geman and M. Yor. Pricing and hedging double-barrier options: a probabilistic approach. *Mathematical Finance*, Vol. 6, No. 4:pp. 365–378, 1996.

H. Geman, D. Madan, and M. Yor. Time changes for Lévy processes. *Mathematical Finance*, Vol. 11:pp. 79–96, 2000.

R. Geske. The valuation of compound options. *Journal of Financial Economics*, Vol. 7, No. 1:pp. 63–81, 1979.

K. Giesecke. Default and information. *Journal of Economic Dynamics & Control*, Vol. 30:pp. 2281–2303, 2006.

K. Giesecke and D. Smelov. Exact sampling of jump-diffusions. *Operations Research, forthcoming*, 2011.

E. Gobet. *Advanced Monte Carlo methods for barrier and related exotic options.* Handbook of Numerical Analysis, Vol. XV, Special Volume: Mathematical Modeling and Numerical Methods in Finance, Elsevier, Netherlands, 2009.

P. Gompers and J. Lerner. *The Venture Capital Cycle*. MIT Press, Cambridge, Massachusetts, 1999.

W. Gompers and J. Lerner. What drives venture capital fundraising? *Working paper*, 2000.

Y. Goncharov. An intensity-based approach to the valuation of mortgage contracts and computation of the endogenous mortgage rate. *International Journal of Theoretical and Applied Finance*, Vol. 9, No. 6:pp. 889–914, 2006.

B. Götz. *Valuation of multi-dimensional derivatives in a stochastic covariance framework*. PhD thesis, TU Munich, 2011.

R. Green. Investment incentives, debt, and warrants. *Journal of Financial Economics*, Vol. 13, No. 1:pp. 115–136, 1984.

S. Griebsch and U. Wystup. On the valuation of fader and discrete barrier options in Heston's stochastic volatility model. *Quantitative Finance*, Vol. 11, No, 5:pp. 693–709, 2011.

A. Groh, R. Baule, and O. Gottschalg. Measuring idiosyncratic risks in leveraged buyout transactions. *Quarterly Journal of Finance and Accounting*, Vol. 47, No. 4:pp. 15–23, 2008.

A. P. Groh and O. Gottschalg. The opportunity cost of capital of US buyouts. *Working paper*, 2009.

T. Guillaume. Window double barrier options. *Review of Derivatives Research*, Vol. 6:pp. 47–75, 2003.

T. Guillaume. Step double barrier options. *Journal of Derivatives*, Vol. 18, No. 1:pp. 59–79, 2010.

S. Guo, E. S. Hotchkiss, and W. Song. Do buyouts (still) create value? *Journal of Finance*, Vol. 66 No. 2:pp. 479–517, 2011.

X. Guo. When the "Bull" meets the "Bear" – A first passage time problem for a hidden Markov process. *Methodology and Computing in Applied Probability*, Vol. 3, No. 2:pp. 135–143, 2001.

S. R. Hakim. Regional diversity, borrower characteristics and mortgage prepayment. *Review of Financial Economics*, Vol. 1, No. 2:pp. 17–29, 1992.

W. J. Hall. The distribution of Brownian motion on linear stopping boundaries. *Sequential Analysis*, Vol. 4:pp. 345–352, 1997.

P. Halpern, R. Kieschnick, and W. Rotenberg. Determinants of financial distress and bankruptcy in highly levered transactions. *The Quarterly Review of Economics and Finance*, Vol. 49, No. 3:pp. 772–783, 2009.

J. D. Hamilton. A new approach to the economic analysis of nonstationary time series and the business cycle. *Econometrica*, Vol. 57, No. 2:pp. 357–384, 1989.

M. Hardy. A regime-switching model of long-term stock returns. *North American Actuarial Journal*, Vol. 3:pp. 185–211, 2001.

H. He, W. Keirstead, and J. Rebholz. Double lookbacks. *Mathematical Finance*, Vol. 8, No. 3:pp. 201–228, 1998.

P. N. Henriksen. Pricing barrier options by a regime switching model. *Journal of Quantitative Finance*, Vol. 11, No. 8:pp. 1221–1231, 2011.

C. Hering, M. Hofert, J.-F. Mai, and M. Scherer. Constructing hierarchical Archimedean copulas with Lévy subordinators. *Journal of Multivariate Analysis*, Vol. 101:pp. 1428–1433, 2010.

S. Heston. A closed-form solution for options with stochastic volatility with applications to bond and currency options. *Journal of Finance*, Vol. 42:pp. 327–343, 1993.

P. Hieber and M. Scherer. Efficiently pricing barrier options in a Markov-switching framework. *Journal of Computational and Applied Mathematics*, Vol. 235:pp. 679–685, 2010.

P. Hieber and M. Scherer. A note on first-passage times of continuously time-changed Brownian motion. *Statistics & Probability Letters*, Vol. 82, No. 1:pp. 165–172, 2012.

P. Hieber and M. Scherer. Modeling credit portfolio derivatives, including both a default and a prepayment feature. *Applied Stochastic Models in Business and Industry*, Vol. 29, No. 5:pp. 479–495, 2013.

N. Hilber, O. Reichmann, C. Schwab, and C. Winter. *Computational Methods for Quantitative Finance: Finite Element Methods for Derivative Pricing.* Springer, 2013.

T. Ho and R. Singer. The value of corporate debt with a sinking-fund provision. *Journal of Business*, Vol. 57, No. 3:pp. 315–336, 1984.

M. Hofert. *Sampling Nested Archimedean Copulas with Applications to CDO Pricing.* PhD thesis, Ulm University, 2010.

M. Hofert and M. Scherer. CDO pricing with nested Archimedean copulas. *Journal of Quantitative Finance*, Vol. 11, No. 5:pp. 775–787, 2011.

J. Hull and A. White. The pricing of options on assets with stochastic volatility. *Journal of Finance*, Vol. 42, No. 2:pp. 281–300, 1987.

T. Hurd. Credit risk modeling using time-changed Brownian motion. *International Journal of Theoretical and Applied Finance*, Vol. 12, No. 8:pp. 1213–1230, 2009.

T. Hurd and A. Kuznetsov. On the first-passage time for brownian motion subordinated by a lévy process. *Journal of Applied Probability*, Vol. 46:pp. 181–198, 2009.

D. Iglehart. Diffusion approximations in collective risk theory. *Journal of Applied Probability*, Vol. 6:pp. 285–292, 1969.

ISDA. Bullet markit LCDX tranche transactions standard terms supplement. Technical report, ISDA Credit Derivatives Determinations Committee, 2010.

V. Ivashina and A. Kovner. The private equity advantage: Leveraged buyout firms and relationship banking. *Review of Financial Studies*, Vol. 24, No. 7:pp. 2462–2498, 2011.

R. Jarrow and R. Protter. Structural versus reduced form models: A new information based perspective. *Journal of Investment Management*, Vol. 2, No. 2:pp. 1–10, 2004.

T. M. Jason. The credit performance of private equity-backed companies in the 'great recession' of 2008/2009. *Working paper*, 2010.

M. Jeanblanc, M. Yor, and M. Chesney. *Mathematical Methods for Financial Markets*. Springer, 2009.

Z. Jiang and M. Pistorius. On perpetual American put valuation and first-passage in a regime-switching model with jumps. *Finance and Stochastics*, Vol. 12, No. 3:pp. 331–355, 2008.

H. Joe. *Multivariate Models and Dependence Concepts*. Chapman & Hall, 1997.

E. Jones, S. Mason, and E. Rosenfeld. Contingent claims analysis of corporate capital structures: an empirical investigation. *Journal of Finance*, Vol. 39, No. 3:pp. 611–625, 1984.

H. Jönsson, W. Schoutens, and G. van Damme. Modeling default and prepayment using Lévy processes: an application to asset backed securities. *Radon Series on Computational and Applied Mathematics*, Vol. 8:pp. 1–23, 2009.

M. Joshi and T. Leung. Using Monte Carlo simulation and importance sampling to rapidly obtain jump-diffusion prices of continuous barrier options. *Journal of Computational Finance*, Vol. 10, No. 4:pp. 93–105, 2007.

S. Kammer. *A general first-passage-time model for multivariate credit spreads and a note on barrier option pricing*. PhD thesis, Justus-Liebig Universität Gießen, 2007.

S. Kaplan and A. Schoar. Private equity performance: Returns, persistence, and capital flows. *Journal of Finance*, Vol. 60, No. 4(4):pp. 1791–1823, 2005.

S. N. Kaplan and P. Strömberg. Leveraged buyouts and private equity. *Journal of Economic Perspectives*, Vol. 23, No. 1:pp. 121–46, 2009.

J. Kau, D. Keenan, W. Muller, and J. Epperson. The valuation and securitization of commercial and multifamily mortgages. *Journal of Banking & Finance*, Vol. 11:pp. 525–546, 1987.

R. Kiesel and M. Lutz. Efficient pricing of constant maturity swap spread options in a stochastic volatility LIBOR market model. *Journal of Computational Finance*, Vol. 14, No. 4:pp. 37–72, 2011.

F. Kilin. Accelerating the calibration of stochastic volatility models. *Journal of Derivatives*, Vol. 18, No. 3:pp. 7–16, 2011.

M. Kim, B.-G. Jang, and H.-S. Lee. A first-passage-time model under regime-switching market environment. *Journal of Banking & Finance*, Vol. 32:pp. 2617–2627, 2008.

C. Kimberling. A probabilistic interpretation of complete monotonicity. *Aequationes Mathematicae*, Vol. 10:pp. 152–164, 1974.

C. Klüppelberg, A. Lindner, and M. Ross. A continuous-time GARCH process driven by a Lévy process: stationarity and second-order behaviour. *Journal of Applied Probability*, Vol. 41, No. 3:pp. 601–622, 2004.

P. Kofman and I. G. Sharpe. Using multiple imputation in the analysis if incomplete observations in finance. *Journal of Financial Econometrics*, Vol. 1, No. 2:pp. 216–249, 2003.

S. Kou, G. Petrella, and H. Wang. Pricing path-dependent options with jump risk via Laplace transforms. *The Kyoto Economic Review*, Vol. 74, No. 1:pp. 1–23, 2005.

S. G. Kou and H. Wang. First passage times of a jump diffusion process. *Advances in Applied Probability*, Vol. 35, No. 2:pp. 504–531, 2003.

N. Kunitomo and M. Ikeda. Pricing options with curved boundaries. *Mathematical Finance*, Vol. 2, No. 4:pp. 275–298, 1992.

A. E. Kyprianou. *Introductory Lectures on Fluctuations of Lévy Processes with applications*. Springer Verlag, 2000.

A. Lewis and E. Mordecki. Wiener-Hopf factorization for Lévy processes having positive jumps with rational transforms. *Journal of Applied Probability*, Vol. 45, No. 1:pp. 118–134, 2008.

J. Liang and Y. Zhou. Valuation of a basket loan credit default swap. *International Journal of Financial Research*, Vol. 1, No. 1:pp. 21–29, 2010.

M. Liang. Valuation of loan CDS and synthetic loan CDO with prepayment risk. working paper, available on http://fileave32.fileave.com/LCDXModel.pdf, 2009.

X. S. Lin. Laplace transform and barrier hitting time distribution. *Actuarial Research Clearing House*, Vol. 1:pp. 165–178, 1999.

A. Lipton. *Mathematical methods for foreign exchange*. World Scientific, 2001.

A. Ljungqvist and M. Richardson. The cash flow, return and risk characteristics of private equity. *NYU, Finance Working Paper*, No. 03-001:pp. 3–44, 2003.

U. Lossen. *Portfolio Strategies of Private Equity Firms: Theory and Evidence*. Gabler, 2006.

D. J. Lucas. Default correlation and credit analysis. *Fixed Income*, Vol. 4, No. 4:pp. 76–87, 1995.

J.-F. Mai and M. Scherer. *Simulating Copulas: Stochastic Models, Sampling Algorithms, and Applications*. Imperial College Press, 2012.

A. W. Marshall and I. Olkin. Families of multivariate distributions. *Journal of the American Statistical Association*, Vol. 83, No. 403:pp. 834–841, 1988.

C. L. Maxam and M. Lacour-Little. Applied nonparametric regression techniques: Estimating prepayments on fixed-rate mortgage-backed securities. *Journal of Real Estate Finance and Economics*, Vol. 23, No. 2:pp. 139–160, 2001.

A. J. McNeil and J. Nešhlová. Multivariate Archimedean copulas, d-monotone functions and l_1-norm symmetric distributions. *The Annals of Statistics*, Vol. 37, No. 5B:pp. 3059–3097, 2009.

R. Merton. On the pricing of corporate debt: The risk structure of interest rates. *Journal of Finance*, Vol. 29, No 2:pp. 449–469, 1974.

R. Merton. Option pricing when the underlying stock returns are discontinuous. *Journal of Financial Economics*, Vol. 3:pp. 125–144, 1976.

S. Metwally and A. Atiya. Using Brownian bridge for fast simulation of jump-diffusion processes and barrier options. *Journal of Derivatives*, Vol. 10:pp. 43–54, 2002.

A. Mijatović and M. Pistorius. Continuously monitored barrier options under Markov process. *Mathematical Finance*, Vol. 23, No. 1:pp. 1–38, 2013.

G. Monsen. The new thinking on prepayments. *Mortgage Banking*, October:pp. 48–56, 1992.

E. Mordecki. Optimal stopping for a diffusion with jumps. *Finance and Stochastics*, Vol. 3, No. 2:pp. 227–236, 1999.

E. Mordecki. Optimal stopping and perpetual options for Lévy processes. *Finance and Stochastics*, Vol. 6, No. 4:pp. 473–493, 2002.

V. Naik. Option valuation and hedging strategies with jumps in the volatility of asset returns. *Journal of Finance*, Vol. 48, No. 5:pp. 1969–1984, 1993.

R. Nelsen. *An introduction to copulas*. Springer Series in Statistics, 2006.

E. Nikoskelainen and M. Wright. The impact of corporate governance mechanisms on value increase in leveraged buyouts. *Journal of Corporate Finance*, Vol. 13, No. 4(4): pp. 511–537, 2007.

J. Nolan. *Stable Distributions - Models for heavy tailed data*. Birkhäuser, 2010.

A. Novikov, V. Frishling, and N. Kordzakhia. Approximations of boundary crossing probabilities for a Brownian motion. *Journal of Applied Probability*, Vol. 36:pp. 1019–1030, 1999.

F. Oberhettinger and L. Badii. *Tables of Laplace transforms*. Springer Verlag, 1973.

T. C. Opler and S. Titman. The determinants of leveraged buyout activity: Free cash flow vs. financial distress costs. *Journal of Finance*, Vol. 48, No. 5(5):pp. 1985–1999, 1993.

L. Overbeck and W. Schmidt. Modeling default dependence with threshold models. *Journal of Derivatives*, Vol. 12, No. 4:pp. 10–19, 2005.

A. Pelsser. Pricing double barrier options using Laplace transforms. *Finance and Stochastics*, Vol. 4:pp. 95–104, 2000.

M. Pistorius and J. Stolte. Fast computation of vanilla prices in time-changed models and implied volatilities using rational approximations. *International Journal of Theoretical and Applied Finance*, Vol. 14, No. 4:pp. 1–34, 2012.

E. Platen and N. Bruti-Liberati. *Numerical solution of stochastic differential equations with jumps in Finance*. Springer-Verlag, 2010.

Y. Prokhorov. Convergence of random processes and limit theorems in probability theory. *Theory of Probability & Its Applications*, Vol. 1, No. 2:pp. 157–214, 1956.

S. Raible. *Lévy processes in finance: Theory, numerics, and empirical facts*. PhD thesis, Freiburg University, 2000.

E. Reiner and M. Rubinstein. Breaking down the barriers. *Risk 4*, Vol. 8:pp. 28–35, 1991.

L. Rogers. Evaluating first-passage probabilities for spectrally one-sided Lévy processes. *Journal of Applied Probability*, Vol. 37:pp. 1173–1180, 2000.

S. Rollin, A. Ferreiro-Castilla, and F. Utzet. A new look at the Heston characteristic function. *Working paper*, 2011.

S. Ross and S. Ghamami. Efficient Monte Carlo barrier option pricing when the underlying security price follows a jump-diffusion process. *Journal of Derivatives*, Vol. 17, No. 3: pp. 45–52, 2010.

K. Rottmann. *Mathematische Formelsammlung*. Spektrum Verlag, 2008.

J. Ruf and M. Scherer. Pricing corporate bonds in an arbitrary jump-diffusion model based on an improved Brownian-bridge algorithm. *Journal of Computational Finance*, Vol. 14, No. 3:pp. 127–145, 2011.

K. Sato. Self-similar processes with independent increments. *Probability Theory and Related Fields*, Vol. 89:pp. 285–300, 1991.

K. Sato. *Lévy Processes and Infinitely Divisible Distributions*. Cambridge Studies in Advanced Mathematics, 1999.

M. Scherer and R. Zagst. Modeling and pricing credit derivatives. *In: Menendez, S.C.; Pérez, J.L.F. (Eds.), Contemporary Mathematics: Mathematics in Finance*, Vol. 515: pp. 111–146, 2010.

R. Schöbel and J. Zhu. Stochastic volatility with an Ornstein-Uhlenbeck process: An extension. *Review of Finance*, Vol. 3, No. 1:pp. 23–46, 1999.

P. Schönbucher and D. Schubert. Copula-dependent default risk in intensity models. working paper, 2001.

P. J. Schönbucher. *Credit derivatives pricing models*. Wiley Finance Series, 2003.

W. Schoutens and J. Cariboni. *Lévy Processes in Credit Risk*. John Wiley & Sons, 2009.

E. Schrödinger. The theory of drop and rise tests on Brownian motion particles. *Physikalische Zeitschrift*, Vol. 16:pp. 289–295, 1915.

E. Schwartz and N. Torous. Mortgage prepayment and default decisions: A Poisson regression approach. *Journal of the American Real Estate and Urban Economics Association*, Vol. 21, No. 4:pp. 431–449, 1993.

A. Sepp. Analytical pricing of double-barrier options under a double-exponential jump diffusion process: Applications of Laplace transform. *International Journal of Theoretical and Applied Finance*, Vol. 7, No. 2:pp. 151–175, 2004.

A. Sepp. Extended CreditGrades model with stochastic volatility and jumps. *Wilmott Magazine*, September:50–62, 2006.

N. J. Sharp, D. P. Newton, and P. W. Duck. An improved fixed-rate mortgage valuation methodology with interacting prepayment and default options. *Journal of Real Estate Finance and Economics*, Vol. 36, No. 3:pp. 307–342, 2007.

P. V. Shevchenko. Addressing the bias in Monte Carlo pricing of multi-asset options with multiple barriers through discrete sampling. *Journal of Computational Finance*, Vol. 6, No. 3:pp. 1–20, 2003.

J. Stapf and T. Werner. How wacky is the DAX. *Discussion Paper Series 1 / Volkswirtschaftliches Forschungszentrum der Deutschen Bundesbank*, Vol. 18:pp. 1–40, 2003.

E. Stein and J. Stein. Stock price distributions with stochastic volatility: An analytical approach. *Review of Financial Studies*, Vol. 4:pp. 727–752, 1991.

P. Strömberg. The new demography of private equity. *The Globalization of Alternative Investments Working Papers Volume 1: The Global Economic Impact of Private Equity Report 2008*, pages 3–26, 2008.

A. Timmermann. Moments of Markov switching models. *Journal of Econometrics*, Vol. 96:pp. 75–111, 2000.

J. von Neumann. Various techniques used in connection with random digits. *Applied Mathematics Series*, Vol. 12:pp. 36–38, 1951.

N. Wilson, M. Wright, and R. Cressy. Private equity and insolvency. *Working Paper*, 2010.

D. Zhang and R. Melnik. First passage time for multivariate jump-diffusion processes in finance and other areas of applications. *Applied Stochastic Models in Business and Industry*, Vol. 25:pp. 565–582, 2009.

C. Zhou. The term structure of credit spreads with jump risk. *Journal of Banking & Finance*, 25:pp. 2015–2040, 2001a.

C. Zhou. Analysis of default correlation and multiple defaults. *The Review of Financial Studies*, Vol. 14, No. 2:pp. 555–576, 2001b.

Index

B

Basic notation
- $\mathbb{E}_{\mathbb{Q},x}[\,]$ 50
- $\mathbb{Q}_x(\,\cdot\,)$ 58
- Cumulative normal distribution Φ . . 12
- Real part Re( ) 66
- Scalar product $\langle\,\cdot\,\rangle$ 32
- Time T 12
- Vector of ones $\mathbf{1}$ 32

BNS model . . . . . *see* Shot-noise process

Brownian bridge 14
- $BB_{ab}(t_{i-1}, t_i, x_{i-1}, x_i)$ 14
- $BB^{\pm}_{ab}(t_{i-1}, t_i, x_{i-1}, x_i)$ 14
- $B_{t_{i-1}} = x_{i-1}$, $B_{t_i} = x_i$ 14

C

CIR process 21
- θ, ν, γ 21, 68

D

Double-exponential jump-diffusion 31
- λ, p, $\alpha_{\oplus}$, $\alpha_{\ominus}$ 31, 68

F

First-exit times
- $T_{P,D}$, $T^{\pm}_{P,D}$ 52
- T_{ab}, $T^{\pm}_{ab}$ 11
- $T_{ab}(i)$, $T^{\pm}_{ab}(i)$ 106ff
- Densities $f_{ab}(t)$, $f^{\pm}_{ab}(t)$ 13
- Fourier densities $\hat{f}_{ab}(\lambda)$, $\hat{f}^{\pm}_{ab}(\lambda)$ 13
- Infinite series $K^N_T(k)$ 13
- Intensity $g^{\pm}_{ab}(t, x_{i-1}, x_i)$ 16
- Laplace transforms $\Psi^{\pm}_{ab}(u)$ 32

H

Heston model . . . . . *see* CIR process
- Correlation ρ 55, 68

I

Implementation
- Absolute error ϵ 25
- Truncation parameter N 25

Insurance applications 103

M

Markov-switching model 57
- Q_0, π, k_{Z_t} 24, 68
- Markov chain $Z = \{Z_t\}_{t\geq 0}$ 24

Multivariate extensions 106
- LTE Generator $\varphi_{\alpha,\theta}(u)$ 116
- α-stable r. v. $W \sim \Lambda(\alpha)$ 117
- Archimedean generator $\varphi(u)$ 111
- Cond. default probability $p^y_i(t)$ 113
- Cond. prepayment probability $q^y_i(t)$ 113
- Copula $C(\cdot,\cdot)$ 110
- Default probability $p_i(t)$ 109
- Exponential r. v. ϵ_i 112
- Gamma r. v. $V \sim \Gamma\,(1/\theta, 1)$ 117
- Kendall's τ 114
- Linear correlation Corr($\cdot$, $\cdot$) 115
- Market factor Y 111
- Portfolio size d 110
- Prepayment probability $q_i(t)$ 109
- Tail coefficients λ_L, λ_U 114

Univariate r. v. U_i 109

O

Option pricing 50
$BO_L(S_0; D, T)$ 53
$C_K(S_0, T)$ 50, 58
$DOC_K(S_0; D, P, T)$ 53
$DOC_K(S_0; D, T)$ 53
$I_K(S_0; D, P, T)$ 53
$I_K(S_0; D, T)$ 53
$K_T := K_0 \exp(\int_0^T r_t dt)$ 50
$B_F(S_0; D, P, T)$ 83
$I_K^{\pm}(S_0; D, P, T)$ 76
Barrier $D_t := D_0 \exp(\int_0^t r_s ds)$ 52
Barrier $P_t := P_0 \exp(\int_0^t r_s ds)$ 52
Barrier derivative $X_{D,P}^{g(S_T)}(S_0)$ 54
Bond $\mathcal{B}_t := \exp(\int_0^t r_s \, ds)$ 52
Characteristic function $\varphi_T(u, S_0)$ . . . 58
Monte–Carlo grid $\triangle$ 76
Payoff $g(S_T)$ 54
Time to maturity T 66
OU process 22
$L(u)$, $M(u)$, $N(u)$ 132
$\varkappa$, k, ξ, σ_0 . . . . . 22, 68

P

Prepayment risk 119
$\Pi_{b,l}^d(t)$ 122
$\Pi_{b,l}^{y,d}(t)$ 121
Loss $L^d(t)$ and notional $N^d(t)$ 123
Number of defaults b 121
Number of prepayments l 121
Portfolio size d 121
Spread $s_{[K_{j-1};K_j]}$ 124
Tranche loss $PV_{[K_{j-1};K_j]}^{loss}$ 124
Tranche notional $PV_{[K_{j-1};K_j]}^{fee}$ 124
Tranches $[K_{j-1}; K_j]$ 124
Private Equity 85
Asset volatility σ 91
Equity volatility σ_E 91
Interest rate c 87
Logarithmic leverage ratio d 89
Market price of debt $V_D(0)$ 90
Market price of equity $V_E(0)$ 137
Redemption rate λ 87
Survival probability $\Phi_{d,\mu,\sigma}(T)$ 89
Process $B = \{B_t\}_{0 \le t \le 1}$
μ 12
σ 12
Barriers a, b 11
Process $B = \{B_t\}_{t \ge 0}$
$\{\tilde{W}_t\}_{t \ge 0}$ 11
Process $S = \{S_t\}_{0 \le t \le 1}$
Ω, $\mathcal{F}$, $\mathbb{Q}$ 52
$\{\sigma_t\}_{t \ge 0} > 0$ 52
$\{r_t\}_{t \ge 0}$ 52
Process $S = \{S_t\}_{t \ge 0}$
$\{\sigma_t\}_{t \ge 0} > 0$ 50

R

Regime switching model . . . . . *see* Markov-switching model

S

Shot-noise process 22
λ_0, δ, ψ, ζ 22, 68
s_i, M_i 22
Stein–Stein model . . . . . *see* OU process

T

Time change 18
Intensity $\lambda = \{\lambda_t\}_{t \ge 0}$ 21
Laplace transform $\vartheta_T(u)$ 21
Time change $\Lambda_T := \int_0^T \lambda_t dt$ 21

Acknowledgements

This research project would not have been possible without the support of many people. Foremost, my thanks go to my advisor Prof. Dr. Matthias Scherer for guiding and supporting me over the last three years. He comes up with many interesting ideas and is always available for discussions on research or other topics. Matthias shared his research experience in many joint projects. Furthermore, he patiently and carefully read earlier versions of this thesis and improved it with valuable comments. He and Prof. Dr. Rudi Zagst provided me with financial support by means of a teaching position. During my PhD studies, those teaching duties have always been a very enjoyable time.

I would also like to thank Prof. Marcos Escobar (Ryerson University, Toronto) who invited me for several research stays and who agreed to serve as a co-examiner of this thesis. Due to his friendliness and commitment, working with him is a real pleasure.

I am very grateful to Prof. Dr. Claudia Klüppelberg for chairing the committee and Prof. Dr. Hansjörg Albrecher for agreeing to serve as referee for this thesis.

Furthermore, I want to thank Prof. Dr. Reiner Braun, Dr. Nico Engel, Lexuri Fernández, and Prof. Dr. Rudi Zagst who also participated in joint research projects that led to this thesis.

I want to thank my colleagues in Munich and Toronto for fruitful discussions and for providing a very nice and friendly atmosphere.

Many thanks go to the German Academic Exchange Service (DAAD) whose financial support enabled my research stays in Toronto. During my research visits, I also received a lot of support from Prof. Luis Seco who allowed me to stay and work at risklab, University of Toronto.

I want to thank Dr. Jörg Marienhagen who pointed me towards the topic of double barrier options.

Finally, I want to thank my family for supporting me throughout my studies.

Some of the results of my PhD studies have previously been published:

R. Braun, N. Engel, P. Hieber, and R. Zagst. The risk appetite of private equity sponsors. *Journal of Empirical Finance*, Vol. 18, No. 5:pp. 815–832, 2011.

M. Escobar, P. Hieber, and M. Scherer. Efficiently pricing barrier derivatives in stochastic volatility models. *Review of Derivatives Research*, in press, 2013.

L. Fernández, P. Hieber, and M. Scherer. Double-barrier first-passage times of jump-diffusion processes. *Monte Carlo Methods and Applications*, Vol. 19, No. 2:pp. 107–141, 2013.

P. Hieber and M. Scherer. Efficiently pricing barrier options in a Markov-switching framework. *Journal of Computational and Applied Mathematics*, Vol. 235:pp. 679–685, 2010.

P. Hieber and M. Scherer. A note on first-passage times of continuously time-changed Brownian motion. *Statistics & Probability Letters*, Vol. 82, No. 1:pp. 165–172, 2012.

P. Hieber and M. Scherer. Modeling credit portfolio derivatives, including both a default and a prepayment feature. *Applied Stochastic Models in Business and Industry*, Vol. 29, No. 5:pp. 479–495, 2013.

Most of the results are joint work with Prof. Dr. Matthias Scherer (Technische Universität München).

- Braun et al. [2011] resulted from a cooperation with Dr. Nico Engel and Prof. Dr. Reiner Braun from the *Center for Entrepreneurial and Financial Studies*, Technische Universität München (Prof. Dr. Dr. Ann-Kristin Achleitner) and is joint work with Prof. Dr. Rudi Zagst.

- Fernández et al. [2013] is joint work with Lexuri Fernández (University of the Basque Country).

- Escobar et al. [2013] is joint work with Prof. Marcos Escobar (Ryerson University, Toronto) and was carried out during a research stay at risklab, University of Toronto.